AD-A084 934 PRATT AND WHITNEY AIRCRAFT GROUP WEST PALM BEACH FL G--ETC F/G 21/5
CUMULATIVE DAMAGE FRACTURE MECHANICS UNDER ENGINE SPECTRA.(U)
JAN 80 J N LARSEN, B J SCHWARTZ, C G ANNIS F33615-77-C-5183
UNCLASSIFIED PWA-FR-11844 AFML-TR-79-4199 NL

1 of 3
AD A084934

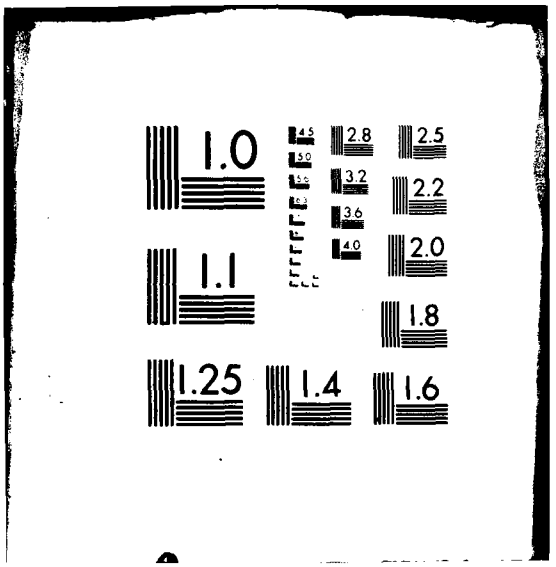
1.0
1.1
1.25
1.4
1.6
1.8
2.0
2.2
2.5
2.8
3.2
3.6
4.0
4.5
5.0

AFML-TR-79-4159

LEVEL II

(2)

4

ADA084934

CUMULATIVE DAMAGE FRACTURE MECHANICS UNDER ENGINE SPECTRA

J. M. LARSEN
B. J. SCHWARTZ
C. G. ANNIS, Jr.
PRATT & WHITNEY AIRCRAFT GROUP
GOVERNMENT PRODUCTS DIVISION
BOX 2691, WEST PALM BEACH, FLORIDA 33402

JANUARY 1980

TECHNICAL REPORT AFML-TR-79-4159
Final Report for period September 1977 through January 1980

AIR FORCE MATERIALS LABORATORY
AIR FORCE WRIGHT AERONAUTICAL LABORATORIES
AIR FORCE SYSTEMS COMMAND
WRIGHT-PATTERSON AIR FORCE BASE, OHIO 45433

NOTICE

When Government drawings, specifications, or other data are used for any purpose other than in connection with a definitely related Government procurement operation, the United States Government thereby incurs no responsibility nor any obligation whatsoever; and the fact that the government may have formulated, furnished, or in any way supplied the said drawings, specifications, or other data, is not to be regarded by implication or otherwise as in any manner licensing the holder or any other person or corporation, or conveying any rights or permission to manufacture, use, or sell any patented invention that may in any way be related thereto.

This report has been reviewed by the Information Office (OI) and is releasable to the National Technical Information Service (NTIS). At NTIS, it will be available to the general public, including foreign nations.

This technical report has been reviewed and is approved for publication.

WALTER H. REIMANN
Project Engineer
Metals Behavior Branch
Metals and Ceramics Division

NATHAN G. TUPPER, Chief
Metals Behavior Branch
Metals and Ceramics Division

"If your address has changed, if you wish to be removed from our mailing list, or if the addressee is no longer employed by your organization please notify AFWAL/MLLN, W-PAFB, OH 45433 to help us maintain a current mailing list."

Copies of this report should not be returned unless return is required by security considerations, contractual obligations, or notice on a specific document.

AIR FORCE/56780/13 May 1980 — 420

SECURITY CLASSIFICATION OF THIS PAGE (When Data Entered)

REPORT DOCUMENTATION PAGE

READ INSTRUCTIONS BEFORE COMPLETING FORM

1. REPORT NUMBER: AFML-TR-79-4159	2. GOVT ACCESSION NO.: AD-A084934
3. RECIPIENT'S CATALOG NUMBER	
4. TITLE (and Subtitle): Cumulative Damage Fracture Mechanics Under Engine Spectra	5. TYPE OF REPORT & PERIOD COVERED: Final Report, Draft 1 Sep 77 - 31 Jan 80
	6. PERFORMING ORG. REPORT NUMBER: FR 11844
7. AUTHOR(s): J. M. Larsen, B. J. Schwartz, C. G. Annis, Jr.	8. CONTRACT OR GRANT NUMBER(s): F33615-77-C-5153
9. PERFORMING ORGANIZATION NAME AND ADDRESS: Pratt & Whitney Aircraft, Government Products Division, P.O. Box 2691, West Palm Beach, Florida 33402	10. PROGRAM ELEMENT, PROJECT, TASK AREA & WORK UNIT NUMBERS: Project 2420 01 08
11. CONTROLLING OFFICE NAME AND ADDRESS: Air Force Materials Laboratory, AFSC Aeronautical Systems Division, Wright-Patterson AFB, Ohio 45433	12. REPORT DATE: Jan 80 13. NUMBER OF PAGES: 221
14. MONITORING AGENCY NAME & ADDRESS (if different from Controlling Office): PWA-FR-11844	15. SECURITY CLASS. (of this report): Unclassified 15a. DECLASSIFICATION DOWNGRADING SCHEDULE

16. DISTRIBUTION STATEMENT (of this Report)

Approved for Public Release; Distribution Unlimited.

17. DISTRIBUTION STATEMENT (of the abstract entered in Block 20, if different from Report)

18. SUPPLEMENTARY NOTES

19. KEY WORDS (Continue on reverse side if necessary and identify by block number)

Fatigue, Crack Propagation, Cumulative Damage, Hyperbolic Sine Model, Crack Retardation, Prestrain

20. ABSTRACT (Continue on reverse side if necessary and identify by block number)

An empirically based mathematical model and computer code capable of predicting cumulative damage effects on fatigue crack growth in engine disks has been developed for Waspaloy (PWA 1007) and IN100 (PWA 1073). The computing software segregates a complex loading mission, applies a multi-parameter interpolation procedure to determine cycle-by-cycle crack growth, and performs a specimen life calculation. The model was developed from a broad matrix of tests of both materials, and a number of auxiliary investigations were conducted to examine the range of applicability of the model.

DD FORM 1 JAN 73 1473 EDITION OF 1 NOV 65 IS OBSOLETE

S/N 0102-LF-014-6601

392887

SECURITY CLASSIFICATION OF THIS PAGE (When Data Entered)

SUMMARY

Cumulative damage fracture mechanics at elevated temperatures is particularly complex, requiring a basic understanding of the variables affecting crack growth and an ability to model material behavior. The synergistic effects of varying load and load sequencing on crack propagation in engine disk materials preclude the use of conventional linear damage accumulation techniques (e.g., Miner's Rule) for accurate life predictions. Failure to consider interaction effects may lead to significant errors in predicted crack growth behavior and in the resulting life prediction. In most cases, the result is an underestimation of propagation life and the concomitant economic penalties of premature removal. Also to be considered is any overestimate of life and the serious implications concerning component safety.

The objective of this contract was to develop and demonstrate an empirically based mathematical model and computer code capable of predicting cumulative damage effects on fatigue crack growth in gas turbine engine disks.

Since the technical approach was empirical in nature, no attempt was made to isolate and describe individual microscopic events associated with propagation interrupted by overloads and/or dwells, but rather synergism resulting from various combinations of these was empirically described using an interpolative mathematical model. The resulting descriptions of generic elemental cumulative damage events could then be used to analyze specific complex mission spectra, and the life under such a mission could then be computed by simple numerical integration of segregated elements. A three-step process of mission segregation, crack growth rate interpolation, and calculation of fatigue crack propagation life was established. This computerized model performs Mission Analysis and Prediction (MAP) of crack growth in gas turbine engine disks subject to complex mission loading.

Development of the MAP computing software was based on an analysis of representative missions for TF30 and F100 engines employing Waspaloy and IN100 turbine disks. Such mission usage is composed of a variety of operational activities including aircraft takeoff, ferry and refueling, terrain-following radar (TFR), bombing runs, and combat under subsonic and supersonic conditions.

Analysis of the turbine disk missions revealed that these low-cycle fatigue loading sequences differ significantly from the high-cycle loading spectra typically experienced by airframe components. The load sequence effects observed in turbine disk operation are characterized by a high occurrence frequency of major throttle excursions (overloads). As a result, immediate post-overload load sequence behavior is of increased significance, while the long-term effects of an overload on crack growth are truncated by the frequently repeated overload. The instantaneous behavior of a crack propagating under fatigue interrupted by frequently occurring overloads was shown to be dominated by delayed retardation. That is, both Waspaloy and IN100 exhibit continuous post-overload deceleration in crack growth until the recurrence of an overload truncates and restarts the load interaction process. This behavior is not effectively described by conventional models of load sequence effects. However, the methodology employed in the MAP system was developed specifically for prediction of mission crack growth with frequently occurring overloads.

Development of the Mission Analysis and Prediction system was based on the P&WA philosophy of empirical synergistic modeling. This philosophy states that any complex mission spectrum can be segregated into elemental damage events that can be quantitatively described. The crack propagation life expected under such a spectrum can then be computed as the linear addition of the damage associated with properly segregated events.

Mission segregation is accomplished by the first of three MAP algorithms: the segregation, interpolation, and computation algorithms. These are described below.

The set of rules by which a mission profile is separated (segregated) into its elemental cumulative damage events constitutes the segregation algorithm. As formulated, the segregation algorithm translates an input isothermal stress-time profile into a parametric, cycle-by-cycle description of the loading sequence. This segregated mission definition provides input compatible with the interpolation algorithm.

The fundamental strength of the MAP system is the interpolative capability provided by the hyperbolic sine model. The application of this procedure is executed by the interpolation algorithm. As formulated, this algorithm performs a complex interpolation to obtain a crack growth rate curve (da/dN us ΔK) as a function of the operating parameters (e.g., stress ratio, temperature, cyclic frequency, and load sequence parameters). These interpolated curves are subsequently used in the computation algorithm to obtain a fatigue crack life calculation.

A cycle-by-cycle integration of the collection of interpolated crack growth curves is performed by the computation algorithm. The resulting life calculation is a prediction of crack propagation resulting from the input mission usage profile.

The accuracy of the cumulative damage fracture mechanics system was evlauated by conducting a number of model demonstration tests simulating engine usage. Using the MAP system, specimen life calculations were obtained for the simulated missions. Subsequently, fatigue crack propagation tests were conducted to evaluate the model accuracy.

The results of the complete model demonstration program established the utility of the MAP system and illustrated the importance of accurate assessment of the cumulative damage fatigue crack growth which results from mission usage of a miltary gas turbine engine.

PREFACE

The major portion of this work was performed under Air Force Materials Laboratory Contract F33615-77-C-5153, "Cumulative Damage Fracture Mechanics Under Engine Spectra." The project engineer was D. E. Macha, reporting to Dr. W. H. Reimann, AFML/LLN. This program was conducted in the Materials and Mechanics Laboratories of Pratt & Whitney Aircraft Government Products Division, West Palm Beach, Florida. The responsible engineer was J. M. Larsen, assisted by B. J. Schwartz and the Program Manager was C. G. Annis, Jr., Group Leader, Fracture Mechanics and Component Life Analysis, reporting to M. C. VanWanderham, General Supervisor, Mechanics of Materials and Structures.

The authors wish to acknowledge D. W. Ogden who directed the material testing, T. Watkins and V. De La Torre, who aided in data analysis, and R. N. Green and Dr. J. H. Griffin for their participation in development of the mission segregation algorithm.

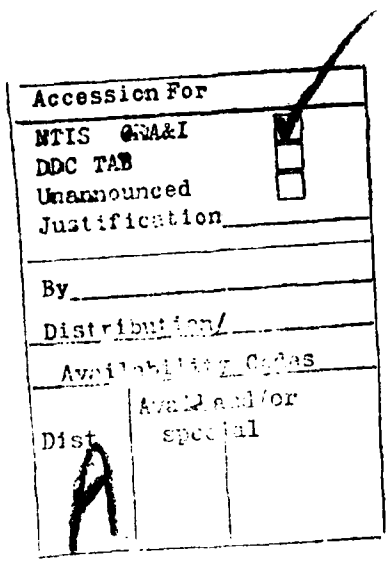

TABLE OF CONTENTS

LIST OF ILLUSTRATIONS

LIST OF ILLUSTRATIONS
(Continued)

LIST OF ILLUSTRATIONS
(Continued)

LIST OF ILLUSTRATIONS
(Continued)

LIST OF ILLUSTRATIONS
(Continued)

LIST OF TABLES

SECTION I
INTRODUCTION

Cumulative damage fracture mechanics at elevated temperatures is particularly complex, requiring a basic understanding of the variables affecting crack growth and an ability to model material behavior. The synergistic effects of varying load and load sequencing on crack propagation in engine disk materials preclude the use of conventional linear damage accumulation techniques (e.g., Miner's Rule) for accurate life predictions. Failure to consider interaction effects may lead to significant errors in predicted crack growth behavior and in the resulting life prediction. In most cases, the result is an underestimation of propagation life and the concomitant economic penalties of premature removal. Also to be considered is any overestimate of life and the serious implications concerning component safety. The desirability of an accurate crack propagation prediction methodology is clearly evident.

The objective of this program was to develop and demonstrate an empirically based mathematical model and computer code, capable of predicting cumulative damage effects on fatigue crack growth in engine disks.

Pratt & Whitney Aircraft Group, under the AFML sponsorship, recently developed an efficient and accurate empirical method for analyzing synergism in crack propagation at elevated temperatures (References 1, 2, and 3). No attempt was made to isolate and describe individual microscopic events associated with propagation interrupted by overloads and/or dwells, but rather synergism resulting from various combinations of these was empirically described using an interpolative mathematical model. The resulting descriptions of generic elemental cumulative damage events were then used to analyze specific complex mission spectra. The life under such a mission was then computed by simple numerical integration of segregated elements. This proven method formed the basis of our technical approach to cumulative damage fracture mechanics.

The program consisted of a 24-month, four-phase technical effort. Phase I, Mission Definition, defined representative composite missions for two advanced Air Force fighter engines that employ Waspaloy and IN100 turbine disks. These results provided the foundation for test matrix formulation. Phase II, Mission Segmentation, defined, segregated, and quantified elemental cumulative damage events. Phase III, Mathematical Model Development, evaluated the data generated in Phase II, integrated these results with relevant pre-existing data, and translated the resulting model into a computer code. Phase IV was Model Demonstration. The Air Force Project Engineer provided two representative mission profiles, upon which life history (a, N) predictions were made. These were recorded with the Air Force Project Engineer prior to demonstration testing. Fatigue crack propagation (FCP) tests on the two materials, IN100 and Waspaloy, addressing the two profiles, and using both compact and surface flaw specimens, were performed to verify the model experimentally. A flow chart of the program operating plan is shown in Figure 1.

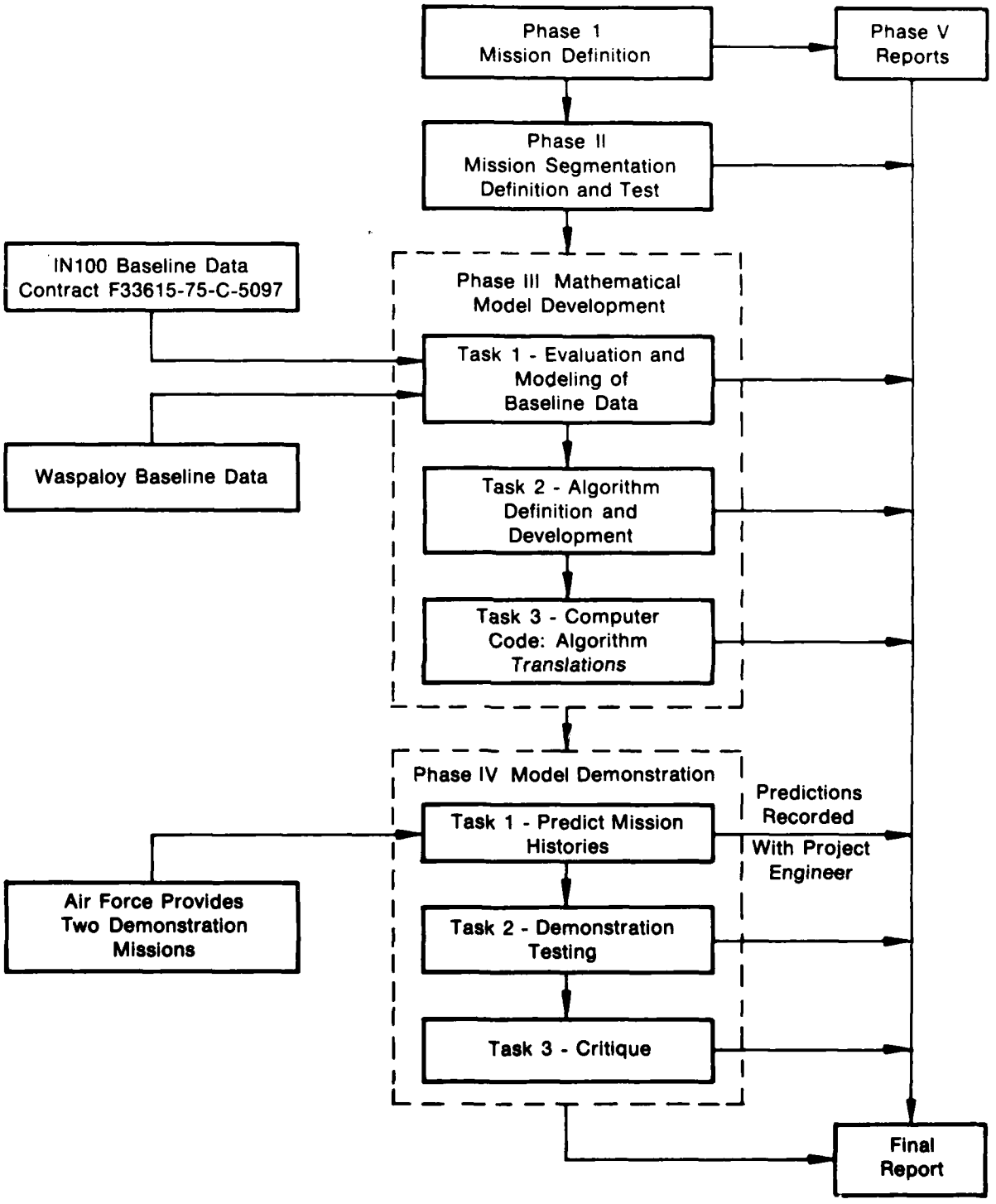

Figure 1. Flow Chart of Program Operating Plan

SECTION II
TECHNICAL PROGRAM AND ACCOMPLISHMENTS

A. PHASE I - MISSION DEFINITION

1. Mission Operating Profile

The objective of the analysis of mission usage data, the Phase I activity, was to provide a basis for formulation of a test and evaluation program for optimum model applicability. Mission usage field data for military aircraft was generally obtained from pilot interviews and event history recorders (EHR) which have been installed on advanced Air Force fighters to acquire real-time engine operating parameters. The compilation and characterization of these raw data define representative engine usage for a variety of operational activities including aircraft takeoff, ferry and refueling, terrain following radar (TFR), bombing runs, and combat under subsonic and supersonic conditions

Representative missions were analyzed for two advanced Air Force fighter engines employing Waspaloy and IN100 turbine disks. For Waspaloy, a composite mission has been prepared to reflect the broad range of operating conditions imposed on this disk. This composite, presented in Figure 2, illustrates the representative duty cycles in terms of rotor speed for the collection of individual mission usages. Figure 3 shows a similar mission for a second engine which employs turbine disks fabricated from IN100. This operating history, given in terms of maximum stress, is based on a Tactical Air Command (TAC) composite mission supplied by the Air Force Materials Laboratory in 1974. This mission has excluded load sequences corresponding to operation of TFR, since this is not a characteristic operating activity for this engine. The two flight missions presented are currently used as the basis for field life predictions for Waspaloy and IN100 disks.

Cumulative damage element event definition, required specimen testing, and model development were based on these two missions.

2. Mission Stress Analysis

A generalized fracture mechanics residual life prediction system capable of addressing crack propagation in disks under mission loading must consider all fracture critical locations in the disk. These include: (1) bore (internal defects), (2) rim (cooling holes, attachments), and (3) web (boltholes). Bore problems are usually associated with inclusions or other intrinsic, subsurface defects where crack propagation is not affected by the surrounding environment. Alternatively, the fracture behavior of surface cracks in wrought nickel-base superalloys may be influenced by strong environmental effects (e.g., oxidation, sulfidation). This program addressed the propagation of surface cracks in air; the propagation of internal defects, or of surface cracks subjected to extremes in environment, was not considered.

The stress analysis of fracture critical disk locations concentrated on boltholes and cooled and uncooled rims of turbine disks. At these locations, stress histories depend on the operating mission profile (Figures 2 and 3), transient thermal gradients, and the geometrical stress concentration. Under a program for the Air Force Aero Propulsion Laboratory, "Structural Life Prediction and Analysis," (Reference 4) a survey was made of estimated bolthole stresses in the two advanced Air Force fighter engines considered in the present contract. The results of the bolthole stress survey were examined as part of the cumulative damage stress analysis performed under the current contract. In addition, bore, bolthole, and rim stress-temperature-time profiles for both Air Force and Navy turbine disks were reviewed.

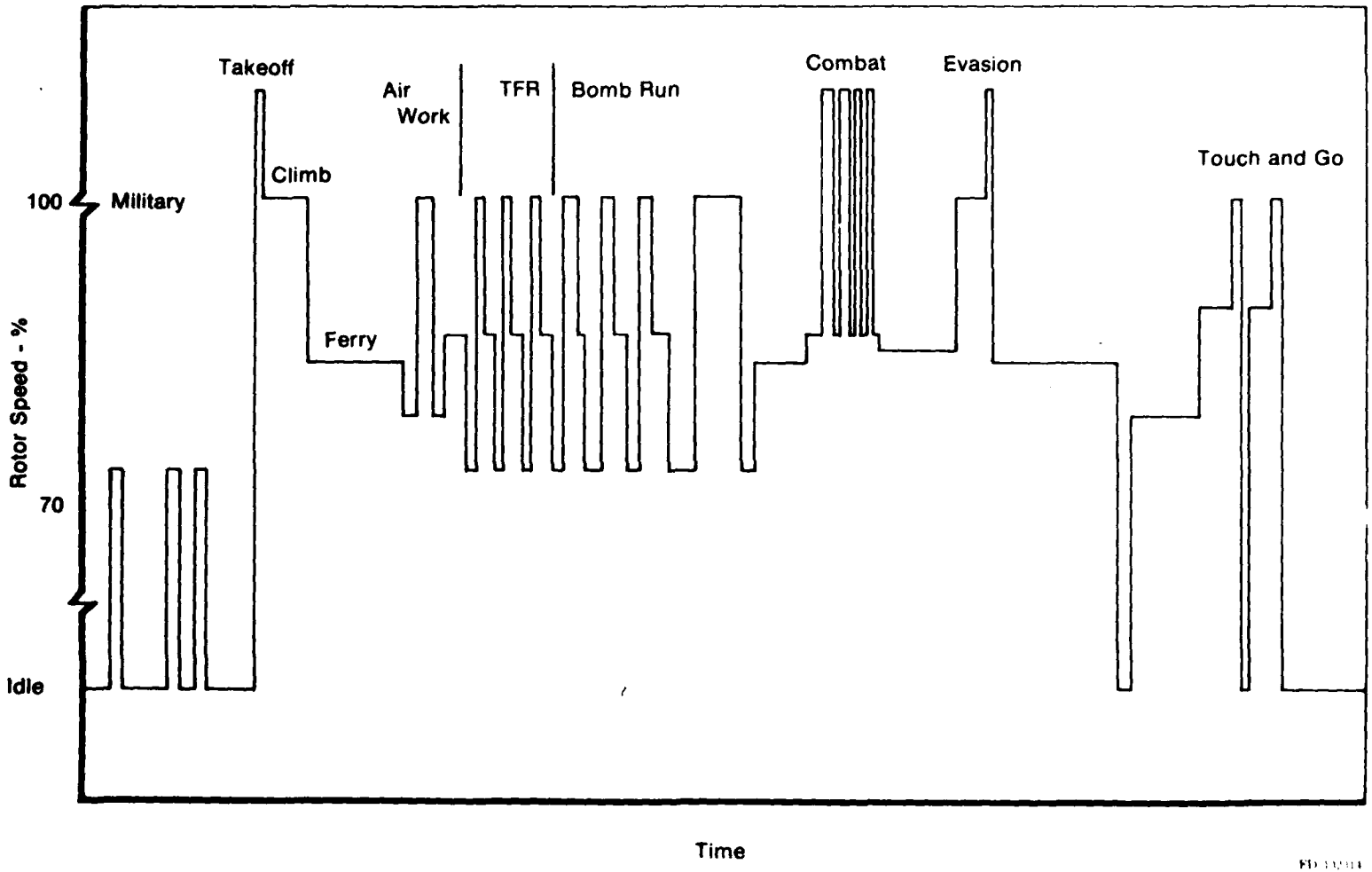

Figure 2. Representative Mission for Waspaloy Disks

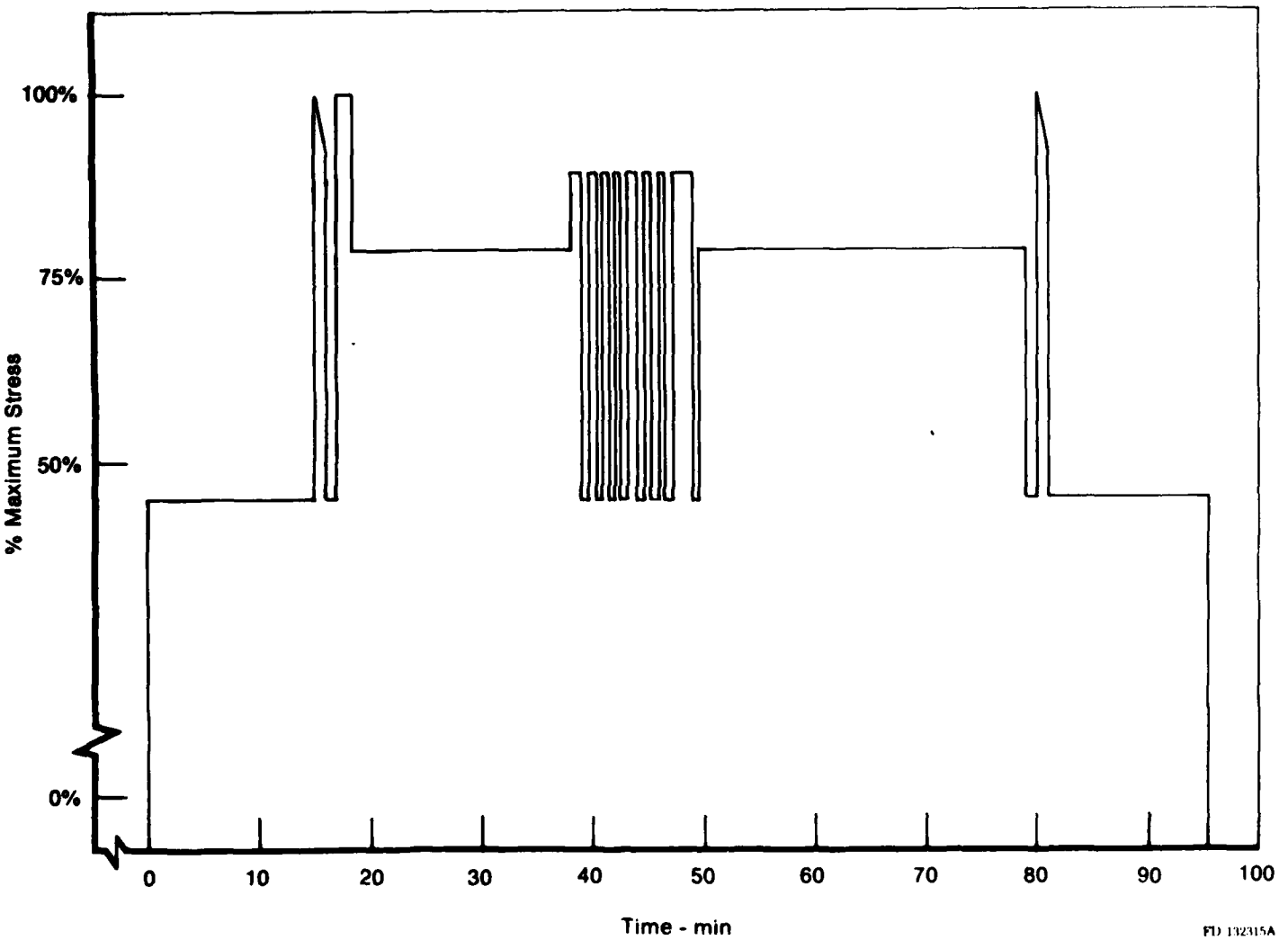

Figure 3. Representative Mission for IN100 Disks

There are as many different stress-temperature-time profiles as there are fracture critical locations on individual disks. Some of these are particularly complex. Figure 4 presents the operational conditions at the fracture critical location for a cooled turbine rim (radial cooling hole) in a Waspaloy disk. Figure 5 presents the stress-temperature-time response for a bolthole in another Waspaloy disk. The stress-temperature-time response of a bolthole in an IN100 disk subjected to a simplified subsonic combat mission is given in Figure 6.

The ultimate objective of this contract was to produce results having general applicability to the analysis of surface cracks in Waspaloy and IN100 turbine disks. Crack propagation data were generated from laboratory specimens having well-defined stress intensity solutions and thickness representative of disk operation. These data represent crack growth in a uniform stress field; the influence of aberrations in the elastic stress field, such as caused by notches, is excluded from the actual test data. The problem of predicting fatigue crack propagation (FCP) in large stress gradients may be solved analytically using advanced crack tip stress intensity solutions such as K developed by P&WA.

B. PHASE II - MISSION SEGMENTATION AND TESTING

1. Philosophy

A thorough understanding of fatigue crack propagation under complex cycling is fundamental to both damage-tolerant-design and retirement-for-cause methodologies. Previous investigations have considered certain aspects of FCP under stress-temperature-time and geometry (thickness) conditions representative of turbine airfoil operation; however, additional study of crack propagation under stress-temperature-time conditions characteristic of turbine disk operation was needed.

The goal of Phase II of this contract was to develop an understanding of cumulative damage FCP suitable for development of an empirical model capable of accurately predicting crack growth for typical USAF turbine disk stress-temperature-time profiles. The approach was to employ a new experimental methodology which examines the macroscopic effects of realistic service loading on FCP. This approach, first demonstrated in AFML contract F33615-75-C-5057 "Applications of Fracture Mechanics at Elevated Temperatures" (Reference 1, 2, and 3), has been extended and optimized for cumulative damage crack growth.

The P&WA philosophy of empirical synergistic modeling is that any complex mission spectrum can be segregated into elemental damage events which can be quantitatively described. The crack propagation life expected under such a spectrum can then be computed as the linear addition of the damage associated with properly segregated events. The following definition is fundamental to understanding this approach:

- An elemental damage event is the smallest repeating load-time sequence which results in FCP not predictable by linear damage accumulation alone.

An analysis of the missions currently used for field life predictions of two advanced USAF fighter engines established cumulative damage elemental events. These events are defined as: (1) constant load amplitude cycling, including dwells, (2) sustained load crack growth, and (3) overload(s)/LCF cycling.

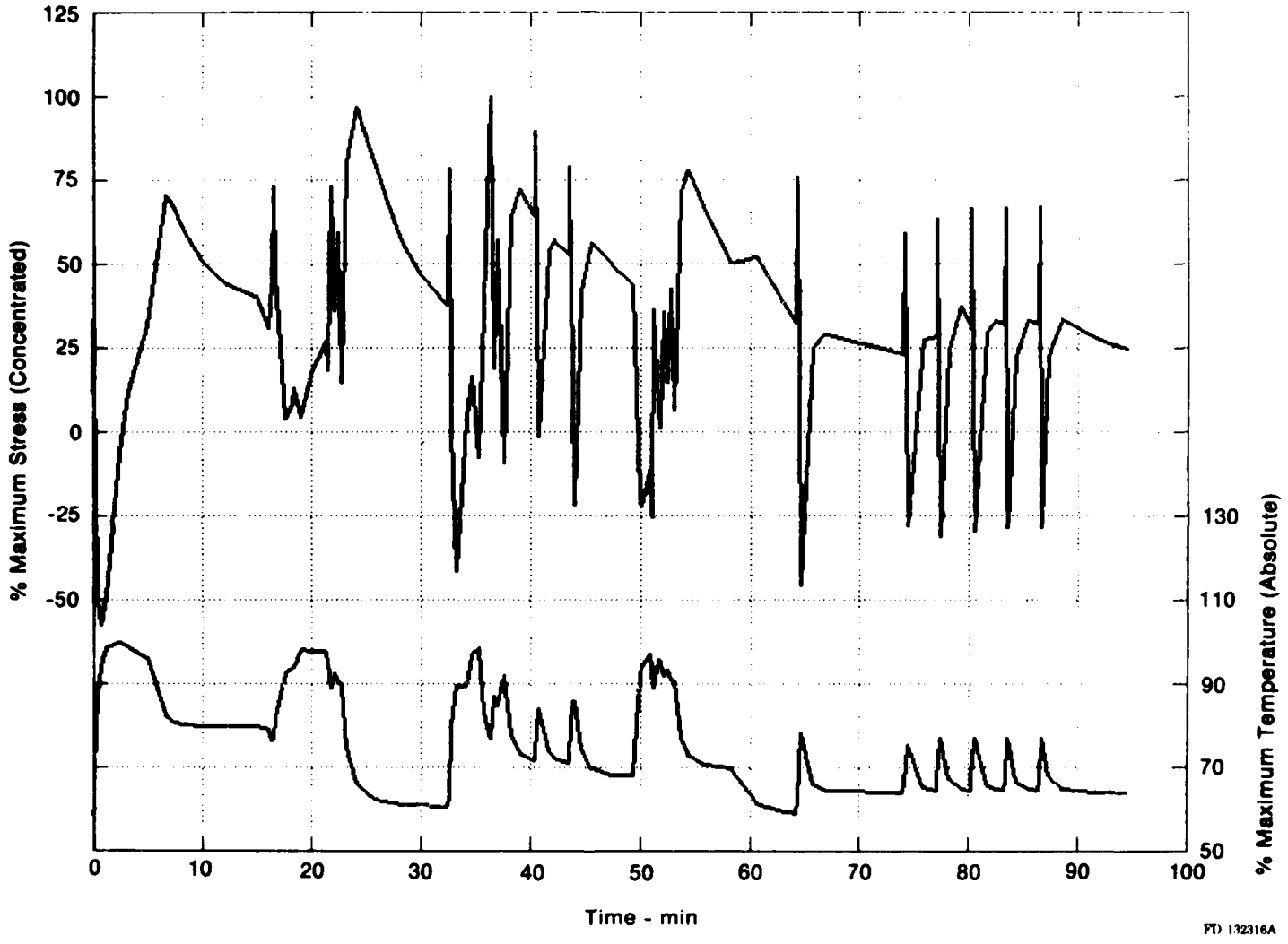

Figure 4. Operational Conditions for a Cooled Turbine Disk Rim (Waspaloy)

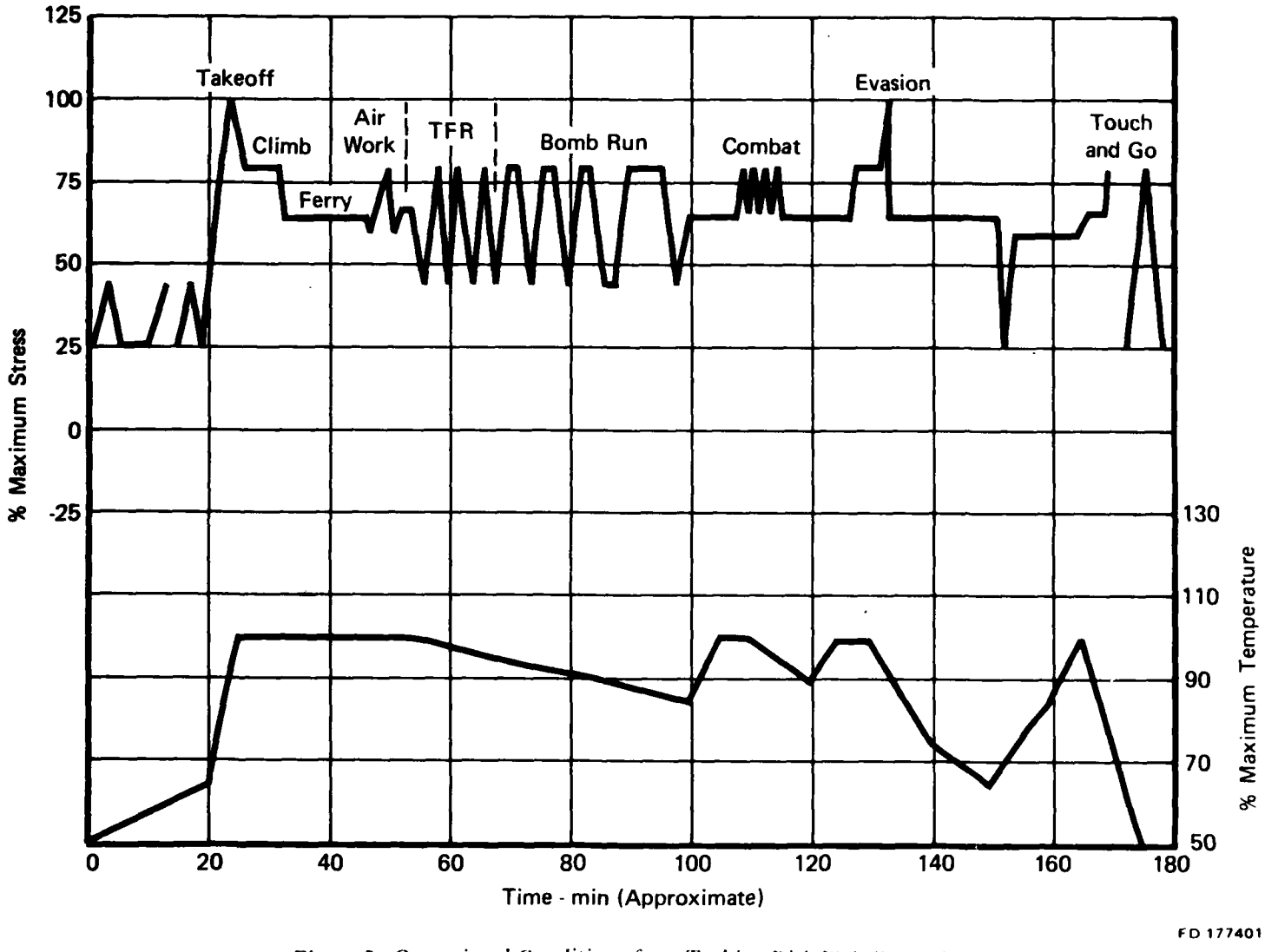

Figure 5. Operational Conditions for a Turbine Disk Web (Waspaloy)

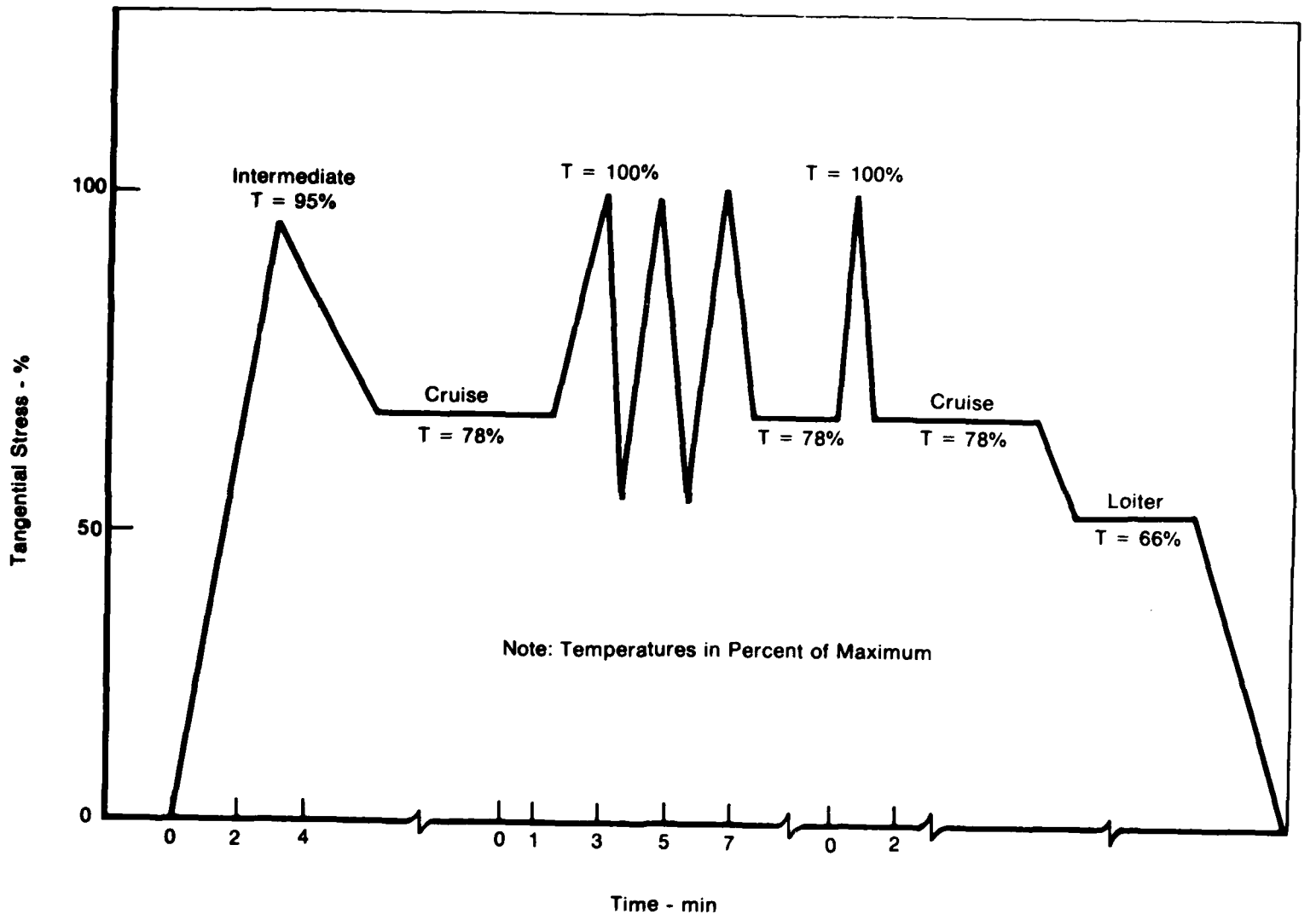

Figure 6. High-Pressure Turbine 2nd-Stage Disk Bolthole Stress vs Time (Subsonic Combat Mission)

2. Metallurgical Analysis

a. *Waspaloy (PWA 1007)*

Three Waspaloy forgings were obtained from Reisner Metals, Inc. The forgings were fabricated from Teledyne Allvac billet, heat No. L568, code WAH. The forgings were 457 mm (18 in.) OD by 40.6 mm (1.6 in.) thick. The chemical composition of Waspaloy (PWA 1007) met or exceeded the specifications shown in Table 1, and the results of mechanical property tests, also given in the table, satisfied material specifications. Typical microstructure of the Waspaloy forgings is shown in Figure 7, and thin foil electron micrographs of representative structure are presented in Figure 8.

b. *GATORIZED® IN100 (PWA 1073)*

Two IN100 forgings were GATORIZED at P&WA/Florida. Material source was Udimet Powder Division of Special Metals Corporation, heat codes F822, B1 and B2. The mechanical properties and chemical composition of the IN100 (PWA 1073) met or exceeded specifications shown in Table 2. Typical microstructure of the IN100 is given in Figure 9. Note the small grain size, ASTM 12-14. Thin-foil transmission electron micrographs of representative dislocation substructure are given in Figure 10.

3. Experimental Program

a. *Applicability of Linear Elastic Fracture Mechanics*

A fundamental assumption implicit in the development of the cumulative damage crack propagation model is the applicability of linear elastic fracture mechanics (LEFM) for Waspaloy and IN100. An examination of this assumption is discussed below. Consideration of nonlinear fracture mechanics concepts is beyond the scope of this contract.

The presence of a crack in a stressed component necessitates redistribution of stresses around the crack. The stress intensity factor is a parameter that reflects this redistribution and is a function of nominal stress, crack size, and specimen and crack geometries. The concept of stress intensity factor was originally defined for an infinitely sharp elastic crack tip, and it is this deformation that gives the material resistance to crack propagation.

The degree of brittleness of a material (and the limit to the applicability of linear elastic fracture mechanics) is directly related to the type of stress redistribution process that occurs at the crack tip. In the high temperature fatigue process, this redistribution of stress is expected to depend on the relative degree of elastic, plastic, creep, and chemical work expended at the crack. In a completely brittle material, relaxation of the crack tip stress field is negligible, and simple reinitiation of a stopped crack is sufficient to promote complete fracture. The absolute limit to the applicability of fracture mechanics is general yielding.

The usefulness of LEFM depends on a uniparametrical relationship between crack growth rate and the stress intensity factor. Crack tip inelasticity, due to material response at elevated temperatures, can preclude general utility of K as the correlative parameter.

The following provides our approach to the development of a system of empirical models for accurate predictions of surface crack growth in Waspaloy in IN100 turbine disks.

Tests are conducted to ensure that the crack tip experiences sufficient geometric constraint and/or environment embrittlement as to render crack growth rate — ΔK relationships independent of component geometry (e.g., thickness).

TABLE 1
CHEMICAL COMPOSITION AND MECHANICAL PROPERTIES OF WASPALOY
(PWA 1007)

	Chemical Composition (%)		
	Minimum	*Maximum*	
Carbon	0.02	0.10	
Manganese	–	0.75	
Sulfur	–	0.020	
Silicon	–	0.75	
Chromium	18.00	21.00	
Colbalt	12.00	15.00	
Molybdenum	3.50	5.00	
Titanium	2.75	3.25	
Aluminum	1.20	1.60	
Zirconium	0.02	0.12	
Boron	0.003	0.010	
Iron	–	2.00	
Copper	–	0.10	
Bismuth	–	0.00005	(0.5 ppm)
Lead	–	0.0010	(10 ppm)
Nickel	remainder		

Mechanical Properties

Tensile

Temperature		*0.2% Yield Strength*		*Ultimate Strength*		*Elongation*	*Reduction in Area*
(°C)	*(°F)*	*(MPa)*	*(ksi)*	*(MPa)*	*(ksi)*	*(%)*	*(%)*
Room	Temp	1062	(154.0)	1373	(199.2)	24.5	37.2
538	(1000)	949	(137.7)	1251	(181.4)	17.0	31.2

Stress Rupture

Temperature		*Applied Stress*		*Time to Failure*	*Elongation*
(°C)	*(°F)*	*(MPa)*	*(ksi)*	*(hr)*	*(%)*
732	(1350)	552	(80.0)	56.7	28.5
816	(1500)	310	(45.0)	67.7	27.0

Mag: 100X

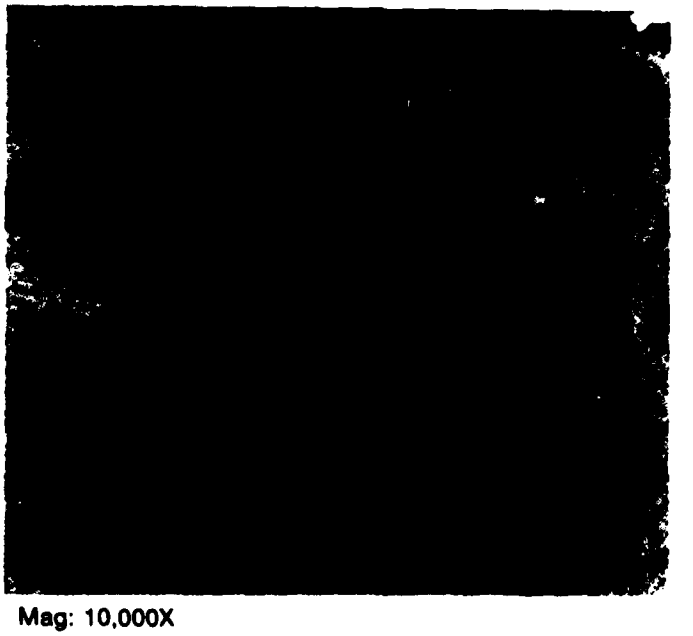

Mag: 10,000X

FD 132319

Figure 7. Typical Microstructure of Waspaloy (PWA 1007) (ASTM Grain Size 3 to 5)

Mag: 10,000X

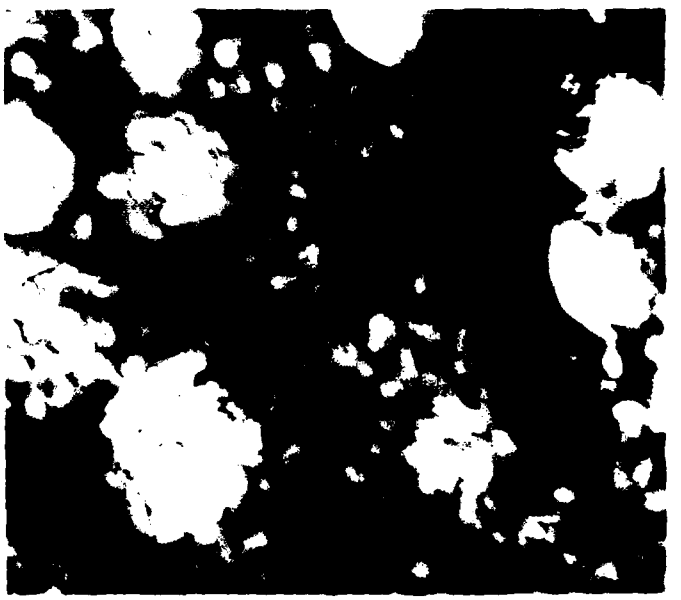

Mag: 70,000X

Figure 8. Thin Foil Transmission Electron Micrographs of Representative Structure from a Waspaloy (PWA 1007) Pancake Forging

TABLE 2
CHEMICAL COMPOSITION AND MECHANICAL PROPERTIES OF GATORIZED® IN100 (PWA 1073)

Chemical Composition (%)	Minimum	Maximum	
Carbon	0.05	0.09	
Manganese	–	0.020	
Sulfur	–	0.010	
Phosphorus	–	0.010	
Silicon	–	0.010	
Chromium	11.90	12.90	
Cobalt	18.00	19.00	
Molybdenum	2.80	3.60	
Titanium	4.15	4.50	
Aluminum	4.80	5.15	
Vanadium	0.58	0.98	
Boron	0.016	0.024	
Zirconium	0.04	0.08	
Tungsten	–	0.05	
Iron	–	0.30	
Copper	–	0.07	
Columbium and Tantalum	–	0.04	
Lead*	–	0.0002	(2 ppm)
Bismuth*	–	0.00005	(0.5 ppm)
Oxygen	–	0.010	(100 ppm)
Nickel	remainder		

*If determined

Mechanical Properties

Tensile

Temperature (°C)	Temperature (°F)	0.2 % Yield Strength (MPa)	0.2 % Yield Strength (ksi)	Ultimate Strength (MPa)	Ultimate Strength (ksi)	Elongation (%)	Reduction in Area (%)
Room	Temp	1166	(169.1)	1631	(236.5)	16.5	29.3
704	(1300)	1113	(161.4)	1241	(180.0)	22.0	27.0

Stress Rupture

Temperature (°C)	Temperature (°F)	Applied Stress (MPa)	Applied Stress (ksi)	Time to Failure (hr)	Time to Elongation (%)	Reduction in Area (%)
732	(1350)	655	(95.0)	22.1	7.5	15.6
732	(1350)	655	(95.0)	29.0	15.0	25.3
732	(1350)	655	(95.0)	27.4	16.7	24.1

Creep

Temperature (°C)	Temperature (°F)	Applied Stress (MPa)	Applied Stress (ksi)	Time to Failure (hr)	Hours to Creep 1%	Hours to Creep 2%
704	(1300)	551.6	(80.0)	161.0	127.1	161.0

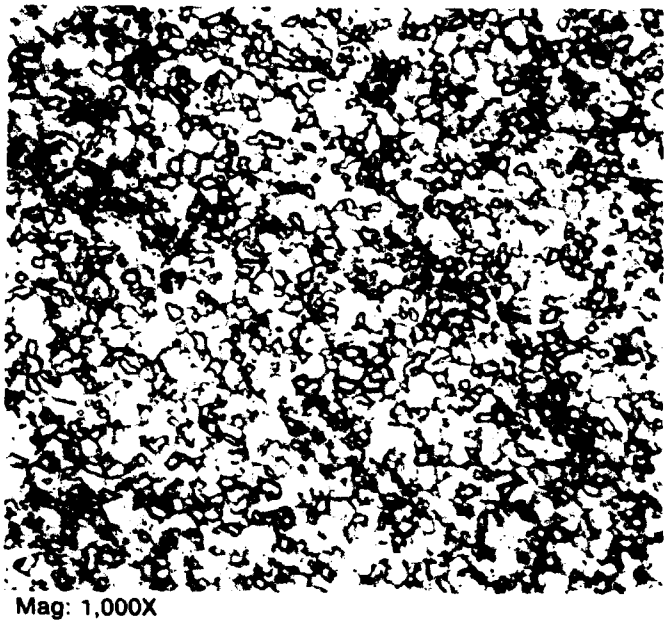

Mag: 1,000X

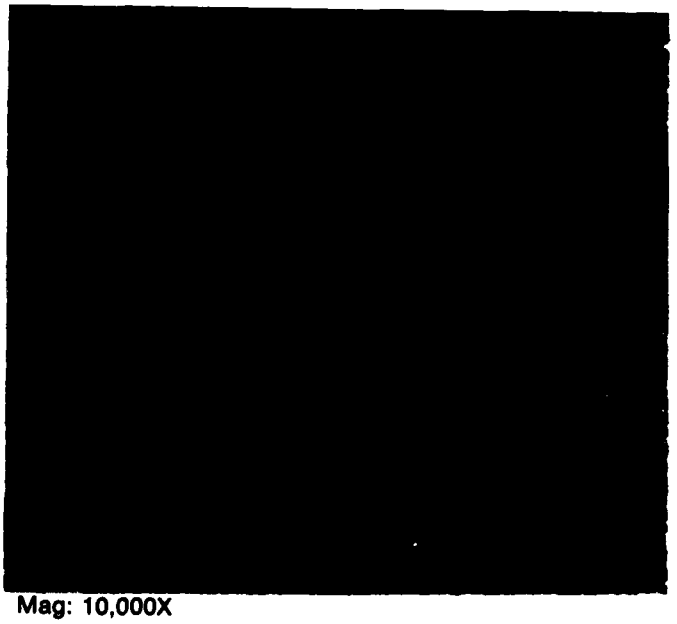

Mag: 10,000X

FD 132721

Figure 9. Typical Microstructure of GATORIZED® IN100 (PWA 1073) (ASTM Grain Size 12 to 14)

Mag: 10,000X

Mag: 70,000X

FD 132322

Figure 10. Thin Foil Transmission Electron Micrographs of Representative Structure from a GATORIZED® IN100 Pancake Forging

While it is known that crack growth rate is related to stress intensity factor for specific conditions, tests are performed to study the generality of the K concept. In one series of tests, crack growth data are obtained in a previously investigated range, but the specimen net section stress is allowed to approach and exceed yield conditions, and deviation from elastic conditions is quantified. Specimen geometry (through-thickness center crack (Figure 11a) and compact specimen (Figure 11b)) and thickness are varied to test the uniqueness of da dN vs ΔK relationship at a given operating condition.

Those geometries and thickness are used where da dN vs ΔK is generally unique for a given operating condition. Well-documented (Reference 5) specimens are used to avoid uncertainties concerning K-calibration. Thicknesses are representative of turbine disks so as to avoid potential mixed-mode crack growth sometimes observed in thin sections.

b. Test Procedure

Test specimens were precracked using procedures outlined in ASTM E-399. Precracking was performed at room temperature at a cyclic frequency of 10 or 20 Hz; anomalous precracking effects were easily recognizable.

Crack propagation testing was conducted on closed-loop servocontrolled equipment operated under load control. Cyclic tests were performed using isosceles triangular load waveforms, and specimen heating was provided by resistance, clamshell furnaces having windows to allow observation of crack growth at the test temperature.

Crack lengths were measured on both surfaces of the propagation specimen using a traveling microscope. This was facilitated by interrupting the cyclic loading and applying the mean test load. This procedure held the specimen rigid while increasing crack tip visibility. A high intensity light was used to provide oblique illumination to the crack and further increase crack visibility. In general, crack length measurements were taken at increments no larger than 0.50 mm (0.020 in.). Crack length measurements are considered to be accurate to within ±0.025 mm (0.001 in.).

c. Test Program

(1) Constant Load Amplitude Cycling

Crack propagation under constant amplitude loading conditions is known to be a function of the applied stress intensity range (within the limits of linear elastic fracture mechanics). This stress intensity range, ΔK, may be viewed as the driving force for crack propagation. Many relationships have been developed to correlate observed crack growth rate and the stress intensity factor. Paris and Erdogan presented the simple relationship:

$$\frac{da}{dN} = C(\Delta K)^n \qquad (1)$$

where C and n are material constants. A major drawback to equations similar to (1) is that they do not account for the effects of load sequence. Additionally, dependencies of crack growth on temperature and loading frequency make the general application of equations such as (1) more difficult.

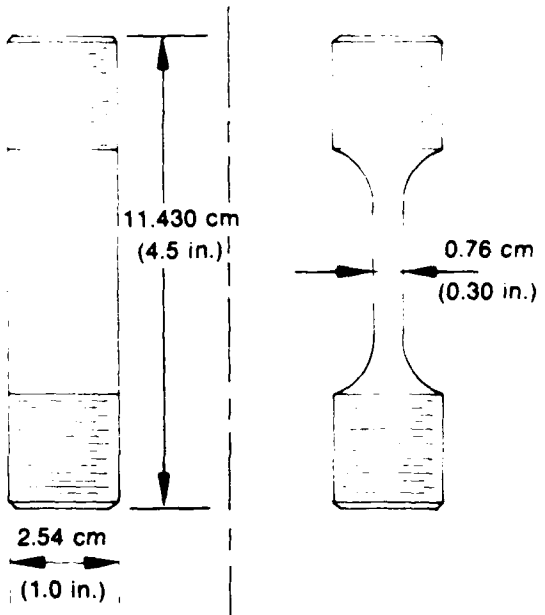

a. Through-Thickness Center Crack Tension Specimen

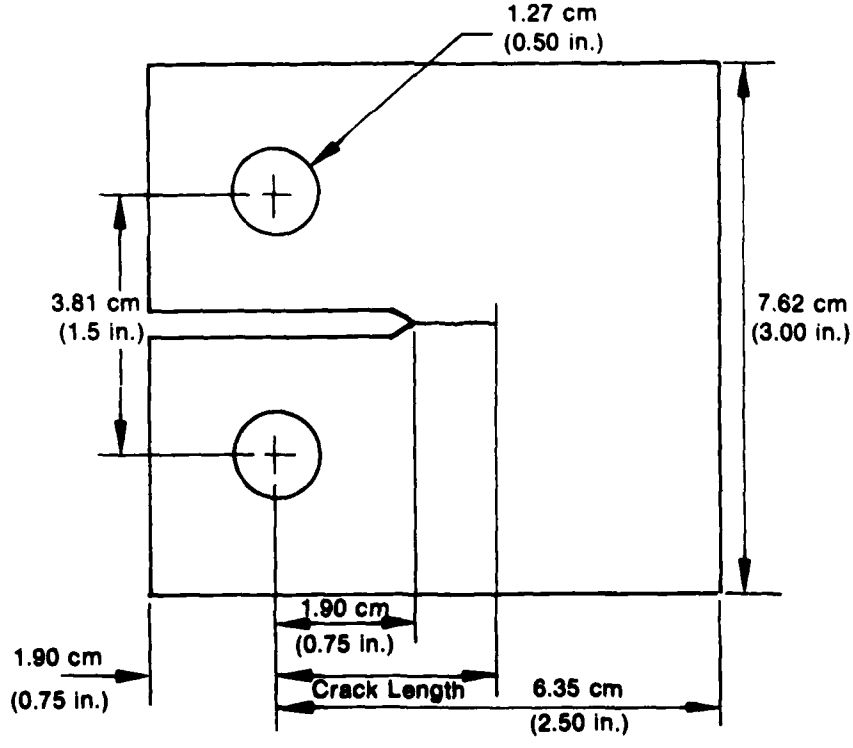

b. Compact Specimen

FD 119166A

Figure 11. Test Specimens Have Documented Fracture Mechanics Analysis

A specific goal of the constant load amplitude testing was to describe the effects of temperature, stress ratio and loading frequency on crack propagation of Waspaloy (PWA 1007) and IN100 (PWA 1073). The fundamental tool used to achieve this objective was developed by P&WA under a separate AFML contract and has been optimized under the current program. The model, which provides an interpolative capability for crack growth rate as a function of several operating parameters (e.g. temperature, stress ratio, frequency), will be presented at length in a later section.

The following tasks were performed in order to provide a basis for an accurate, interpolative model for constant load amplitude FCP; the matrix of these basic propagation tests is given in Table 3. All tests employed saw tooth, constant load amplitude cycling.

(a) Heat-to-Heat Variation

With few exceptions, specimens tested in this program were taken from the same heats of material (Waspaloy and IN100) and were different from those of existing data. The heats of material for this program met P&WA specifications, and tests were performed to ensure compatibility with existing data. In order to determine and quantify any significant variations from heat-to-heat, test conditions were selected to overlap preexisting data.

No significant variations in crack propagation behavior were found among available heats of material. The extremely rigid controls of alloy chemistry imposed on both IN100 and Waspaloy ensure consistent composition. Processing and heat treatment specifications, supported by a quality control inspection of microstructure and mechanical properties, also limit the performance variability of each alloy. As was shown in Figure 9, the characteristic microstructure of GATORIZED® IN100 (PWA 1073) is extremely uniform, having a very small grain size (ASTM 12 to 14). The crack growth behavior of this material is correspondingly well behaved. The microstructure of conventionally forged Waspaloy (PWA 1007), Figure 8, possesses a much larger characteristic grain size (ASTM 3 to 5), and the allowable variability in grain size is generally ASTM 2 to 7. While the heats of WAspaloy evaluated under this contract did not display significant heat-to-heat variability, the potential for limited variation in the elevated temperature cracking behavior of this alloy exists as a result of grain size flexibility.

(b) Effect of Loading Rate (Frequency)

Tests to determine the influence of cyclic frequency on elevated temperature crack propagation in Waspaloy were performed under the current program, and similar data has been generated for IN100 (References 1, 2, and 3). The range of frequencies examined (0.00833 Hz (0.5 cpm) to 20 Hz) was chosen so as to reflect actual loading of a turbine disk as defined in Phase I.

(c) Effect of Stress Ratio

An investigation of the effect of stress ratio ($R = \sigma_{max}/\sigma_{min}$) on crack growth was conducted over the range of $0.1 \leq R \leq 0.8$ for a broad range of temperatures. The influence of negative stress ratios was examined under an auxiliary investigation to be discussed later.

(d) Effect of Temperature

The effect of operating temperature on subcritical crack growth was investigated for Waspaloy under the test program of this contract. The effect of temperature for IN100 had been previously characterized (Reference 2). For both materials, the range of interest was 427 to 732°C (800 to 1350°F), and the environment was laboratory air.

TABLE 3
BASIC PROPAGATION TEST MATRIX

Stress Ratio	*Frequency (Hz)*	*Thickness (mm)*	*(in.)*	*Temperature* ^{o}C *427*	(^{o}F) *(800)*	^{o}C *649*	(^{o}F) *(1200)*	^{o}C *732*	(^{o}F) *(1350)*	*Number of Tests Waspaloy*	*IN100*
0.05	0.167	2.54	(0.1)		X*		X*		X*	3	0
0.05	0.167	7.62	(0.3)		XX†		X†		X†	4	0
0.05	0.167	12.70	(0.5)		X†		X*			2	0
0.10	0.167	7.60	(0.3)				XX‡			1	2
0.10	20 Hz	7.62	(0.3)		X†		XX†			3	0
0.10	120 sec dwell	7.62	(0.3)						X*	1	0
0.10	600 sec dwell	7.62	(0.3)						X	1	0
0.10	0.00833	7.62	(0.3)				X		X†	1	2
0.50	0.167	7.62	(0.3)		X†		X°			2	0
0.80	0.167	7.62	(0.3)		X†		X			2	1
0.80	20	7.62	(0.3)				X†			1	0
Sustained Load (da/dt)		7.62	(0.3)				X*		X*	9/30	0/5

°R = 0.55
‡IN100 only
†Waspaloy only
*Existing data for IN00

(2) Crack Propagation Under Periodic Load Dwell

This task examined the crack propagation of Waspaloy and IN100 under fatigue cycling with a dwell at maximum load, Figure 12. The testing, outlined in Table 3, was conducted to characterize the effect of period of load dwell and operating temperature on subcritical crack growth.

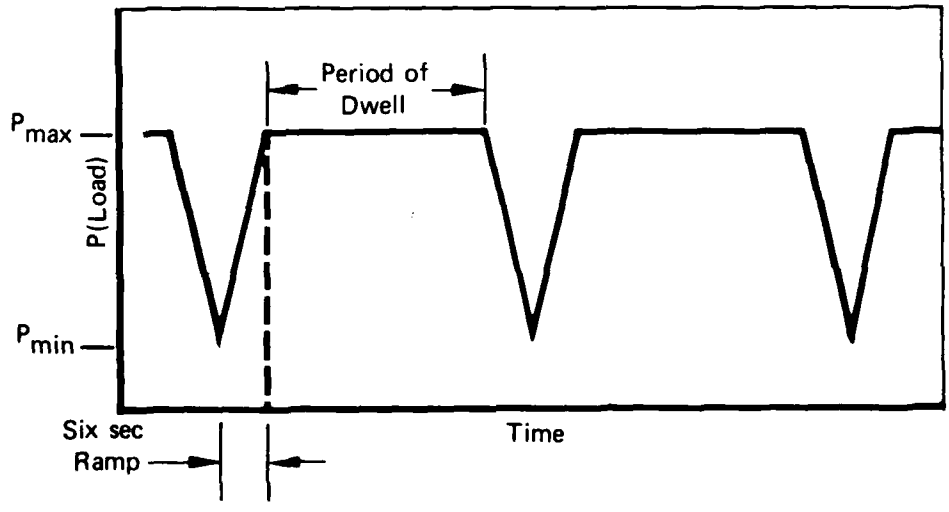

Figure 12. Loading Waveform for Periodic Load Dwell Testing

(3) Sustained Load Crack Growth

The methodology used to determine sustained load crack growth relationship for Waspaloy and IN100 was developed by P&WA under an AFML contract, and is described in Reference 2. The test effort employed compact specimens and examined creep crack growth over the range of 649 to 732°C (1200 to 1350°F). This work, discussed in detail in a later section, resulted in an interpolative model of sustained load crack growth as a function of temperature. The test matrix for this task is included in Table 3.

(4) Synergistic Crack Propagation

The majority of the crack growth studies outlined thus far employ constant load amplitude fatigue cycling. These tests, while necessary, are not completely representative of component operating conditions. As discussed under Phase I, Mission Definition, gas turbine components experience complex load and temperature histories. Crack growth relationships are complicated by load sequence effects, and the influence of elevated temperature operation on load interaction phenomena is unclear.

The objective of the testing in this task was to establish possible synergistic effects among secondary parameters affecting crack propagation. Testing was designed to investigate the effects of low cycle fatigue (LCF) — dwell interactions at constant peak load, interactions of major load excursions (overloads) with less severe cycling with variable stress ratio, and interactions of high amplitude sustained load on LCF.

The generated data provided a basis for development of a mathematical model capable of predicting cumulative crack growth during a complex stress-temperature-time spectrum for typical Waspaloy and IN100 turbine disks.

A typical operating mission consists of a complex thermal-mechanical stress history such as that shown in Figure 4. Our approach is to separate and isolate those stress-time histories most suspected of having synergistic effects on crack growth in Waspaloy and IN100. This approach to model development calls for isothermal testing only, thus minimizing complicated and costly thermal mechanical testing.

For each test performed under the current task, crack propagation data was obtained using procedures described earlier, and crack length (a) vs cumulative cycles (N) data was generated. See Appendix C. The actual test performed, defined in the following tasks, was composed of repetitive segments containing an isolated load sequence (elemental damage event).

(a) Task 1 — LCF-Dwell Interaction at Constant Peak Stress

The purpose of Task 1 was to investigate possible synergistic effects of combined LCF and dwell. All tests were performed with constant peak stress (load), and two temperatures were investigated, 649 and 732°C (1200 and 1350°F). A schematic of the stress-time history is given in Figure 13. The test matrix is presented in Table 4.

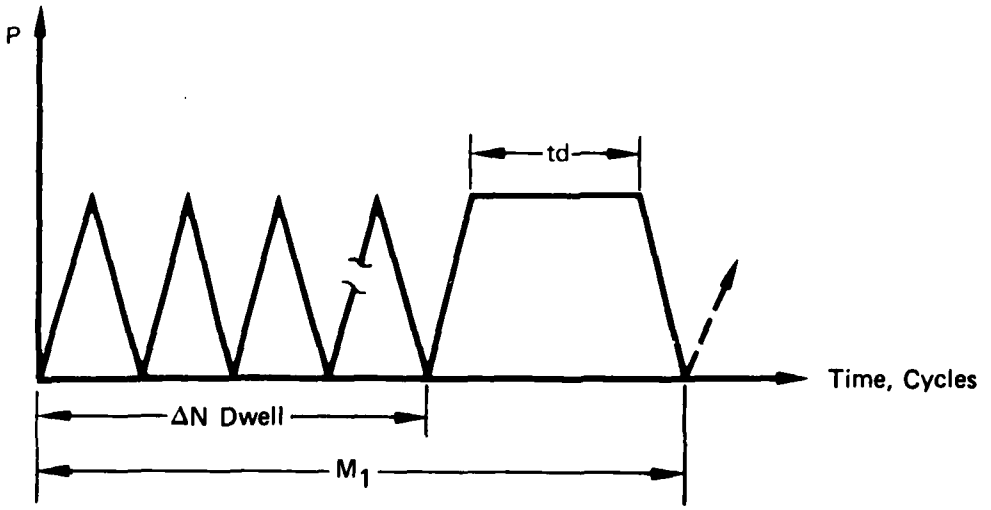

LCF Frequency = 0.167 Hz (10 cpm)

ΔN_{Dwell} = Number of LCF Cycles
td = Dwell Time, Minutes
R = P_{min}/P_{max}

td = 2 min
N_1 = 10 = 1 min
N_1 = 20 = 2 min
N_1 = 40 = 4 min
R = 0.1

FD 132142

Figure 13. Low Cycle Fatigue-Dwell Interaction at Constant Peak Stress

TABLE 4
SYNERGISTIC FCP TEST MATRIX

Test Description	Dwell Time (min)	Cycles Between Overloads	Overload Ratio	Temperature = 649°C (1200°F) Stress Ratio 0.1	Temperature = 649°C (1200°F) Stress Ratio 0.5	Temperature = 732°C (1350°F) Stress Ratio 0.1	Temperature = 732°C (1350°F) Stress Ratio 0.5	Number of Tests Required Waspaloy	Number of Tests Required IN100
LCF-Overload	0	40	1.5		X*			1	0
		20		X*	XX*	X	X*	6	1
		5			X*			1	0
		40	1.25		X*			1	0
		20		X*	X*	X	X*	4	1
		5			X*			1	0
LCF-dwell	2	40	1.0	X*		X*		2	0
		20		X*	X*	X*	X*	4	0
		10		X*		X*		2	0
				Total				24	2

Specimen Thickness = 7.62 mm (0.3 in.)
*Existing data for IN100

A Task 1 mission, M_1 was defined as ΔN_{Dwell} LCF cycles plus a 2-min dwell. As the test matrix defines, ΔN_{Dwell} varied so that the total time for LCF cyclic crack growth was less than, equal to, and greater than the dwell period. The tests investigated the interaction as a function of the ratio of LCF to sustained load crack growth within a single mission.

Crack growth relations, da/dN vs ΔK, were obtained for each of the test conditions using procedures described later. The relations defining crack growth will also be discussed in a later section.

(b) Task 2 — Variable Stress Ratio Interaction with Major Load (LCF — Overload)

The purpose of Task 2 was to investigate possible synergistic effects of major load excursions on LCF crack growth in Waspaloy and IN100. The test temperatures were 649 and 732°C (1200 and 1350°F). A schematic of the stress-time history is given in Figure 14 and the test matrix for Task 2 is presented in Table 4.

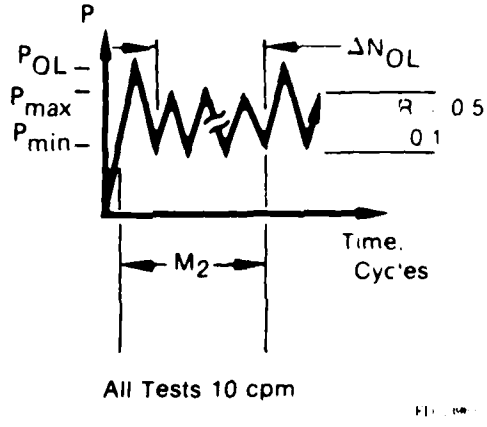

Figure 14. Variable Stress Ratio With Major Load Excursions

(c) Task 3 — Interaction of High Amplitude Sustained Load with LCF

The purpose of Task 3 was to investigate the possible synergistic effects of high amplitude sustained loads on LCF of Waspaloy and IN100. However, initial construction of the test matrix was accomplished without complete knowledge of the form of typical mission profiles giving stress and temperature as a function of time. The missions (Figures 2 thorugh 6), defined under Phase 1 of this contract, represent the results of the most current engine usage and analyses conducted and describe conditions encountered by a disk operated in a military gas turbine engine. A review of these profiles shed question on the ultimate value the overload dwell-LCF tests proposed under this task. The form of these tests is illustrated in Figure 15.

The testing was designed to measure the effect of a dwell at overload upon subsequent FCP; however, no such overload dwells were observed in the mission profiles. Since all other load sequences were addressed in testing and modeling, the tests of this task were replaced with other, more pertinent, tests. These include the auxiliary negative stress ratio tests as well as selected tests designed to complement and extend the original matrix.

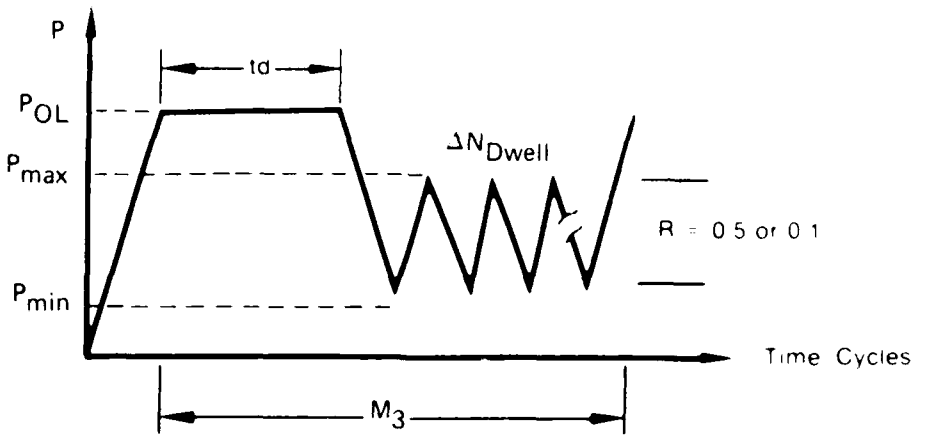

td = Dwell Time, min
N = Number of Cycles

Figure 15. Interaction of Sustained High Load With LCF

(5) Auxiliary Investigations

The testing described in the following sections was conducted to supplement the data generated for use in model development. The results of these investigations provide insight into the nature of crack propagation under a variety of test conditions which are beyond the scope of the model development for this program. While not actually used in crack propagation modeling, the auxiliary data provide a means to assess the limits of applicability of the model.

(a) Effect of Negative Stress Ratio

Fatigue cycling which is characterized by tension-compression loading ($R < 0$) may occur in turbine disks under some circumstances. For example, thermally and mechanically induced strain gradients may produce local compressive stresses in a disk under mission operation, Figure 4. The negative R tests of Table 5 were conducted in order to evaluate this effect on crack propagation in Waspaloy and IN100.

(b) Effect of Net Section Stress

The through-thickness center flaw crack propagation specimen (shown in Figure 11a) was used to determine the effect of stress levels greater than 0.8 times the yield strength of Waspaloy. Similar tests were performed on IN100 previously. This specimen was selected due to the small initial crack size (approximately 0.762 mm (0.030 in.)) obtainable. The small crack provides the capability to obtain the necessary high net section stress with corresponding stress intensities (ΔK approximately 55 MPa $\sqrt{m}$ (50 ksi $\sqrt{in.}$)) that are comparable to existing linear elastic crack propagation curves.

TABLE 5
AUXILIARY INVESTIGATIONS

	Test Description	Stress Ratio	Frequency (Hz)	Thickness (mm)	Thickness (in.)	Temperature °C 427	Temperature (°F) (800)	Temperature °C 649	Temperature (°F) (1200)	Number of Tests Waspaloy	Number of Tests IN100
1	$\sigma_{op} > 0.8\ \sigma_y$	0.1	0.167	7.62	(0.3)				X*	2	0
2	Prior Plastic Deformation	0.1	0.167	7.62	(0.3)		X		X	2	1
3	Negative Stress Ratio	-0.5	0.167	7.62	(0.3)		X		X	2	2
		-1.0	0.167	7.62	(0.3)		X		X	2	2
4	Thermal Mechanical Fatigue	0.05	0.0167	7.62	(0.3)		800 1300F			1	0
5	Overload-Underload-LCF	0.5	0.167	7.62	(0.3)				X+	1	0
				Total						10	5

*Existing data for IN100
+Waspaloy only.

(c) Effect of Prior Plastic Deformation

The purpose of this task was to investigate the influence of prior plastic cycling on subsequent crack propagation. Crack growth in material which has previously been yielded is representative of the initial stages of propagation of a flaw which initiated in the region of a stress concentrator. These tests are outlined in Table 5.

(d) Effect of Overload-Underload-LCF Sequencing

The crack propagation testing upon which the cumulative damage modeling was based is isothermal in nature. It was assumed that a nonisothermal mission may be suitably represented by a series of isothermal segments. The purpose of this investigation was a brief examination of crack propagation of Waspaloy (PWA 1007) subject to thermal-mechanical fatigue (Table 5).

(e) Thermal-Mechanical Fatigue

The crack propagation testing upon which the cumulative damage modeling was based is isothermal in nature. It was assumed that a nonisothermal mission may be suitably represented by a series of isothermal segments. The purpose of this investigation was a brief examination of crack propagation of Waspaloy (PWA 1007) subject to thermal-mechanical fatigue (Table 5).

(f) Effect of Thickness

The goal of this task was to investigate the effect of specimen thickness on crack propagation in Waspaloy (PWA 1007). Of specific concern was the qualification of crack propagation data as thickness independent (i.e., representative of the most severe geometric constraint).

C. PHASE III — MATHEMATICAL MODEL DEVELOPMENT

1. Model Description

To analyze a complex mission spectrum in terms of consistently accurate cumulative damage accounting requires two basic tools: (1) a mathematical model describing crack propagation at frequencies , temperatures, and stress ratios representative of turbine disk operation, and (2) a model which describes cumulative damage synergistic effects such as:

- Overloads of varying degree and occurrence frequency
- Dwells of varying duration
- Combinations of these with simple cyclic crack growth behavior.

The requisite tool is the Interpolative Synergistic Hyperbolic Sine Model, SINH.

a. *Mathematical Formulation*

The model is based on the hyperbolic sine equation,

$$\log (da\ dN) = C_1 \sinh (C_2 (\log (\Delta K) + C_3)) + C_4 \quad (2)$$

where the coefficients have been shown (References 1, 2, and 3) to be functions of test frequency, stress ratio, and temperature:

C_1 = material constant
$C_2 = f_2 (\upsilon, R, T)$
$C_3 = f_3 (\upsilon, R, T)$
$C_4 = f_4 (\upsilon, R, T)$

Additionally, Equation 2 may also be used to describe crack propagation data as a function of load sequence parameters.

Descriptions of the mathematical model (SINH) and the hyperbolic sine function (sinh) on which it is based are provided in the following paragraphs.

b. *Characteristics of the sinh*

The hyperbolic sine is defined as

$$y = \sinh x = \frac{e^x - e^{-x}}{2} \quad (3)$$

and when presented on Cartesian coordinates it appears as shown in Figure 16. The function is zero at $x = 0$ and has its inflection there.

The introduction of the four regression coefficients, C_1 through C_4, permits relocation of the point of inflection and scaling of both axes. In the equation

$$(y - C_4) = \sinh (x + C_3), \quad (4)$$

C_3 establishes the horizontal location of the hyperbolic sine point of inflection and C_4 locates its vertical position.

To scale the axes, C_1 and C_2 are introduced

$$\frac{(y - C_4)}{C_2} = \sinh (C_2(x + C_3)) \quad (5)$$

which can be rewritten as

$$y = C_1 \sinh (C_2 (x + C_3)) + C_4 \quad (6)$$

of which Equation 2 is a special case where $y = \log (da/dN)$ and $x = \log (\Delta K)$. Note that C_3 has units of $\log (\Delta K)$ and C_4 has units of $\log (da/dN)$; C_1 and C_2 are dimensionless and can be conceptualized as stretching the curve vertically and horizontally, respectively. Experience indicates that, for a given material, C_1 can be fixed without adversely affecting model flexibility.

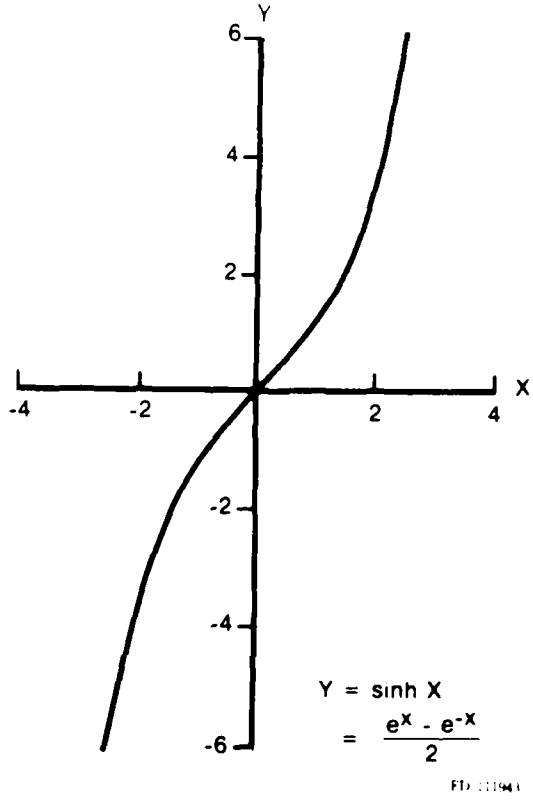

Figure 16. Hyperbolic Sine on Cartesian Coordinates

Experience has also shown that the materials considered here (Waspaloy and IN100) exhibit symmetrical da/dN vs ΔK relationships for simple cycling. For materials which do not display this symmetry, an asymmetric variation of the model is available. Here, the shape coefficient, C_2, is separated into similar coefficients C_2 and C'_2. The first of these coefficients determines model curvature above the point of inflection, while C'_2 controls curvature below inflection. The model remains a continuous function, and when the data is symmetric $C_2 = C'_2$, and the model reverts to its original form.

The hyperbolic sine equation was selected as the model for the following reasons:

- It exhibits the overall shape of typical da dN vs ΔK plots, obtained over several decates of crack growth rates.

- All or part of the equation may be used to fit data, since the sinh has both a concave and a convex half and a nearly linear portion near inflection. Also, the slope at inflection can vary with the fitting constants. (By comparison, the slope of an x^3 model is always zero at inflection.)

- The sinh is not periodic (e.g., trigonometric tangent) nor asymptotic (e.g., tangent, or inverse hyperbolic tangent); therefore, when extrapolation becomes necessary, the sinh behaves well at distances removed from the data, quite unlike most polynomial, periodic, or asymptotic functions.

- This model requires no information other than (a vs N) data. By comparison, some other models in current use require both K_{th} and K_{Ic}, in addition to (a vs N) data, to model crack growth behavior. Both K_{th} and K_{Ic} are difficult to obtain experimentally, K_{th} because of the extremely small crack growth measurements necessary and K_{Ic} because of gross plasticity at the crack tip encountered in fracture-toughness testing at elevated temperatures.

c. *SINH Descriptions of Basic Propagation*

The hyperbolic sine model is easily adapted to describe fundamental parametric effects of operating conditions such as stress ratio, frequency, and temperature on crack growth rate.

Figure 17 schematically depicts the qualitative effects on crack propagation rate of frequency (Figure 17a), stress ratio (Figure 17b), and temperature (Figure 17c).

Because of the simple relationships observed between the coefficients of the SINH model and the fundamental propagation-controlling parameters, interpolations are straightforward. It is here that the model demonstrates its great usefulness: *the hyperbolic sine model provides descriptions of crack propagation characteristics where data are unavailable.* The interpolation algorithm is described under Algorithm Definition and Development.

2. Advanced Regression Considerations

Interpolative modeling of crack propagation as a function of operating parameters such as frequency, stress ratio, and temperature (Figure 17) requires a multiple regression capability which allows simultaneous consideration of several different collections of data, each differing from the others by only one FCP — controlling parameter. Separate regression of the individual data sets contributing to an interpolative model does not allow data at one condition to influence the model at another condition. However, the final model was to have broad interpolative capability with behavior at one condition used to describe FCP at another condition. Therefore, it is desirable to permit the data to exhibit their mutual influence during the modeling process.

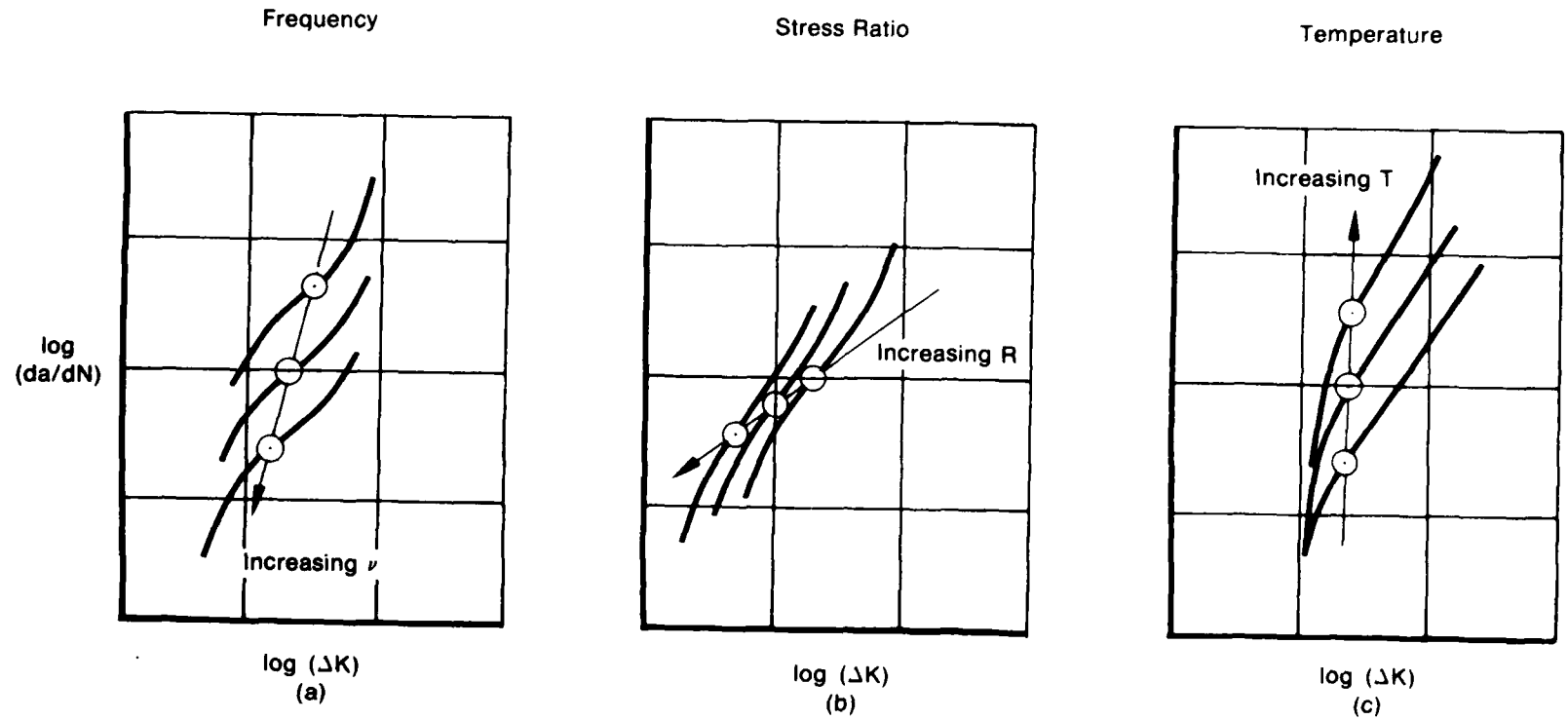

Figure 17. Crack Propagation as Influenced by (a) Frequency, (b) Stress Ratio, and (c) Temperature

Pratt & Whitney Aircraft has developed a mathematical technique to accomplish this. Individual sets of data are treated independently relative to some of the SINH coefficients, while the entire collection is treated as an entity with respect to the interpolative coefficients (functions of ν, R, T, etc.). This improved method was used to develop the propagation models presented in this report. The actual computational procedure employed in the modeling, referred to as the Method of Least Squares, is described in the following paragraphs.

The goal of this procedure is to determine model coefficients for which the resulting curve through the data will have the least (minimum) summed squared error between calculated and observed values for the dependent variable (see Figure 18). In this instance, the independent and dependent variables, x and y, are log (ΔK) and log (da/dN), respectively.

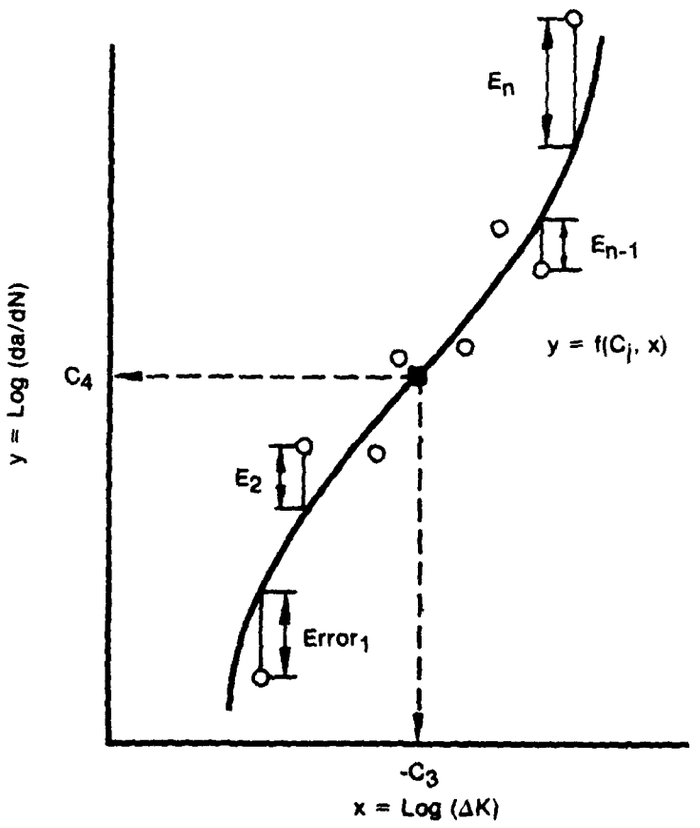

Figure 18. Method of Least Squares

Define the sum of the squared errors as

$$E^2 = \sum_{i=1}^{n} E_i^2 = \sum (y_{cal_i} - y_i)^2 \tag{7}$$

Since $y_{cal_i} = f(C_2, C_3, C_4, x_i)$, E is also a function of C_2, C_3, C_4.

Now, E^2 will be a minimum when each of its partial derivatives is zero simultaneously. That is

$$\frac{\partial E^2}{\partial C_2} = \frac{2E\partial E}{\partial C_2} = 0 \tag{8}$$

$$\frac{\partial E^2}{\partial C_3} = \frac{2E\partial E}{\partial C_3} = 0 \tag{9}$$

$$\frac{\partial E^2}{\partial C_4} = \frac{2E\partial E}{\partial C_4} = 0 \tag{10}$$

when f is the SINH model,

$$E_i = C_1 \text{ SINH } (C_2(x_i + C_3)) + C_4 - y_i \tag{11}$$

and

$$\frac{\partial E}{\partial C_2} = C_1 \cosh (C_2(x_i + C_3))(x_i + C_3) \tag{12}$$

$$\frac{\partial E}{\partial C_3} = C_1 \cosh (C_2(x_i + C_3))(C_2) \tag{13}$$

$$\frac{\partial E}{\partial C_4} = 1 \tag{14}$$

Now, substituting Equations 11, 12, 13, and 14 into Equations 8, 9, and 10, and solving* the resulting three simultaneous equations provides the values for C_2, C_3, and C_4 for which Equation 7 will be a minimum.

The foregoing discussion explains the procedure for determining the coefficients for SINH curve. Suppose further that each SINH representation of FCP is related to the others, the relationship depending on differences in frequency, stress ratio, temperature, etc. Consider frequency as an example, and assume that the points of inflection are linearly related, viz:

$$C_{3,j} = C_{33} + C_{34}(C_4,j) \tag{15}$$

for j different SINH curves.

---

*In this instance, the resulting simultaneous equations are nonlinear in C_2, C_3, and C_4. The solution therefore requires some iterati e procedure such as an N-dimensional Newton-Raphson method.

Assume also that C_2 and C_4 are related to test frequency by Equations 16 and 17:

$$C_4, j = C_{35} + C_{36} (\log (\upsilon)) \tag{16}$$

$$C_2, j = C_{37} + C_{38} (\log (\upsilon)) \tag{17}$$

Coefficients C_{33} through C_{38} can be then determined by substituting Equations 15, 16, and 17 into Equation 11 and differentiating with respect to C_{33} through C_{38} in a manner analogous to that used in determining C_2, C_3, C_4 in the foregoing discussion.

3. Algorithm Definition and Development

The computer code developed under Phase III has as its mathematical formulation three algorithms: the segregation, interpolation, and computation algorithms.

a. The Segregation Algorithm

The set of rules by which a mission profile is separated (segregated) into its elemental cumulative damage events constitutes the segregation algorithm. As formulated, the segregation algorithm translates an input isothermal stress-time profile, such as illustrated in Figure 5, into a parametric, cycle-by-cycle description of the loading sequence. This segregated mission definition, given in terms of the elemental mission segments addressed in the test program, provides input compatible with the interpolation algorithm.

Development of the segregation algorithm was based on the mission definition described under Phase I, Figures 2 through 6. A characteristic of these representative operational profiles is a high occurrence frequency for major load excursions (overloads). As discussed in Appendix A (Reference 6), the implication of this observation is to diminish the importance of long term overload effects and to place increased significance on the synergistic interaction which occurs immediately following the overload. As a result, a primary investigation conducted under the test program was to characterize the short term effects of overloading. Similarly, the interpolation algorithm, developed to address mission profiles representative of turbine disk operation, is not routinely applicable to missions which may contain infrequent overloads (e.g. airframe loading spectra).

The general procedure employed in the segregation algorithm is outlined as follows:

1. Define isothermal operating temperature
2. Locate load dwells
3. Locate major load excursions (overloads)
4. Calculate the number of cycles between successive overloads
5. Calculate overload ratio for each less severe cycle following an overload
6. Determine stress ratio and frequency of all fatigue cycles.

Upon completion of mission segregation, the data is passed to the interpolation algorithm, and the appropriate crack growth rate curves are obtained.

b. The Interpolation Algorithm

The fundamental strength of the hyperbolic sine model is its interpolative capacity. The procedure known as the interpolation algorithm for calculating the SINH coefficients, describing FCP under the influence of a segregated elemental event, is illustrated in the following paragraphs. For simplicity, the example considers only simple cycling with varying frequency, stress ratio, and temperature (υ, R, T). The actual computer software includes other life-controlling parameters: period of load dwell, overload ratio, and cycles between overloads.

The coefficient (e.g., C_2, C_3, and C_4) at any intermediate value of an element life-controlling parameter, can be determined from Equation 18.

$$C_j = C_{jbase} + \Delta C_j; \qquad j = 2,3,4 \tag{18}$$

where:

$$C_j = \begin{bmatrix} C_2 \\ C_3 \\ C_4 \end{bmatrix} = \text{interpolated values of coefficients}$$

and:

$$\Delta C_j = \begin{bmatrix} \Delta C_2 \\ \Delta C_3 \\ \Delta C_4 \end{bmatrix} = \text{differences from baseline values.}$$

Since the SINH coefficients are linear functions of the controlling parameters,* it is evident that:

$$\underset{N\,X\,1}{\begin{bmatrix} \Delta C_2 \\ \Delta C_3 \\ \Delta C_4 \end{bmatrix}} = \underset{N\,X\,N}{\begin{bmatrix} \partial C_2/\partial v, \partial C_2/\partial R, \partial C_2/\partial T \\ \partial C_3/\partial v, \partial C_3/\partial R, \partial C_3/\partial T \\ \partial C_4/\partial v, \partial C_4/\partial R, \partial C_4/\partial T \end{bmatrix}} X \underset{N\,X\,1}{\begin{bmatrix} \Delta v \\ \Delta R \\ \Delta T \end{bmatrix}}$$

where:

$$\begin{bmatrix} \Delta v \\ \Delta R \\ \Delta T \end{bmatrix} = \text{differences from baseline values}$$

and the N X N partial derivative matrix is easily determined from the slopes of the lines relating each coefficient with each rate controlling parameter. The computation of the intermediate coefficients, using Equation 18, is then straightforward.

c. *The Computational Algorithm*

The product of the interpolation algorithm is a collection of SINH descriptions of crack propagation corresponding to the segregated mission cycles. The interpolated crack growth curves are representative of the cycle-by-cycle crack growth under the individual loading conditions, and the effects of load sequence synergism are implicit. The method of computation of crack growth under the complex mission.

A simple cycle-by-cycle integration is used to sum the incremental crack advances, Δa_i, which comprise the incremental cyclic life, ΔN_i, (or event life, ΔE_i)

$$da/dN = f(a, \Delta K. . .) \tag{20}$$

$$\Delta a_i = f(a, \Delta K . . .)\, \Delta N_i \tag{21}$$

*Strictly speaking, the coefficients are nonlinear functions of v, R, and T; however, they are linear functions of other functions. This simplification was used here for presentation clarity.

The sum of all these incremental crack advances results in the crack propagation during one mission, $\Delta a_{mission}$

$$\Delta a_{mission} = \sum_{i=1}^{n} \Delta a_i$$

where n is the number of elemental events comprising the mission profile.

The total mission lifetime, $N_{missions}$, is similarly calculated as the number of mission crack advances, $\Delta a_{mission}$, required to reach critical cracklength.

$$a_{critical} = a_o + \sum_{i=1}^{N_{missions}} \Delta a_{mission}$$

This summed numerical integration procedure is referred to as the computational algorithm.

4. SINH Descriptions of Crack Propagation

Interpolative crack propagation models developed from the data generated under the test programs outlined in Tables 3 and 4 are presented in the following pages. Each of the individual models describes the influence of a single test variable (e.g., temperature, frequency, stress ratio) upon crack propagation. The combination of these models forms a unified description of the crack growth behavior over the range of operating conditions addressed in the test matrices. This unified description is formalized in the interpolation algorithm.

a. Waspaloy (PWA 1007) Crack Propagation

The majority of the Waspaloy data presented in this report were generated under the current contract and represent crack propagation in a single heat of material. A limited amount of additional data (Reference 7), generated from a second heat of this same alloy, was also used. The inclusion of additional data aided in model refinement and extension.

Regression of the crack length vs cycle (a, N) data to produce crack growth rate vs applied stress intensity range (da/dN, ΔK) data, in general, was accomplished with the seven-point incremental polynomial technique (Reference 8). This reduction technique was found desirable for Waspaloy data but less beneficial when reducing IN100 data, since typical scatter in (da/dN, ΔK) data in Waspaloy is considerably more severe than in IN100.

The severity of data scatter in these two alloys is closely linked to grain size. Elevated temperature fatigue of Waspaloy and IN100 results in discontinuous advances of the observed surface crack, and the increments of discontinuous advance are on the order of the material grain size. As the magnitude of the discontinuous crack advance (Δa_{disc}) increases, the variability of the increment in crack growth (Δa) increases by a value within the range ± 2 (Δa_{disc}), and the associated scatter in da/dN increases. The large grain size of Waspaloy (ASTM 2-7) makes this a significant effect, while the fine crystalline structure of IN100 (ASTM 12-14) results in much less inherent scatter in crack growth rate.

The mathematical procedure employed in the seven-point incremental polynomial technique for data reduction produces five fewer (da/dN, ΔK) data points than does the direct secant method. Generally, this presents no significant problem; however, (a, N) data sets containing a small number of points may be severely diminished during data reduction. Therefore, small data sets were reduced by the direct secant method and their specimen numbers bear the prefix "100." Data reduced with the seven-point incremental polynomial method have identification numbers beginning with "7AN" (See Appendix C).

(1) Basic Propagation, Constant Load Amplitude Cycling

(a) Effect of Loading Rate (Frequency)

Experience with turbine disk alloys indicates that changing test frequency, while holding stress ratio and temperature constant, produces crack growth curves similar in shape but shifted along a nearly vertical line passing through the points of inflection. The location of these inflection points is related to test frequency; reduced frequency (increased cycle duration) is observed to accelerate crack growth rate.

Figures 19 and 20 illustrate the effects of cyclic frequency on FCP in Waspaloy, at 649°C (1200 °F), R = 0.1. The four curves represent crack growth under frequencies of 0.00833, 0.167, 0.333, and 20 Hz (0.5 cpm, 10 cpm, 20 cpm, 20 Hz). Note that points of inflection describe a straight line, i.e.: $C_3 = C_{33} + C_{34} \times C_4$. Figure 21 demonstrates the interrelationships of the other SINH coefficients and test frequency. Note that the coefficients *exactly* describe a straight line, so that any aberrations in the model appear when the SINH curve is plotted with the data it represents. This model completely describes the effect of frequency on FCP in Waspaloy at this temperature by interpolation of the equations given in Figure 21.

(b) Effect of Stress Ratio, 0.167 Hz (10 cpm)

The influence of stress ratio (R) on crack propagation in Waspaloy (PWA 1007) fatigued at 0.167 Hz (10 cpm) 649°C (1200°F) is illustrated in Figures 22 through 24. Data from tests at four difference stress ratios were used to develop a model (Figures 22 and 23) of this effect for $0.05 \leq R \leq 0.80$. A plot of the correlative parameters and the defining equations is given in Figure 24. Each of the SINH coefficients is defined as a linear function of log (1 - R) for the range of positive stress ratios.

This relationship should not be extrapolated into the range of negative stress ratios (i.e., tension-compression fatigue). Data gathered from tests at R = -0.5 and R = -1.0 demonstrate the invalid nature of this extrapolation. Crack propagation under negative stress ratio fatigue is discussed under "Auxiliary Investigations" later in this report.

(c) Effect of Stress Ratio, 20 Hz

The effect of stress ratio on fatigue crack propagation of Waspaloy is a function of the associated cyclic frequency of the loading. In order to address this functional dependence, testing was conducted at a frequency of 20 Hz and $0.05 \leq R \leq 0.80$. The resulting model is illustrated in Figures 25 and 26. A plot of the correlative parameters is shown in Figure 27. The combination of the 20 Hz stress ratio model and the similar 0.167 Hz model provides full interpolative capability for crack growth rate as a function of stress ratio and frequency simultaneously.

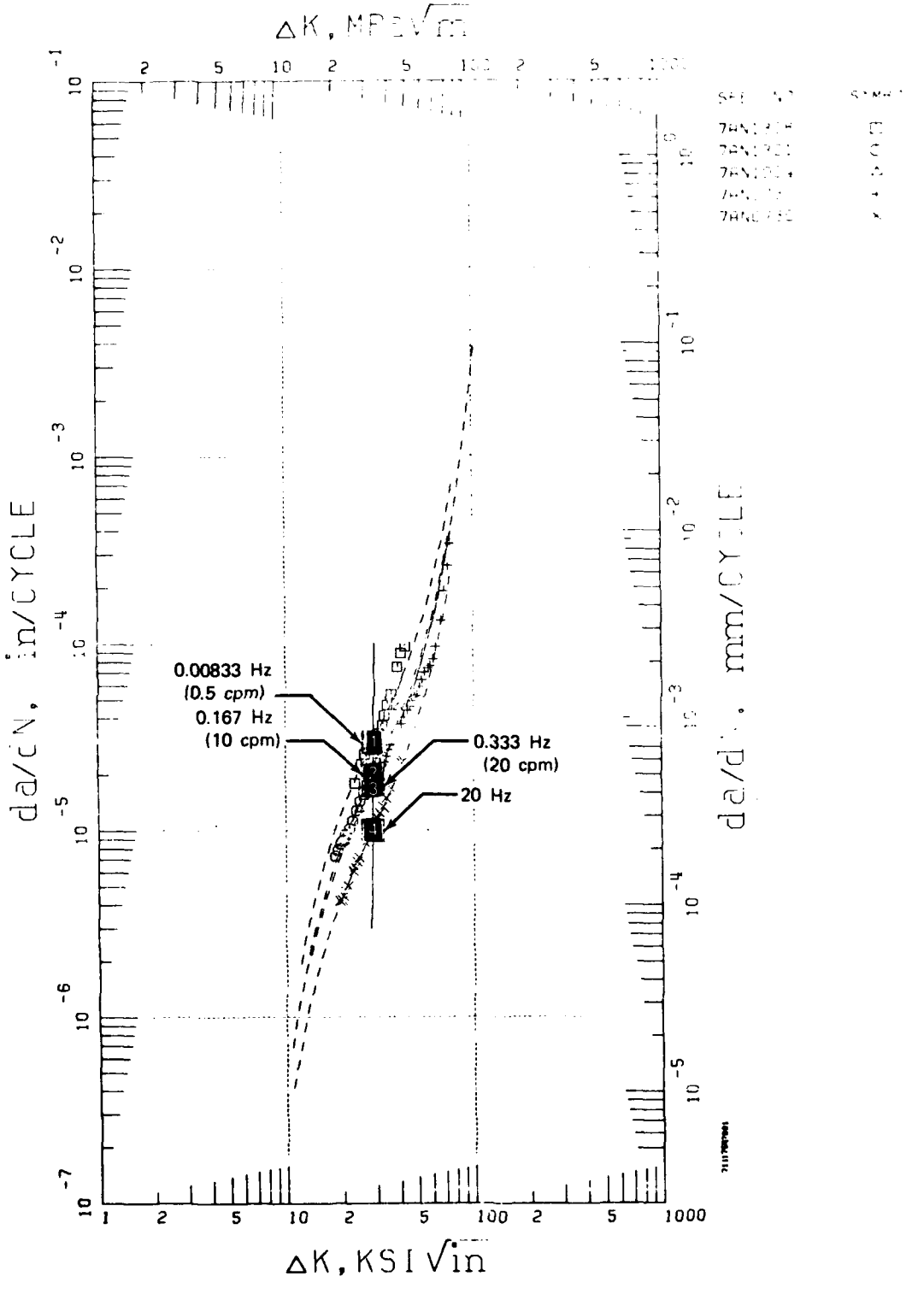

Figure 19. Waspaloy (PWA 1007) Crack Propagation, Frequency Model, 649°C (1200°F)

PAGE 71117547901

R=0.1 T=1200F FREQ=0.5 CPM — 3 34 36 38 — GROUP NO. 1

SPEC NO	MATERIAL	TEMP	ATM	FREQ	R	TYPE	THIK	REMARKS
7AN1328	PWA 1007	1200F	AIR	.5 CPM	R=.1	RB	CN	.299

□ RSQRD 0.9759 SEE 0.0709

-0.26 0. Y=0.5000 SINH(4.102 (X -1.468)) -4.527

NAFT 2 (METRIC) Y=0.5000 SINH(4.102 (X -1.509)) -3.122

*** IMPORTANT *** THIS EQUATION IS VALID BETWEEN X= 23.31 , AND X= 43.79 ONLY. DO NOT EXTRAPOLATE.

R=.05 T=1200F FREQ=10CPM — 34 36 38 — GROUP NO. 2

SPEC NO	MATERIAL	TEMP	ATM	FREQ	R	TYPE	THIK	REMARKS
7AN1301	PWA 1007	1200F	AIR	10 CPM	R=.05	RB	MCT	.501
7AN1004	PWA 1007	1200F	AIR	10 CPM	R=.05		CN	.301

○
△ RSQRD 0.9802 SEE 0.0313

-0.26 0. Y=0.5000 SINH(4.102 (X -1.465)) -4.709

NAFT 2 (METRIC) Y=0.5000 SINH(4.102 (X -1.506)) -3.304

*** IMPORTANT *** THIS EQUATION IS VALID BETWEEN X= 18.31 , AND X= 39.98 ONLY. DO NOT EXTRAPOLATE.

R=.05 T=1200F FREQ=20CPM — 34 36 38 — GROUP NO. 3

SPEC NO	MATERIAL	TEMP	ATM	FREQ	R	TYPE	THIK	REMARKS
7AN0730	PWA 1007	1200F	AIR	20 CPM	R=.05	RB	MCT	.447

+ RSQRD 0.9915 SEE 0.0378

-0.26 0. Y=0.5000 SINH(4.102 (X -1.464)) -4.751

NAFT 2 (METRIC) Y=0.5000 SINH(4.102 (X -1.505)) -3.346

*** IMPORTANT *** THIS EQUATION IS VALID BETWEEN X= 30.31 , AND X= 75.74 ONLY. DO NOT EXTRAPOLATE.

R=.05 T=1200F FREQ=20HZ — 34 36 38 — GROUP NO. 4

SPEC NO	MATERIAL	TEMP	ATM	FREQ	R	TYPE	THIK	REMARKS
7AN0736	PWA 1007	1200F	AIR	20 HZ	R=.05	RB	MCT	.432 WG

× RSQRD 0.9971 SEE 0.0145

-0.26 0. Y=0.5000 SINH(4.102 (X -1.461)) -5.000

NAFT 2 (METRIC) Y=0.5000 SINH(4.102 (X -1.502)) -3.595

*** IMPORTANT *** THIS EQUATION IS VALID BETWEEN X= 19.27 , AND X= 42.41 ONLY. DO NOT EXTRAPOLATE.

OVERALL STATISTICS FOR THIS COLLECTION OF GROUPS. TOTAL RSQRD = 0.9820, AND STD.ERROR.EST. = 0.0624

FO 168088

Figure 20. Statistics for Waspaloy (PWA 1007) Crack Propagation, Frequency Model, 649°C (1200°F)

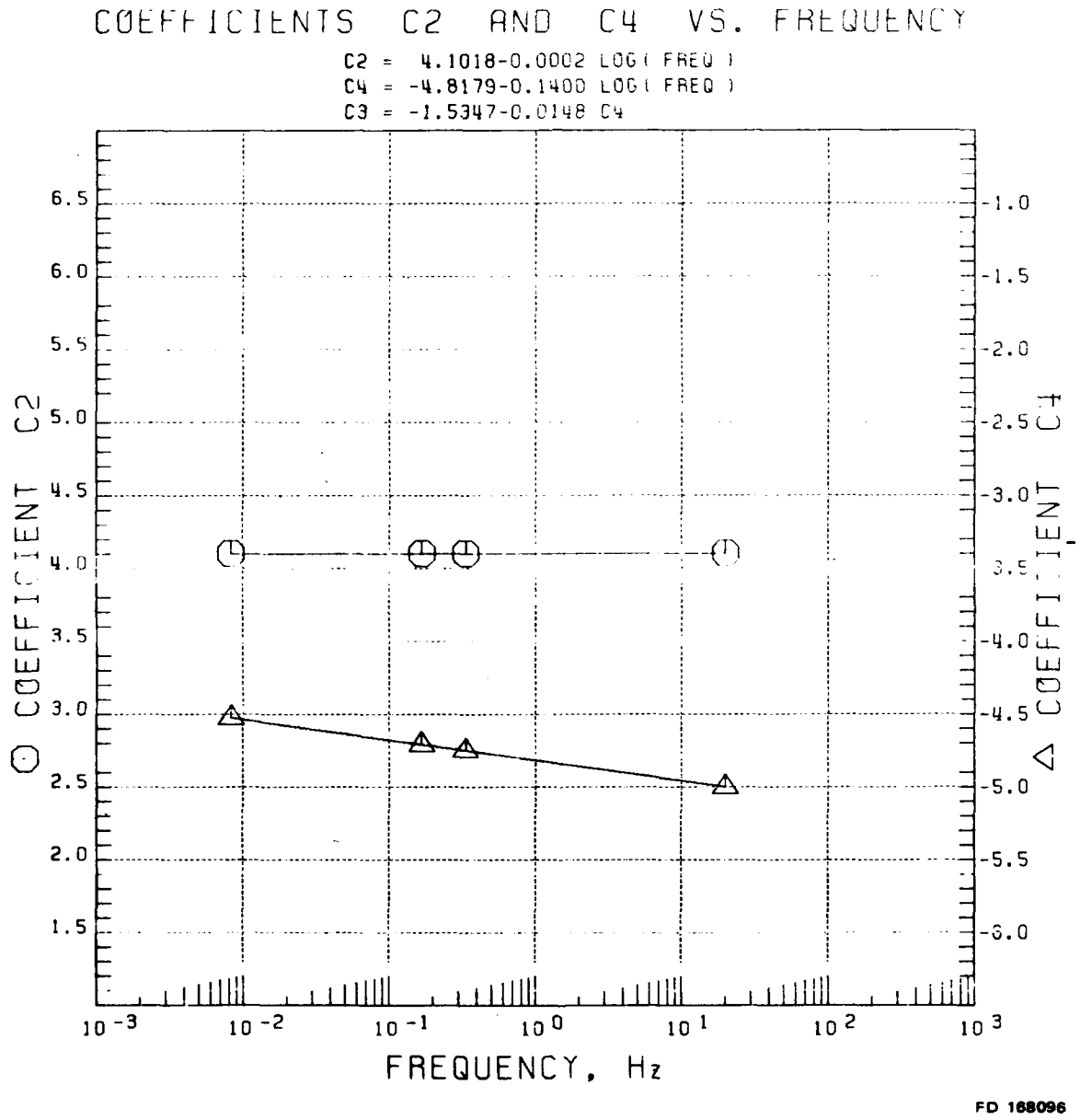

Figure 21. Waspaloy (PWA 1007) Frequency Model Correlative Parameters, 649°C (1200°F)

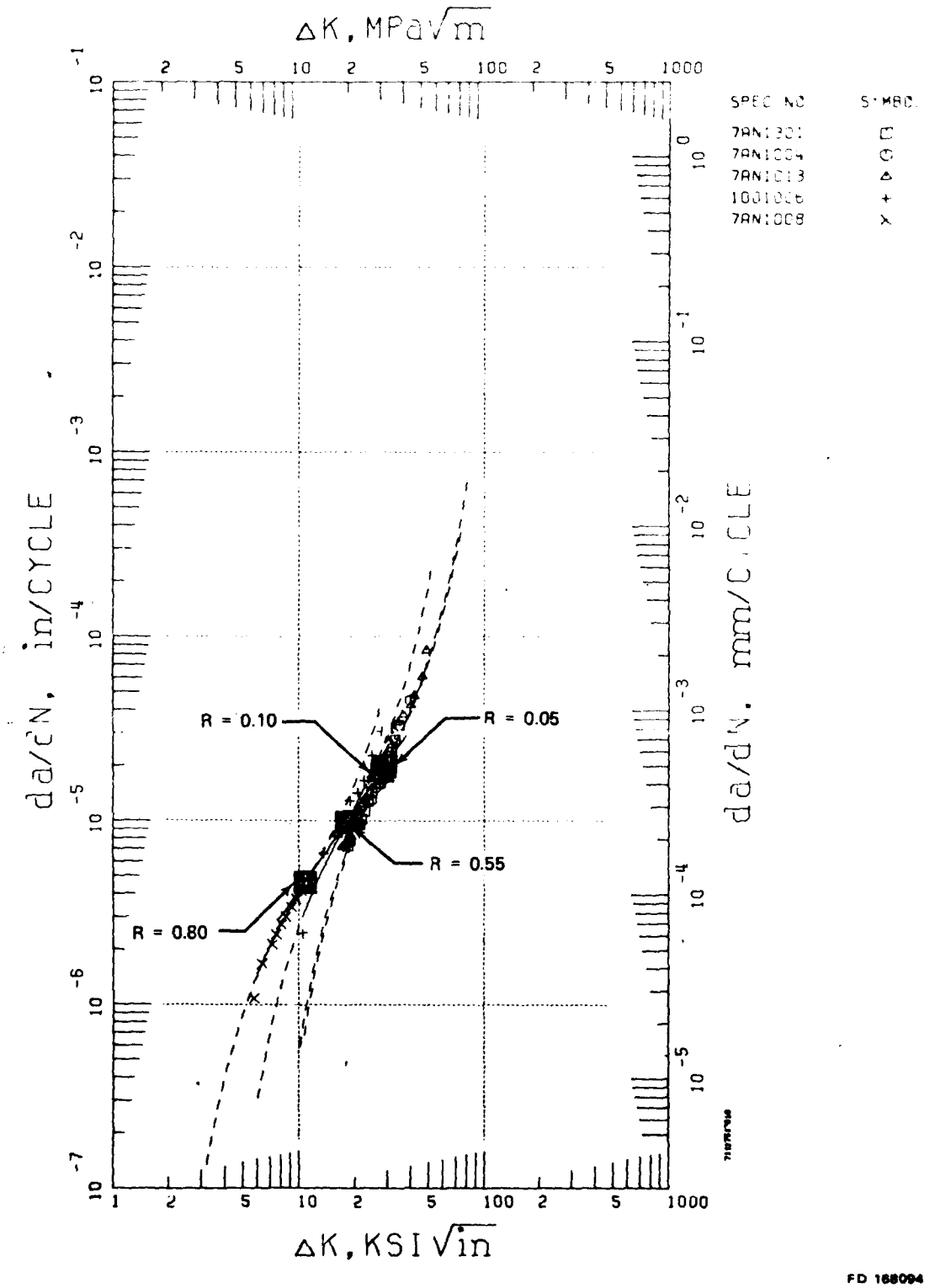

Figure 22. Waspaloy (PWA 1007) Crack Propagation, Stress Ratio Model, 0.167 Hz (10 cpm), 649°C (1200°F)

PAGE 71117517910

R=.05 T=1200F FREQ=10CPM 2 34 36 38 GROUP NO. 1

SPEC NO	MATERIAL	TEMP	ATM	FREQ	R	TYPE	THIK	REMARKS
7AN1301	PWA 1007	1200F	AIR	10 CPM	R=.05	BAR MCT	.501	
7AN1004	PWA 1007	1200F	AIR	10 CPM	R=.05	CN	.301	

□
○ RSQRD 0.9808 SEE 0.0313

-0.34 10. Y=0.5000 SINH(4.102 (X -1.465)) -4.709
NRFT 1 (METRIC) Y=0.5000 SINH(4.102 (X -1.506)) -3.304
*** IMPORTANT *** THIS EQUATION IS VALID BETWEEN X= 18.31 . AND X= 39.98 ONLY. DO NOT EXTRAPOLATE.

R=.1 T=1200F FREQ=10CPM 3 34 36 38 GROUP NO. 2

SPEC NO	MATERIAL	TEMP	ATM	FREQ	R	TYPE	THIK	REMARKS
7AN1013	PWA 1007	1200F	AIR	10 CPM	R=.1	BAR MCT	.318	

△ RSQRD 0.9932 SEE 0.0201

-0.34 10. Y=0.5000 SINH(4.080 (X -1.450)) -4.731
NRFT 1 (METRIC) Y=0.5000 SINH(4.080 (X -1.491)) -3.326
*** IMPORTANT *** THIS EQUATION IS VALID BETWEEN X= 17.09 . AND X= 49.06 ONLY. DO NOT EXTRAPOLATE.

R=.55 T=1200F FREQ=10CPM 3 34 36 38 GROUP NO. 3

SPEC NO	MATERIAL	TEMP	ATM	FREQ	R	TYPE	THIK	REMARKS
1001006	PWA 1007	1200F	AIR	10 CPM	R=.55	CN	.287	

+ RSQRD 0.9891 SEE 0.0305

-0.34 10. Y=0.5000 SINH(3.802 (X -1.259)) -5.009
NRFT 1 (METRIC) Y=0.5000 SINH(3.802 (X -1.300)) -3.604
*** IMPORTANT *** THIS EQUATION IS VALID BETWEEN X= 10.53 . AND X= 27.87 ONLY. DO NOT EXTRAPOLATE.

R=.8 T=1200F FREQ=10CPM 3 34 36 38 GROUP NO. 4

SPEC NO	MATERIAL	TEMP	ATM	FREQ	R	TYPE	THIK	REMARKS
7AN1008	PWA 1007	1200F	AIR	10 CPM	R=.8	CN	.300	

× RSQRD 0.9452 SEE 0.0319

-0.34 10. Y=0.5000 SINH(3.470 (X -1.035)) -5.335
NRFT 1 (METRIC) Y=0.5000 SINH(3.470 (X -1.070)) -3.930
*** IMPORTANT *** THIS EQUATION IS VALID BETWEEN X= 5.77 . AND X= 11.06 ONLY. DO NOT EXTRAPOLATE.

OVERALL STATISTICS FOR THIS COLLECTION OF GROUPS. TOTAL RSQRD = 0.9854. AND STD.ERROR.EST. = 0.0288

FD 168095

Figure 23. Statistics for Waspaloy (PWA 1007) Crack Propagation, Stress Ratio Model, 0.167 Hz (10 cpm), 649°C (1200°F)

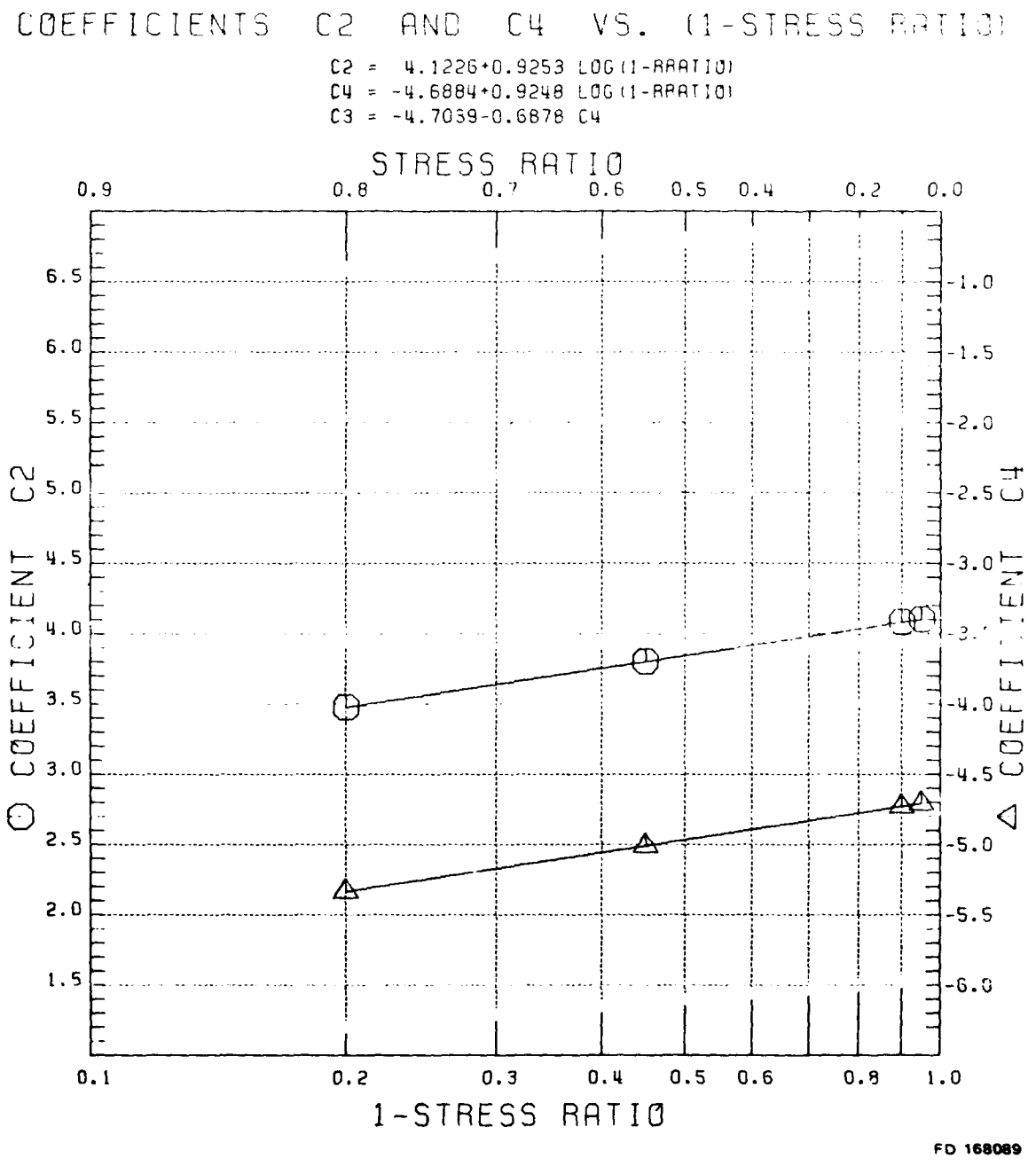

Figure 24. Waspaloy (PWA 1007) Stress Ratio Model Correlative Parameters, 0.167 Hz (10 cpm), 649°C (1200°F)

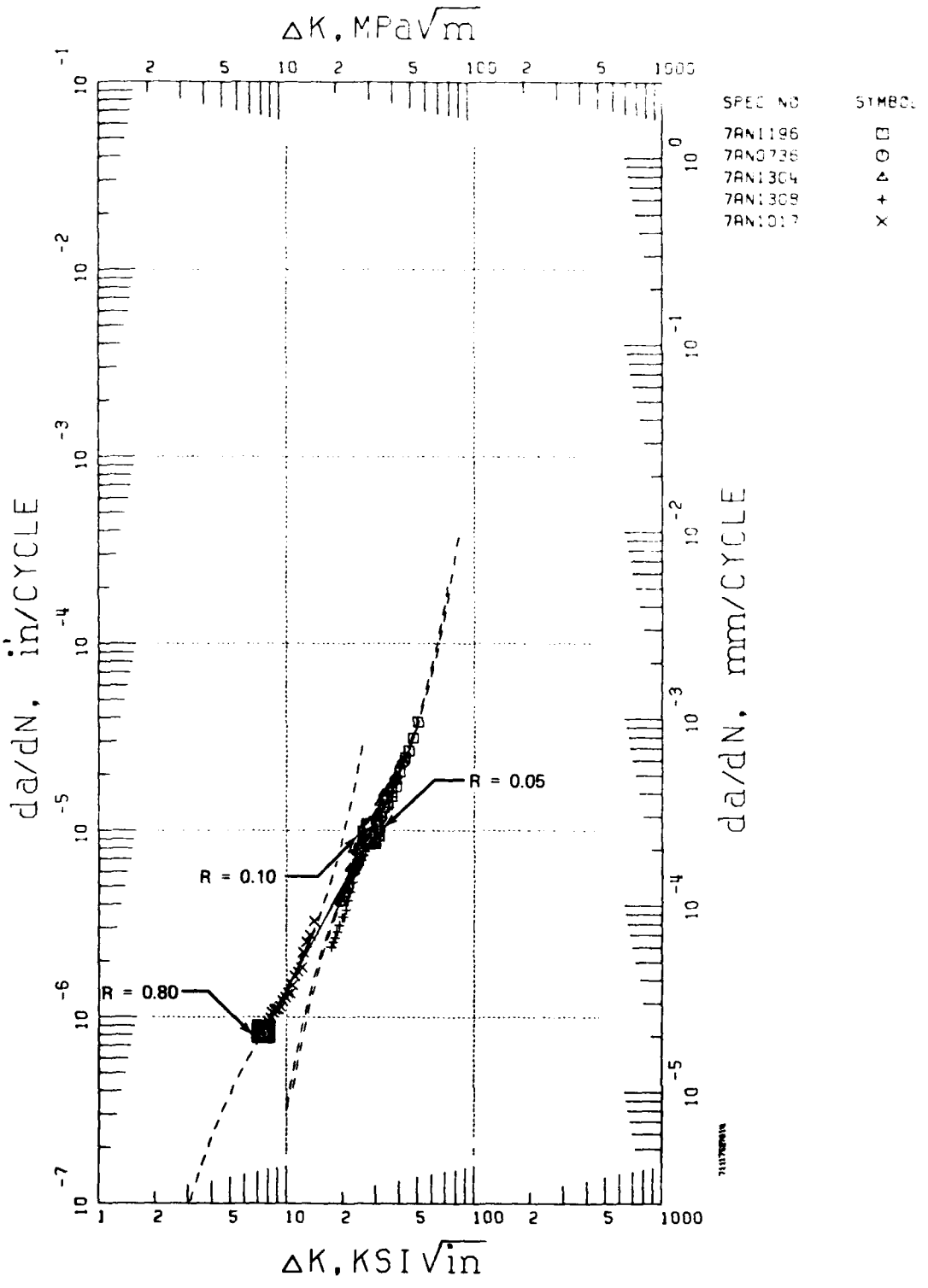

Figure 25. Waspaloy (PWA 1007) Crack Propagation, Stress Ratio Model, 20.0 Hz, 649°C (1200°F)

PAGE 71117527914

6 33 34 35 36 37 38 GROUP NO. 1

SPEC NO	MATERIAL	TEMP	ATM	FREQ	R	TYPE	THIK	REMARKS
7AN1196	PWA 1007	1200F	AIR	20 HZ	R=.05	RAD MCT	.753	KEYHOLE
7AN0736	PWA 1007	1200F	AIR	20 HZ	R=.05	RAD MCT	.432	W6

□
○ RSQRD 0.9969 SEE 0.0154

-0.53 0. Y=0.5000 SINH(4.102 (X -1.461)) -5.000
NRFT 1 (METRIC) Y=0.5000 SINH(4.102 (X -1.502)) -3.595
*** IMPORTANT *** THIS EQUATION IS VALID BETWEEN X= 19.27 , AND X= 50.28 ONLY. DO NOT EXTRAPOLATE.

6 33 34 35 36 37 38 GROUP NO. 2

SPEC NO	MATERIAL	TEMP	ATM	FREQ	R	TYPE	THIK	REMARKS
7AN1304	PWA 1007	1200F	AIR	20 HZ	R=.1	RAD MCT	.500	
7AN1308	PWA 1007	1200F	AIR	20 HZ	R=.1	RAD MCT	.302	

△
+ RSQRD 0.9305 SEE 0.0744

-0.53 0. Y=0.5000 SINH(4.081 (X -1.441)) -5.037
NRFT 1 (METRIC) Y=0.5000 SINH(4.081 (X -1.482)) -3.632
*** IMPORTANT *** THIS EQUATION IS VALID BETWEEN X= 17.36 , AND X= 40.18 ONLY. DO NOT EXTRAPOLATE.

6 33 34 35 36 37 38 GROUP NO. 3

SPEC NO	MATERIAL	TEMP	ATM	FREQ	R	TYPE	THIK	REMARKS
7AN1017	PWA 1007	1200F	AIR	20 HZ	R=.8	RAD MCT	.300	

× RSQRD 0.9751 SEE 0.0300

-0.53 0 Y=0.5000 SINH(3.506 (X -0.879)) -6.077
NRFT 1 (METRIC) Y=0.5000 SINH(3.506 (X -0.920)) -4.672
*** IMPORTANT *** THIS EQUATION IS VALID BETWEEN X= 6.92 , AND X= 14.07 ONLY. DO NOT EXTRAPOLATE.

OVERALL STATISTICS FOR THIS COLLECTION OF GROUPS. TOTAL RSQRD = 0.9855. AND STD.ERROR.EST. = 0.0545

FD 169877

Figure 26. Statistics for Waspaloy (PWA 1007) Crack Propagation, Stress Ratio Model, 20.0 Hz, 649°C (1200°F)

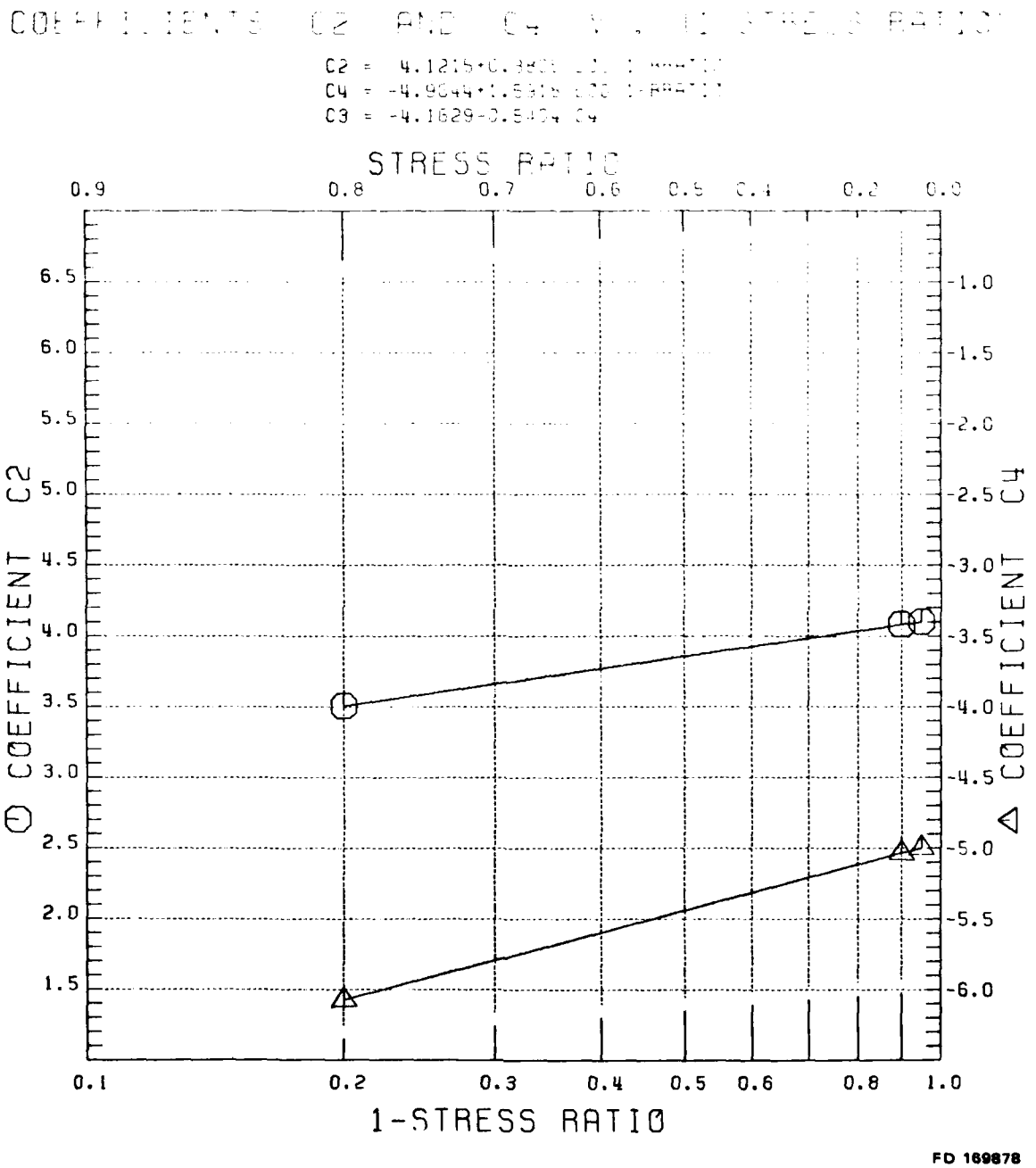

Figure 27. Waspaloy (PWA 1007) Stress Ratio Model Correlative Parameters, 20 Hz, 649°C (1200°F)

(d) Effect of Temperature

The effect of operating temperature on crack propagation of Waspaloy (PWA 1007) is illustrated in the composite plot of Figure 28. (See also Figure 29.) This SINH model describes the detrimental influence of increasing temperature on crack growth in this alloy. The relationships defining the associated SINH coefficients are presented in Figure 30.

(2) Crack Propagation Under Periodic Load Dwell

(a) Effect of Load Dwell, 649°C (1200°F)

Crack propagation in Waspaloy (PWA 1007) under periodic load dwell, Figure 12, at 649°C (1200°F) is a function of the period of dwell. Tests conducted with dwells ranging from 120 to 900 sec, were used to develop the interpolative SINH model of the effect of dwell shown in Figure 31. (See also Figure 32.) While experience has demonstrated that the SINH coefficients are linear functions of the log of the period of dwell, this relationship does not completely describe the behavior of data of Figure 31. Coefficients C_2 and C_3 are linear functions, but two linear segments are required to define the behavior of C_4 with period of load dwell. This is shown in the plot of Figure 33.

(b) Effect of Load Dwell, 732°C (1350°F)

The crack propagation behavior of Waspaloy (PWA 1007) under periodic load dwell displays a significant dependence on operating temperature. A SINH model developed from data generated in Waspaloy at 732°C (1350°F) under dwells of 120 and 900 sec, is presented in Figure 34. (See also Figure 35.) The interpolative functions describing this behavior are given in Figure 36.

Comparison of the 649°C dwell data with data generated under similar loading at 732°C indicates that crack propagation rate under 900 sec dwell conditions is nearly independent of temperature. However, under 120 sec dwell loading, crack propagation at 732°C is significantly slower than at 649°C as shown in Figure 37. The reduced crack growth rate at the higher temperature is attributed to crack tip blunting which results from an appreciable creep component at 732°C. During the 732°C, 900 sec dwell test, crack tip blunting resulted in crack arrest at values of $\Delta K < 35$ MPa $\sqrt{m}$ and in general, severely complicated data generation at this condition.

The interactive effect of periodic load dwell and operating temperature is included in the general interpolation algorithm developed under this contract.

(3) Sustained Load Crack Growth

Conventional experimental methods for determination of crack propagation behavior under sustained loading call for incremental crack length measurements over the duration of the test. This allows generation of crack growth rate vs applied stress intensity (da/dt vs K) data which characterize crack growth under the conditions of testing.

We have applied an alternative procedure to elevated temperature sustained load crack propagation testing (Reference 2). The underlying assumption of this method is that the sustained load crack growth curve exhibits a sigmoidal shape definable by an equation of the form:

$$da/dt = 10^{**} (C_1 \text{ SINH } (C_2 (\log K + C_3)) + C_4). \quad (24)$$

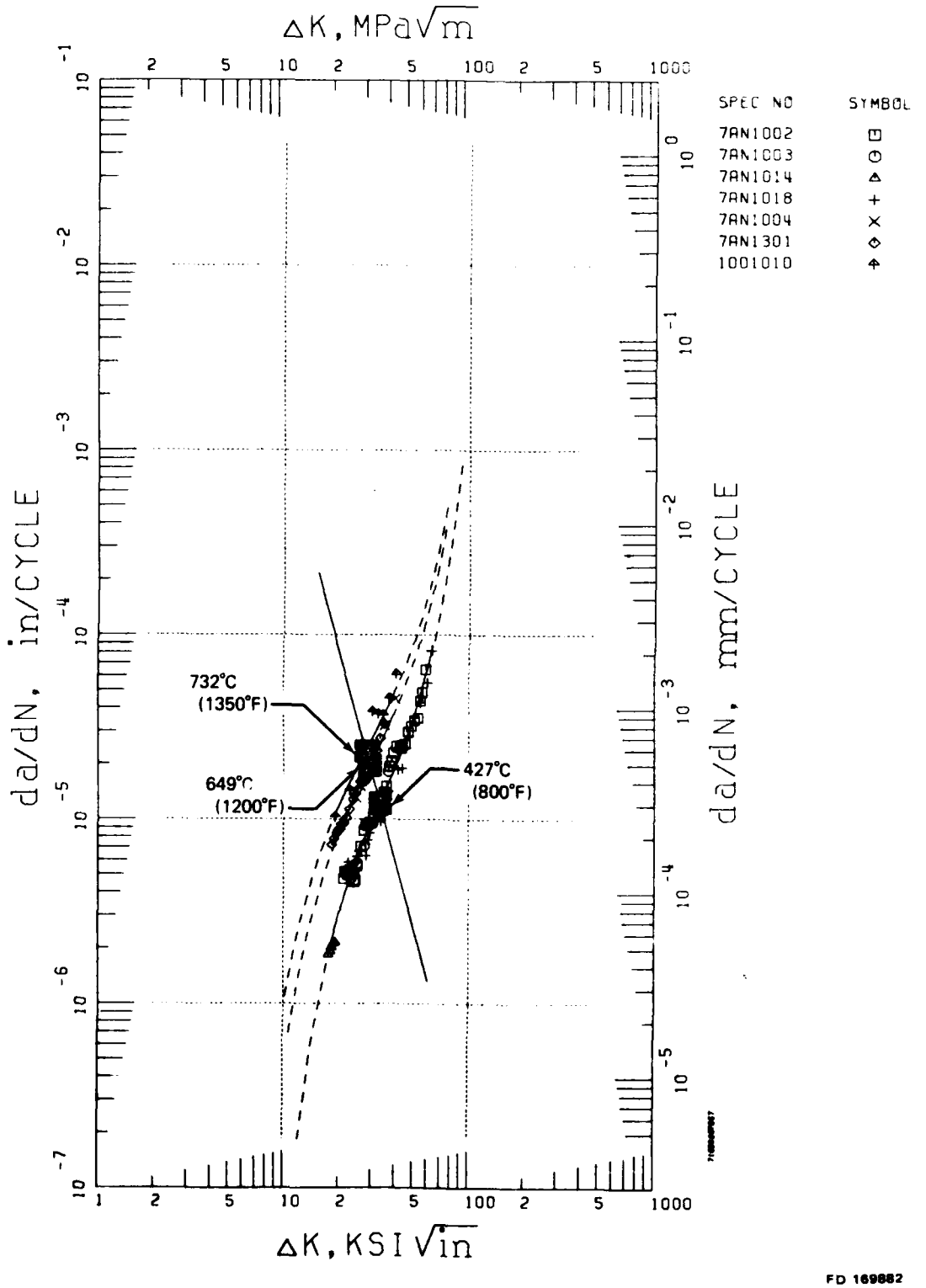

Figure 28. Waspaloy (PWA 1007) Crack Propagation, Temperature Model, R = 0.05, 0.167 Hz (10 cpm)

PAGE 71630267957

R=.05 T=800F FREQ=10CPM 6 33 34 35 36 37 38 GROUP NO. 1

SPEC NO	MATERIAL	TEMP	ATM	FREQ	R	TYPE	THIK	REMARKS	
7AN1002	PWA 1007	800F	AIR	10 CPM	R=.05	RAD MCT	.499		□
7AN1003	PWA 1007	800F	AIR	10 CPM	R=.05	CN	.303		○
7AN1014	PWA 1007	800F	AIR	10 CPM	R=.05	RAD MCT	.300	PARTIAL	△
7AN1018	PWA 1007	800F	AIR	10 CPM	R=.05	RAD MCT	.298		+ RSQRD 0.9786 SEE 0.0571

-0.35 0. Y=0.5000 SINH(4.604 (X -1.520)) -4.914

NRFT 3 (METRIC) Y=0.5000 SINH(4.604 (X -1.561)) -3.509

*** IMPORTANT *** THIS EQUATION IS VALID BETWEEN X= 17.55 , AND X= 62.89 ONLY. DO NOT EXTRAPOLATE.

R=.05 T=1200F FREQ=10CPM 6 33 34 35 36 37 38 GROUP NO. 2

SPEC NO	MATERIAL	TEMP	ATM	FREQ	R	TYPE	THIK	REMARKS	
7AN1004	PWA 1007	1200F	AIR	10 CPM	R=.05	CN	.301		×
7AN1301	PWA 1007	1200F	AIR	10 CPM	R=.05	RAD MCT	.501		◇ RSQRD 0.9818 SEE 0.0311

-0.35 0. Y=0.5000 SINH(4.102 (X -1.465)) -4.709

NRFT 3 (METRIC) Y=0.5000 SINH(4.102 (X -1.506)) -3.304

*** IMPORTANT *** THIS EQUATION IS VALID BETWEEN X= 18.31 , AND X= 39.98 ONLY. DO NOT EXTRAPOLATE.

R=.05 T=1350F FREQ=10CPM 6 33 34 35 36 37 38 GROUP NO. 3

SPEC NO	MATERIAL	TEMP	ATM	FREQ	R	TYPE	THIK	REMARKS	
1001010	PWA 1007	1350F	AIR	10 CPM	R=.05	CN	.301		◆ RSQRD 0.9582 SEE 0.0866

-0.35 0. Y=0.5000 SINH(3.913 (X -1.444)) -4.632

NRFT 3 (METRIC) Y=0.5000 SINH(3.913 (X -1.485)) -3.227

*** IMPORTANT *** THIS EQUATION IS VALID BETWEEN X= 18.94 , AND X= 40.47 ONLY. DO NOT EXTRAPOLATE.

OVERALL STATISTICS FOR THIS COLLECTION OF GROUPS. TOTAL RSQRD = 0.9785, AND STD.ERROR.EST. = 0.0534

FD 169883

Figure 29. Statistics for Waspaloy (PWA 1007) Crack Propagation, Temperature Model, R = 0.05, 0.167 Hz (10 cpm)

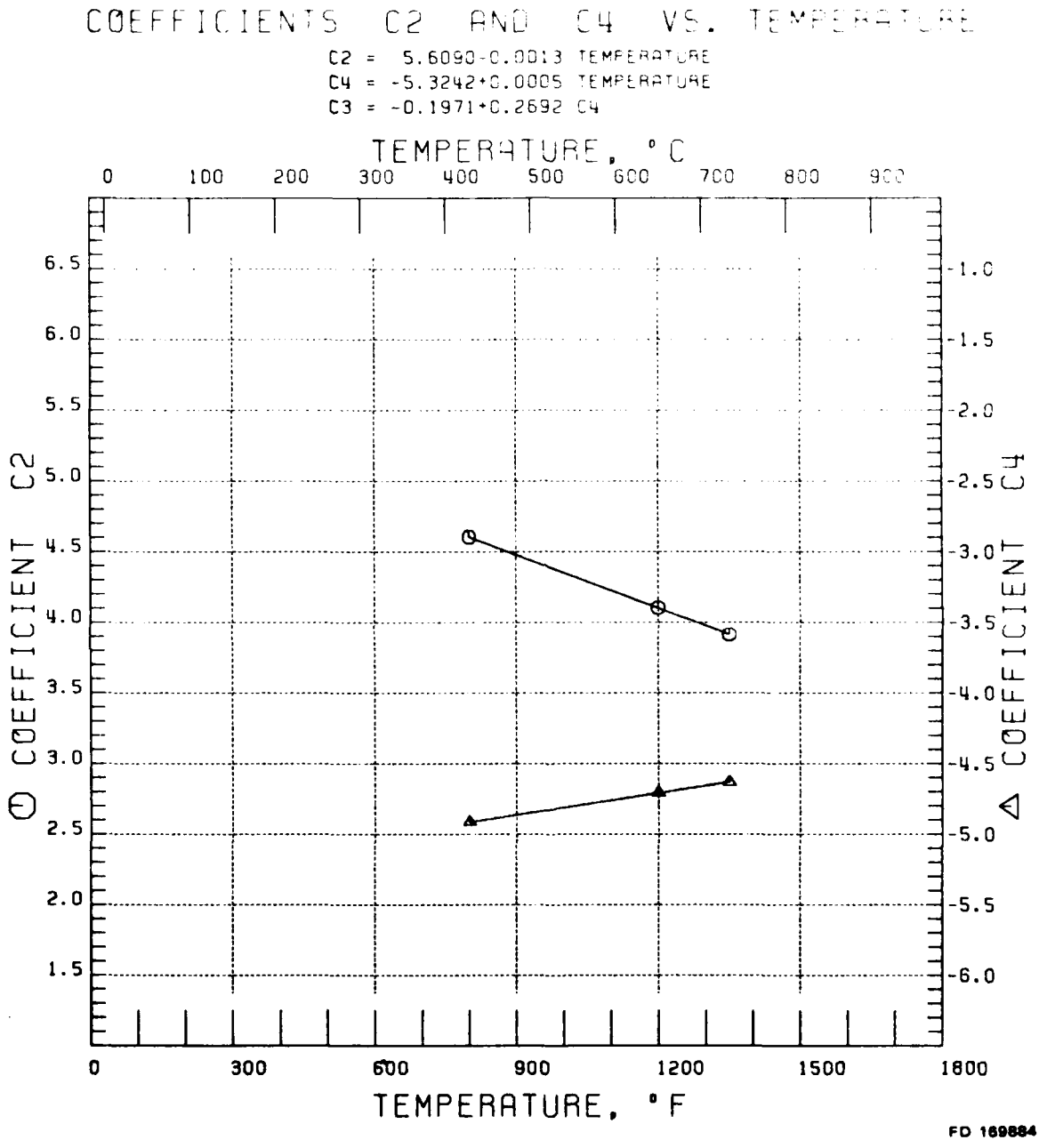

Figure 30. Waspaloy (PWA 1007) Temperature Model Correlative Parameters, R = 0.05, 0.167 Hz (10 cpm)

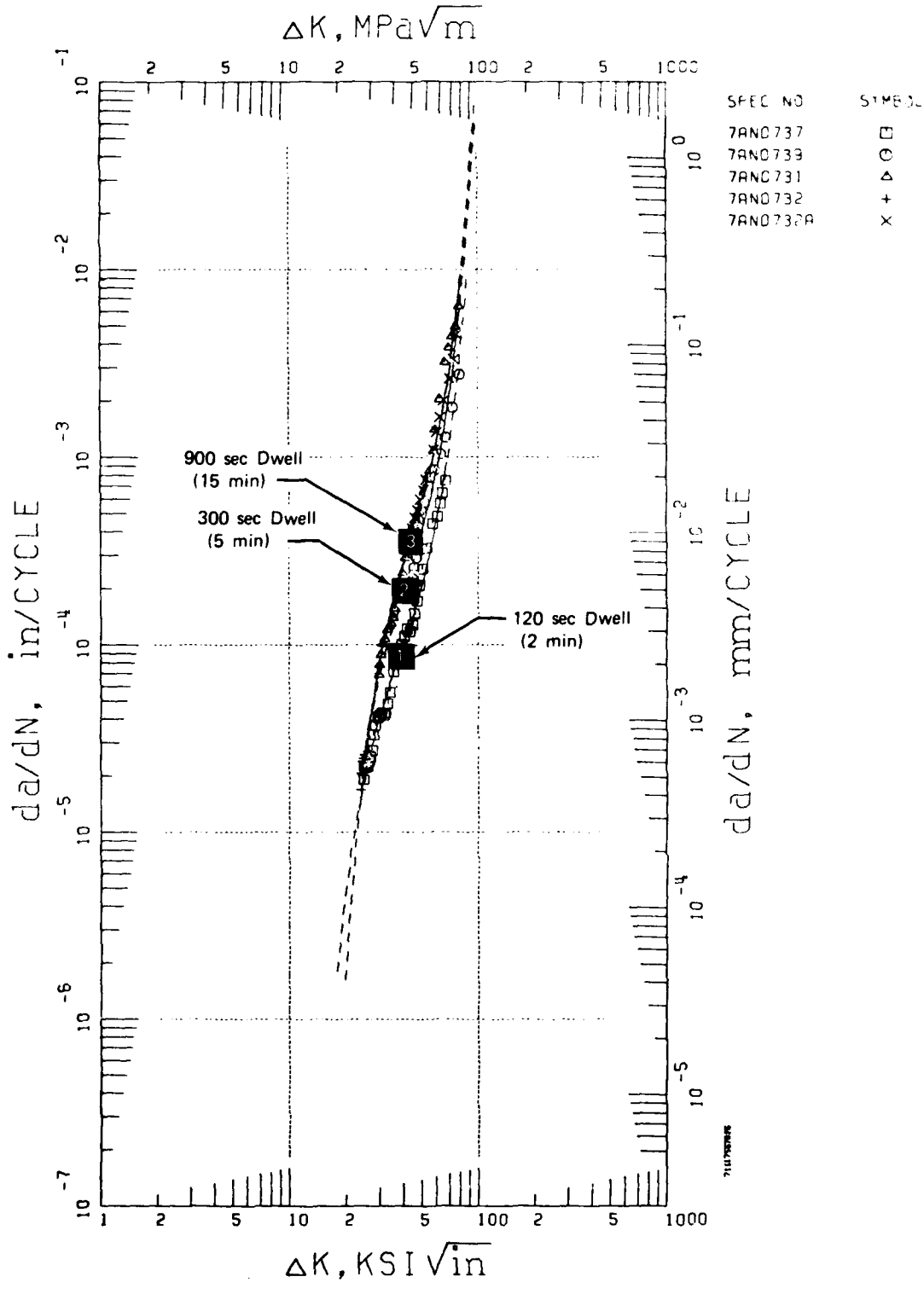

Figure 31. Waspaloy (PWA 1007) Crack Propagation, Dwell Model, R = 0.05, 649°C (1200°F)

PAGE 71117557925

TEST CONDITIONS 9 2 3 4 6 7 8 10 11 12 GROUP NO. 1

SPEC NO	MATERIAL	TEMP	ATM	FREQ	R	TYPE	THIK	REMARKS	
7AN0737	PWA 1007	1200F	AIR	2 MDWL	R=.05	RAD MCT	.316		□ RSQRD 0.9924 SEE 0.0433

-0.74 0. Y=0.5000 SINH(5.820 (X -1.584))-4.054

NRFT 4 (METRIC) Y=0.5000 SINH(5.820 (X -1.625))-2.649

*** IMPORTANT *** THIS EQUATION IS VALID BETWEEN X= 24.68 . AND X= 67.84 ONLY. DO NOT EXTRAPOLATE.

TEST CONDITIONS 9 2 3 4 6 7 8 10 11 12 GROUP NO. 2

SPEC NO	MATERIAL	TEMP	ATM	FREQ	R	TYPE	THIK	REMARKS	
7AN0739	PWA 1007	1200F	AIR	5 MDWL	R=.05	RAD MCT	.377		○ RSQRD 0.9161 SEE 0.1365

-0.74 0. Y=0.5000 SINH(6.140 (X -1.610))-3.707

NRFT 4 (METRIC) Y=0.5000 SINH(6.140 (X -1.651))-2.302

*** IMPORTANT *** THIS EQUATION IS VALID BETWEEN X= 45.03 . AND X= 79.98 ONLY. DO NOT EXTRAPOLATE.

TEST CONDITIONS 9 2 3 4 6 7 8 10 11 12 GROUP NO. 3

SPEC NO	MATERIAL	TEMP	ATM	FREQ	R	TYPE	THIK	REMARKS	
7AN0731	PWA 1007	1200F	AIR	15MDWL	R=.05	RAD MCT	.417		△
7AN0732	PWA 1007	1200F	AIR	15MDWL	R=.05	RAD MCT	.422	LOW K	+
7AN0732A	PWA 1007	1200F	AIR	15MDWL	R=.05	RAD MCT	.422	HI K	× RSQRD 0.9921 SEE 0.0214

-0.74 0. Y=0.5000 SINH(6.523 (X -1.641))-3.453

NRFT 4 (METRIC) Y=0.5000 SINH(6.523 (X -1.682))-2.048

*** IMPORTANT *** THIS EQUATION IS VALID BETWEEN X= 23.99 . AND X= 79.75 ONLY. DO NOT EXTRAPOLATE.

OVERALL STATISTICS FOR THIS COLLECTION OF GROUPS. TOTAL RSQRD = 0.9893, AND STD.ERROR.EST. = 0.0221

FD 169889

Figure 32. Statistics for Waspaloy (PWA 1007) Crack Propagation, Dwell Model, R = 0.05, 649°C (1200°F)

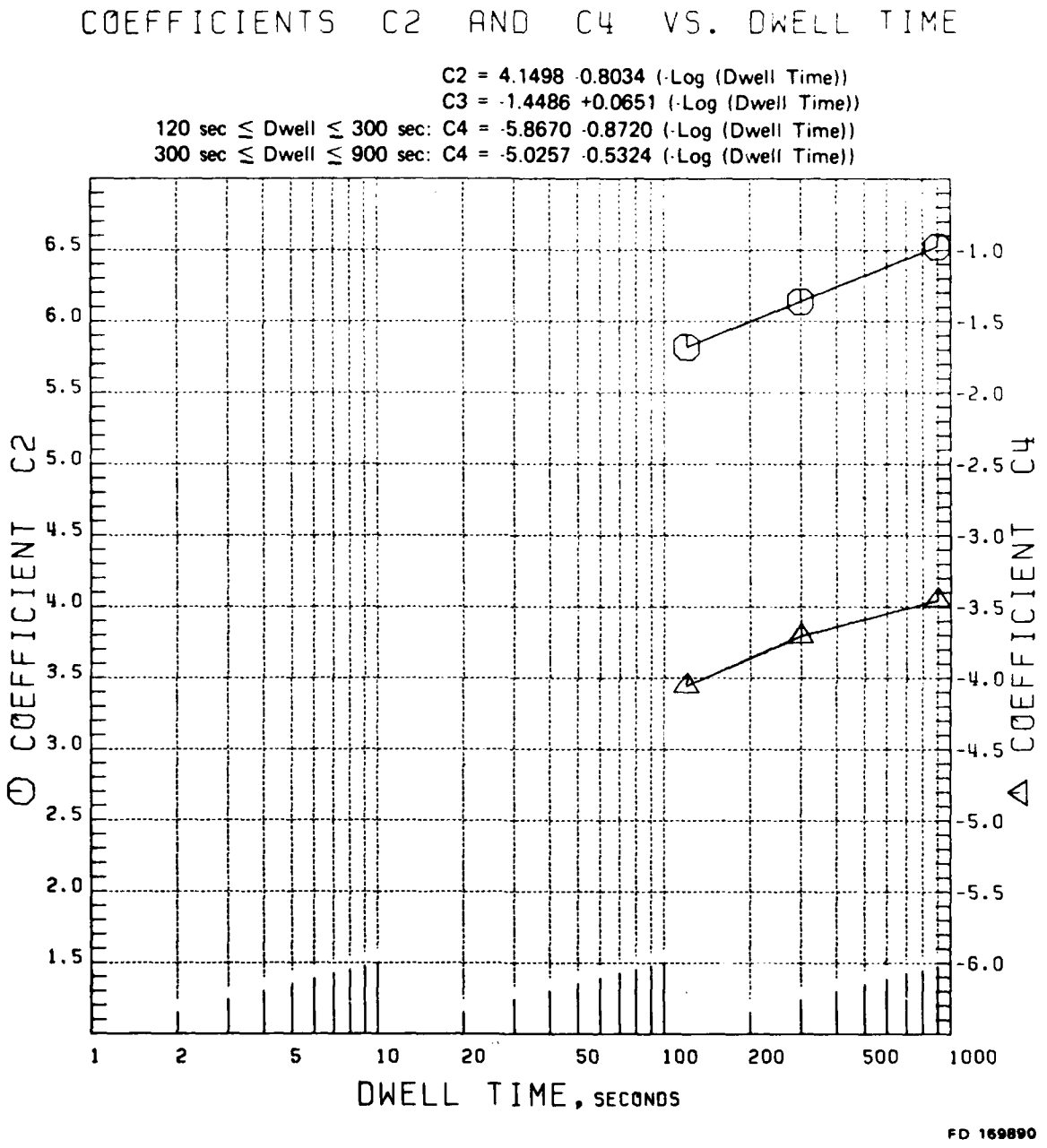

Figure 33. Waspaloy (PWA 1007) Dwell Model Correlative Parameters, R = 0.05, 649°C (1200°F)

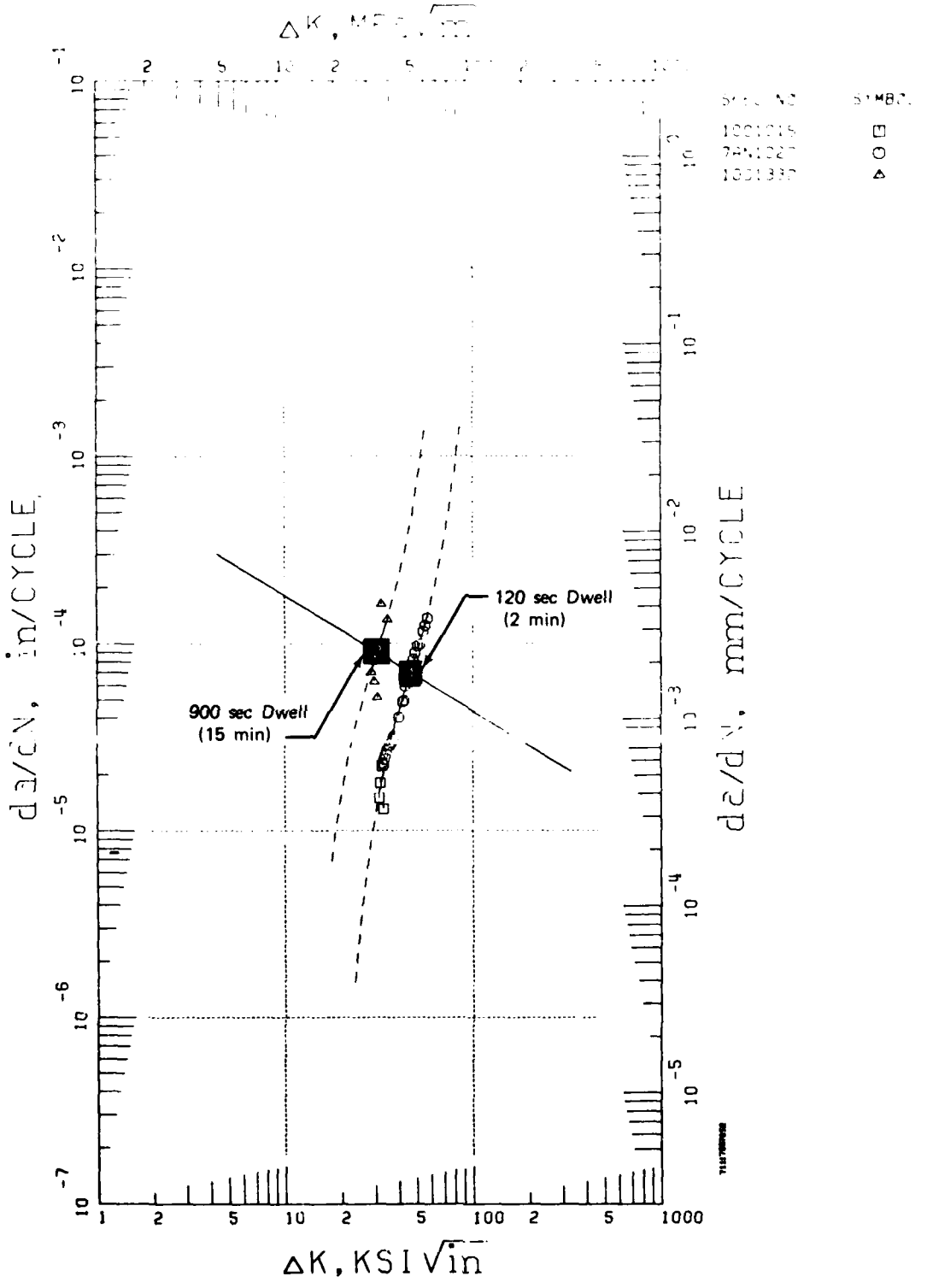

Figure 34. Waspaloy (PWA 1007) Crack Propagation, Dwell Model, R = 0.10, 732°C (1350°F)

PAGE 71117557952

TEST CONDITIONS 3 343638 GROUP NO. 1

SPEC NO	MATERIAL	TEMP	ATM	FREQ	R	TYPE	THIK	REMARKS
1001015	PWA 1007	1350F	AIR	2 MDWL	R=.1	RAD MCT	.300	PARTIAL
7AN1027	PWA 1007	1350F	AIR	2 MDWL	R=.1	RAD MCT	.299	

□
○ RSQRD 0.9703 SEE 0.0551

-0.00 0. Y=0.5000 SINH(6.402 (X -1.668))-4.156

NAFT 4 (METRIC) Y=0.5000 SINH(6.402 (X -1.709))-2.751

*** IMPORTANT *** THIS EQUATION IS VALID BETWEEN X= 31.69 , AND X= 57.41 ONLY. DO NOT EXTRAPOLATE.

TEST CONDITIONS 3 343638 GROUP NO. 2

SPEC NO	MATERIAL	TEMP	ATM	FREQ	R	TYPE	THIK	REMARKS
1001330	PWA 1007	1350F	AIR	15 MDL	R=.1	RAD CN	.299	

△ RSQRD 0.4457 SEE 0.1902

-0.00 0. Y=0.5000 SINH(6.315 (X -1.490))-4.046

NAFT 4 (METRIC) Y=0.5000 SINH(6.315 (X -1.531))-2.641

*** IMPORTANT *** THIS EQUATION IS VALID BETWEEN X= 28.38 , AND X= 35.16 ONLY. DO NOT EXTRAPOLATE.

OVERALL STATISTICS FOR THIS COLLECTION OF GROUPS. TOTAL RSQRD = 0.9401 , AND STD.ERROR.EST. = 0.0784

FD 169894

Figure 35. Statistics for Waspaloy (PWA 1007) Crack Propagation, Dwell Model, R = 0.10, 732°C (1350°F)

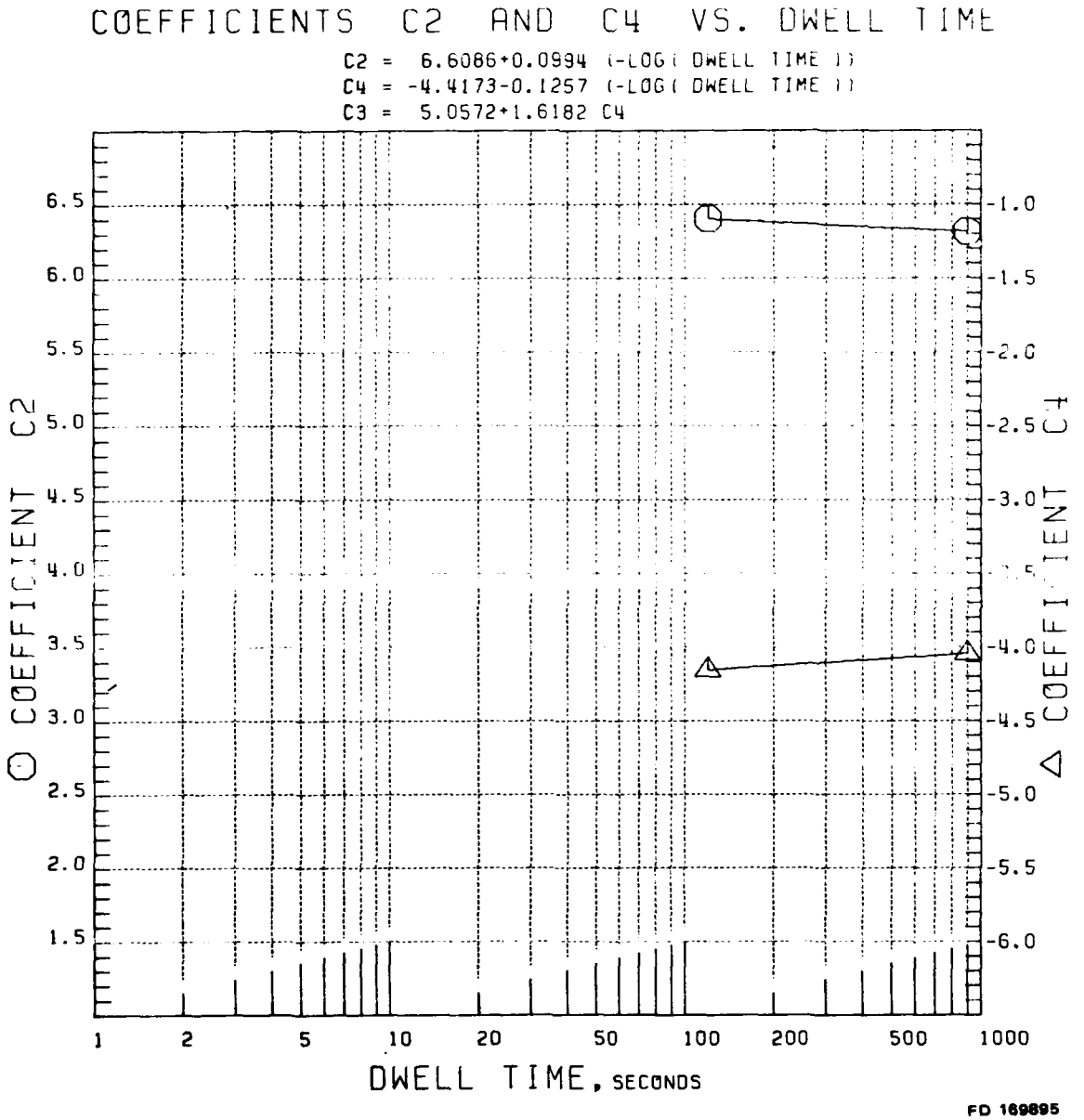

Figure 36. Waspaloy (PWA 1007) Dwell Model Correlative Parameters, R = 0.10, 732°C (1350°F)

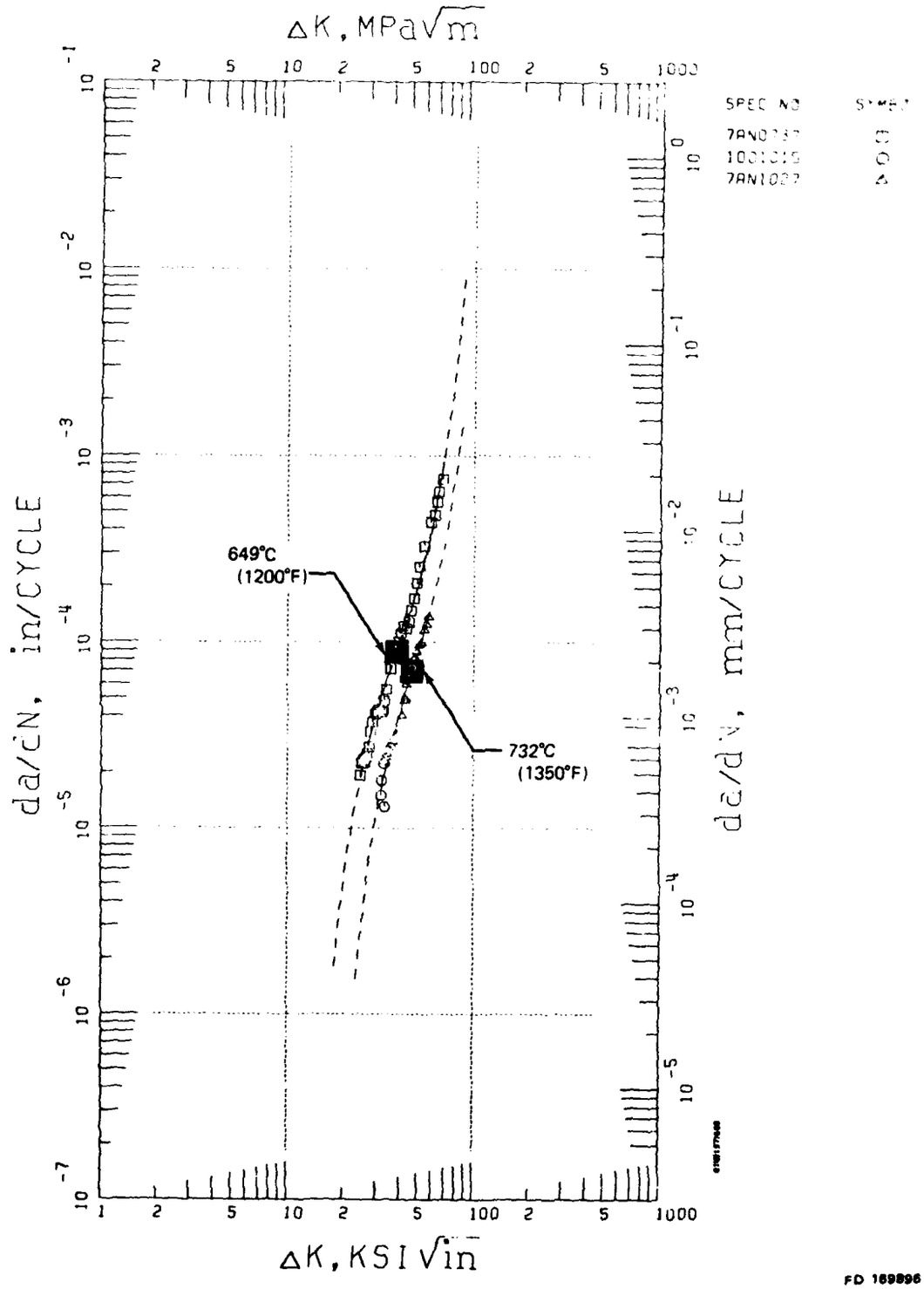

Figure 37. Waspaloy (PWA 1007), Effect of Temperature on Crack Propagation, 120 sec Dwell Loading

The experimental procedure requires sustained load testing of a series of compact specimens which have been previously fatigue precracked. Test loads for the individual specimens are selected to produce a range of values of initial applied stress intensity for the collection of specimens. Assuming that cracking of all of the specimens follows a mutual propagation (da/dt, K) curve, data from the collection of tests may be used to define this propagation curve. The data required include: times of specimen failure, test load, initial (a_i) and final (a_f) crack length, and specimen geometry. The following mathematical procedure is employed to produce the crack growth curve:

- Initialize the coefficients of the crack growth curve at values which are characteristic of the material in question.
- Integrate the reciprocal of the crack growth curve from initial to final crack length to obtain calculated lives (time to failure) for each of the individual test specimens.
- Calculate the summed squared error for the actual vs observed lives for the test specimens.
- Generate a new set of SINH coefficients using the Newton-Raphson to minimize the calculated summed squared error.
- Repeat the last three steps above until convergence is achieved.

This procedure was applied to determine the sustained load crack growth behavior of Waspaloy (PWA 1007). Nine compact specimens were tested, five at 649°C (1200°F) and four at 732°C , to generate the crack growth model shown in Figure 38. (See also Figure 39.) The range of validity of these curves is approximately 45 MPa $\sqrt{m} \leq K \leq$ 110 MPa $\sqrt{m}$, and plotted crack growth rates are approximately equivalent. The crossing of the curves is an artifact of the range of testing, and extrapolation beyond the range of the data should not be attempted.

A plot of the actual vs calculated times to failure for all specimens used to generate the SINH curves is presented in Figure 40. Excellent correlation between actual and calculated lives is shown for the 649°C data. However, considerable difficulty was encountered in modeling sustained load crack propagation at 732°C. The data at this temperature display much less consistency than at 649°C. The basis for the inconsistency probably lies with a combination of factors which include ill-defined crack fronts and crack tunneling.

(4) Synergistic Crack Propagation

(a) LCF — Overload Interaction

Variable amplitude load sequences produce synergistic effects on crack propagation which complicate the life prediction procedure. The nature and significance of crack retardation experienced in turbine disks are discussed in Appendix A. Individual SINH models describing the effects on crack growth under representative load sequences are presented below. The analysis was performed on data generated using repetitive mission cycles as illustrated in Figure 14. As discussed previously (and in Appendix A), the overload-LCF sequence is defined as an "elemental damage event."

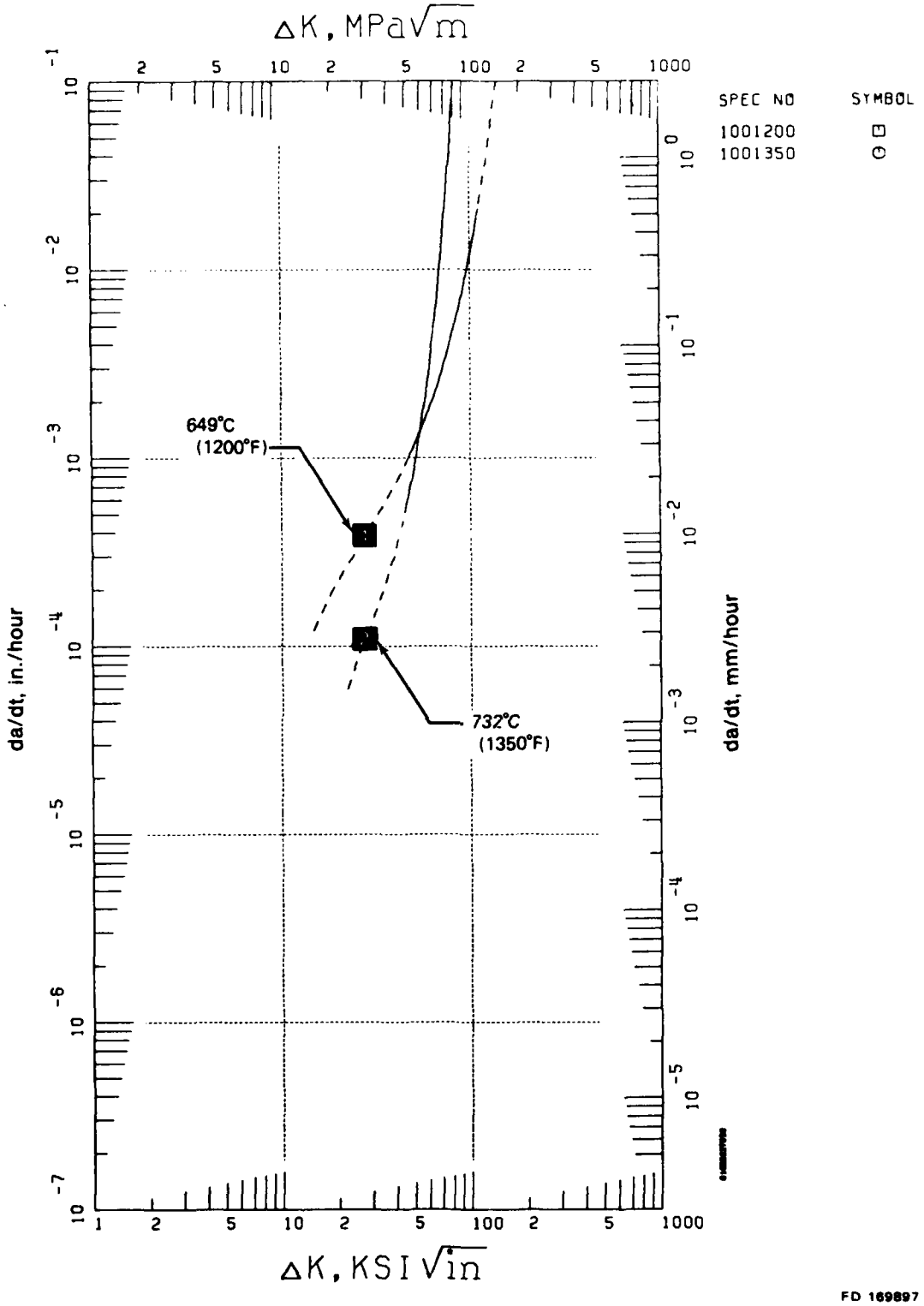

Figure 38. Waspaloy (PWA 1007) Crack Propagation Under Sustained Loading

PAGE 81002227958

TEST CONDITIONS 6 1 2 304 5 6 GROUP NO. 1

SPEC NO	MATERIAL	TEMP	ATM	FREQ	R	TYPE	THIK	REMARKS
1200								
	-0.45 6.			Y=0.5000 SINH(3.234 (X -1.440))-3.413				
	NAFT 0			(METRIC) Y=0.5000 SINH(3.234 (X -1.481))-2.008				

① RSQRD 0.0000 SEE 0.0000

*** IMPORTANT *** THIS EQUATION IS VALID BETWEEN X= 45.00 , AND X= 110.00 ONLY. DO NOT EXTRAPOLATE.

TEST CONDITIONS 6 1 2 304 5 6 GROUP NO. 2

SPEC NO	MATERIAL	TEMP	ATM	FREQ	R	TYPE	THIK	REMARKS
1350								
	-0.45 6.			Y=0.5000 SINH(5.197 (X -1.440))-3.962				
	NAFT 0			(METRIC) Y=0.5000 SINH(5.197 (X -1.481))-2.557				

② RSQRD 0.0000 SEE 0.0000

*** IMPORTANT *** THIS EQUATION IS VALID BETWEEN X= 45.00 , AND X= 110.00 ONLY. DO NOT EXTRAPOLATE.

OVERALL STATISTICS FOR THIS COLLECTION OF GROUPS. TOTAL RSQRD = 0.0000. AND STD.ERROR.EST. = 0.0000

FD 169898

Figure 39. Statistics for Waspaloy (PWA 1007) Crack Propagation Under Sustained Loading

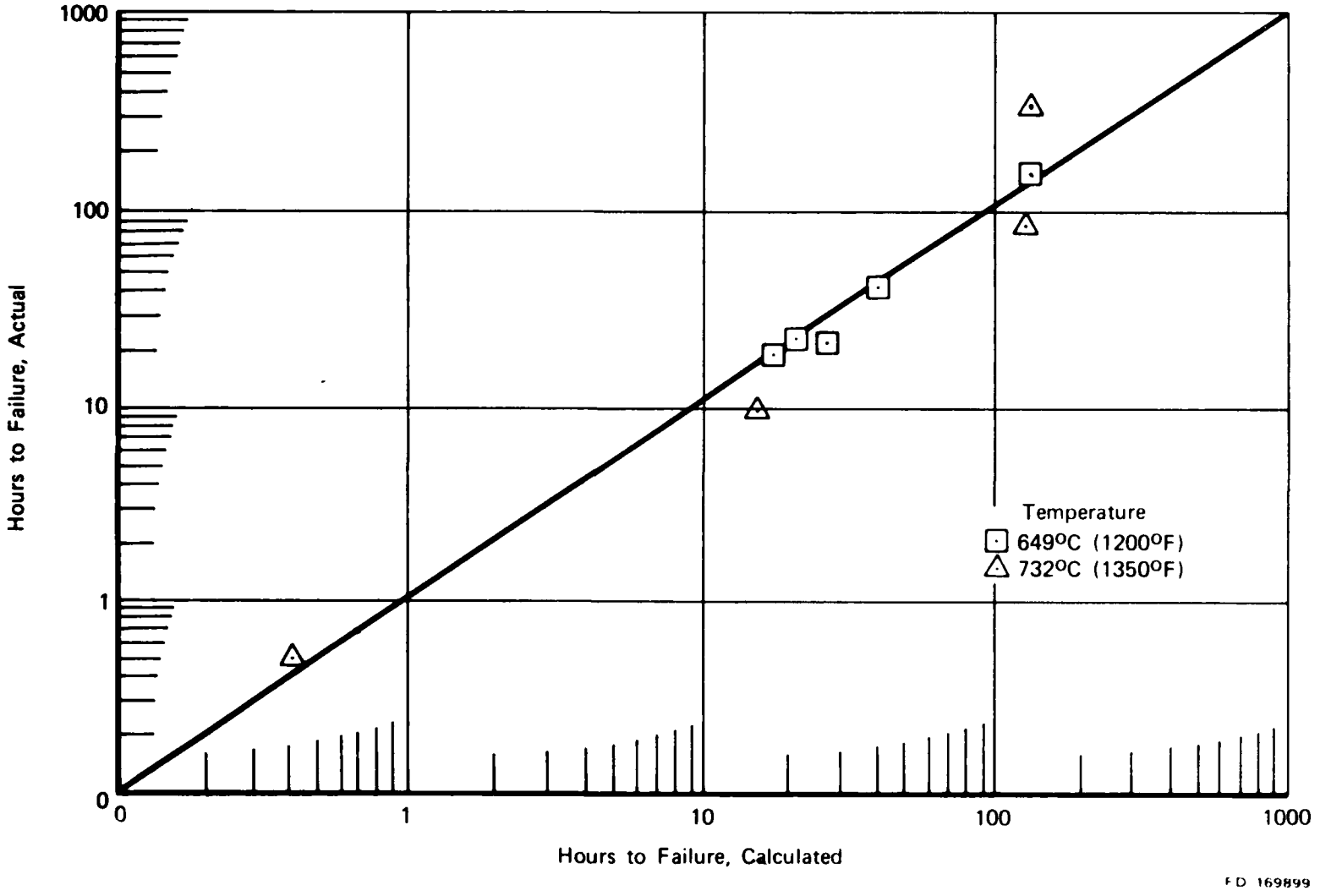

Figure 40. Waspaloy (PWA 1007), Actual vs Calculated Time to Failure of Sustained Load Crack Growth Specimens

(1) Effect of Number of Cycles Between Overloads

The number (ΔN_{OL}) of baseline fatigue cycles between successive overloads has a pronounced effect on the average crack growth rate produced by the repetitive loading of Figure 14. For tests under representative load sequence, da/dN vs ΔK data were generated with da/dN defined as the average crack growth per cycle ($\Delta a_{mission}/(\Delta N_{OL} + 1)$) and ΔK defined for the load range ($P_{max} - P_{min}$). Thus, the repetitive overload is treated as an isolated variable influencing crack growth, and the ΔK associated with the overhead is, by convention, equivalent to the baseline ΔK.

The results of testing of Waspaloy (PWA 1007) conducted under conditions of R = 0.5, 0.167 Hz, 649°C (1200°F), OLR = P_{OL}/P_{max} = 1.50, and $5 \leq \Delta N_{OL} \leq 40$ are presented in a composite, Figure 41. Figure 42 lists the statistics. Under the stated conditions, crack growth rate decreases as ΔN_{OL} increases. The SINH curves represent an interpolative model of the effect of the number of cycles between overloads. As shown in Figure 43, each of the defining SINH coefficients is a linear function of ($\Delta N_{OL} + 1$).

(2) Effect of Overload Ratio

Waspaloy (PWA 1007) crack propagation data generated under periodic overload-fatigue, Figure 14, with overload ratios of 1.25 and 1.50 were investigated. The other conditions of testing were equivalent: ΔN_{OL} = 40, R = 0.50, 0.167 Hz, and 649 °C (1200°F). Under these conditions, average crack growth rate increases as OLR approaches one. When OLR is equal to one, K_{OL} equals K_{max}, and an observable ΔN_{OL} vanishes. Therefore, for OLR= 1.0 the effect of overload ratio reduces to baseline crack growth. This is shown in Figure 44, and the statistics are summarized in Figure 45. The SINH curve for OLR = 1.0 is that predicted by the constant load amplitude stress ratio model presented earlier. As shown in Figure 46, the SINH coefficients describing the effect of overload ratio are a linear function of OLR.

(b) LCF — Dwell Interaction

Investigation of possible synergistic interaction within an LCF-dwell sequence was performed using the repetitive mission shown in Figure 13. Crack propagation tests employing this mission were conducted for Waspaloy (PWA 1007) at 649°C (1200°F) and 732°C (1350°F). The crack growth data were reduced with da/dN calculated as the average crack advance per cycle, with the dwell cycle counted as one load cycle.

The results of three 649°C (1200°F) tests of 10, 20, and 40 sawtooth fatigue cycles between dwells of 120 sec produced similar crack growth rates, Figure 47. Furthermore, all of this data is adequately described by the previously developed model of baseline fatigue (0.167 Hz, R = 0.10, 649°C). Apparently, there is little interaction or effect on crack growth produced by the periodic application of the load dwell at maximum load under the conditions of testing.

The FCP rate under similar loading at 732°C (1350°F) was also found to be independent of the number of sawtooth cycles separating the periodic load dwells of 120 sec. The data presented in Figure 48 represent three different test conditions: 10, 20, and 40 cycles between dwells. All of this data is described by the single SINH curve shown. An interpolative model of the effect of temperature on crack growth under LCF-Dwell loading is illustrated in Figure 49 and the statistics shown on Figure 50. As shown, crack growth rate is independent of the number of cycles between dwells ($10 \leq \Delta N_{Dwell} \leq 40$) and is a linear function of temperature as shown in Figure 51.

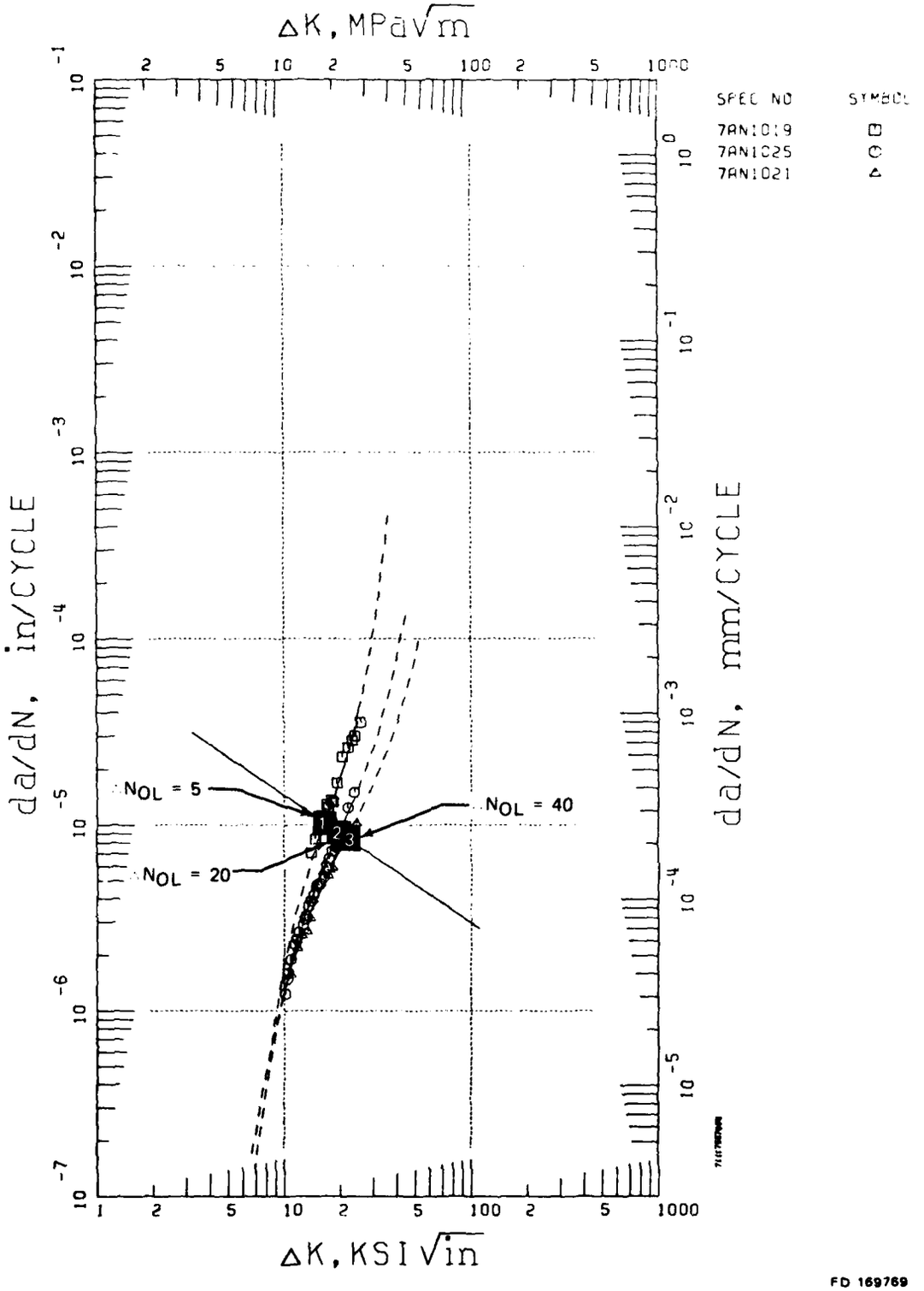

Figure 41. Waspaloy (PWA 1007) Crack Propagation, Model of Effect of the Number of Cycles Between Overloads, R = 0.50, 0.167 Hz (10 cpm), 649°C (1200°F)

PAGE 81407407900

3 34 36 38

SPEC NO	MATERIAL	TEMP	ATM	FREQ	R	TYPE	THIK	REMARKS
7AN1019	PWA 1007	1200F	AIR	10 CPM	R=.5	RAD MCT	.299	OL1.5+5CY

-0.29 0. Y=0.5000 SINH(5.615 (X -1.218))-4.993

NRFT 5 (METRIC) Y=0.5000 SINH(5.615 (X -1.259))-3.588

*** IMPORTANT *** THIS EQUATION IS VALID BETWEEN X= 14.12 . AND X= 25.66 ONLY. DO NOT EXTRAPOLATE.

GROUP NO. 1

□ RSQRD 0.9728 SEE 0.0027

3 34 36 38

SPEC NO	MATERIAL	TEMP	ATM	FREQ	R	TYPE	THIK	REMARKS
7AN1025	PWA 1007	1200F	AIR	10 CPM	R=.5	RAD MCT	.300	OL1.5+20CY

-0.29 0. Y=0.5000 SINH(4.461 (X -1.294))-5.043

NRFT 5 (METRIC) Y=0.5000 SINH(4.461 (X -1.335))-3.638

*** IMPORTANT *** THIS EQUATION IS VALID BETWEEN X= 10.16 . AND X= 23.77 ONLY. DO NOT EXTRAPOLATE.

GROUP NO. 2

○ RSQRD 0.9939 SEE 0.0311

3 34 36 38

SPEC NO	MATERIAL	TEMP	ATM	FREQ	R	TYPE	THIK	REMARKS
7AN1021	PWA 1007	1200F	AIR	10 CPM	R=.5	RAD MCT	.302	OL1.5+40

-0.29 0. Y=0.5000 SINH(3.845 (X -1.334))-5.070

NRFT 5 (METRIC) Y=0.5000 SINH(3.845 (X -1.375))-3.605

*** IMPORTANT *** THIS EQUATION IS VALID BETWEEN X= 10.91 . AND X= 24.29 ONLY. DO NOT EXTRAPOLATE.

GROUP NO. 3

△ RSQRD 0.9959 SEE 0.0181

OVERALL STATISTICS FOR THIS COLLECTION OF GROUPS. TOTAL RSQRD = 0.9863. AND SEE,FRACTN,FIT. 0.0427

FD 169770

Figure 42. Statistics for Waspaloy (PWA 1007) Crack Propagation, Model of Effect of the Number of Cycles Between Overloads, R = 0.50, 0.167 Hz (10 cpm), 649°C (1200°F)

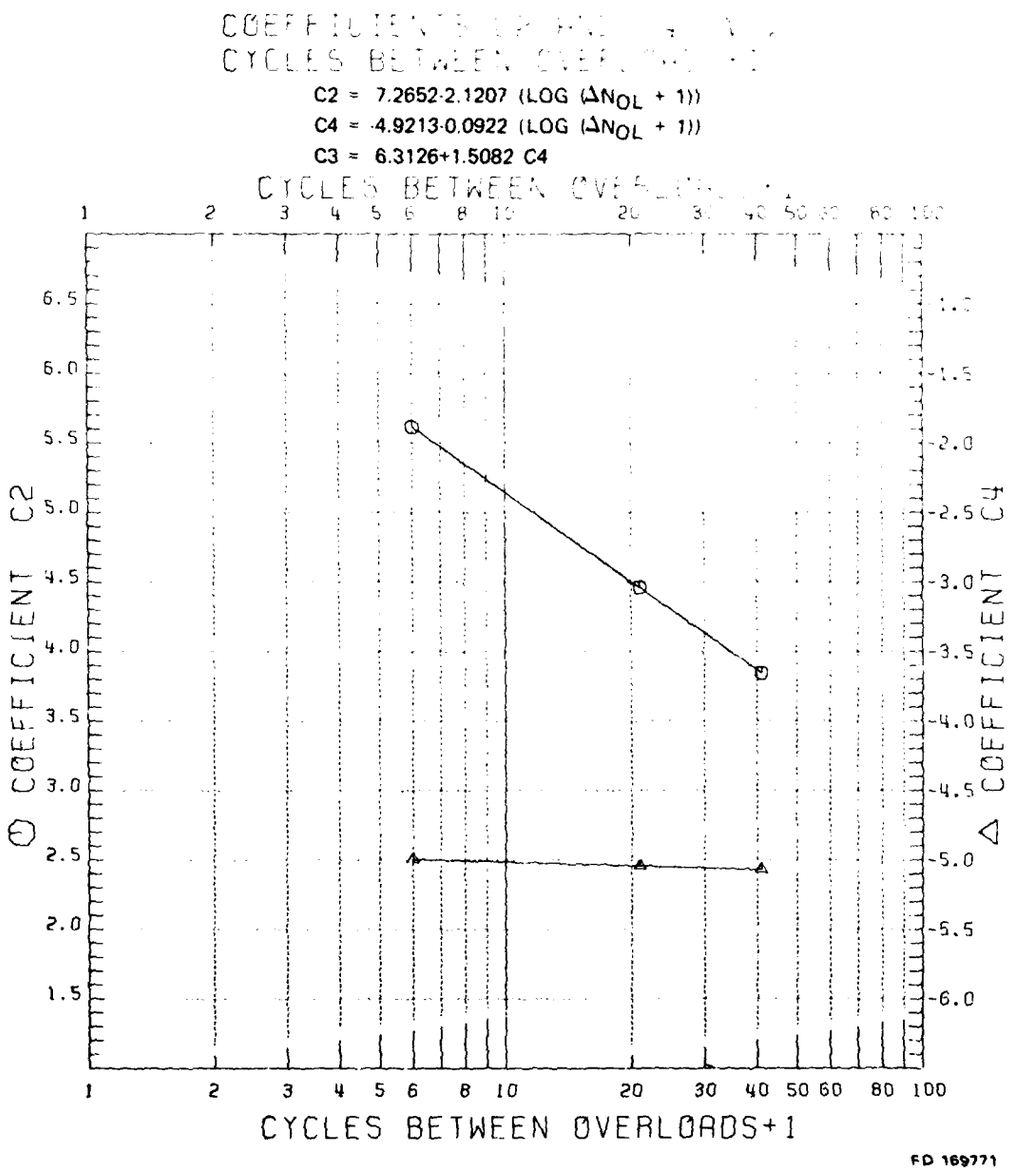

Figure 43. Waspaloy (PWA 1007) Crack Propagation, Correlative Parameters, Model of Effect of ΔN_{OL}, R = 0.50, 0.167 Hz (10 cpm), 649°C (1200°F)

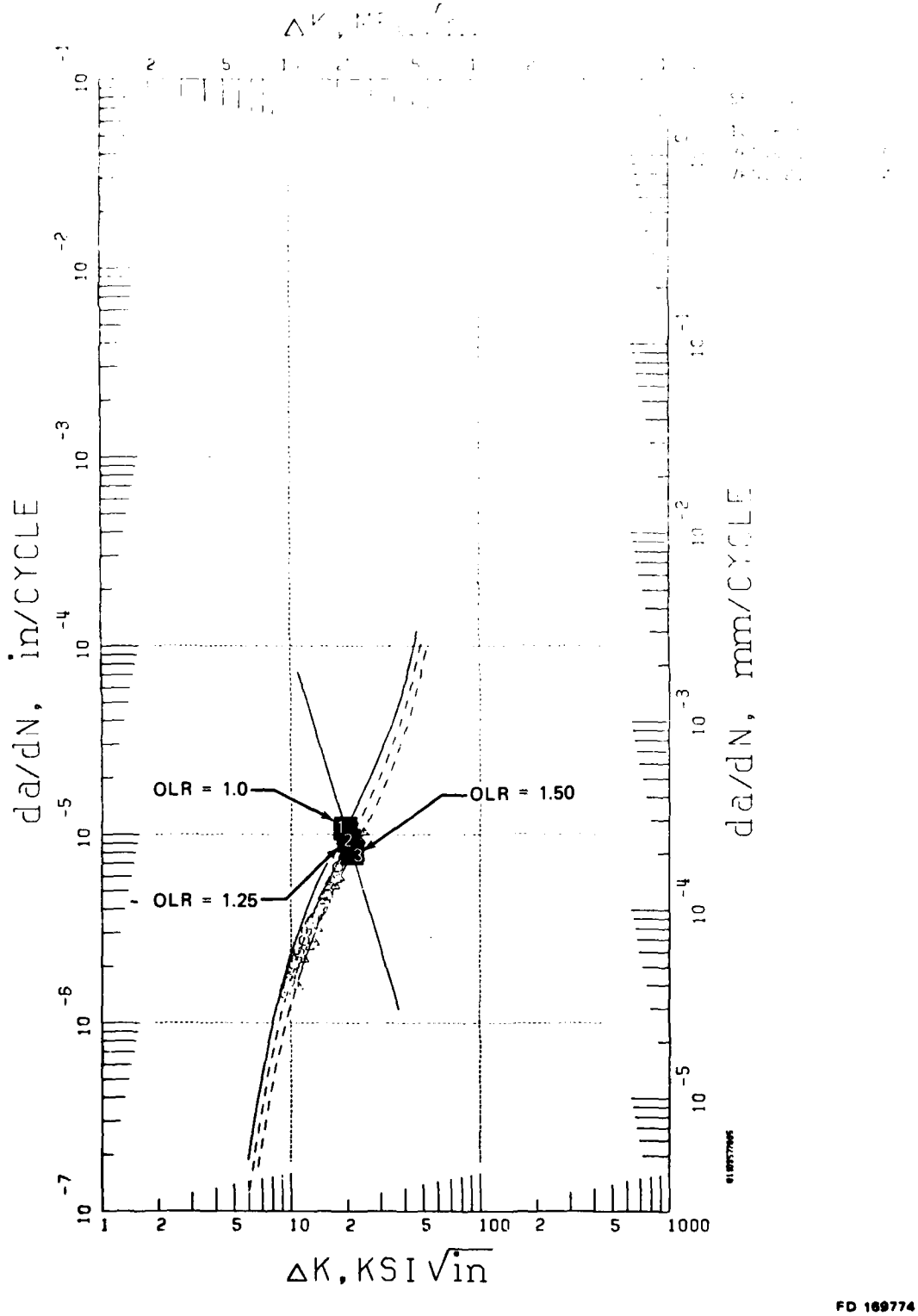

Figure 44. Waspaloy (PWA 1007) Crack Propagation, Overload Ratio Model, R = 0.50, 0.167 Hz (10 cpm), 649°C (1200°F)

```
PAGE   81407387929

  OLR =1.00
                                                    3  34 36 38
SPEC NO    MATERIAL   TEMP  ATM     FREQ      R     TYPE     THIK  REMARKS                    GROUP NO.    1
100 BASE   PWA 1007   1200F  AIR    10 CPM   R = 0.5
        -1.45 0.                 Y=0.5000 SINH(3.844 (X -1.288 ))-4.967                  □ RSQRD 0.0000  SEE 0.0000
       NAFT 6          (METRIC) Y=0.5000 SINH(3.844 (X -1.329 ))-3.562
     *** IMPORTANT ***  THIS EQUATION IS VALID BETWEEN  X= 1.00    , AND  X= 1000.000NLY.   DO NOT EXTRAPOLATE.

  OLR =1.25 + 40 CYCLES
                                                    3  34 36 38
SPEC NO    MATERIAL   TEMP  ATM     FREQ      R     TYPE     THIK  REMARKS                    GROUP NO.    2
7AN1028    PWA 1007  1200F AIR    10 CPM   R=.5   RA.  MCT  .301 OL1.25+40
        -1.45 0.                 Y=0.5000 SINH(3.845 (X -1.311 ))-5.018                  ○ RSQRD 0.9903  SEE 0.0546
       NAFT 6          (METRIC) Y=0.5000 SINH(3.845 (X -1.352 ))-3.613
     *** IMPORTANT ***  THIS EQUATION IS VALID BETWEEN  X= 9.26    , AND  X= 22.53   ONLY.   DO NOT EXTRAPOLATE.

  OLR = 1.50 + 40 CYCLES
                                                    3  34 36 38
SPEC NO    MATERIAL   TEMP  ATM     FREQ      R     TYPE     THIK  REMARKS                    GROUP NO.    3
7AN1021    PWA 1007  1200F AIR    10 CPM   R=.5   RA.  MCT  .302 OL1.5+40
        -1.45 0.                 Y=0.5000 SINH(3.846 (X -1.334 ))-5.069                  △ RSQRD 0.9971  SEE 0.0463
       NAFT 6          (METRIC) Y=0.5000 SINH(3.846 (X -1.375 ))-3.664
     *** IMPORTANT ***  THIS EQUATION IS VALID BETWEEN  X= 10.91   , AND  X= 24.29   ONLY.   DO NOT EXTRAPOLATE.

   OVERALL STATISTICS FOR THIS COLLECTION OF GROUPS.   TOTAL RSQRD = 0.8131,  AND   STD.ERROR.EST. = 1.0455
```

FD 169775

Figure 45. Statistics for Waspaloy (PWA 1007) Crack Propagation, Overload Ratio Model, R = 0.50, 0.167 Hz (10 cpm), 649°C (1200°F)

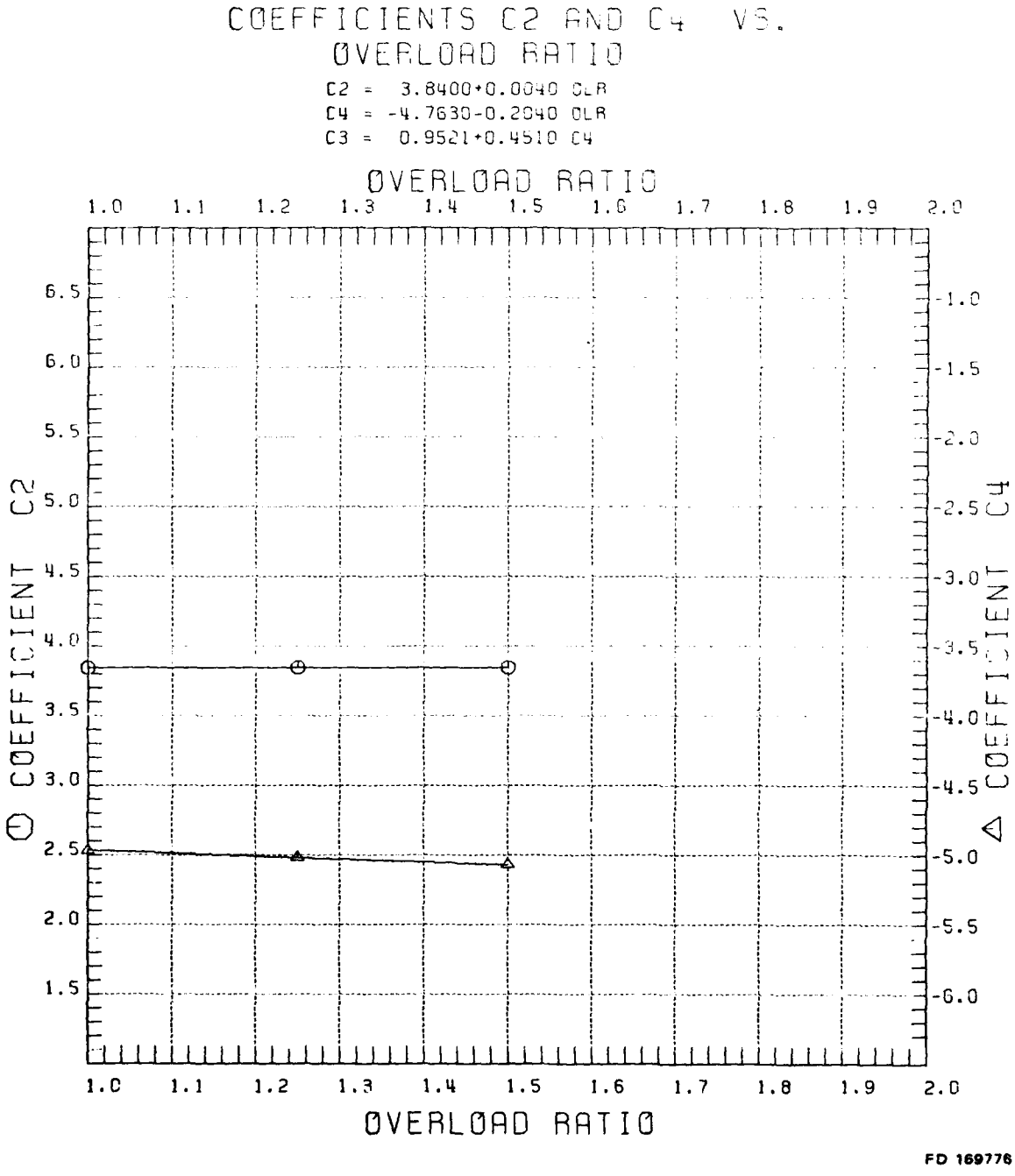

Figure 46. Waspaloy (PWA 1007) Crack Propagation, Overload Ratio Model Correlative Parameters, R = 0.50, 0.167 Hz (10 cpm), 649°C (1200°F)

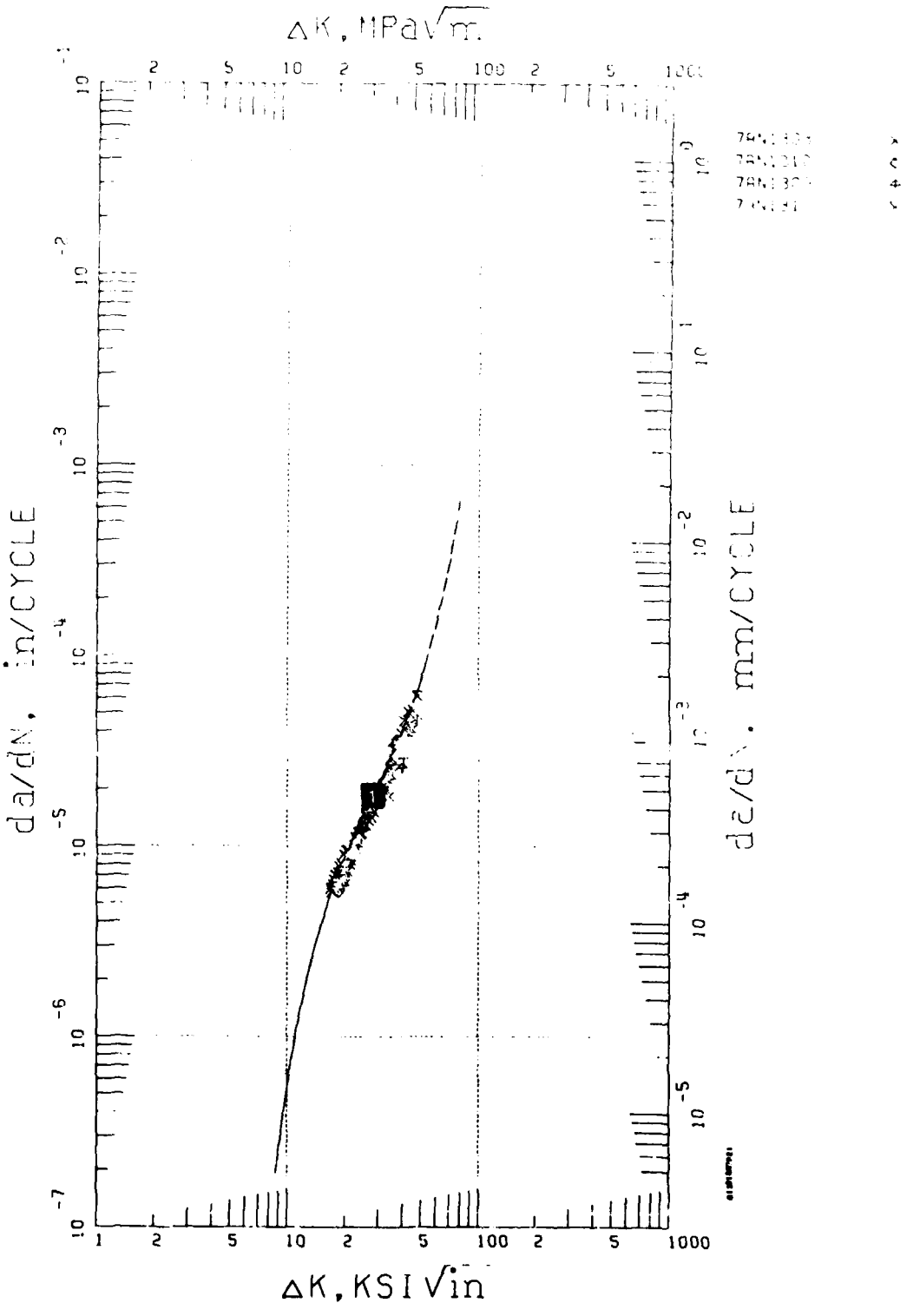

Figure 47. Waspaloy (PWA 1007) Crack Propagation, LCF-Dwell, R = 0.10, 649°C (1200°F), 0.167 (10 cpm) Sawtooth Fatigue Interrupted by Periodic 120 sec Load Dwell, ΔN_{Dwell} = 10, 20, and 40

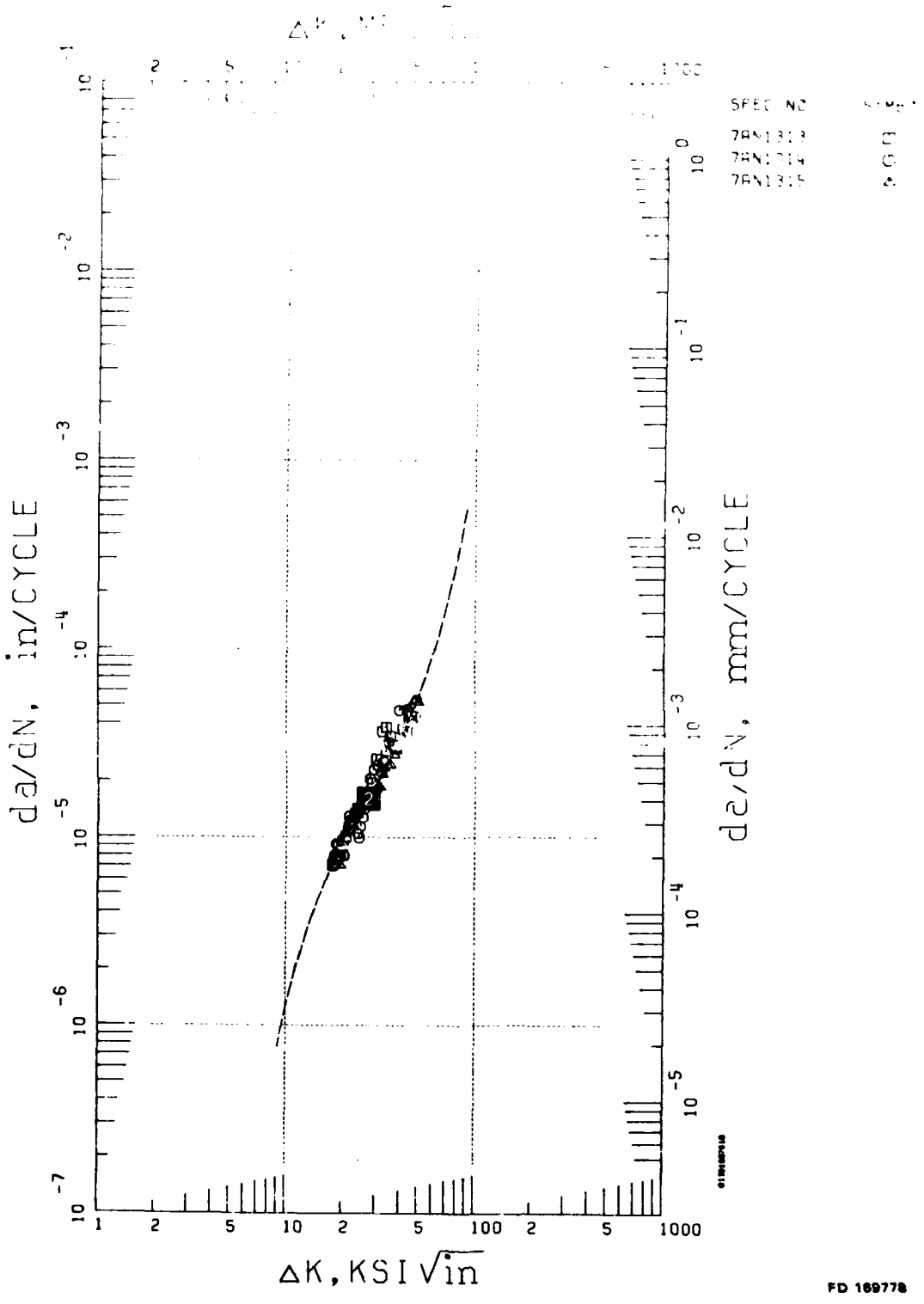

Figure 48. Waspaloy (PWA 1007) Crack Propagation, LCF - Dwell, R = 0.10, 732°C (1350°F), 0.167 (10 cpm) Sawtooth Fatigue Interrupted by Periodic 120 sec Load Dwell, ΔN_{Dwell} = 10, 20, and 40

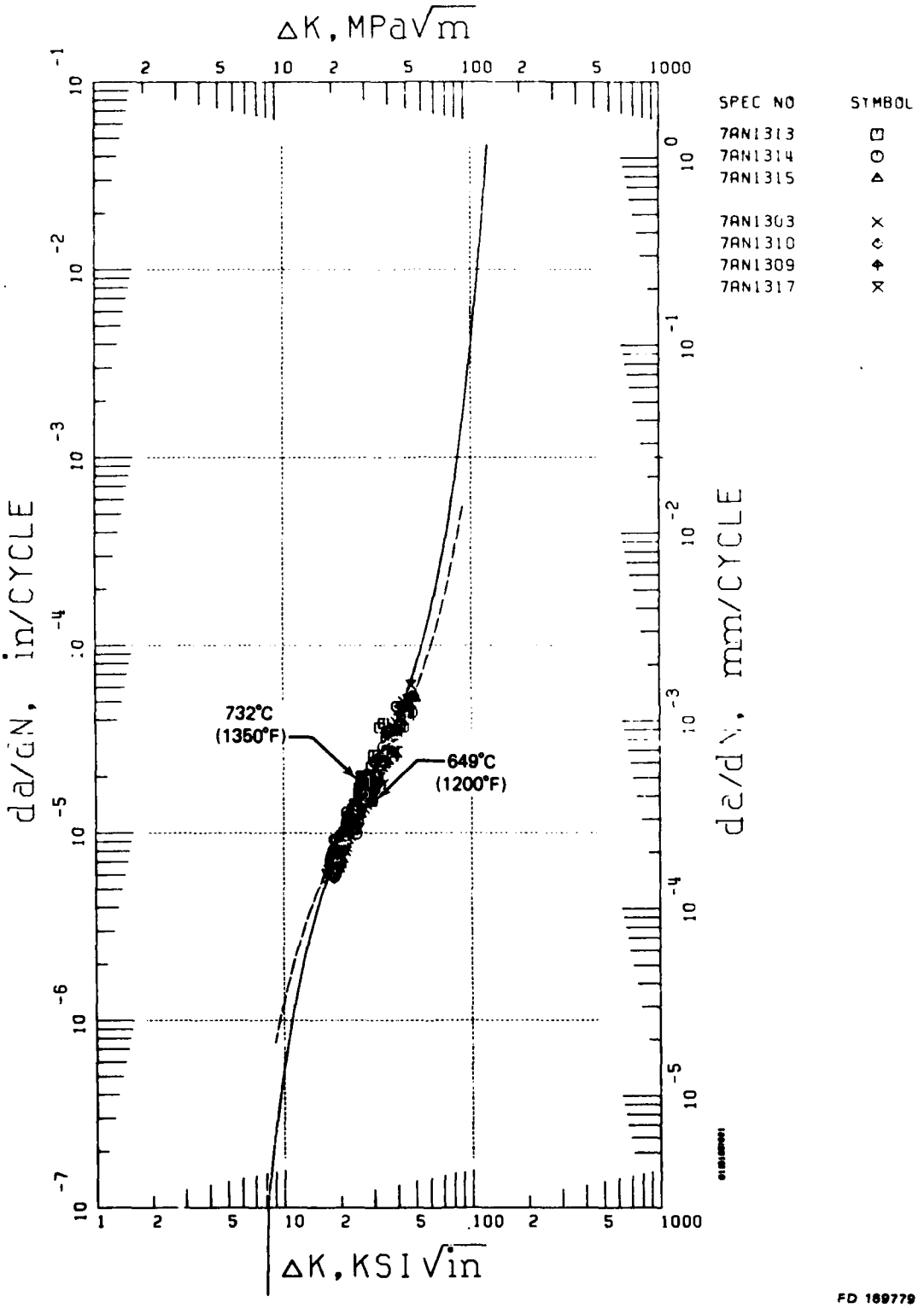

Figure 49. Waspaloy (PWA 1007) Temperature Model of LCF - Dwell Fatigue, R = 0.10

PAGE 81607167903

1350F, R=.1, 3 2 3 4 GROUP NO. 1

SPEC NO	MATERIAL	TEMP	ATM	FREQ	R	TYPE	THIK	REMARKS	
7AN1313	PWA 1007	1350F	AIR	10 CPM	R=.1	RAD MCT	.302	2MDWL+40CY	□
7AN1314	PWA 1007	1350F	AIR	10 CPM	R=.1	RAD MCT	.294	2MDWL+20CY	○
7AN1315	PWA 1007	1350F	AIR	10 CPM	R=.1	RAD MCT	.299	2MDWL+10CY	△ RSQRD 0.4679 SEE 1.3765

-0.78 0. Y=0.5000 SINH(3.534 (X -1.434))-4.796

NAFT 0 (METRIC) Y=0.5000 SINH(3.534 (X -1.475))-3.391

*** IMPORTANT *** THIS EQUATION IS VALID BETWEEN X= 17.75 , AND X= 50.53 ONLY. DO NOT EXTRAPOLATE.

1200F, R=.1, 3 2 3 4 GROUP NO. 2

SPEC NO	MATERIAL	TEMP	ATM	FREQ	R	TYPE	THIK	REMARKS	
7AN1303	PWA 1007	1200F	AIR	10 CPM	R=.1	RAD MCT	.500	2MDWL+20CY	×
7AN1310	PWA 1007	1200F	AIR	10 CPM	R=.1	RAD MCT	.292	2MDWL+20CY	◇
7AN1309	PWA 1007	1200F	AIR	10 CPM	R=.1	RAD MCT	.304	2MDWL+40CY	+
7AN1317	PWA 1007	1200F	AIR	10 CPM	R=.1	RAD MCT	.302	2MDWL+10CY	⊠ RSQRD 0.7072 SEE 1.3059

-0.78 0. Y=0.5000 SINH(4.080 (X -1.450))-4.731

NAFT 0 (METRIC) Y=0.5000 SINH(4.080 (X -1.491))-3.326

*** IMPORTANT *** THIS EQUATION IS VALID BETWEEN X= 16.86 , AND X= 48.17 ONLY. DO NOT EXTRAPOLATE.

OVERALL STATISTICS FOR THIS COLLECTION OF GROUPS. TOTAL RSQRD = 0.6130. AND STD.ERROR.EST. = 1.3272

FD 1697 80

Figure 50. Statistics for Waspaloy (PWA 1007) Temperature Model of LCF-Dwell Fatigue, R = 0.10

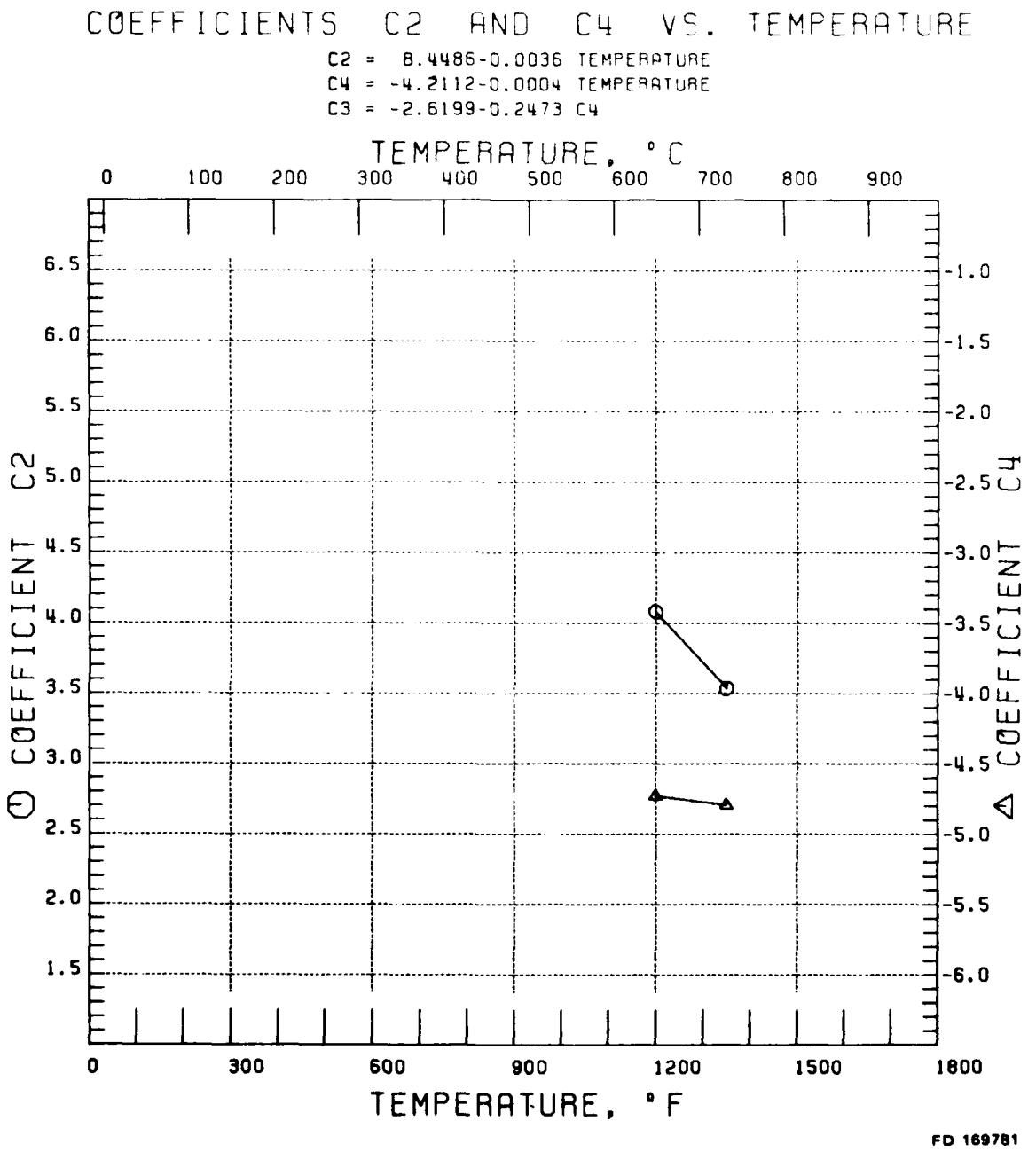

Figure 51. Waspaloy (PWA 1007) Crack Propagation, Correlative Parameters, for Temperature Model of LCF - Dwell Fatigue, R = 0.10

b. *GATORIZED*® IN100 (PWA 1073) Crack Propagation

The majority of the IN100 crack growth data presented in this section were generated under a previous AFML contract (References 1, 2, and 3). Additional data have been produced in testing under the current contract, and data from both sources have been employed in model development. The models are presented in the following sections.

(1) Basic Propagation, Constant Load Amplitude Cycling

(a) Effect of Loading Rate (Frequency)

The influence of cyclic frequency on crack growth in IN100 was examined over the range 0.00833 (0.5 cpm) ≤ frequency ≤ 20 Hz, at 649°C and R = 0.1. An interpolative model of the effect of frequency developed from this data is shown in Figure 52 and Figure 53 shows the statistics. The SINH coefficients C2 and C4 are linear functions of log (frequency) over the full range of the model. However, this is not the case for the coefficient C3 which locates the abscissa of the SINH inflection points. As illustrated in Figure 54, C3 is represented as a linear function for 0.00833 Hz (0.5 cpm) ≤ frequency ≤ 0.167 Hz (10 cpm), and a second function is defined over the range 0.167 Hz (10 cpm) ≤ frequency ≤ 20 Hz. This relationship was required in order to produce an adequate description of the data over the range of testing. The 0.00833 Hz (0.5 cpm) data exhibit anomalous test-to-test variability. All specimens were tested at identical conditions (0.00833 Hz (10 cpm), R = 0.10, 649°C); however, specimen 604 AF exhibited a much slower crack growth rate than the population of tests. In fact, the data of 604 AF agree well with the results of 0.167 (10 cpm). This variability cannot be attributed to heat-to-heat effects, since specimen 605 AF (which is in agreement with the remaining data) was taken from the same heat of material as 604 AF. While no error in the 604 AF data analysis or the recorded test conditions can be found, an unknown error in testing is believed to be responsible for the anomalous behavior.

(b) Effect of Stress Ratio, 0.167 Hz

An interpolative model of the effect of stress ratio on crack propagation in IN100 (PWA 1073) was developed from data over the range 0.1 ≤ R ≤ 0.8. The cyclic frequency was 0.167 Hz and the test temperature was 649°C. The base condition of R = 0.10 is defined by a collection of data from six tests and three heats of material. The composite SINH model for the effect of stress ratio is illustrated in Figure 55 and Figure 56 gives the statistics. The associated correlative parameters are linear functions of log (1-R) for positive stress ratios as shown in Figure 57.

The effect of negative stress ratio fatigue on crack propagation of IN100 is discussed under auxiliary investigations.

(c) Effect of Stress Ratio, 20 Hz

The effect of stress ratio on crack growth in IN100 (PWA 1073) fatigued at a frequency of 20 Hz, is described by the model shown in Figure 58, and Figure 59 reviews the statistics. The defining SINH coefficients are illustrated in Figure 60.

(d) Effect of Temperature

Results of crack propagation testing of IN100 (PWA 1073) conducted at 0.167 Hz, R = 0.1, and 538°C (1000°F) ≤ T ≤ 732°C (1350°F), were used to develop an interpolative SINH model of the effect of temperature. This model is presented in Figure 61, the statistics presented in Figure 62, and the defining SINH coefficients are given in Figure 63.

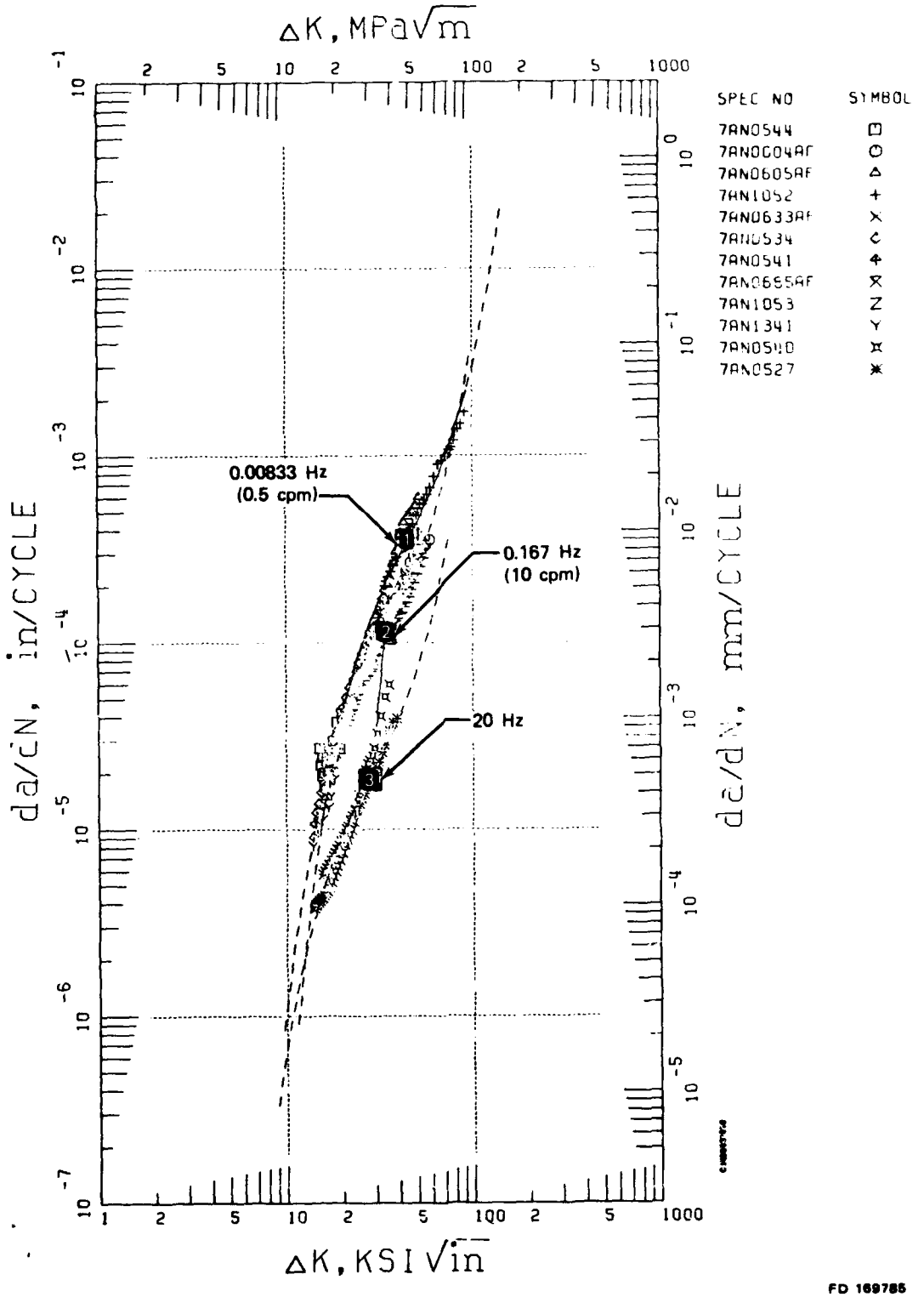

Figure 52. IN100 (PWA 1073) Crack Propagation, Frequency Model, R = 0.10, 649°C (1200°F)

```
PAGE  81409437948

  R=.1 T=1200F FREQ=.5CPM                          3 3 7 11                          GROUP NO.    1
SPEC NO    MATERIAL   TEMP  ATM    FREQ     R    TYPE    THIK  REMARKS
7AN0544    PWA 1073   1200F AIR    .5 CPM  R=.1  RAD MCT  .469 BAER                  □
7AN0604AF  PWA 1073   1200F AIR    .5 CPM  R=.1  RAD MCT                           ○
7AN0605AF  PWA 1073   1200F AIR    .5 CPM  R=.1  RAD MCT                           △
7AN1052    PWA 1073   1200F AIR    .5 CPM  R=.1  RAD MCT  .285                     + RSQRD 0.9380  SEE 0.1357
        -1.87 0.              Y=0.5000 SINH(3.960 (X -1.651 ))-3.454
       NRFT 2          (METRIC)Y=0.5000 SINH(3.960 (X -1.692 ))-2.650
     *** IMPORTANT *** THIS EQUATION IS VALID BETWEEN  X= 15.11  , AND  X= 90.97  ONLY.  DO NOT EXTRAPOLATE.

  R=.1 T=1200 FREQ=10CPM                           3 3 7 11                          GROUP NO.    2
SPEC NO    MATERIAL   TEMP  ATM    FREQ     R    TYPE    THIK  REMARKS
7AN0633AF  PWA 1073   1200F AIR   10 CPM  R=.1  RAD MCT  .250                     X
7AN0534    PWA 1073   1200F AIR   10 CPM  R=.1  RAD MCT  .5                       ◇
7AN0541    PWA 1073   1200F AIR   10 CPM  R=.1  RAD MCT .4995 HAEP               ✦
7AN0685AF  PWA 1073   1200F AIR   10 CPM  R=.1  RAD MCT  .870                     ⋈
7AN1053    PWA 1073   1200F AIR   10 CPM  R=.1  RAD MCT  .299                     Z
7AN1341    PWA 1073   1200F AIR   10 CPM  R=.1  RAD CR   .296                     Y RSQRD 0.9803  SEE 0.0531
        -1.87 0.              Y=0.5000 SINH(3.961 (X -1.529 ))-3.947
       NRFT 2          (METRIC)Y=0.5000 SINH(3.961 (X -1.570 ))-2.542
     *** IMPORTANT *** THIS EQUATION IS VALID BETWEEN  X= 13.76  , AND  X= 55.79  ONLY.  DO NOT EXTRAPOLATE.

  R=.1 T=1200F FREQ=20HZ                           3 3 7 11                          GROUP NO.    3
SPEC NO    MATERIAL   TEMP  ATM    FREQ     R    TYPE    THIK  REMARKS
7AN0540    PWA 1073   1200F AIR    20 HZ   R=.1  RAD MCT  .412                     ⋈
7AN0527    PWA 1073   1200F AIR    20 HZ   R=.1  RAD MCT  .25  BA1080H28  R       * RSQRD 0.9486  SEE 0.0817
        -1.87 0.              Y=0.5000 SINH(3.962 (X -1.448 ))-4.734
       NRFT 2          (METRIC)Y=0.5000 SINH(3.962 (X -1.489 ))-3.329
     *** IMPORTANT *** THIS EQUATION IS VALID BETWEEN  X= 14.07  , AND  X= 39.07  ONLY.  DO NOT EXTRAPOLATE.

   OVERALL STATISTICS FOR THIS COLLECTION OF GROUPS.   TOTAL RSQRD = 0.9789.  AND   STD.ERROR.EST. = 0.0861
                                                                                    FD 189786
```

Figure 53. Statistics for IN100 (PWA 1073) Crack Propagation, Frequency Model, R = 0.10, 649°C (1200°F)

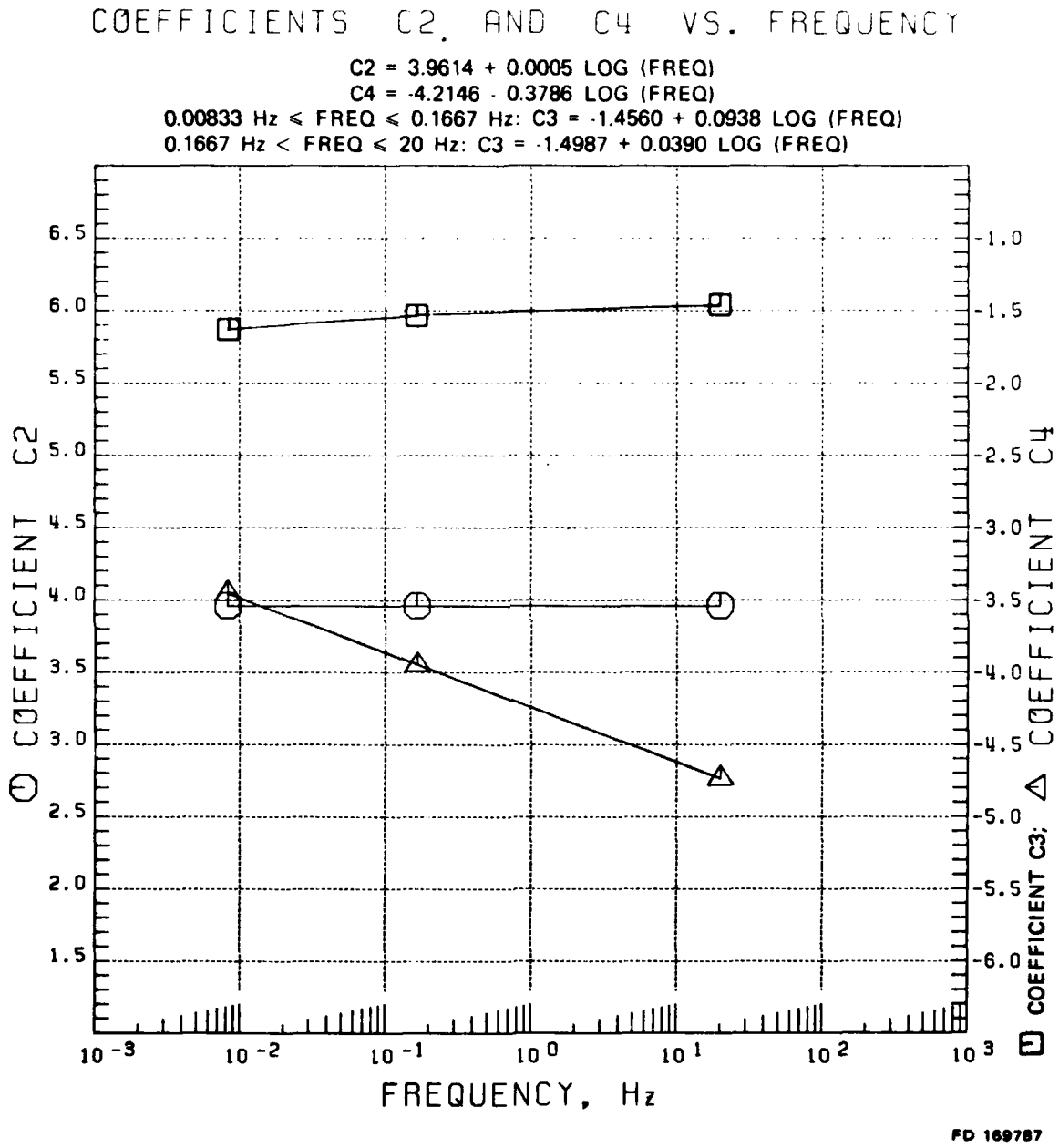

Figure 54. IN100 (PWA 1073) Crack Propagation, Frequency Model Correlative Parameters, R = 0.10, 649°C (1200°F)

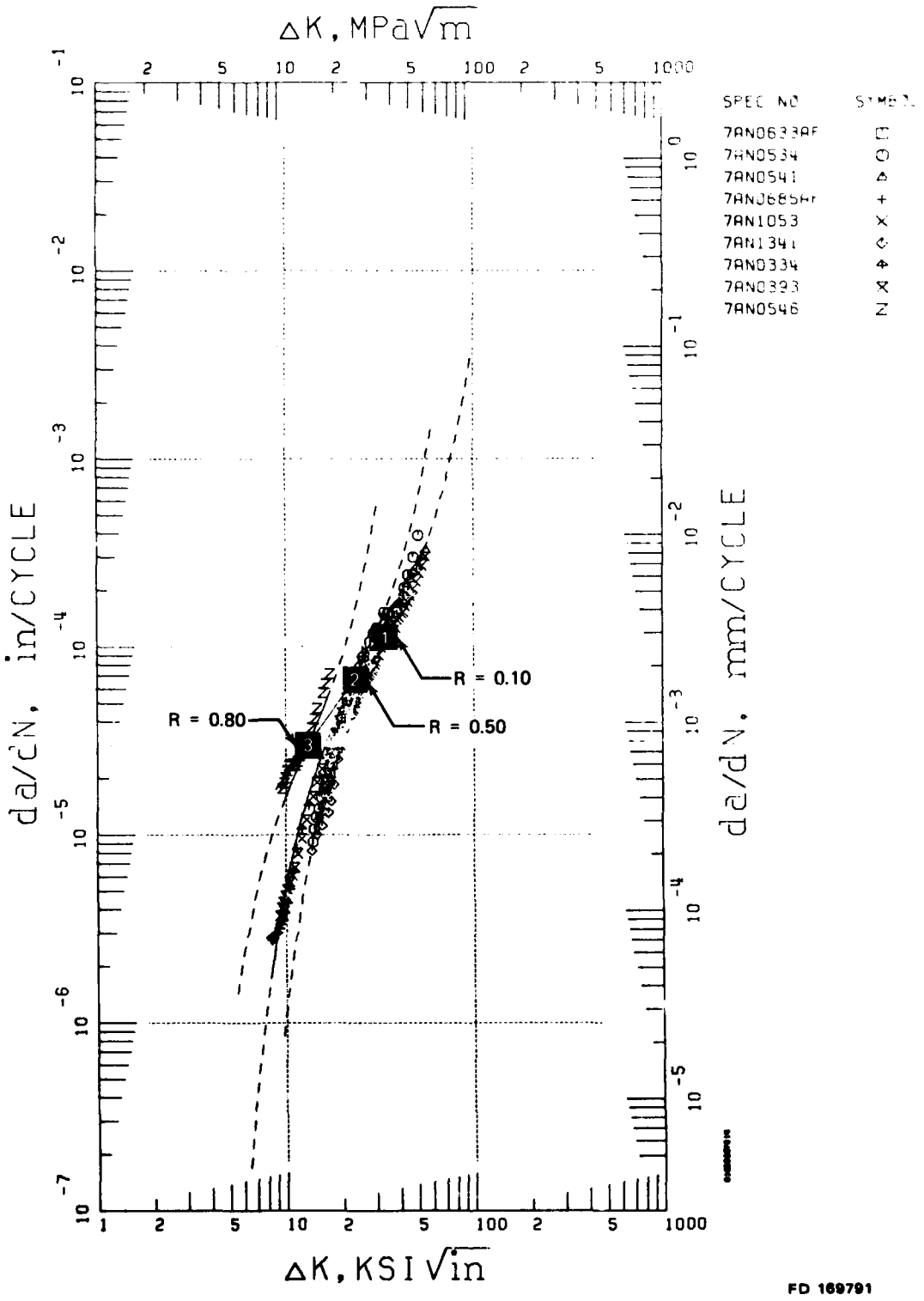

Figure 55. IN100 (PWA 1073) Crack Propagation, Stress Ratio Model, 0.167 Hz (10 cpm), 649° (1200°F)

PAGE 81608267914

R=.1 T=1200F FREQ=10CPM 6 33 34 35 36 37 38 GROUP NO. 1

SPEC NO	MATERIAL	TEMP	ATM	FREQ	R	TYPE	THIK	REMARKS	
7AN0633AF	PWA 1073	1200F	AIR	10 CPM	R=.1	RAD MCT	.250		□
7AN0534	PWA 1073	1200F	AIR	10 CPM	R=.1	RAD MCT	.5		○
7AN0541	PWA 1073	1200F	AIR	10 CPM	R=.1	RAD MCT	.4995	HAEP	△
7AN0685AF	PWA 1073	1200F	AIR	10 CPM	R=.1	RAD MCT	.870		+
7AN1053	PWA 1073	1200F	AIR	10 CPM	R=.1	RAD MCT	.299		×
7AN1341	PWA 1073	1200F	AIR	10 CPM	R=.1	RAD CN	.296		◇ RSQRD 0.9803 SEE 0.0531

-1.16 0. Y=0.5000 SINH(3.961 (X -1.529))-3.947
NAFT 1 (METRIC) Y=0.5000 SINH(3.961 (X -1.570))-2.542
*** IMPORTANT *** THIS EQUATION IS VALID BETWEEN X= 13.76 . AND X= 55.79 ONLY. DO NOT EXTRAPOLATE.

R=.5 T=1200F FREQ=10CPM 6 33 34 35 36 37 38 GROUP NO. 2

SPEC NO	MATERIAL	TEMP	ATM	FREQ	R	TYPE	THIK	REMARKS	
7AN0334	PWA 1073	1200F	AIR	10 CPM	R=.5	RAD MCT	.5	BAEPB3H9	▲
7AN0393	PWA 1073	1200F	AIR	10 CPM	R=.5	RAD MCT	.5		⊠ RSQRD 0.9845 SEE 0.0793

-1.15 0. Y=0.5000 SINH(4.192 (X -1.368))-4.172
NAFT 1 (METRIC) Y=0.5000 SINH(4.192 (X -1.409))-2.767
*** IMPORTANT *** THIS EQUATION IS VALID BETWEEN X= 8.33 . AND X= 33.17 ONLY. DO NOT EXTRAPOLATE.

R=.8 T=1200F FREQ=10CPM 6 33 34 35 36 37 38 GROUP NO. 3

SPEC NO	MATERIAL	TEMP	ATM	FREQ	R	TYPE	THIK	REMARKS	
7AN0546	PWA 1073	1200F	AIR	10 CPM	R=.8	RAD MCT	.503	HAEP	Z RSQRD 0.9689 SEE 0.0841

-1.16 0. Y=0.5000 SINH(4.551 (X -1.117))-4.522
NAFT 1 (METRIC) Y=0.5000 SINH(4.551 (X -1.158))-3.117
*** IMPORTANT *** THIS EQUATION IS VALID BETWEEN X= 9.55 . AND X= 17.15 ONLY. DO NOT EXTRAPOLATE.

OVERALL STATISTICS FOR THIS COLLECTION OF GROUPS. TOTAL RSQRD = 0.9842. AND STD.ERROR.EST. = 0.0604

FD 169792

Figure 56. Statistics for IN100 (PWA 1073) Crack Propagation, Stress Ratio Model, 0.167 Hz (10 cpm), 649°C (1200°F)

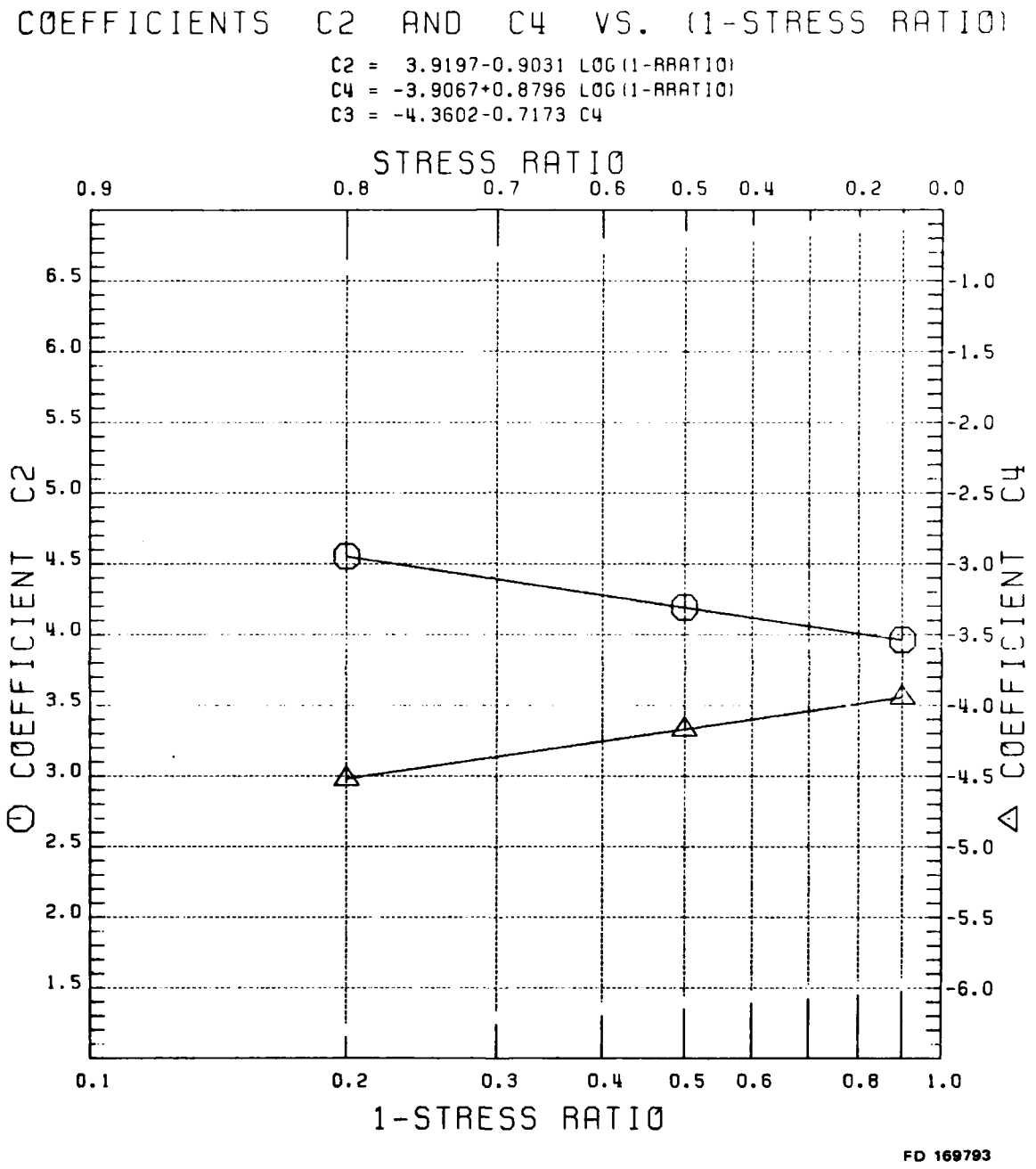

Figure 57. IN100 (PWA 1073) Crack Propagation, Stress Ratio Model Correlative Parameters, 0.167 Hz (10 cpm), 649°C (1200°F)

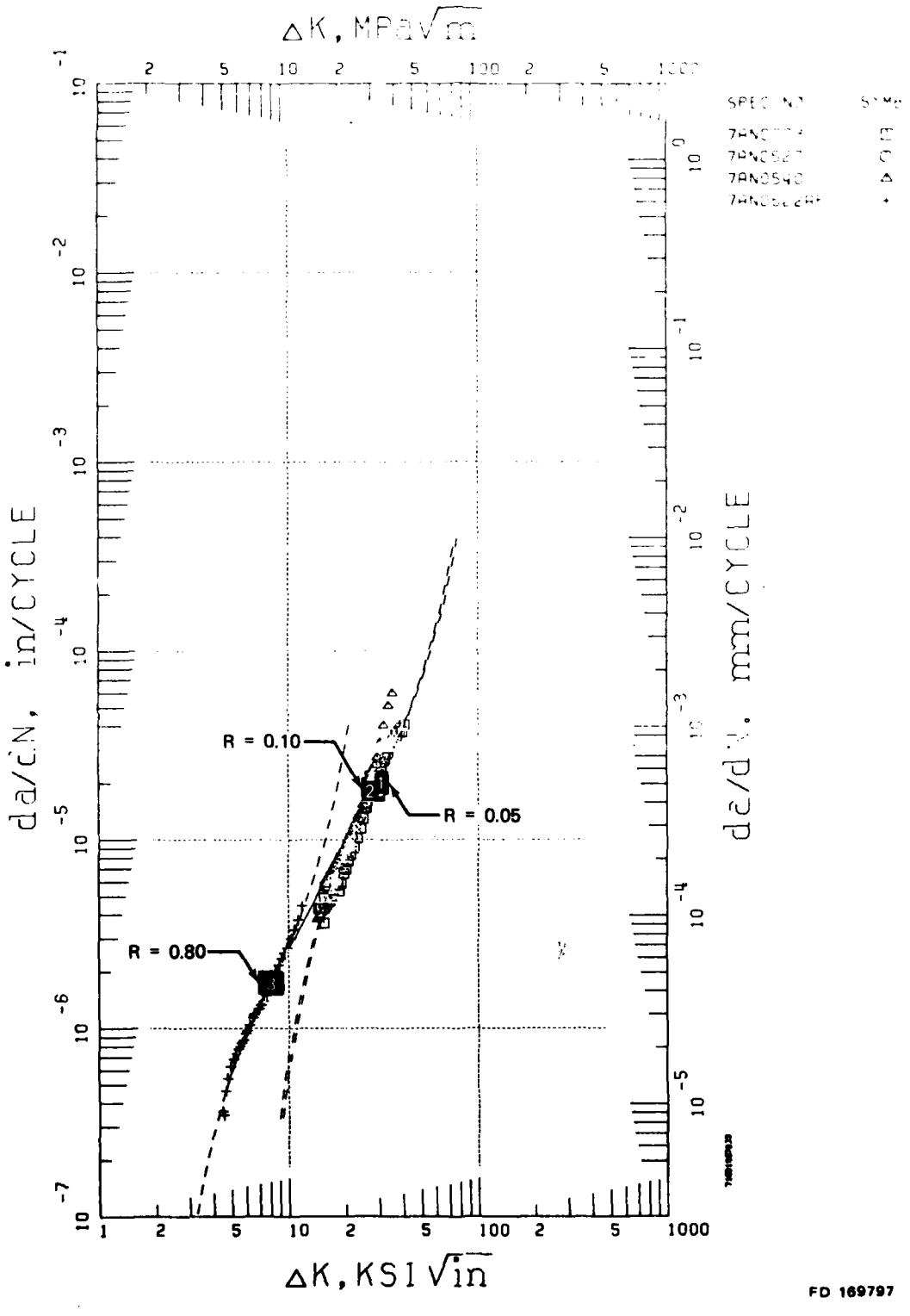

Figure 58. IN100 (PWA 1073) Crack Propagation, Stress Ratio Model, 20 Hz, 649°C (1200°F)

PAGE 71031487933

1200F, R=.05, IN100 F MODEL 3 34 36 38 GROUP NO. 1

SPEC NO	MATERIAL	TEMP	ATM	FREQ	R	TYPE	THIK	REMARKS
7AN0703	PWA 1073	1200F	AIR	20 HZ	R=.05	RAD MCT	.249	

□ RSQRD 0.9570 SEE 0.0748

-0.41 0. Y=0.5000 SINH(3.955 (X -1.468))-4.697

NAFT 1 (METRIC) Y=0.5000 SINH(3.955 (X -1.508))-3.292

*** IMPORTANT *** THIS EQUATION IS VALID BETWEEN X= 14.38 , AND X= 41.30 ONLY. DO NOT EXTRAPOLATE.

1200F, R=.1, 20 HZ, IN100 3 34 36 38 GROUP NO. 2

SPEC NO	MATERIAL	TEMP	ATM	FREQ	R	TYPE	THIK	REMARKS
7AN0527	PWA 1073	1200F	AIR	20 HZ	R=.1	RAD MCT	.25	BA10B3H28 R
7AN0540	PWA 1073	1200F	AIR	20 HZ	R=.1	RAD MCT	.442	

○

△ RSQRD 0.9487 SEE 0.0817

-0.41 0. Y=0.5000 SINH(3.962 (X -1.448))-4.734

NAFT 1 (METRIC) Y=0.5000 SINH(3.962 (X -1.489))-3.329

*** IMPORTANT *** THIS EQUATION IS VALID BETWEEN X= 14.07 , AND X= 39.07 ONLY. DO NOT EXTRAPOLATE.

1200F, R=.8, 20 HZ, IN100 3 34 36 38 GROUP NO. 3

SPEC NO	MATERIAL	TEMP	ATM	FREQ	R	TYPE	THIK	REMARKS
7AN0622AF	PWA 1073	1200F	AIR	20 HZ	R=.8	RAD MCT	.206	

+ RSQRD 0.9910 SEE 0.0[illegible]

-0.41 0. Y=0.5000 SINH(4.170 (X -0.904))-5.758

NAFT 1 (METRIC) Y=0.5000 SINH(4.170 (X -0.945))-4.353

*** IMPORTANT *** THIS EQUATION IS VALID BETWEEN X= 4.48 , AND X= 11.78 ONLY. DO NOT EXTRAPOLATE.

OVERALL STATISTICS FOR THIS COLLECTION OF CRC FS, TOTAL RSQRD = 0.9827, AND STD.ERROR.EST. = 0.0095

FD 169799

Figure 59. Statistics for IN100 (PWA 1073) Crack Propagation, Stress Ratio Model, 20 Hz, 649°C (1200°F)

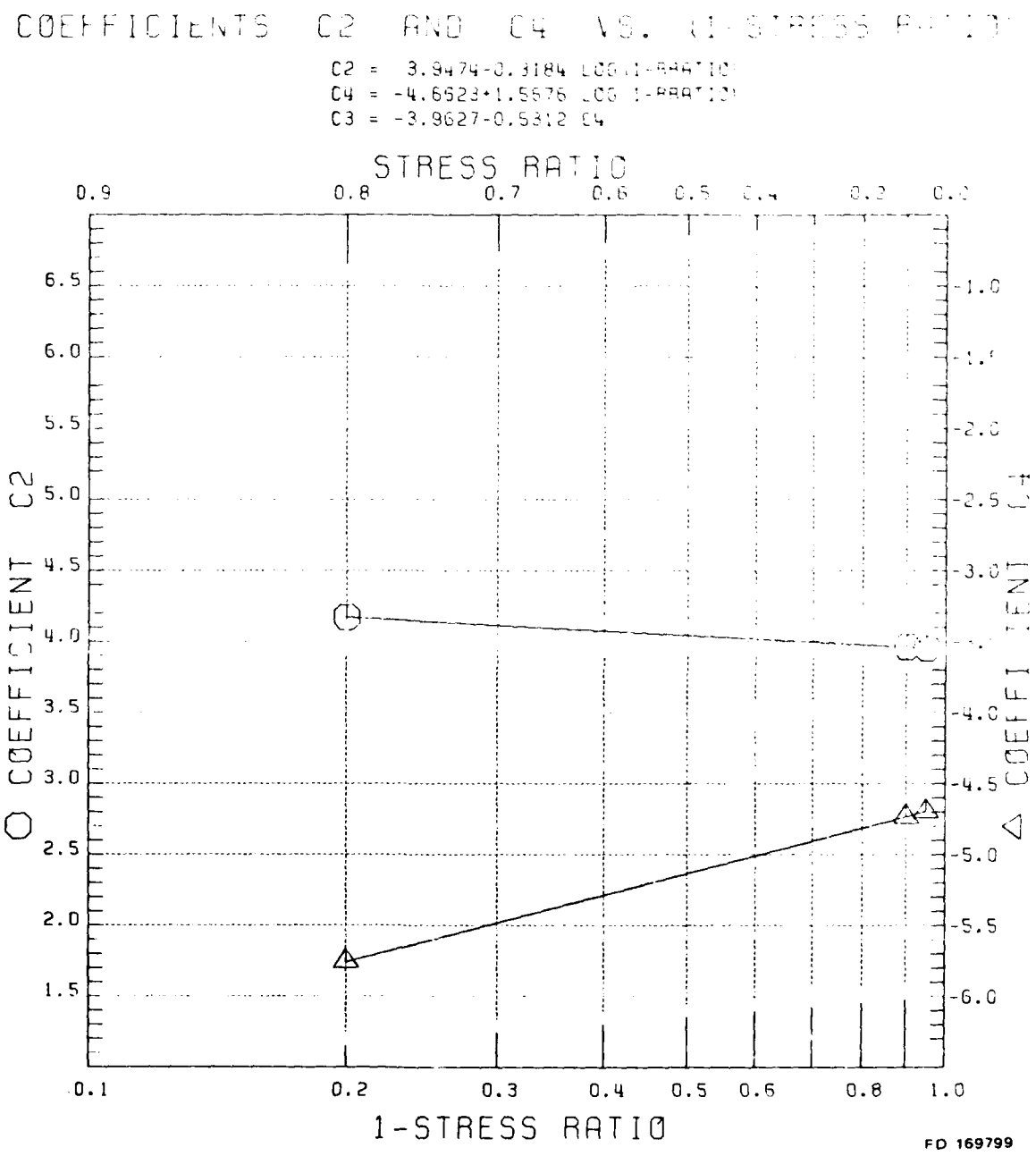

Figure 60. IN100 (PWA 1073) Crack Propagation, Stress Ratio Model Correlative Parameters, 20 Hz, 649°C (1200°F)

AD-A084 934 PRATT AND WHITNEY AIRCRAFT GROUP WEST PALM BEACH FL G--ETC F/G 21/5
CUMULATIVE DAMAGE FRACTURE MECHANICS UNDER ENGINE SPECTRA.(U)
JAN 80 J M LARSEN, B J SCHWARTZ, C G ANNIS F33615-77-C-5153
UNCLASSIFIED PWA-FR-11844 AFML-TR-79-4189 NL

2 OF 3
AD
A084934

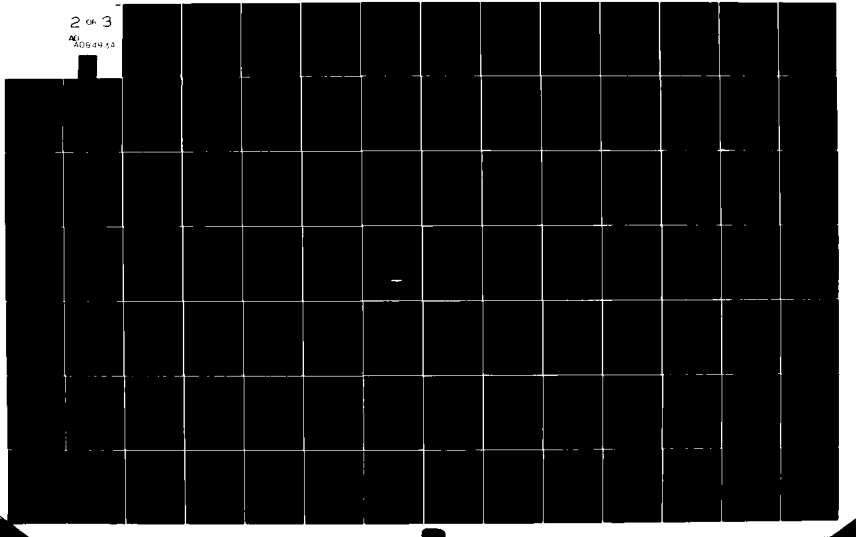

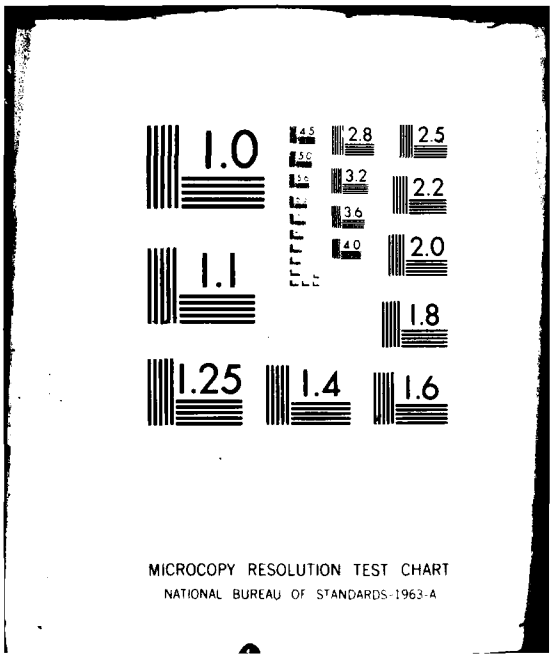
1.0
1.1
1.25
1.4
1.6
1.8
2.0
2.2
2.5
2.8
3.2
3.6
4.0
MICROCOPY RESOLUTION TEST CHART
NATIONAL BUREAU OF STANDARDS-1963-A

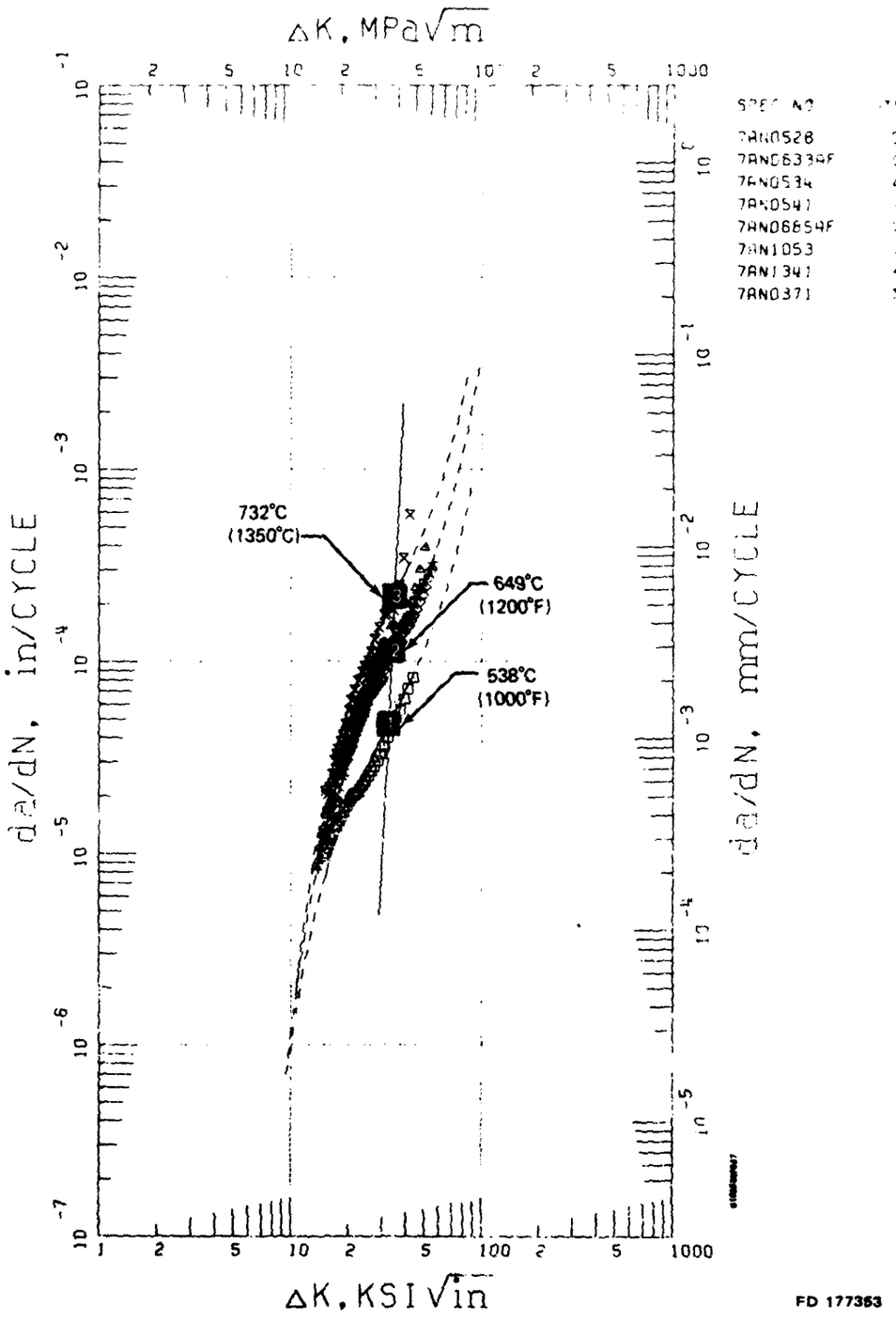

Figure 61. IN100 (PWA 1073) Crack Propagation, Temperature Model, R = 0.10, 0.167 Hz (10 cpm)

PAGE 81608237937

R=.1 T=1000F FREQ=10CPM 3 34 36 38 GROUP NO. 1

SPEC NO	MATERIAL	TEMP	ATM	FREQ	R	TYPE	THIK	REMARKS	
7AN0528	PWA 1073	1000F	AIR	10 CPM	R=.1	RAD MCT	.250	BA10B3H28	□ RSQRD 0.9778 SEE 0.0735

-0.09 0. Y=0.5000 SINH(3.761 (X -1.511))-4.327

NRFT 3 (METRIC) Y=0.5000 SINH(3.761 (X -1.552))-2.922

*** IMPORTANT *** THIS EQUATION IS VALID BETWEEN X= 14.77 . AND X= 43.91 ONLY. DO NOT EXTRAPOLATE.

R=.1 T=1200F FREQ=10CPM 3 34 36 38 GROUP NO. 2

SPEC NO	MATERIAL	TEMP	ATM	FREQ	R	TYPE	THIK	REMARKS	
7AN0633AF	PWA 1073	1200F	AIR	10 CPM	R=.1	RAD MCT	.250		○
7AN0534	PWA 1073	1200F	AIR	10 CPM	R=.1	RAD MCT	.5		△
7AN0541	PWA 1073	1200F	AIR	10 CPM	R=.1	RAD MCT	.4995	HAEP	+
7AN0685AF	PWA 1073	1200F	AIR	10 CPM	R=.1	RAD MCT	.870		×
7AN1053	PWA 1073	1200F	AIR	10 CPM	R=.1	RAD MCT	.299		◇
7AN1341	PWA 1073	1200F	AIR	10 CPM	R=.1	RAD CN	.296		♠ RSQRD 0.9803 SEE 0.0531

-0.09 0. Y=0.5000 SINH(3.961 (X -1.529))-3.947

NRFT 3 (METRIC) Y=0.5000 SINH(3.961 (X -1.570))-2.542

*** IMPORTANT *** THIS EQUATION IS VALID BETWEEN X= 13.76 . AND X= 55.79 ONLY. DO NOT EXTRAPOLATE.

R=.1 T=1350F FREQ=10CPM 3 34 36 38 GROUP NO. 3

SPEC NO	MATERIAL	TEMP	ATM	FREQ	R	TYPE	THIK	REMARKS	
7AN0371	PWA 1073	1350F	AIR	10CPM	R=.1	RAD MCT			⧖ RSQRD 0.9816 SEE 0.0628

-0.09 0. Y=0.5000 SINH(4.111 (X -1.543))-3.662

NRFT 3 (METRIC) Y=0.5000 SINH(4.111 (X -1.584))-2.257

*** IMPORTANT *** THIS EQUATION IS VALID BETWEEN X= 15.18 . AND X= 42.06 ONLY. DO NOT EXTRAPOLATE.

OVERALL STATISTICS FOR THIS COLLECTION OF GROUPS. TOTAL RSQRD = 0.9801. AND STD.ERROR.EST. = 0.0563

FD 177354

Figure 62. Statistics for IN100 (PWA 1073) Crack Propagation, Temperature Model, R = 0.10, 0.167 Hz (10 cpm)

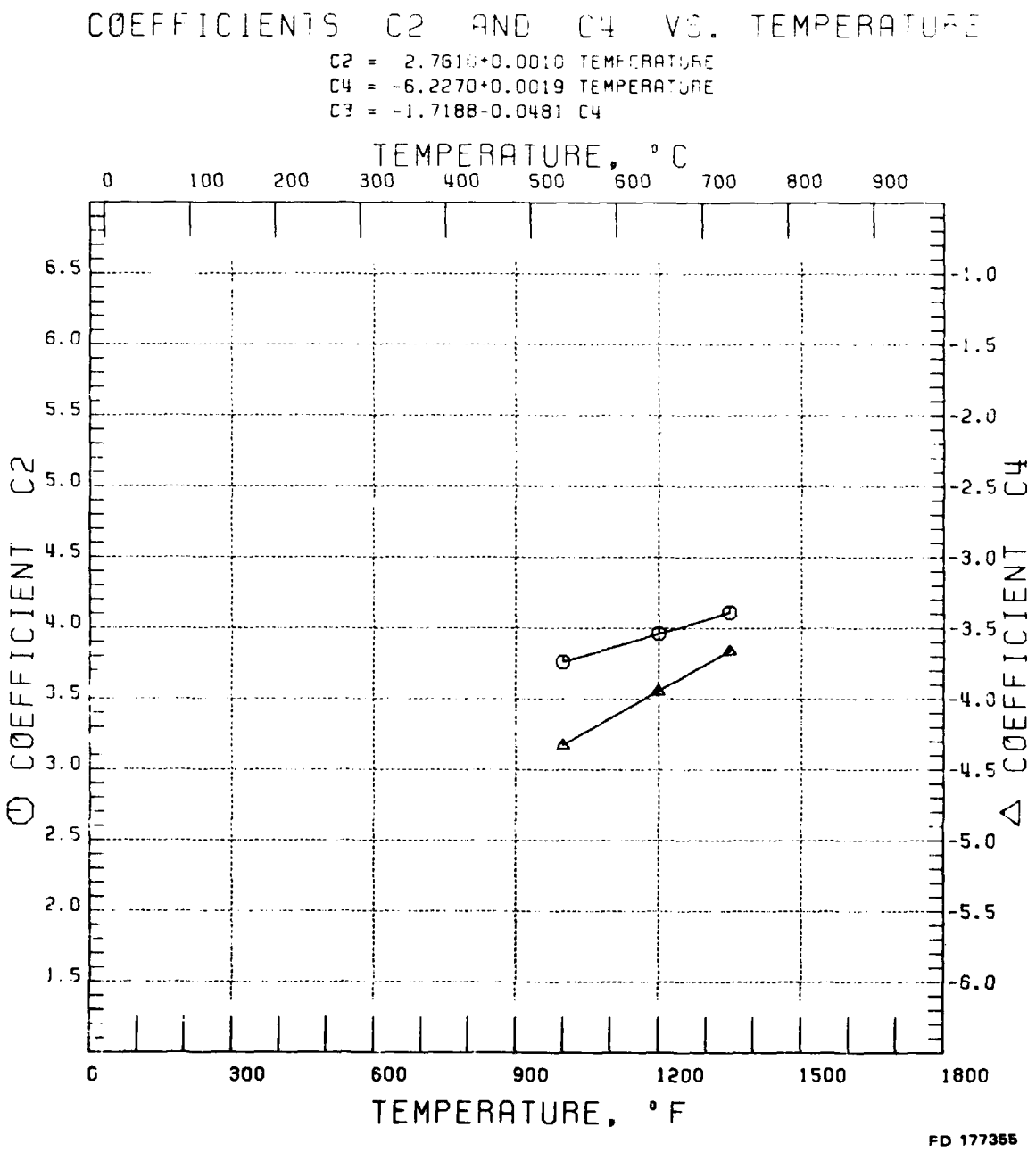

Figure 63. IN100 (PWA 1073) Crack Propagation, Temperature Model Correlative Parameters, R = 0.10, 0.167 Hz (10 cpm)

(2) Crack Propagation Under Periodic Load Dwell

(a) Effect of Load Dwell, 649°C (1200°F)

Crack propagation under periodic load dwell in GATORIZED® IN100 (PWA 1073) was investigated using the repetitive loading shown in Figure 12. The period of load dwell was 60, 120, and 600 sec, in three tests where R = 0.10 and T = 649°C. The composite model of the effect of the period of load dwell is illustrated in Figure 65. Figure 64 lists the statistics. The interpolative SINH coefficients are shown in Figure 66.

(b) Effect of Load Dwell, 732°C (1350°F)

The effect of period of load dwell on crack growth in IN100 tested at 732°C is described by the interpolative SINH model presented in Figure 67. Figure 68 gives the statistics. The increased crack growth rate associated with increased dwell period is correlated with the SINH coefficients as shown in Figure 69.

(3) Sustained Load Crack Growth

Under a previous Air Force program the sustained load crack growth behavior of IN100 (PWA 1073) was determined (Reference 2). The experimental and analytical procedures used were the same as described earlier in this report for Waspaloy sustained load crack growth. The results of the IN100 investigation, presented in Figures 70 and 71, demonstrate the deleterious influence of increasing temperature on sustained load crack growth. The correlation between these curves and 10 tests of 12.7 mm (0.50 in.) thick compact specimens is illustrated in Figure 72.

(4) Synergistic Crack Propagation

(a) LCF -- Overload Interaction

The nature of crack retardation resulting from load sequencing representative of military gas turbine operation is discussed in Appendix A. Testing based on the repetitive load cycle shown in Figure 14 was used to characterize synergistic interaction for LCF-overload fatigue of GATORIZED® IN100. Interpolative models of crack propagation as a function of overload occurence frequency and relative magnitude are presented below.

(1) Effect of Cycles Between Overloads

Under constant load amplitude fatigue (R = 0.50) at 649°C (1200°F) periodically interrupted by a single overload (OLR = 1.5), crack propagation in IN100 displays a strong dependence on the number of baseline fatigue cycles between overloads (ΔN_{OL}). Results of crack propagation tests conducted with ΔN_{OL} = 5, 20, and 40 cycles are plotted in composite fashion in Figure 73. Figure 74 presents the statistics. The associated SINH curves represent an interpolative model of the effect of number of cycles between successive periodic overloads. As shown in Figure 75, the defining SINH coefficients are linear functions of the logarithm of the number of cycles per repetitive mission ($\log(\Delta N_{OL} + 1)$).

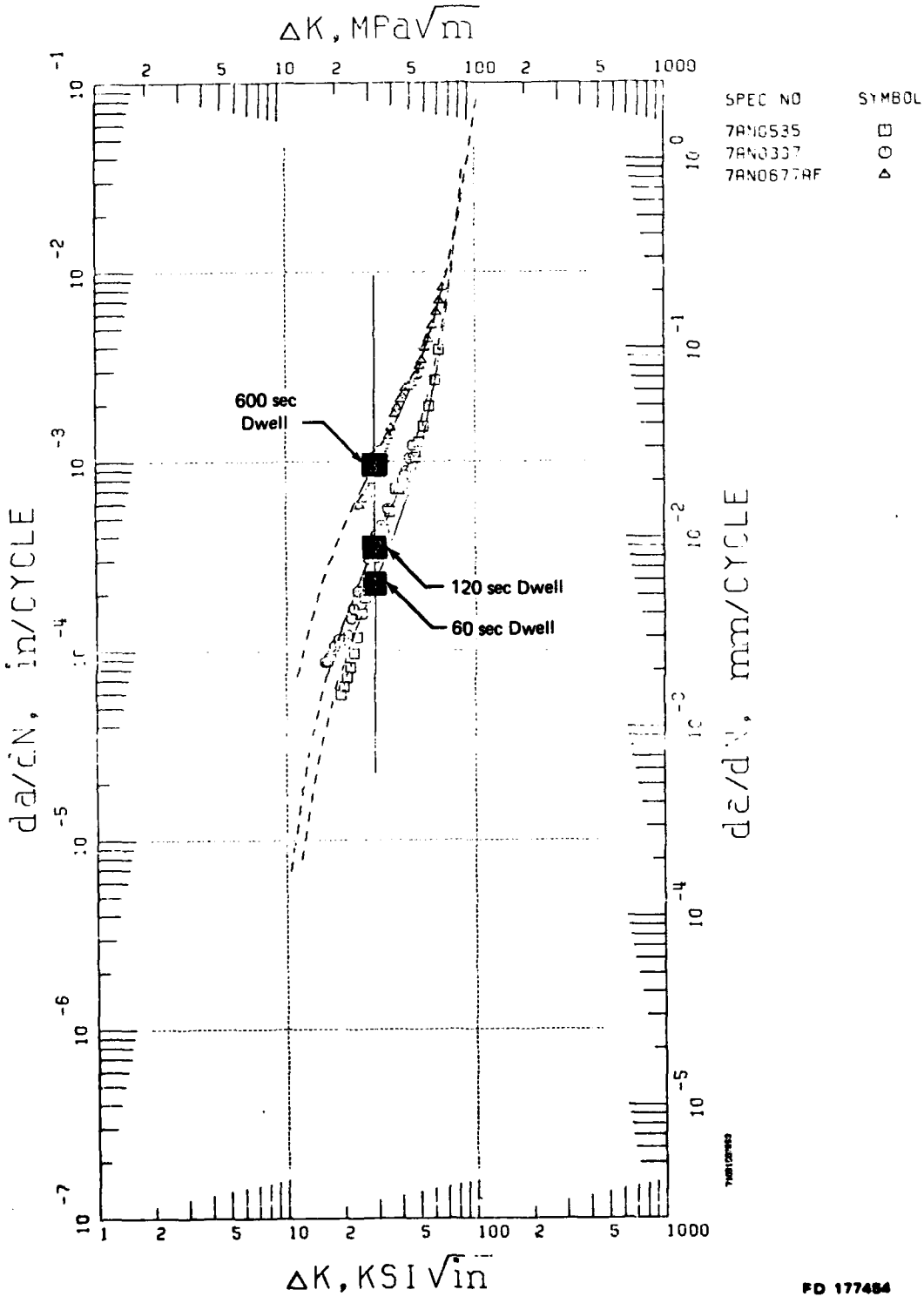

Figure 64. IN100 (PWA 1073) Crack Propagation, Dwell Model, R = 0.10, 649°C (1200°F)

PAGE 71031507953

TEST CONDITIONS 9 2 3 4 6 7 8 10 11 12 GROUP NO. 1

SPEC NO	MATERIAL	TEMP	ATM	FREQ	R	TYPE	THIK	REMARKS
7AN0535	PWA 1073	1200F	AIR	1 MDWL	R=.1	RAD MCT	.465	BAER

□ RSQRD 0.9683 SEE 0.1272

-1.16 0. Y=0.5000 SINH(4.663 (X -1.466))-3.644

NAFT 4 (METRIC) Y=0.5000 SINH(4.663 (X -1.507))-2.239

*** IMPORTANT *** THIS EQUATION IS VALID BETWEEN X= 19.48 , AND X= 64.16 ONLY. DO NOT EXTRAPOLATE.

TEST CONDITIONS 9 2 3 4 6 7 8 10 11 12 GROUP NO. 2

SPEC NO	MATERIAL	TEMP	ATM	FREQ	R	TYPE	THIK	REMARKS
7AN0337	PWA 1073	1200F	AIR	2 MDWL	R=.1	RAD MCT	.44	BAEPBGHS

○ RSQRD 0.9823 SEE 0.0572

-1.16 0. Y=0.5000 SINH(4.402 (X -1.466))-3.456

NAFT 4 (METRIC) Y=0.5000 SINH(4.402 (X -1.507))-2.051

*** IMPORTANT *** THIS EQUATION IS VALID BETWEEN X= 16.06 , AND X= 46.80 ONLY. DO NOT EXTRAPOLATE.

TEST CONDITIONS 9 2 3 4 6 7 8 10 11 12 GROUP NO. 3

SPEC NO	MATERIAL	TEMP	ATM	FREQ	R	TYPE	THIK	REMARKS
7AN0677AF	PWA 1073	1200F	AIR	10MDWL	R=.1	MCT		

△ RSQRD 0.9857 SEE 0.0424

-1.16 0. Y=0.5000 SINH(3.795 (X -1.466))-3.019

NAFT 4 (METRIC) Y=0.5000 SINH(3.795 (X -1.507))-1.814

*** IMPORTANT *** THIS EQUATION IS VALID BETWEEN X= 24.38 , AND X= 67.70 ONLY. DO NOT EXTRAPOLATE.

OVERALL STATISTICS FOR THIS COLLECTION OF GROUPS. TOTAL RSQRD = 0.9830, AND STD.ERROR.EST. = 0.0789

FD 177455

Figure 65. Statistics for IN100 (PWA 1073) Crack Propagation, Dwell Model, R = 0.10, 649°C (1200°F)

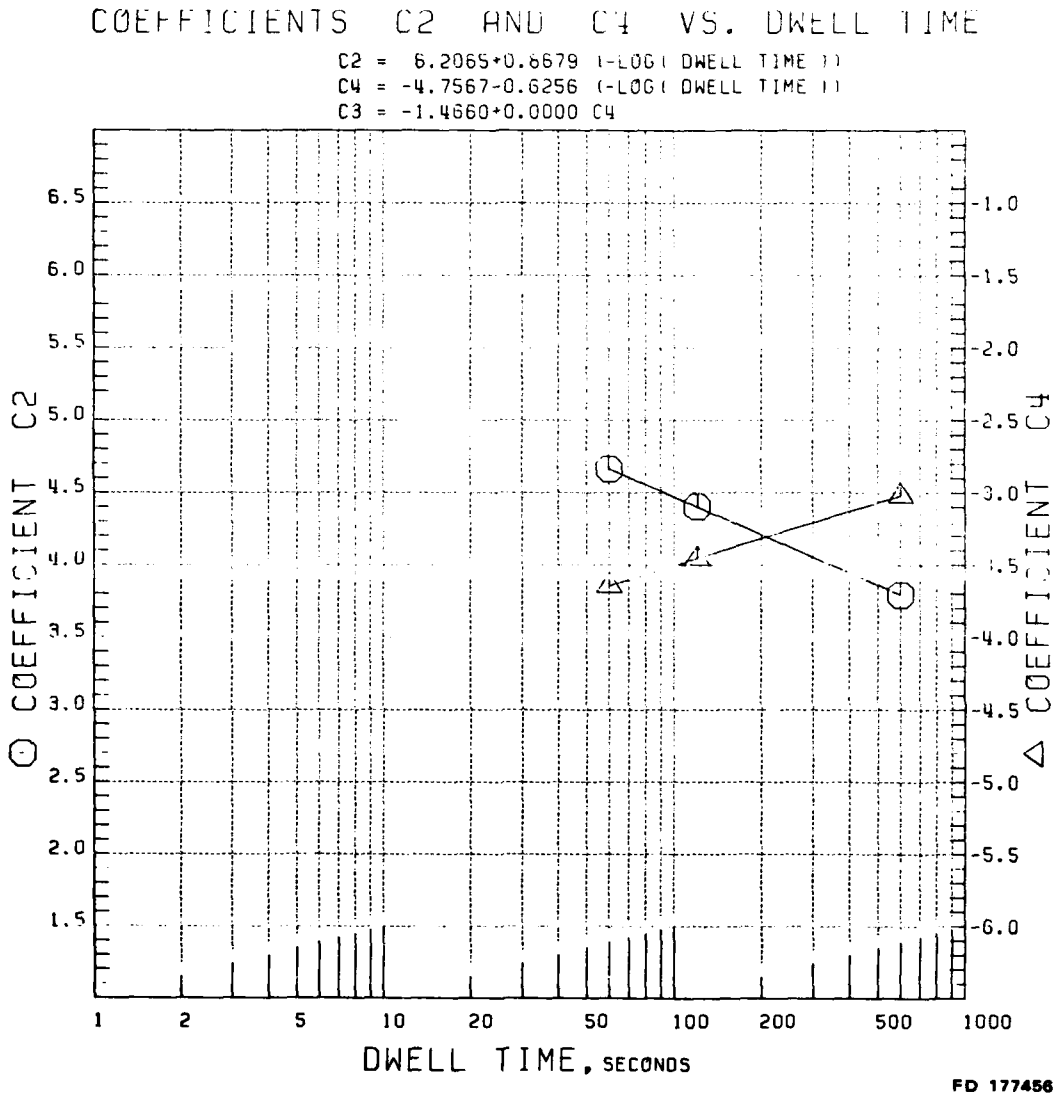

Figure 66. IN100 (PWA 1073) Crack Propagation, Dwell Model Correlative Parameters, R = 0.10, 649°C (1200°F)

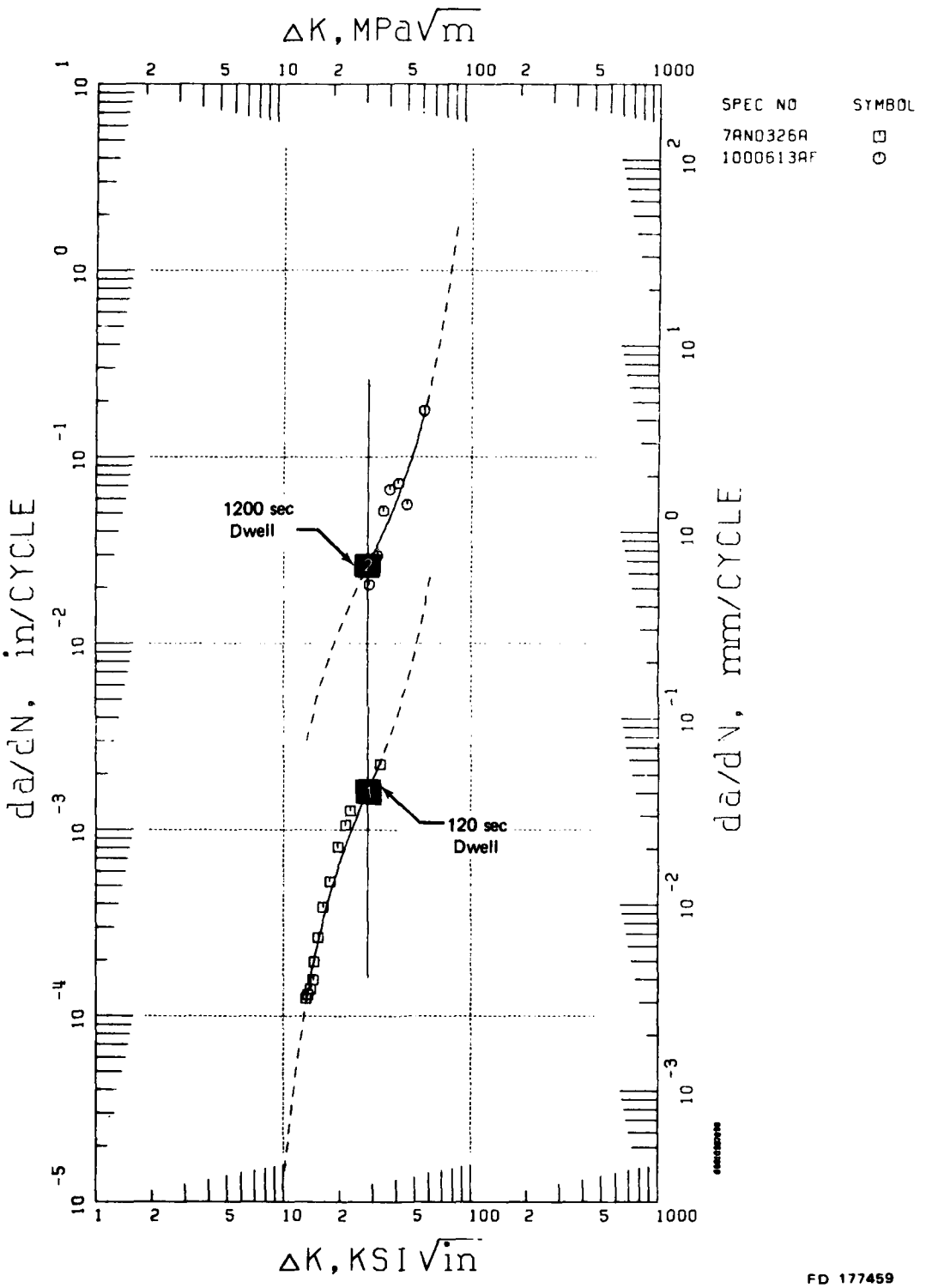

Figure 67. IN100 (PWA 1073) Crack Propagation, Dwell Model, R = 0.10, 732°C (1350°F)

PAGE 80910367936

GROUP NO. 1

TEST CONDITIONS 6 33 34 35 36 37 38

SPEC NO	MATERIAL	TEMP	ATM	FREQ	R	TYPE	THIK	REMARKS
7AN0326A	PWA 1073	1350F	AIR	2 MDWL	R=.1	RAD MCT	.436	BAEPH986

□ RSQRD 0.9817 SEE 0.0826

-0.77 0.

Y=0.5000 SINH(4.762 (X -1.450))-2.792

NAFT 4

(METRIC) Y=0.5000 SINH(4.762 (X -1.491))-1.387

*** IMPORTANT *** THIS EQUATION IS VALID BETWEEN X= 13.27 , AND X= 32.85 ONLY. DO NOT EXTRAPOLATE.

GROUP NO. 2

TEST CONDITIONS 6 33 34 35 36 37 38

SPEC NO	MATERIAL	TEMP	ATM	FREQ	R	TYPE	THIK	REMARKS
1000613AF	PWA 1073	1350F	AIR	20MDWL	R=.1	RAD MCT	.25	20MIN.DWELL

○ RSQRD 0.8358 SEE 0.1479

-0.77 0.

Y=0.5000 SINH(4.263 (X -1.450))-1.582

NAFT 4

(METRIC) Y=0.5000 SINH(4.263 (X -1.491))-0.177

*** IMPORTANT *** THIS EQUATION IS VALID BETWEEN X= 28.65 , AND X= 55.75 ONLY. DO NOT EXTRAPOLATE.

OVERALL STATISTICS FOR THIS COLLECTION OF GROUPS. TOTAL RSQRD = 0.9939, AND STD.ERROR.EST. = 0.1070

FD 177460

Figure 68. Statistics for IN100 (PWA 1073) Crack Propagation, Dwell Model, R = 0.10, 732°C (1350°F)

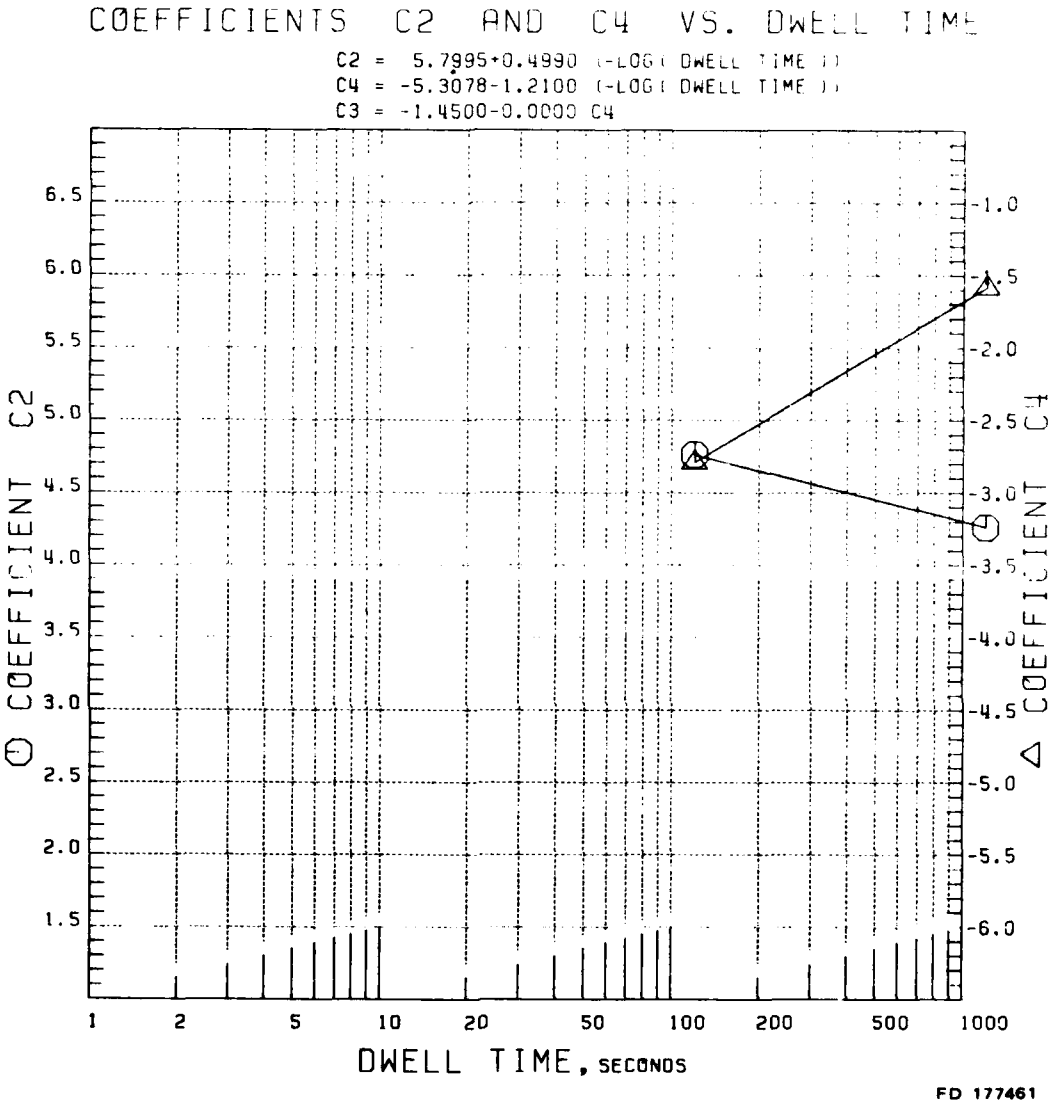

Figure 69. IN100 (PWA 1073) Crack Propagation, Dwell Model Correlative Parameters, R = 0.10, 732°C (1350°F)

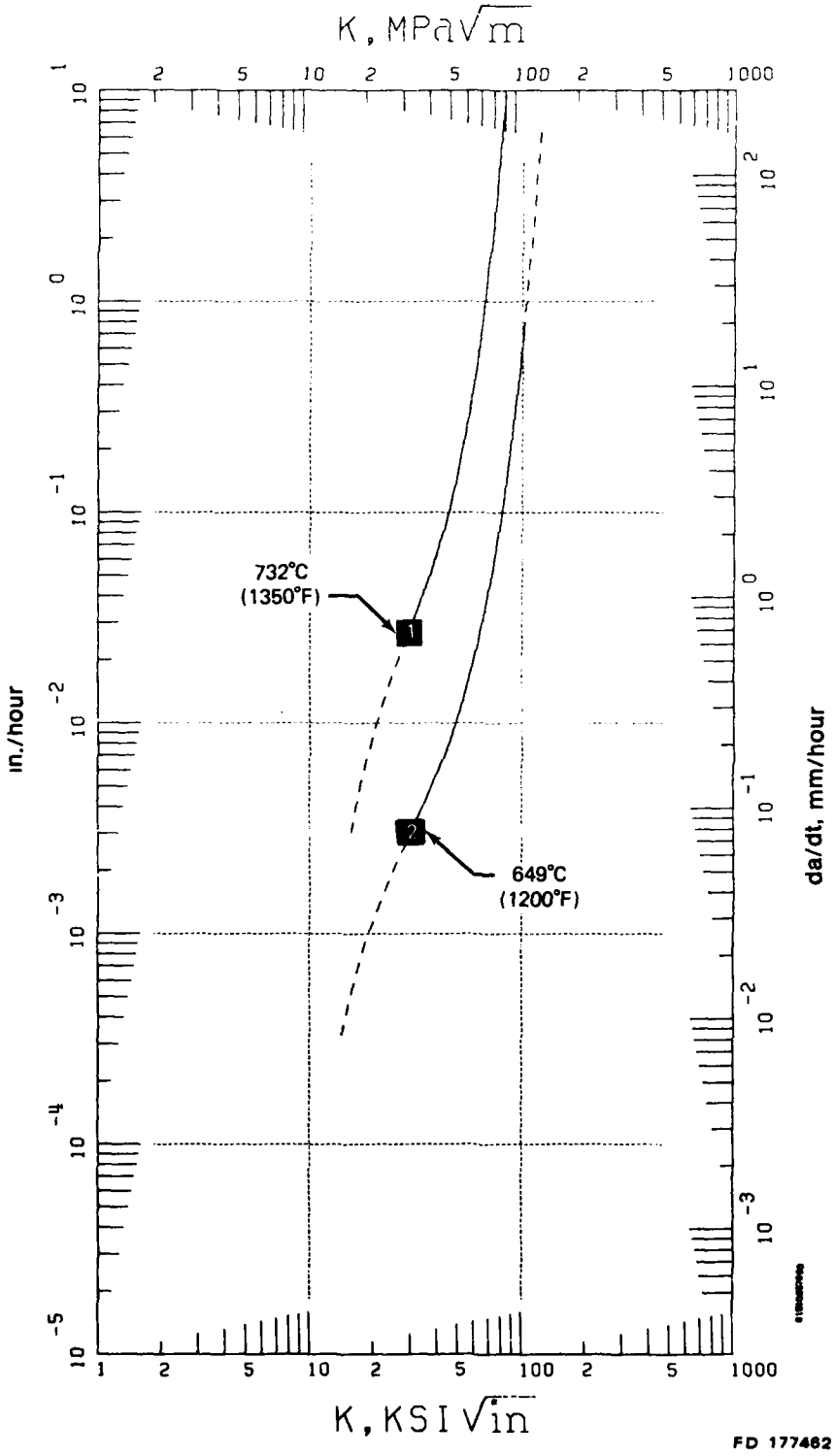

Figure 70. IN100 (PWA 1073) Crack Propagation Under Sustained Loading, 649°C (1200°F) and 732°C (1350°F)

PAGE 81510247959

GROUP NO. 1

3 2 3 4

MATERIAL	TEMP	ATM	FREQ	R	TYPE	THIK	REMARKS
PWA 1007	1200	AIR	DA/DT		MCT	0.50	

-8.52 0. Y=0.5000 SINH(4.297 (X -1.479))-2.519

NRFT 0 (METRIC) Y=0.5000 SINH(4.297 (X -1.520))-1.114

*** IMPORTANT *** THIS EQUATION IS VALID BETWEEN X= 30.00 . AND X= 100.00 ONLY. DO NOT EXTRAPOLATE.

GROUP NO. 2

3 2 3 4

MATERIAL	TEMP	ATM	FREQ	R	TYPE	THIK	REMARKS
PWA 1007	1350	AIR	DA/DT		MCT	0.50	

-8.52 0. Y=0.5000 SINH(5.200 (X -1.467))-1.570

NRFT 0 (METRIC) Y=0.5000 SINH(5.200 (X -1.508))-0.165

*** IMPORTANT *** THIS EQUATION IS VALID BETWEEN X= 30.00 . AND X= 100.00 ONLY. DO NOT EXTRAPOLATE.

FD 177463

Figure 71. Statistics for IN100 (PWA 1073) Crack Propagation Under Sustained Loading, 649°C (1200°F) and 732°C (1350°F)

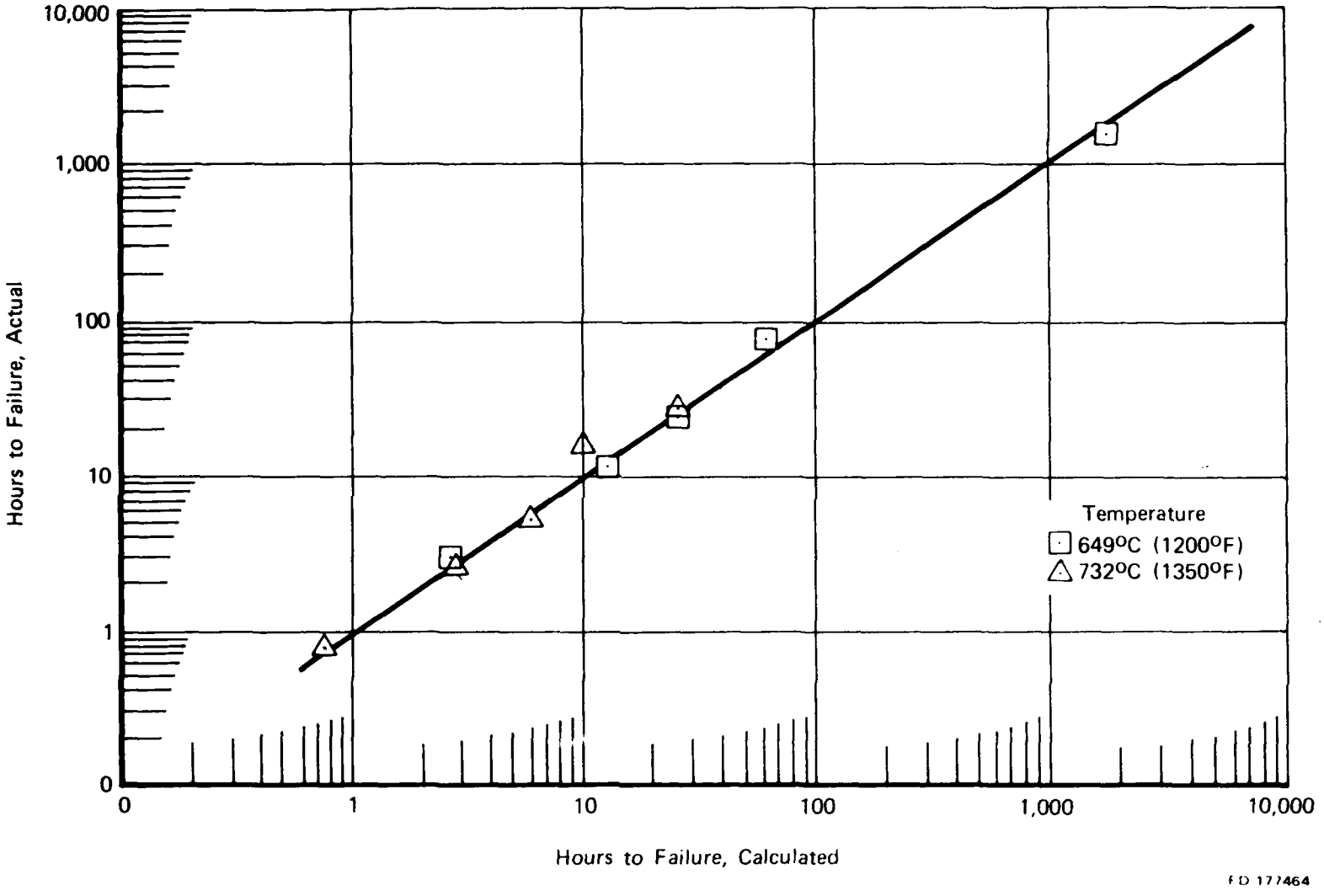

Figure 72. Actual vs Calculated Times to Failure for 10 Compact Specimens Tested Under Sustained Load at 649°C (1200°F) and 732°C (1350°F)

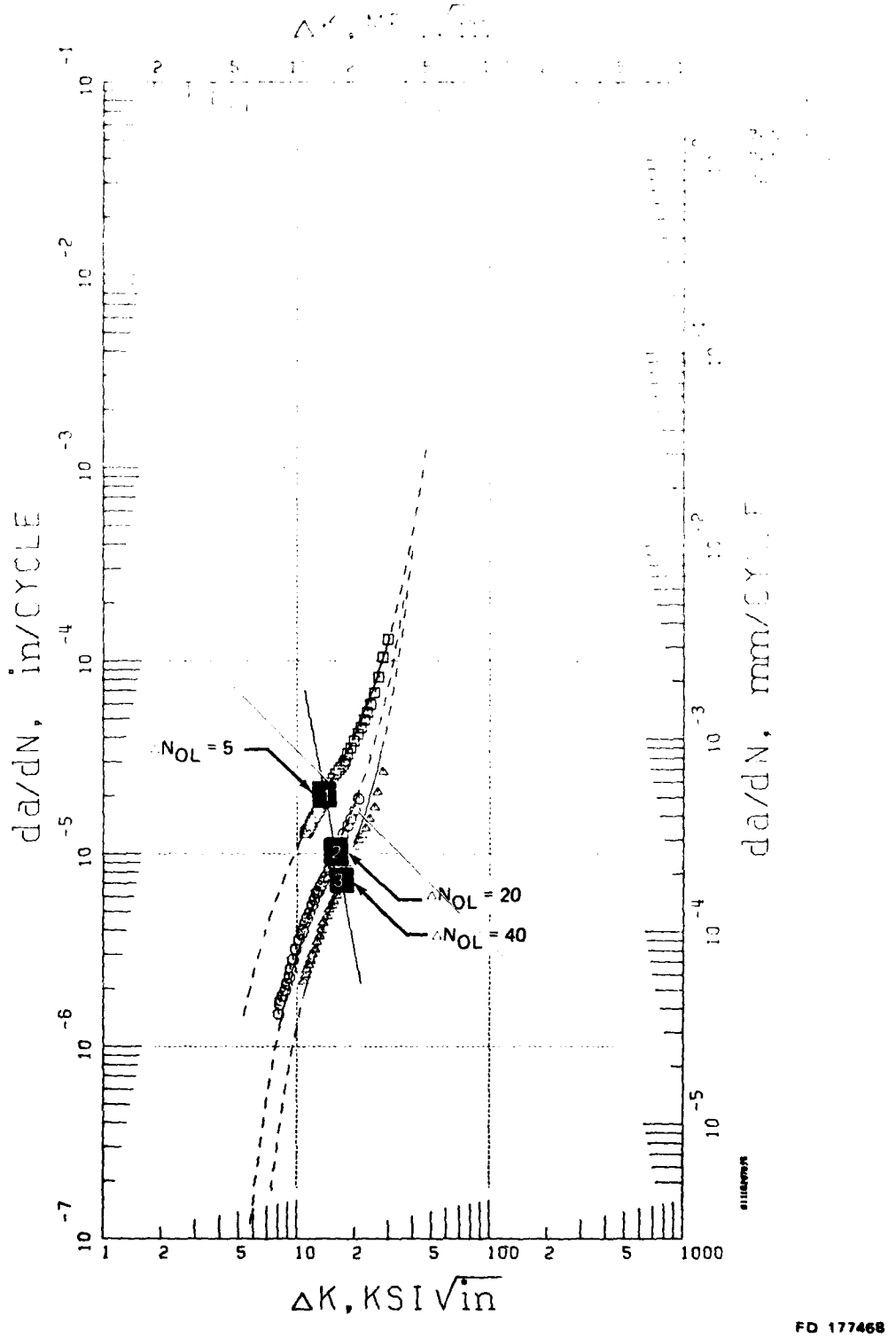

Figure 73. IN100 (PWA 1073) Crack Propagation, Model of the Effect of the Number of Cycles Between Overloads, R = 0.50, 0.167 Hz (10 cpm), 649°C (1200°F) OLR = 1.50

```
PAGE   81116297935

                                                    3 34 36 38                                          GROUP NO.    1
SPEC NO    MATERIAL  TEMP  ATM     FREQ      R     TYPE     THIK  REMARKS
7AN0680AF PWA 1073  1200F AIR     MIX     R=.5  RAD MCT  .251 OL1.5+5CY                  □ RSQRD 0.9970  SEE 0.0277
       -0.51 0.                Y=0.5000 SINH(3.766 (X -1.143 )) -4.690
     NRFT 5          (METRIC) Y=0.5000 SINH(3.766 (X -1.184 )) -3.285
   *** IMPORTANT ***  THIS EQUATION IS VALID BETWEEN  X= 11.13   , AND  X= 29.63  ONLY.  DO NOT EXTRAPOLATE.

                                                    3 34 36 38                                          GROUP NO.    2
SPEC NO    MATERIAL  TEMP  ATM     FREQ      R     TYPE     THIK  REMARKS
7AN0671AF PWA 1073  1200F AIR     MIX     R=.5  RAD MCT  .253 OL1.5+20CY                 ○ RSQRD 0.9992  SEE 0.0487
       -0.51 0.                Y=0.5000 SINH(4.741 (X -1.198 )) -4.981
     NRFT 5          (METRIC) Y=0.5000 SINH(4.741 (X -1.239 )) -3.576
   *** IMPORTANT ***  THIS EQUATION IS VALID BETWEEN  X= 8.05    , AND  X= 20.88  ONLY.  DO NOT EXTRAPOLATE.

                                                    3 34 36 38                                          GROUP NO.    3
SPEC NO    MATERIAL  TEMP  ATM     FREQ      R     TYPE     THIK  REMARKS
7AN0675AF PWA 1073  1200F AIR     MIX                MCT  .251 OL1.5+40CY                 △ RSQRD 0.9961  SEE 0.0[illegible]
       -0.51 0.                Y=0.5000 SINH(5.262 (X -1.228 )) -5.136
     NRFT 5          (METRIC) Y=0.5000 SINH(5.262 (X -1.269 )) -3.731
   *** IMPORTANT ***  THIS EQUATION IS VALID BETWEEN  X= 10.78   , AND  X= 27.85  ONLY.  DO NOT EXTRAPOLATE.

  OVERALL STATISTICS FOR THIS COLLECTION OF GROUPS.   TOTAL RSQRD = 0.9953.  AND  STD.ERROR.EST. = 0.0488
```

FD 177469

Figure 74. ***Statistics for IN100 (PWA 1073) Crack Propagation, Model of the Effect of the Number of Cycles Between Overloads R = 0.50, 0.167 Hz (10 cpm), 649°C (1200°F) OLR = 1.50***

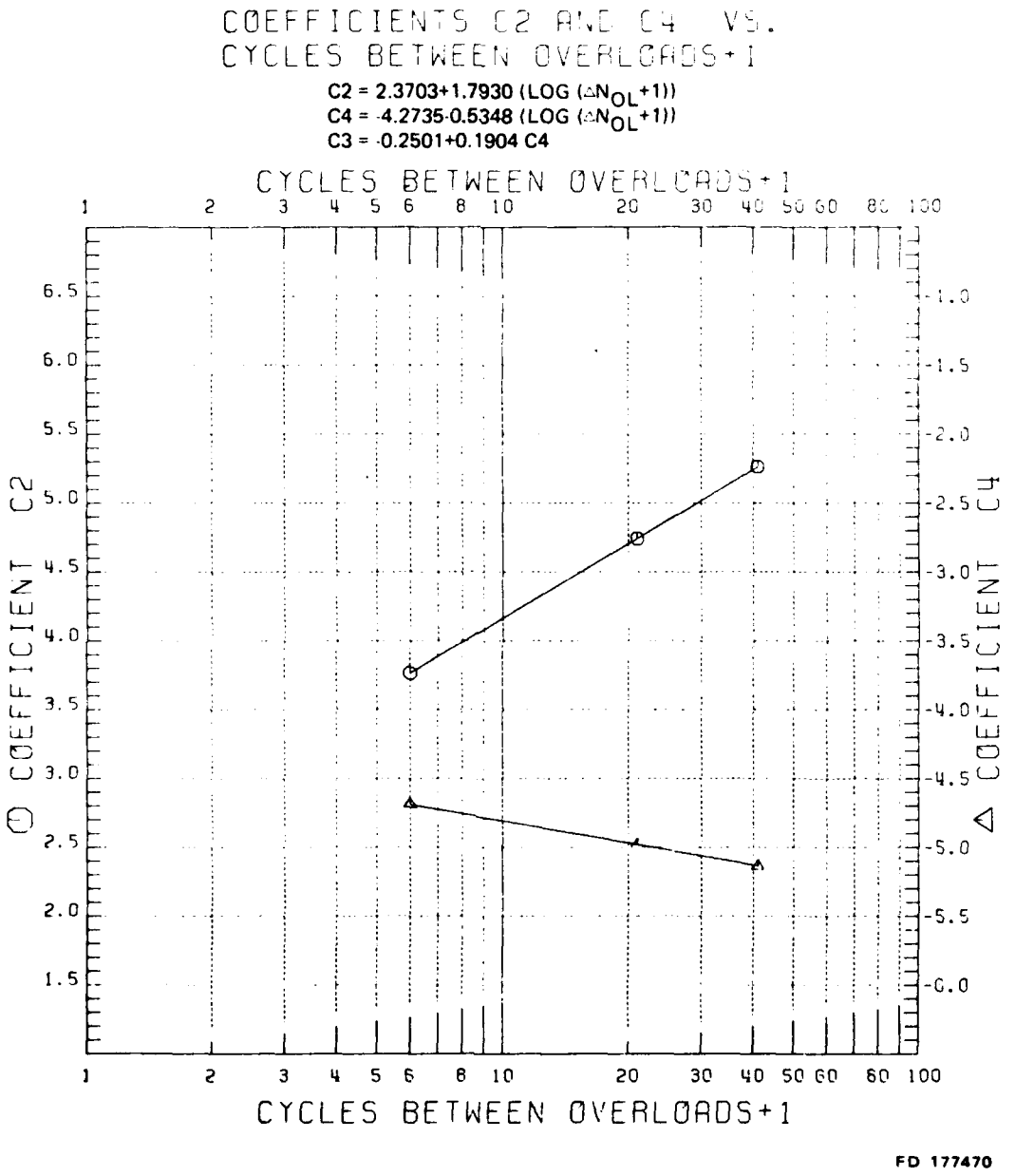

Figure 75. IN100 (PWA 1073) Crack Propagation, Correlative Parameters Model of Effect of ΔN_{OL}, R = 0.50, 0.167 Hz (10 cpm), 649°C (1200°F), OLR = 1.50

(2) Effect of Overload Ratio

Under periodic overload-fatigue the effect of increasing overload ratio (P_{OL}/P_{max}) while holding ΔN_{OL} constant is to decrease the average rate of crack propagation produced by the load sequencing. Tests of IN100 were conducted using the repetitive load sequence shown in Figure 14. Similar to the tests discussed above, the temperature was 649°C (1200°F), R = 0.50, and the cyclic frequency was 0.167 Hz (10 cpm). The number of cycles between overloads, ΔN_{OL}, was held constant at 40, and overload ratio was varied over the range $1.0 \leq OLR \leq 1.50$.

Under an overload ratio of 1.0, the load range is constant and crack growth reduces to the case of the constant ΔP baseline. For overload ratios of 1.25 and 1.50 average growth rate is reduced. A composite of these data, and the associated SINH model, is presented in Figure 76. Figure 77 gives the statistics. The defining SINH coefficients are linear functions of OLR as illustrated in Figure 78.

(b) LCF — Dwell Interaction

Crack propagation testing of IN100 fatigued at 649°C (1200°F) under the repetitive LCF-dwell sequence shown in Figure 13 revealed little or no effect of the periodic dwell. As illustrated in Figure 79, data generated with 10, 20, and 40 cycles of 0.167 Hz (10 cpm) sawtooth fatigue (R = 0.1)between dwells correlated well with the crack growth curve representing sawtooth fatigue only. Figure 80 presents the statistics.

Similar tests conducted at 732°C (1350 °F) demonstrated a mild effect of the periodic load dwell. The results of tests conducted with 10, 20, and 40 cycles between dwells are shown in a composite presented in Figure 81. Figure 82 presents the statistics. For purposes of comparison, the SINH curves describing crack growth under baseline fatigue (732°C, 0.167, R = 0.10) and repetitive dwell (732°C, 120 sec dwell, R = 0.10) are also shown. The SINH curves representing the individual LCF-dwell data sets are given by an interpolative model of this effect, and the defining coefficients are illustrated in Figure 83.

5. Auxiliary Investigation

a. Negative Stress Ratio Effects

Tension-compression fatigue ($R \leq O$) may occur in isolated disk locations during mission operation as shown in Figure 4. Fatigue crack propagation under such negative stress ratio cycling is not accurately predicted by a simple extrapolation of a stress ratio model developed for tension-tension ($R \geq O$) fatigue. Due to a difference in the mechanism of crack growth associated with the positive vs negative load excursion, a separate evaluation of crack growth is required for $R \leq O$.

Considering the work of Elber (Reference 7), the effective stress intensity range operating at the crack tip is $\Delta K_{eff} = (K_{max} - K_{closure})$, where $K_{closure}$ is the stress intensity at which physical closing of the crack tip occurs on unloading. Under a compressive stress field, a crack tip singularity does not exist, and K = 0 for all $\sigma_{applied} \leq O$. While for a given K_{max}, the applied stress intensity range ($\Delta K = K_{max} - K_{min}$) remains constant for negative stress ratio fatigue, $\Delta K_{effective}$ is increased slightly as $K_{closure}$ decreases due to compressive yielding.

In order to examine the effect of representative tension-compression fatigue on crack growth in Waspaloy and IN100, the matrix of tests outlined in Table 5 was conducted. The investigation was performed at 427°C (800°F) and 649°C (1200°F) and spanned the range of $-1.0 \leq R \leq 0.0$; the cyclic frequency was 0.167 Hz (10 cpm). The crack growth specimen employed in these tests was of through-thickness center crack geometry, Figure 11a.

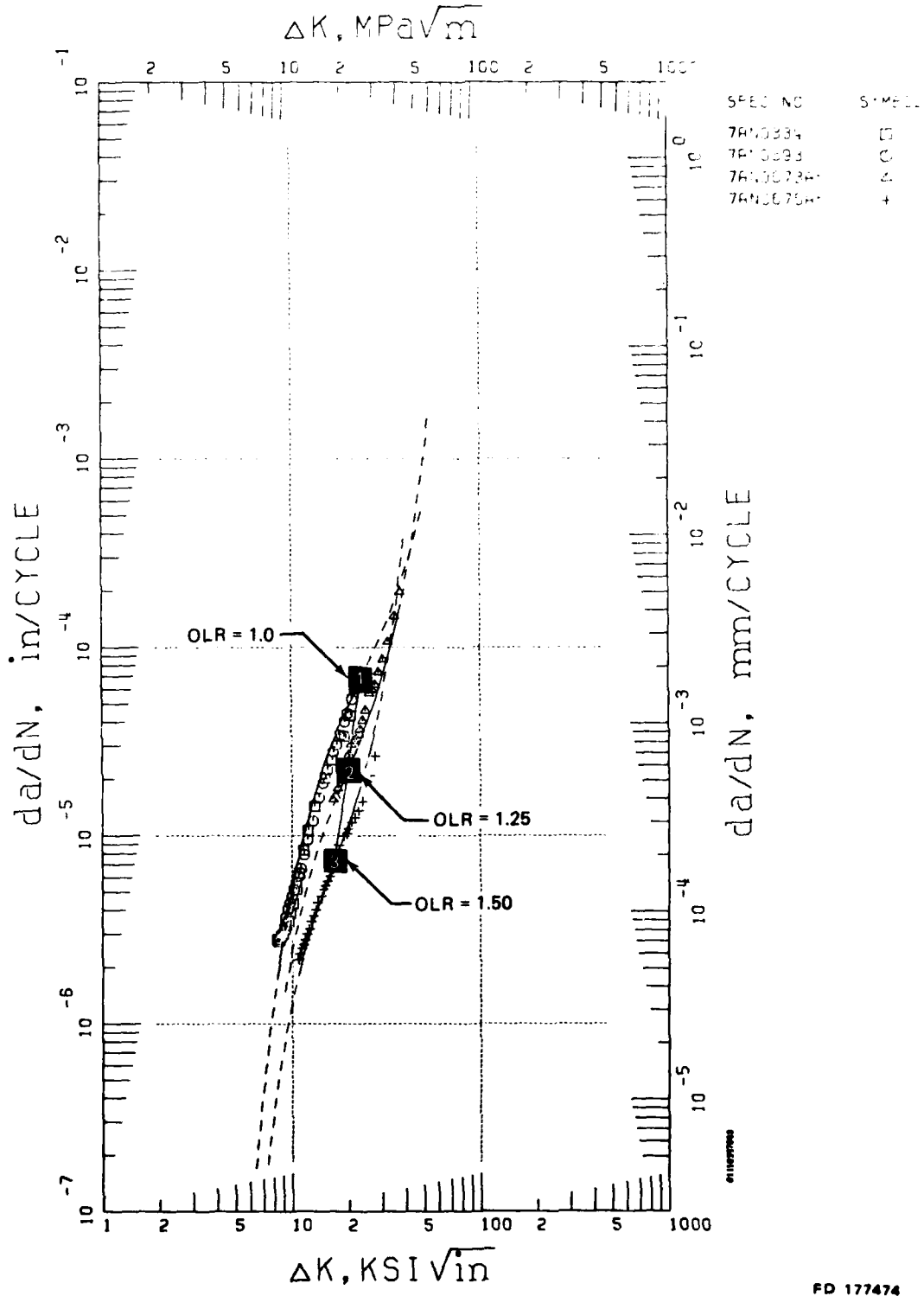

Figure 76. IN100 (PWA 1073) Crack Propagation, Overload Ratio Model, R = 0.50, 0.167 Hz (10 cpm), 649°C (1200°F), ΔN_{OL} = 40

PAGE 81116357943

OLR =1.00 3 34 36 38 GROUP NO. 1

SPEC NO	MATERIAL	TEMP	ATM	FREQ	R	TYPE	THIK	REMARKS
7AN0334	PWA 1073	1200F	AIR	10 CPM	R=.5	RAD MCT	.5	BAEPB3H9
7AN0393	PWA 1073	1200F	AIR	10 CPM	R=.5	RAD MCT	.5	

□ RSQRD 0.9791 SEE 0.0849

-7.17 33. Y=0.5000 SINH(4.192 (X -1.368))-4.172

NAFT 6 (METRIC) Y=0.5000 SINH(4.192 (X -1.409))-2.767

*** IMPORTANT *** THIS EQUATION IS VALID BETWEEN X= 8.33 , AND X= 21.89 ONLY. DO NOT EXTRAPOLATE.

OLR =1.25 + 40 CYCLES 3 34 36 38 GROUP NO. 2

SPEC NO	MATERIAL	TEMP	ATM	FREQ	R	TYPE	THIK	REMARKS
7AN0673AF	PWA 1073	1200F	AIR	MIX	R=.5	RAD MCT	OL1.25+40	

△ RSQRD 0.9962 SEE 0.0767

-7.17 33. Y=0.5000 SINH(4.727 (X -1.298))-4.654

NAFT 6 (METRIC) Y=0.5000 SINH(4.727 (X -1.339))-3.249

*** IMPORTANT *** THIS EQUATION IS VALID BETWEEN X= 16.61 , AND X= 37.69 ONLY. DO NOT EXTRAPOLATE.

OLR = 1.50 + 40 CYCLES 3 34 36 38 GROUP NO. 3

SPEC NO	MATERIAL	TEMP	ATM	FREQ	R	TYPE	THIK	REMARKS
7AN0675AF	PWA 1073	1200F	AIR	MIX		MCT	.251	OL1.5+40CY

+ RSQRD 0.9962 SEE 0.0663

-7.17 33. Y=0.5000 SINH(5.262 (X -1.228))-5.136

NAFT 6 (METRIC) Y=0.5000 SINH(5.262 (X -1.269))-3.731

*** IMPORTANT *** THIS EQUATION IS VALID BETWEEN X= 10.78 , AND X= 27.85 ONLY. DO NOT EXTRAPOLATE.

OVERALL STATISTICS FOR THIS COLLECTION OF GROUPS. TOTAL RSQRD = 0.9768. AND STD.ERROR.EST. = 0.0748

FD 177475

Figure 77. Statistics for IN100 (PWA 1073) Crack Propagation, Overload Ratio Model, R = 0.50, 0.167 Hz (10 cpm) 649°C (1200°F) $\Delta N_{OL} = 40$

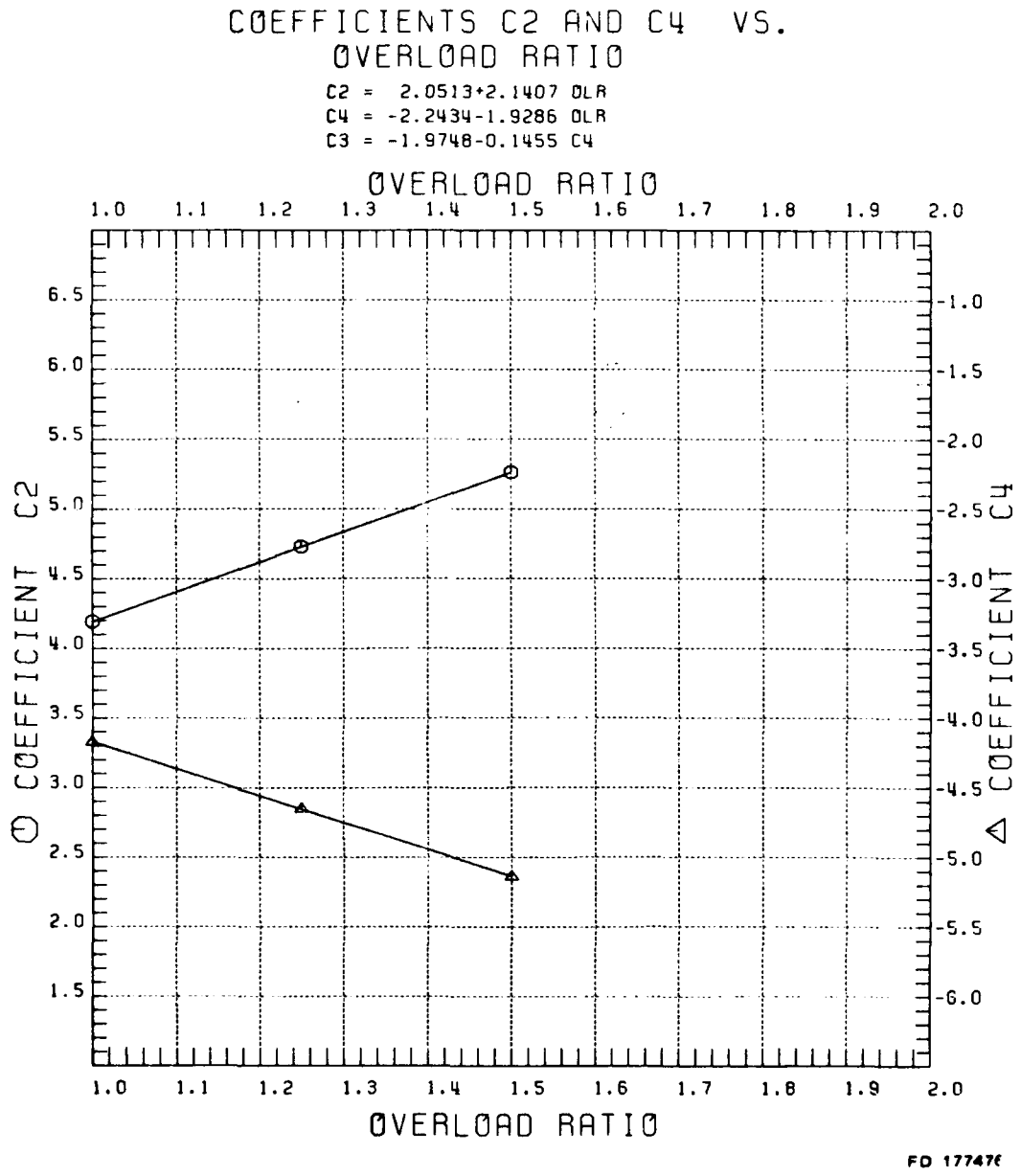

Figure 78. IN100 (PWA 1073) Crack Propagation, Overload Ratio Model Correlative Parameters, R = 0.50, 0.167 Hz (10 cpm), 649°C (1200°F), ΔN_{OL} = 40

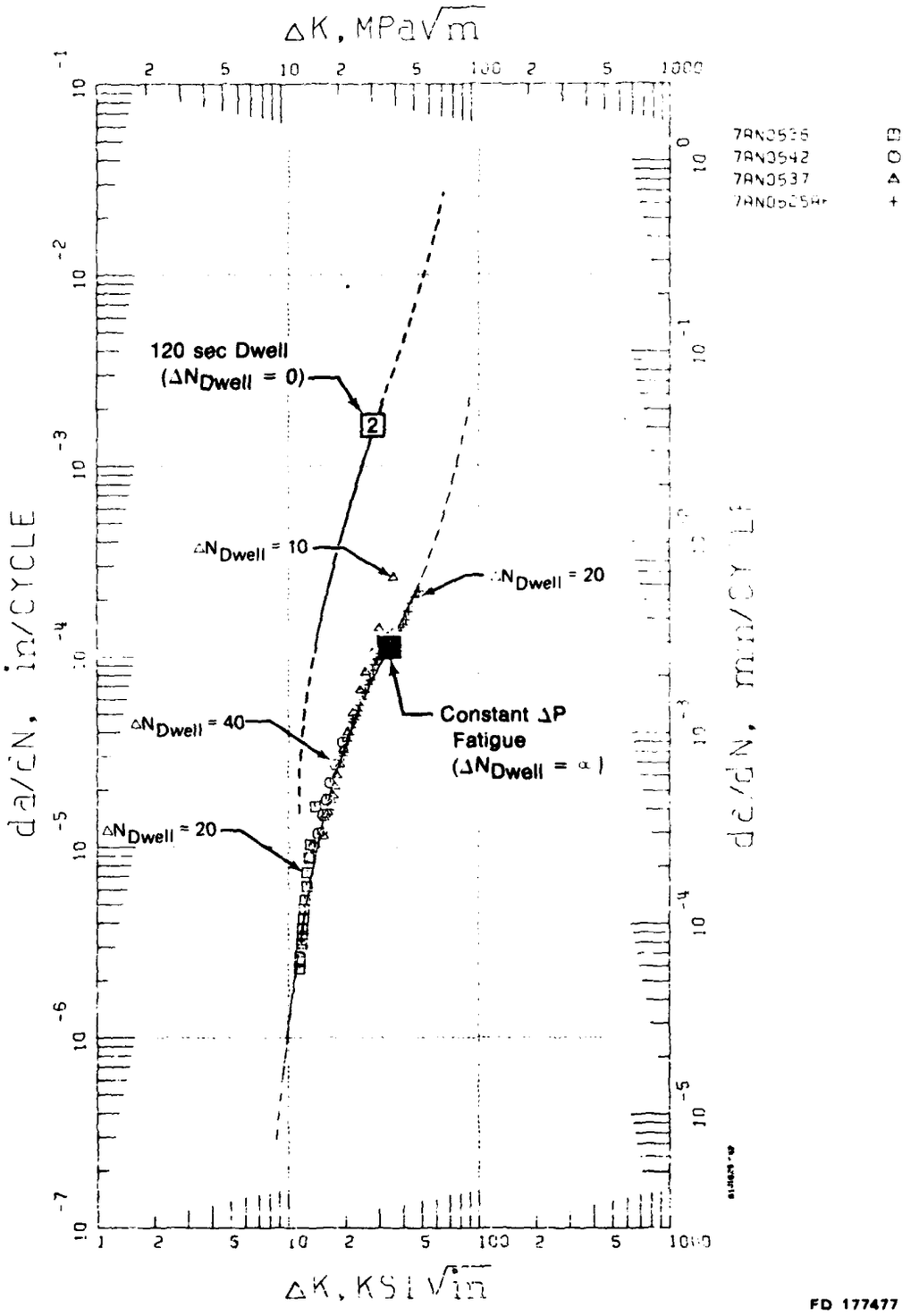

Figure 79. IN100 (PWA 1073) Crack Propagation, R = 0.10, 649°C (1200°F), 0.167 Hz (10 cpm) Sawtooth Fatigue Interrupted by Periodic 120 Dwell at Peak Load, ΔN_{Dwell} = 10, 20, and 40

PAGE 61316297942

1200F, R=.1, 20CBD — 6 2 3 4 6 7 8 — GROUP NO. 1

SPEC NO	MATERIAL	TEMP	ATM	FREQ	R	TYPE	THK	REMARKS
7AN0536	PWA 1073	1200F	AIR	MIX	R=.1	RAD MCT	.470	20CY + 2MDWL

□ RSQRD 0.9992 SEE 0.1326

-0.24 0. Y=0.5000 SINH(3.961 (X -1.529)) -3.947

VRFT 0 (METRIC) Y=0.5000 SINH(3.961 (X -1.570)) -2.542

*** IMPORTANT *** THIS EQUATION IS VALID BETWEEN X= 11.39 , AND X= 13.83 ONLY. DO NOT EXTRAPOLATE.

1200F, R=.1, 40CBD — 6 2 3 4 6 7 8 — GROUP NO. 2

SPEC NO	MATERIAL	TEMP	ATM	FREQ	R	TYPE	THK	REMARKS
7AN0542	PWA 1073	1200F	AIR	MIX	R=.1	RAD MCT	.500	40CY + 2MDWL

○ RSQRD 0.9973 SEE 0.1058

-0.24 0. Y=0.5000 SINH(3.961 (X -1.529)) -3.947

VRFT 0 (METRIC) Y=0.5000 SINH(3.961 (X -1.570)) -2.542

*** IMPORTANT *** THIS EQUATION IS VALID BETWEEN X= 12.98 , AND X= 19.14 ONLY. DO NOT EXTRAPOLATE.

1200F, R=.1, 10CBD — 6 2 3 4 6 7 8 — GROUP NO. 3

SPEC NO	MATERIAL	TEMP	ATM	FREQ	R	TYPE	THK	REMARKS
7AN0537	PWA 1073	1200F	AIR	MIX	R=.1	RAD MCT	.470	10CY + 2MDWL

△ RSQRD 0.9921 SEE 0.1197

-0.24 0. Y=0.5000 SINH(3.961 (X -1.529)) -3.947

VRFT 0 (METRIC) Y=0.5000 SINH(3.961 (X -1.570)) -2.542

*** IMPORTANT *** THIS EQUATION IS VALID BETWEEN X= 15.11 , AND X= 35.41 ONLY. DO NOT EXTRAPOLATE.

1200F, R=.1, 20CBD — 6 2 3 4 6 7 8 — GROUP NO. 4

SPEC NO	MATERIAL	TEMP	ATM	FREQ	R	TYPE	THK	REMARKS
7AN0625F	PWA 1073	1200F	AIR	MIX	R=.1	RAD MCT	.294	20CY + 2MDWL

+ RSQRD 0.9847 SEE 0.0342

-0.24 0. Y=0.5000 SINH(3.961 (X -1.529)) -3.947

VRFT 0 (METRIC) Y=0.5000 SINH(3.961 (X -1.570)) -2.542

*** IMPORTANT *** THIS EQUATION IS VALID BETWEEN X= 19.47 , AND X= 48.34 ONLY. DO NOT EXTRAPOLATE.

FD 177478

Figure 80. Statistics for IN100 (PWA 1073) Crack Propagation, R = 0.10, 649°C (1200°F) 0.167 Hz (10 cpm), Sawtooth Fatigue Interrupted by Periodic 120 Dwell at Peak Load, ΔN_{Dwell} = 10, 20, and 40

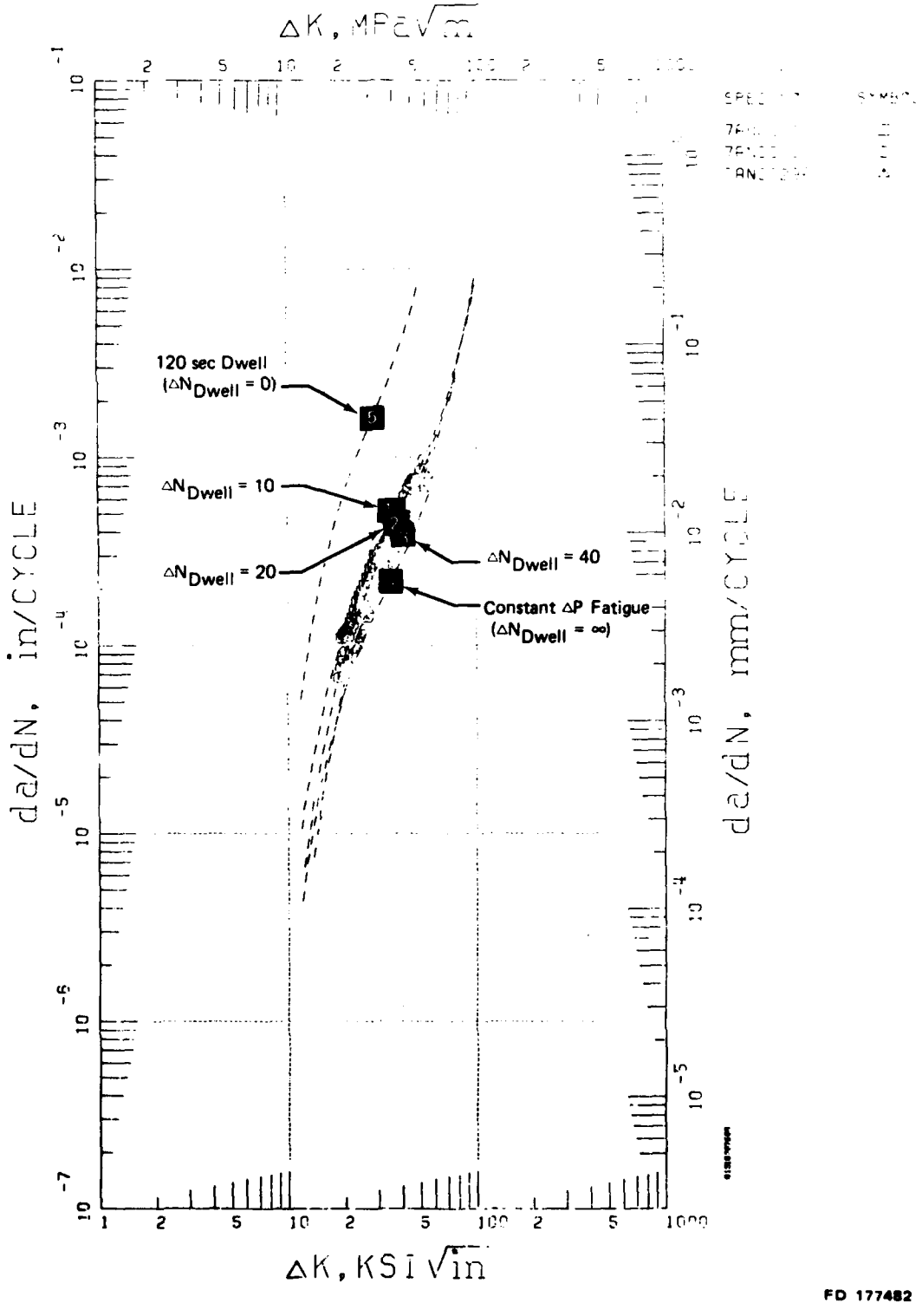

Figure 81. IN100 (PWA 1073) Crack Propagation, Model of LCF-Dwell Interaction, R = 0.10, 732°C (1350°F)

PAGE 81316287906

1350F, R=.1, 10CPM — 3 2 3 4 — GROUP NO. 1

SPEC NO | MATERIAL | TEMP | ATM | FREQ | R | TYPE | THIK | REMARKS

7R[illegible]21AF | PWA 1073 | 1350F | AIR | MIX | R=.1 | RAD MCT | .237 | 10CY + 2MDWL | ☐ RSQRD 0.9908 SEE 0.0358

-1.35 0. Y=0.5000 SINH(3.828 (X -1.568))-3.323

NRFT 0 (METRIC) Y=0.5000 SINH(3.828 (X -1.609))-1.918

*** IMPORTANT *** THIS EQUATION IS VALID BETWEEN X= 19.19 . AND X= 47.26 ONLY. DO NOT EXTRAPOLATE.

1350F, R=.1, 20CPM — 3 2 3 4 — GROUP NO. 2

SPEC NO | MATERIAL | TEMP | ATM | FREQ | R | TYPE | THIK | REMARKS

7R[illegible]26AF | PWA 1073 | 1350F | AIR | MIX | R=.1 | RAD MCT | .240 | 20CY + 2MDWL | ⊙ RSQRD 0.9955 SEE 0.0411

-1.35 0. Y=0.5000 SINH(4.065 (X -1.580))-3.360

NRFT 0 (METRIC) Y=0.5000 SINH(4.065 (X -1.621))-1.955

*** IMPORTANT *** THIS EQUATION IS VALID BETWEEN X= 18.50 . AND X= 52.18 ONLY. DO NOT EXTRAPOLATE.

1350F, R=.1, 40CPM — 3 2 3 4 — GROUP NO. 3

SPEC NO | MATERIAL | TEMP | ATM | FREQ | R | TYPE | THIK | REMARKS

7R[illegible]29AF | PWA 1073 | 1350F | AIR | MIX | R=.1 | RAD MCT | .251 | 40CY + 2MDWL | ▲ RSQRD 0.9924 SEE 0.0397

-1.35 0. Y=0.5000 SINH(4.301 (X -1.592))-3.398

NRFT 0 (METRIC) Y=0.5000 SINH(4.301 (X -1.633))-1.993

*** IMPORTANT *** THIS EQUATION IS VALID BETWEEN X= 20.80 . AND X= 55.82 ONLY. DO NOT EXTRAPOLATE.

GROUP NO. 4

SPEC NO | MATERIAL | TEMP | ATM | FREQ | R | TYPE | THIK | REMARKS

PWA 1073 1350 AIR 10 cpm R = 0.1

-1.35 0. Y=0.5000 SINH(4.111 (X -1.543))-3.662

NRFT 0 (METRIC) Y=0.5000 SINH(4.111 (X -1.584))-2.257

GROUP NO. 5

SPEC NO | MATERIAL | TEMP | ATM | FREQ | R | TYPE | THIK | REMARKS

PWA 1073 1350 AIR 2 MDWL R = 0.1

-1.35 0. Y=0.5000 SINH(4.762 (X -1.450))-2.792

NRFT 0 (METRIC) Y=0.5000 SINH(4.762 (X -1.491))-1.[illegible]

FD 177483

Figure 82. Statistics for IN100 (PWA 1073) Crack Propagation, Model of LCF-Dwell Interaction, R = 0.10, 732°C (1350°F)

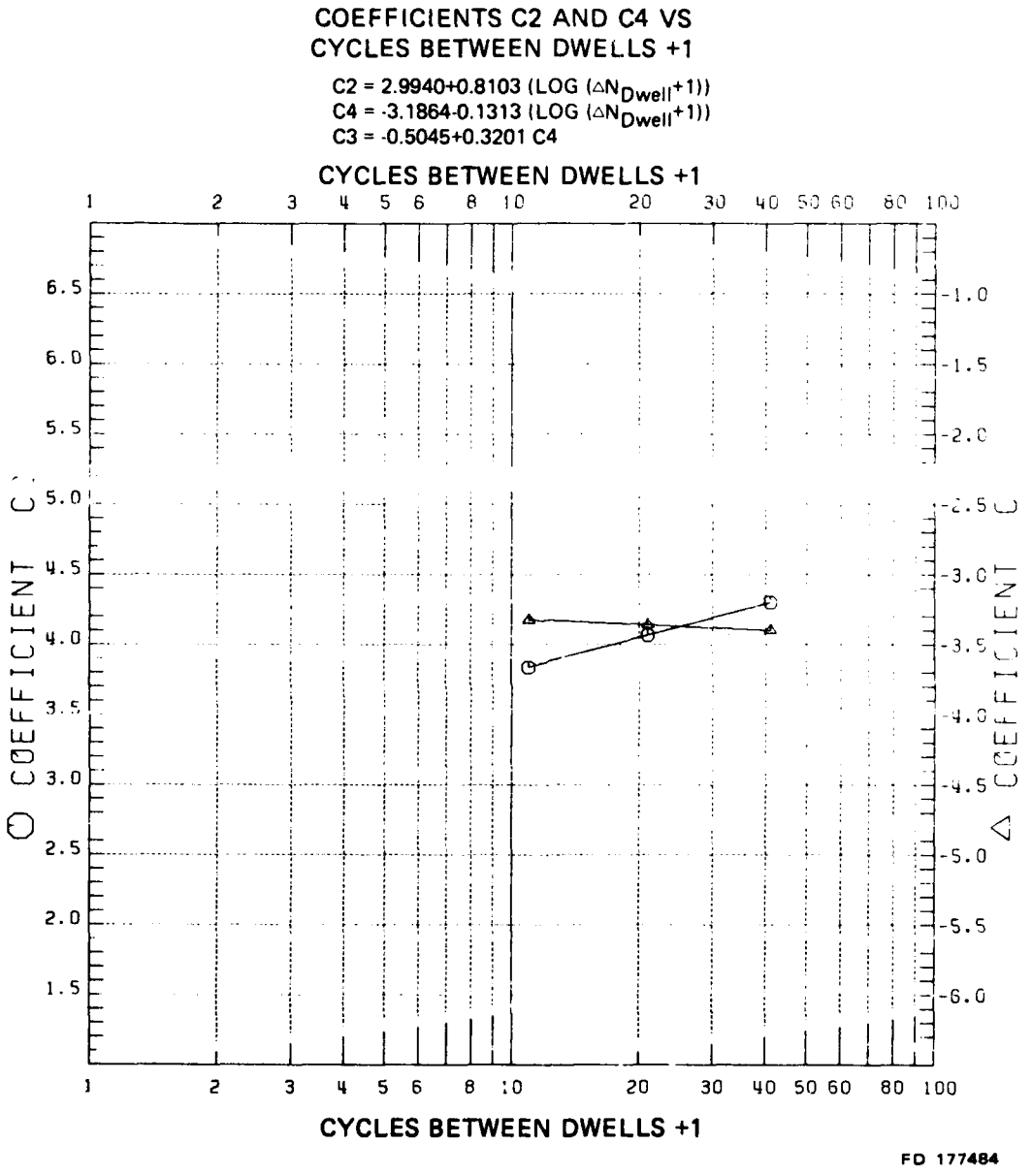

Figure 83. IN100 (PWA 1073) Crack Propagation, Correlative Parameters for Model of LCF-Dwell Interaction, R = 0.10, 732°C (1350°F)

All tests were conducted with the specimen carefully aligned and ends rigidly fixed. In spite of such efforts to achieve a uniform nominal stress field in the specimen, crack growth irregularities observed in several specimens suggested the presence of a bending stress. The irregular crack growth was characterized by unequal rates of propagation at the opposing specimen surfaces, producing crack front asymmetry. This condition required the rejection of data from several completed tests and subsequent retesting.

(1) Waspaloy

The results of the 427°C (800°F) negative stress ratio tests for Waspaloy are presented in Figure 84. The rate of crack propagation is observed to be similar for R = -0.5 and R = -1.0 fatigue, and crack growth under both of these stress ratios is more rapid than the illustrated curve for R = 0 cycling. Since all data are regressed with K_{min} = 0 for compressive stress excursions, the comparison of the negative R data with the R = 0 curve isolates the influence of the compressive excursion.

The effect of negative stress ratio cycling on crack propagation of Waspaloy at 649°C (1200°F) is illustrated in Figure 85. Again the compressive loading is observed to increase crack growth above the rate produced by R = 0 fatigue.

(2) IN100

Crack propagation in IN100 subject to negative stress ratio exhibited anomalous behavior. At 427°C (800°F), Figure 86, the effect of R = -0.5 fatigue is nearly equivalent to behavior under R = 0 cycling, however, decreasing stress ratio to R = -1.0 (specimen 793) is observed to reduce crack growth rate significantly below that of baseline (R = 0) fatigue. Close examination of the data from specimen 793 revealed no satisfactory explanation for the slower crack growth. While this specimen was taken from a separate heat of IN100, experience with this alloy indicates that the anomalous behavior cannot be explained as a heat-to-heat effect.

Anomalous crack growth was also observed in 649°C (1200°F) negative stress ratio testing of IN100. As illustrated in Figure 87, crack propagation under R = -0.5 fatigue was observed to be more rapid than under R = -1.0 cycling. Propagation under both conditions was more severe than for R = 0 fatigue.

(3) Interpolative Modeling of Crack Growth

The basis for the anomalies in crack propagation exhibited by the negative stress ratio data is believed to be the tendency for asymmetric crack growth, as previously discussed. While the data presented were taken from specimens displaying very limited crack asymmetry, such behavior appears to be the source of appreciable test-to-test variability for tension-compression fatigue. Similar crack asymmetry and data variability were not observed under tension-tension fatigue. The use of a large capacity testing machine, having a very rigid load train, should significantly reduce the variability for tension-compression fatigue. Such equipment was not available for the current program.

In the light of the observed variability in the generated crack propagation data for negative stress ratio fatigue, interpolative models of crack growth behavior could not be reliably developed. Multiple tests at each condition are suggested in order to appropriately characterize the effect of tension-compression cycling.

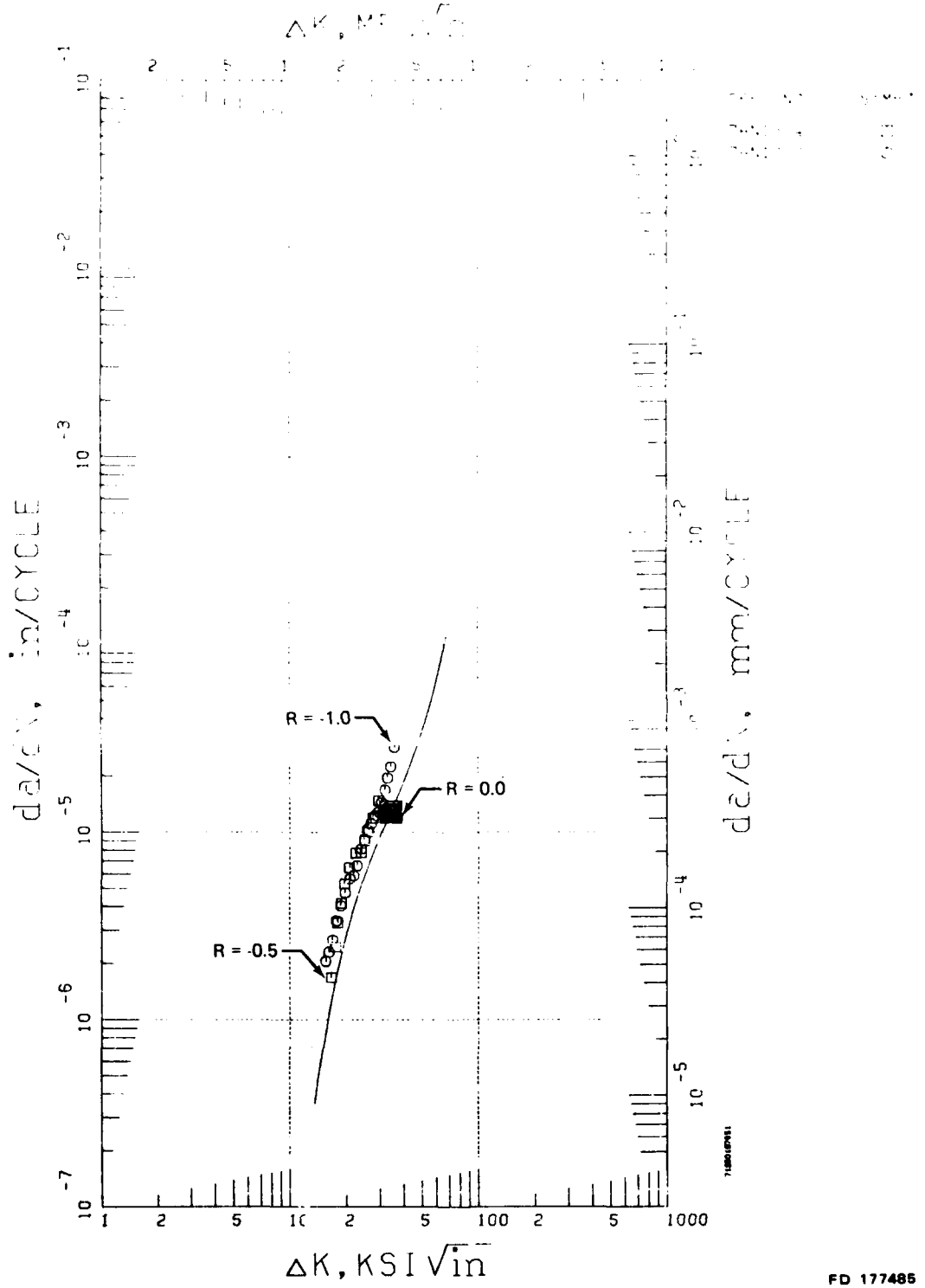

Figure 84. Waspaloy (PWA 1007) Crack Propagation, Negative Stress Ratio Effect, 0.167 Hz (10 cpm), 427°C (800°F)

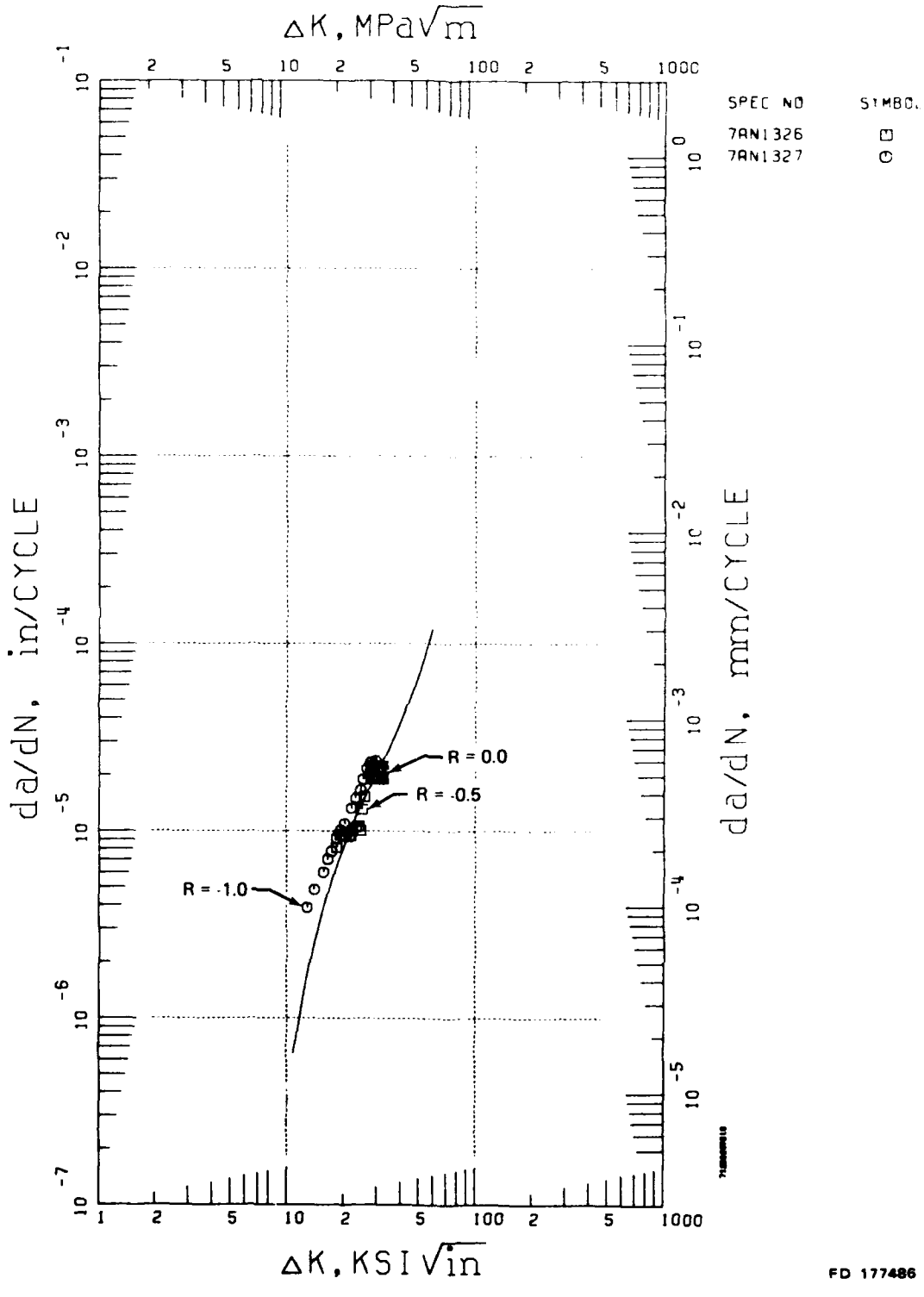

Figure 85. Waspaloy (PWA 1007) Crack Propagation, Negative Stress Ratio Effect, 0.167 Hz (10 cpm), 649°C (1200°F)

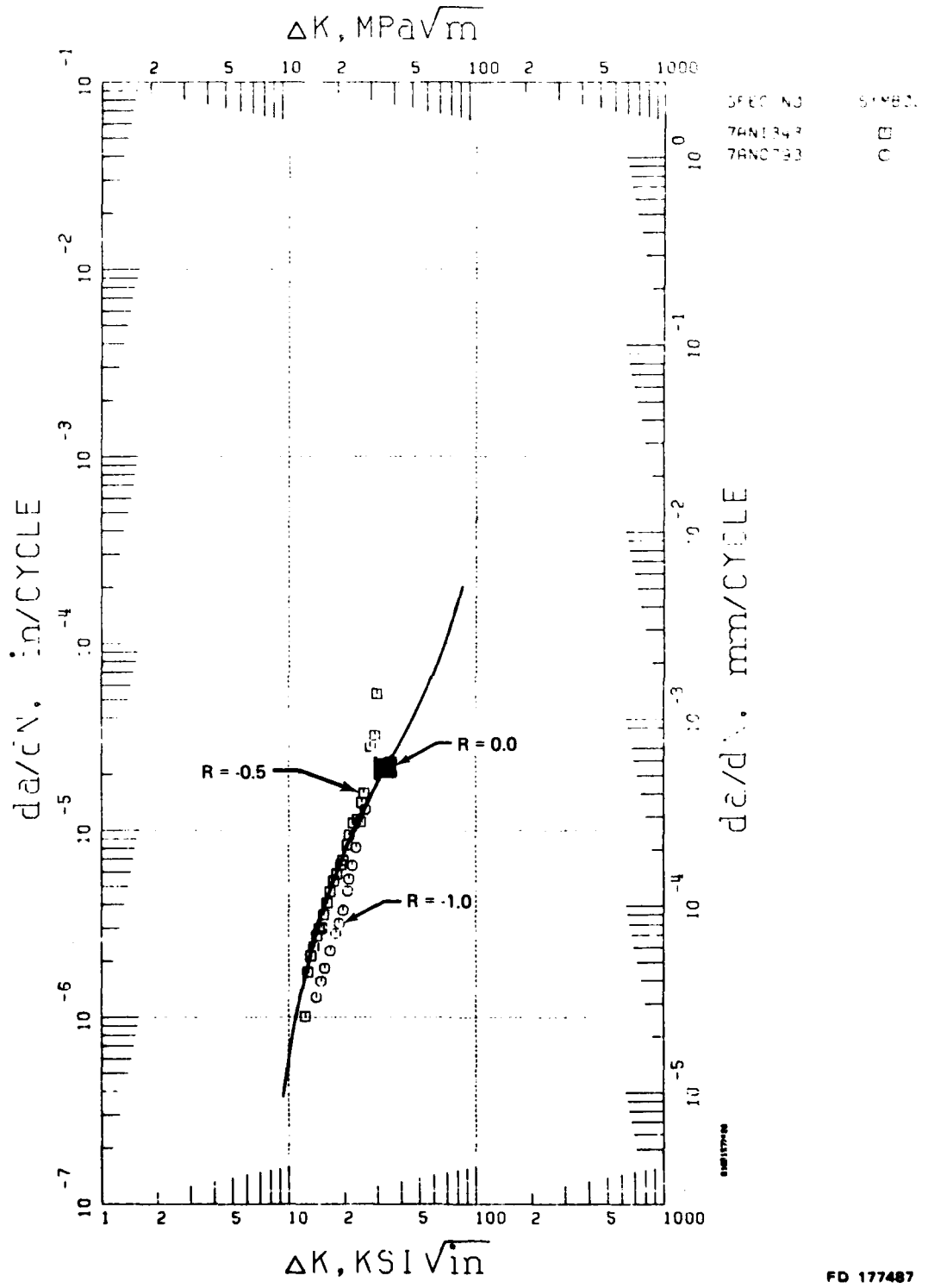

Figure 86. IN100 (PWA 1073) Crack Propagation, Negative Stress Ratio Effect, 0.167 Hz (10 cpm), 427°C (800°F)

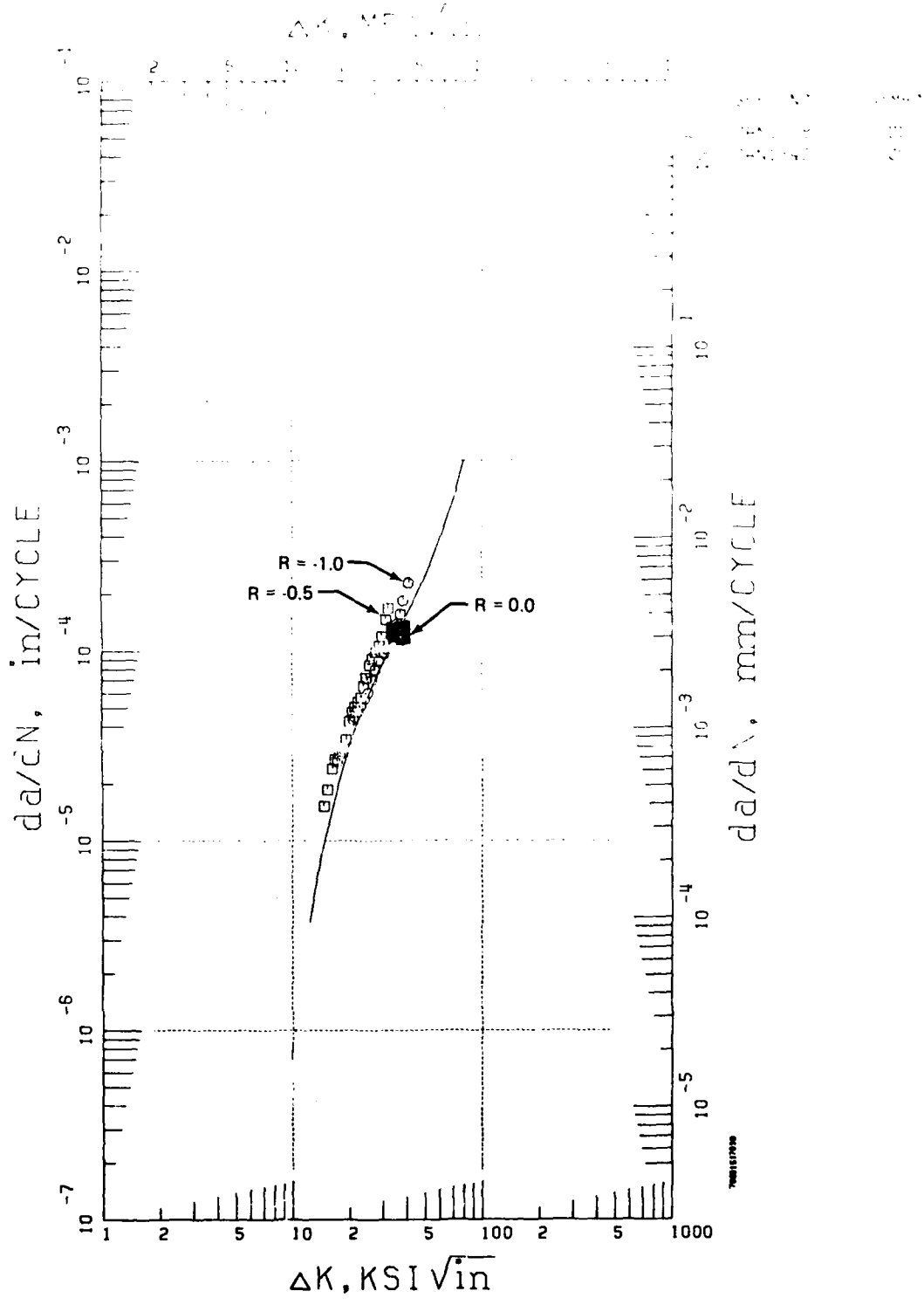

Figure 87. IN100 (PWA 1073) Crack Propagation, Negative Stress Ratio Effect, 0.167 Hz (10 cpm) 649°C (1200°F)

b. *Effect of Net Section Stress*

The effect of high net section stress on crack propagation in Waspaloy (PWA 1007) was investigated using the through-thickness center crack specimen in Figure 11a. This specimen was selected for its small obtainable crack size and the ability to achieve high net section stresses at stress intensities comparable with those of the baseline testing. Tests of two specimens were conducted with $\sigma_{net} > 0.8\ \sigma_{yield}$, T = 649°C (1200°F), R = 0.05, and a frequency of 0.167 Hz (10 cpm). The resulting data are presented in Figure 88, and their relationship to the baseline crack growth curve is illustrated. Crack propagation under the high stress loading is observed to be slightly less rapid than under equivalent test conditions with significantly reduced stress. Thus, the interpolative models of crack propagation in Waspaloy (PWA 1007) should be applicable, but slightly conservative when used to predict crack growth in a stress field of magnitude approaching the material yield strength.

Similar findings have been reported (Reference 2) for the effect of high net section stress on elevated temperature crack propagation in GATORIZED® IN100 (PWA 1073).

c. *Prior Plastic Deformation*

Component crack propagation life predictions are made using da/dN data obtained from virgin (unstrained) material. However, cracks occuring in real hardware often initiate in regions of high stress concentration such as boltholes or blade attachment areas. Material in these regions may be subjected to many strain cycles in excess of 1.0%. It is assumed that FCP behavior (da/DN vs ΔK) in this material is essentially the same as that for virgin material and that data generated on virgin specimens can be used to describe FCP in pre-strained material. The purpose of this auxiliary investigation was to test this hypothesis, using Waspaloy (PWA 1007) and IN100 (PWA 1073).

(1) Waspaloy

In order to simulate the cyclic loading experienced in the vicinity of a bolthole in a Waspaloy turbine disk, 1.0% tensile strain range cycling ($\epsilon_{mean} = \frac{1}{2}\ \epsilon_{max}$) was applied to unnotched center-crack specimens (Figure 11a). The specimens (1321 and 1323) were cycled at 649°C (1200°F) and 0.167 Hz (10 cpm) for 10% (200 cycles) of the expected crack initiation life. Determination of the cyclic stress-strain behavior of Waspaloy was performed using the strain control specimen of Figure 89, and typical hysteresis loops are presented in Figure 90. During the elevated temperature pre-strain cycling, specimen 1321 was monitored with acoustic emission equipment, and a plot of the resulting emission count is presented in Figure 91. The initially high acoustic activity attenuated to a stable level within the first 50 cycles. Acoustic emission reflects damage accumulation during testing. No detectable flaws resulted from the pre-straining.

The unnotched specimens were removed from the test machine, and a through-thickness center flaw was machined in each using electric discharge methods. From this point the specimens were treated the same as virgin specimens. The notched specimens were returned to the testing machine, precracked at room temperature, and the crack was propagated to failure under constant load amplitude fatigue T = 649°C (1200°F), 0.167 Hz (10 cpm), and a stress ratio of 0.1. The crack propagation data (da/dN vs ΔK) and a SINH curve representing crack propagation in virign (unstrained) Waspaloy are presented in Figure 92. Crack growth in the pre-strained material is approximately 30% faster than in virgin material. The crack growth rate in the pre-strained specimens is approximately 30% faster than observed from the virgin material tests. However, this deviation is explainable by intrinsic data scatter for crack propagation testing.

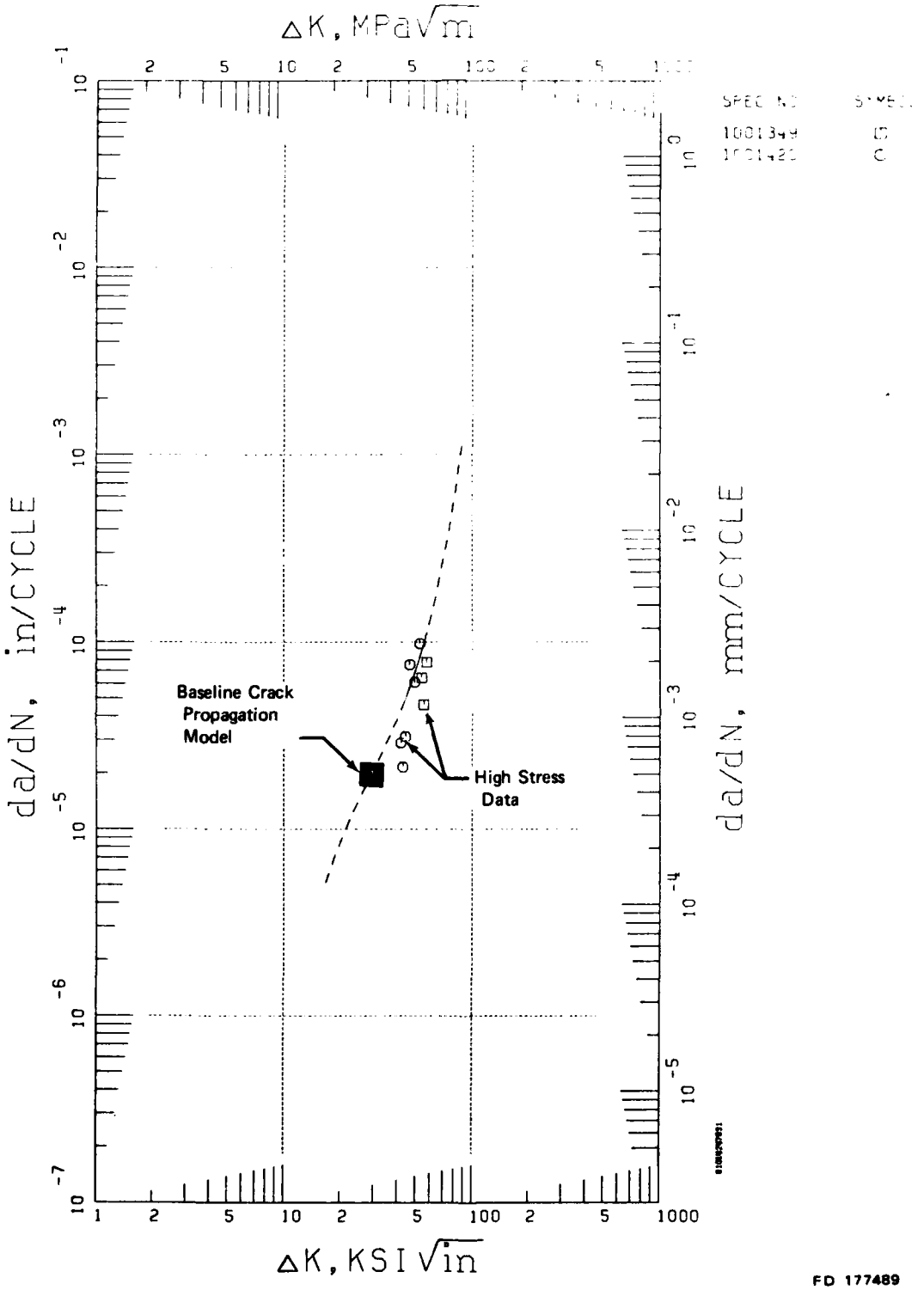

Figure 88. Waspaloy (PWA 1007) Crack Propagation, High Stress Effect, R = 0.05, 0.167 Hz (10 cpm), 649°C (1200°F)

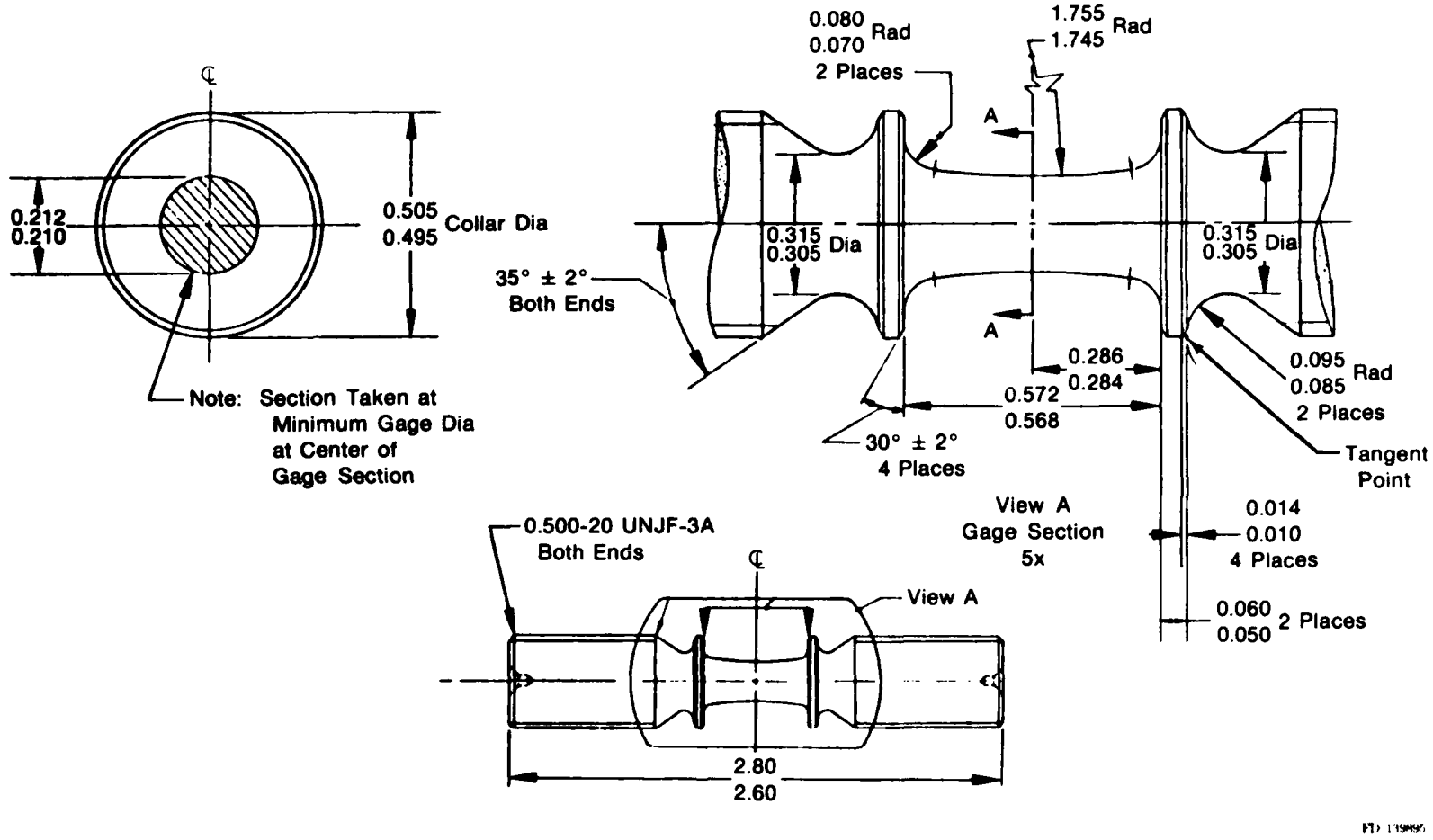

Figure 89. Strain Controlled Low Cycle Fatigue Specimen

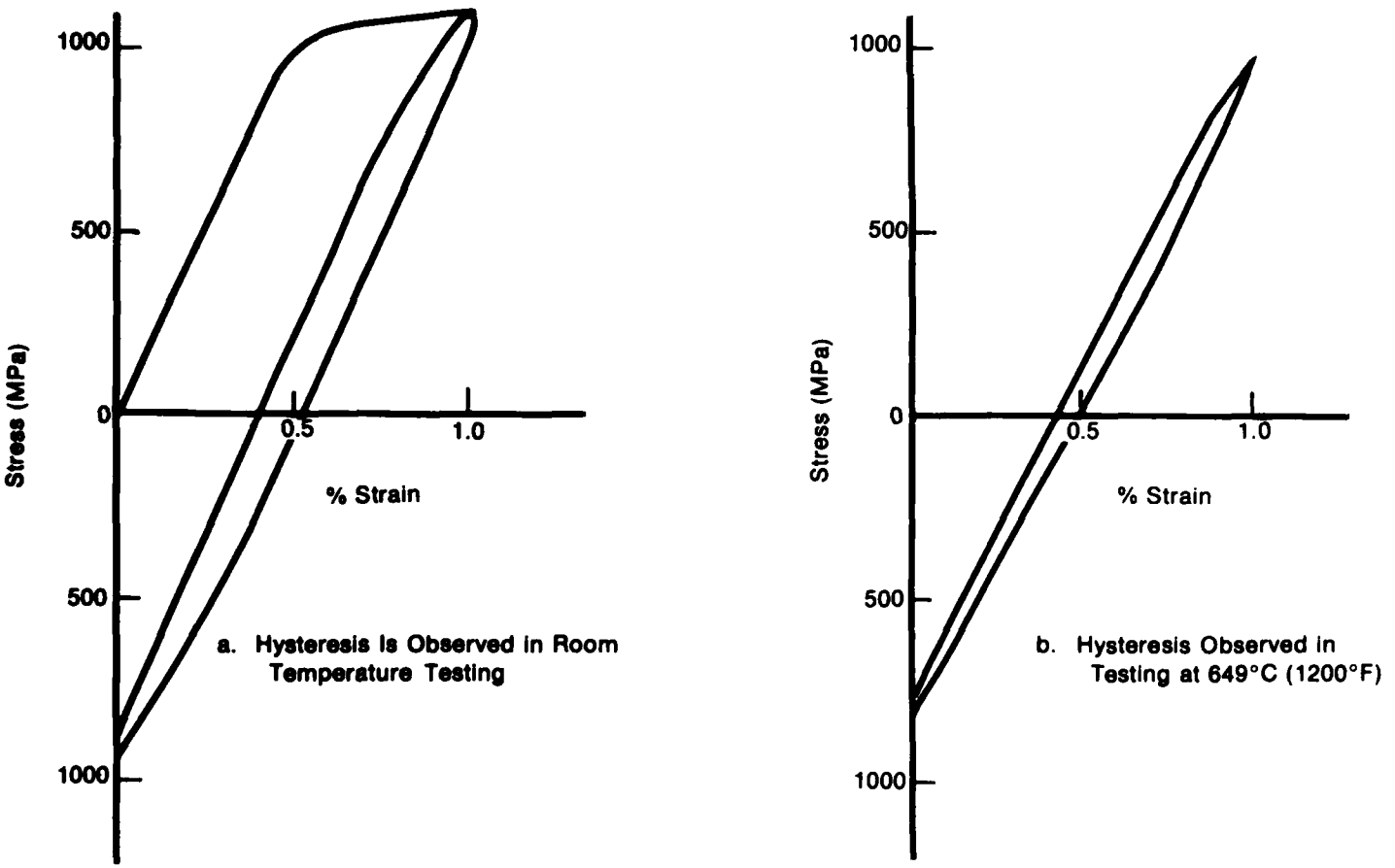

Figure 90. Hysteresis Observed in 1.0% Strain Controlled Testing

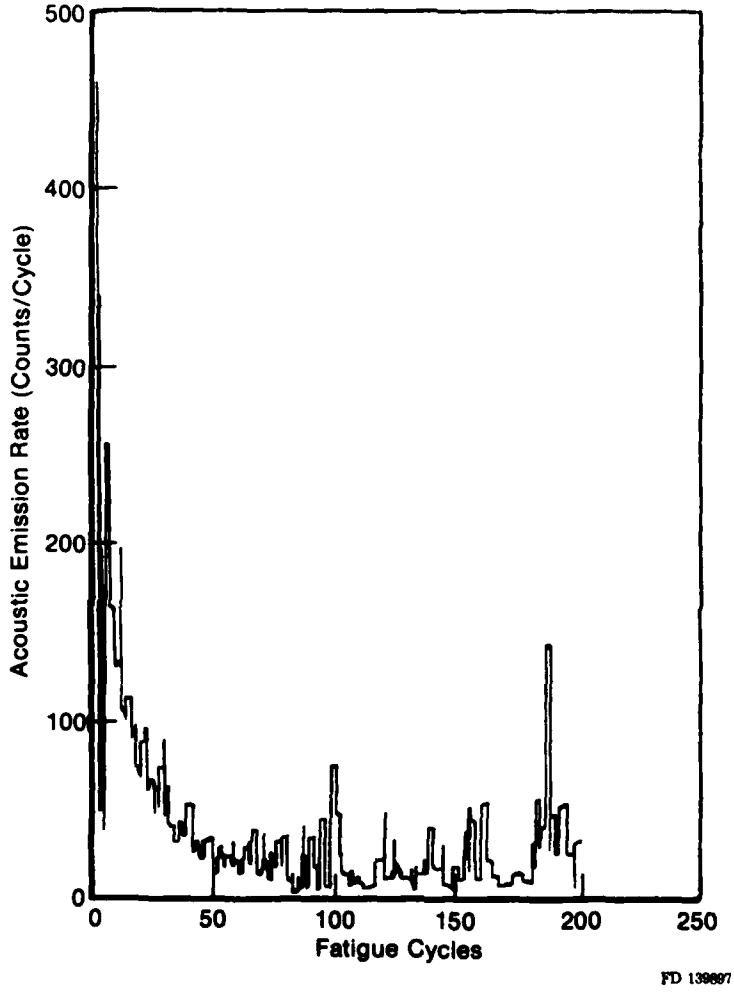

Figure 91. Acoustic Emission Record of Prestrain Cycling of Waspaloy (PWA 1007) Specimen

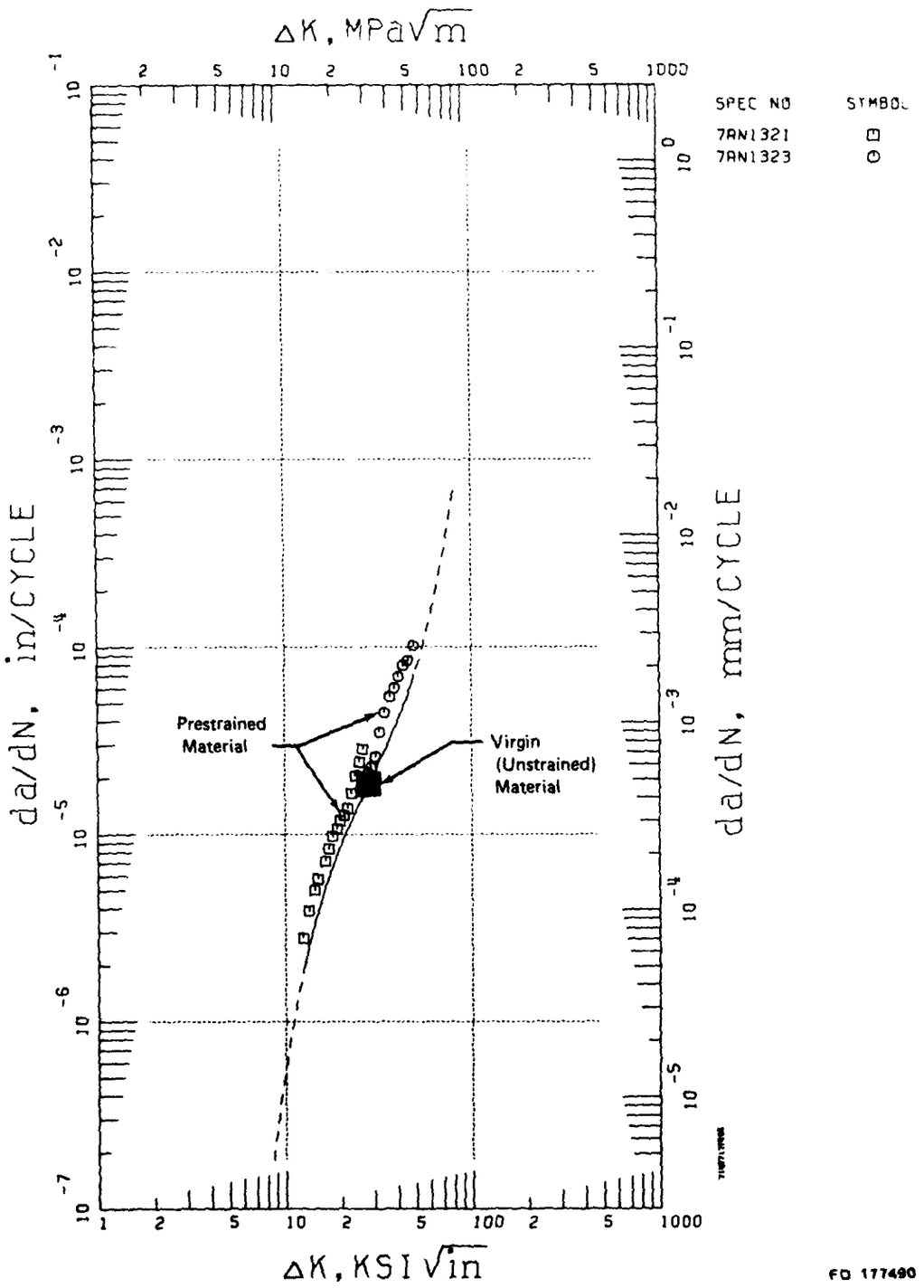

Figure 92. Waspaloy (PWA 1007) Crack Propagation, Effect of Prior Plastic Deformation, R = 0.10, 0.167 Hz (10 cpm), 649°C (1200°F)

(2) IN100

The effect of 1.0% strain cycling prior to crack propagation was also examined in IN100. The procedure was as described for Waspaloy, and the results are illustrated in Figure 93. Crack propagation in pre-strained IN100 was observed to be generally equivalent to characteristic crack growth in virgin IN100.

(3) Component Life Prediction

The results of the Waspaloy and IN100 tests discussed above indicate different effects of 1.0% pre-strain cycling. Using a crack growth model developed for virgin material data, prediction of fatigue crack life in pre-strained Waspaloy (PWA 1007) are expected to be slightly anticonservative, while for IN100, little model bias is indicated. However, the tests results for both materials fall within the range of intrinsic data scatter. Therefore, fatigue crack growth models representing virgin material data from both alloys are applicable to life prediction in pre-strained material.

d. Overload-Underload-LCF Interaction

Flight mission stress analysis which was conducted under Phase I of this contract revealed the existence of compressive stresses within the loading spectrum of a cooled turbine disk (Figure 4). The compressive stresses occurred immediately following a major tensile load excursion (overload) and were expected to have a detrimental influence upon crack propagation rate by reducing the beneficial effect of the overload.

A test was conducted to examine the effect on crack propagation of compressive loading in the repetitive mission sequence of overload-underload-low cycle fatigue, Figure 94. The resulting data was reduced with the hyperbolic sine model and is presented in the comparative plot of Figure 95. The three data sets are from tests of IN100 at 649°C (1200°F) and (1) constant load amplitude fatigue, R = 0.5; (2) constant load amplitude fatigue, R = 0.5, interrupted by a periodic overload (Overload Ratio = P_{OL}/P_{max} = 1.5) every 21 cycles; and (3) identical to (2) with the addition of a single compressive load excursion with an underload of (P_{UL}/P_{max}) = -0.45.

Crack propagation resulting from the overload-LCF loading (curve 2) is significantly less rapid than under similar constant load amplitude fatigue (curve 1). However, the overload-underload-LCF mission produces crack propagation which is slightly more severe than under constant ΔP fatigue. That is, in IN100 (PWA 1073) cycled at 649°C (1200°F) the effect of the minor compressive load excursion (U_{OL} = -0.45) following an overload (OLR = 1.5, ΔN_{OL} = 20) is to erase the beneficial effect of the overload, and the combined effect of the overload-underload sequence is detrimental to the crack propagation life.

Further examination of the influence of overload-underload-LCF sequencing on crack growth is beyond the scope of the present contract. Such research is suggested for a future program.

e. Thermal-Mechanical Fatigue

Because the study of thermal-mechanical synergism is particularly complex, it has been assumed that the effects of frequency, stress ratio, dwells, and overloads occurring with changing temperature can be approximated by considering the isothermal increments of each parameter. The results of a survey test, discussed below, tend to substantiate this approach.

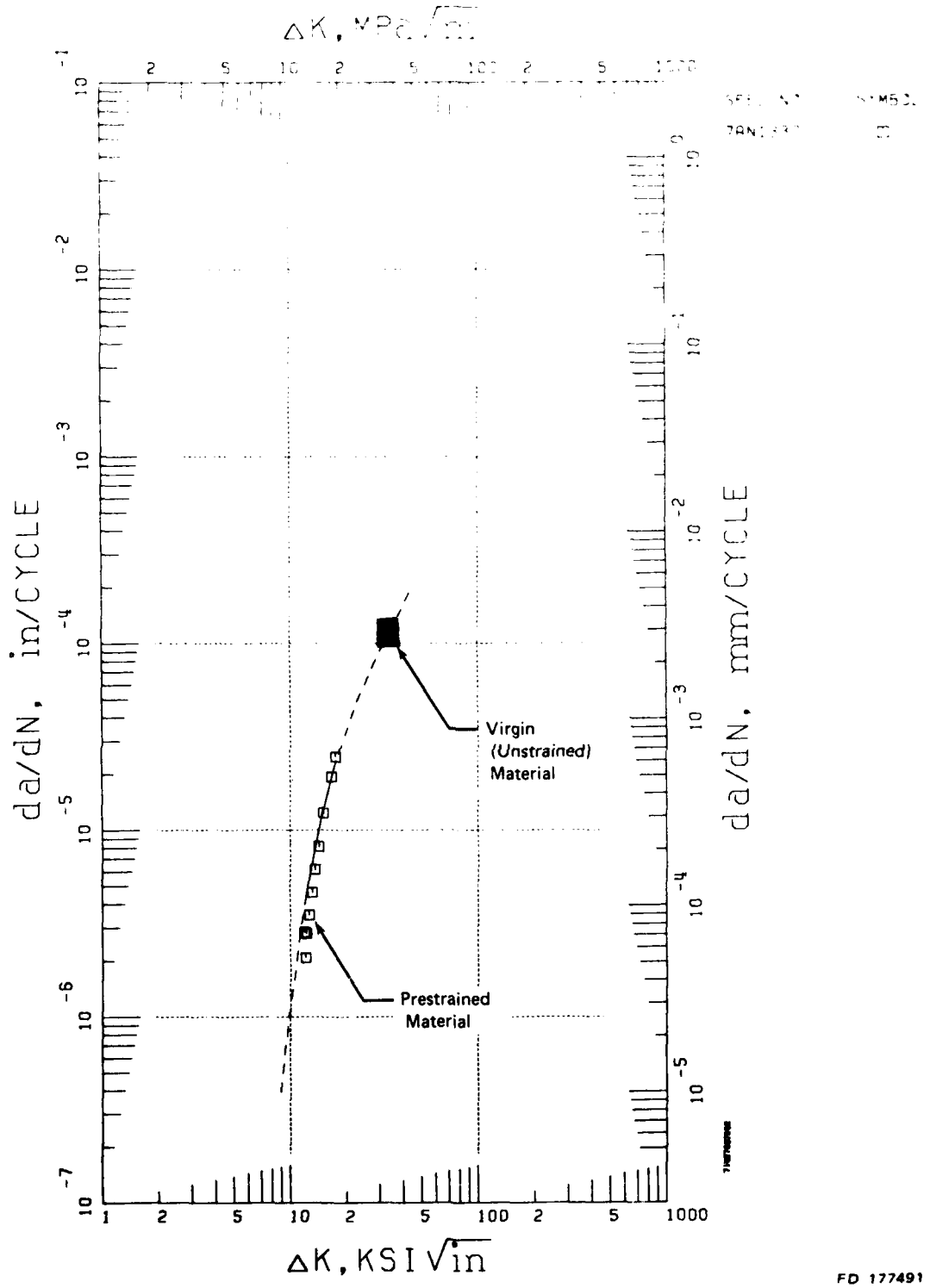

Figure 93. IN100 (PWA 1073) Crack Propagation, Effect of Prior Plastic Deformation, R = 0.10, 0.167 Hz (10 cpm), 649°C (1200°F)

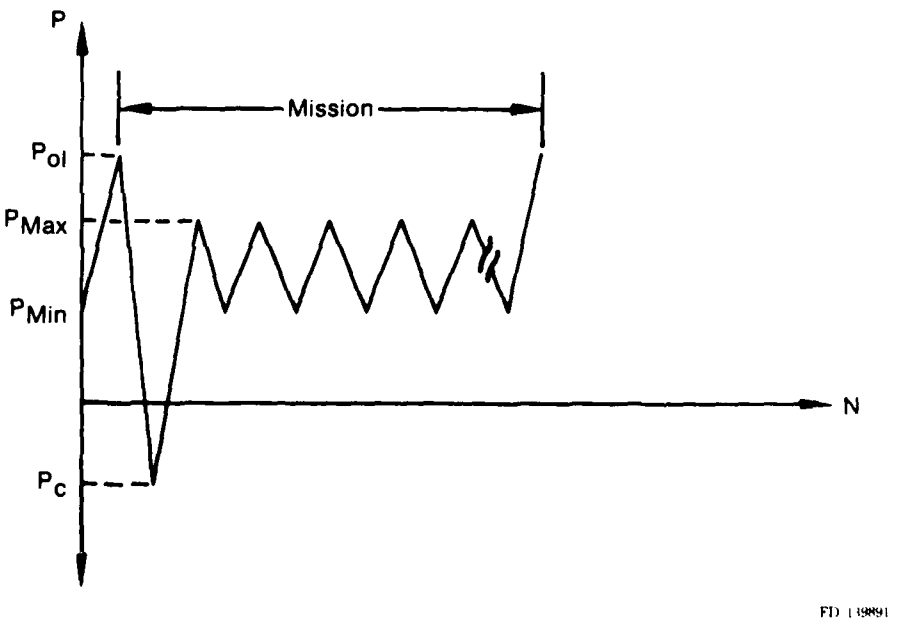

Figure 94. Overload-Underload-LCF Mission

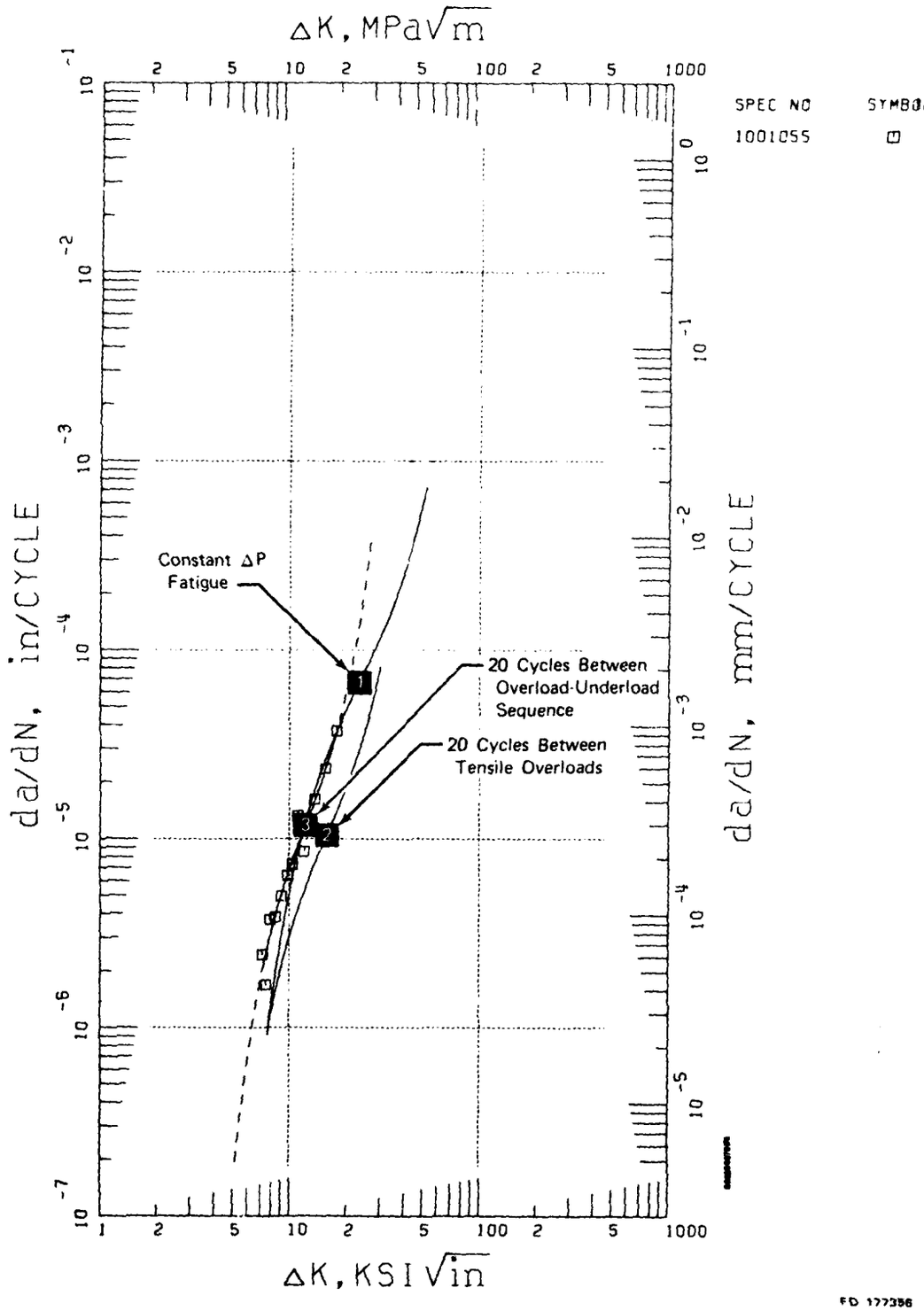

Figure 95. IN100 (PWA 1073) Crack Propagation, Effect of Overload-Underload Sequence, R = 0.50, 0.167 Hz (10 cpm), 649°C (1200°F), OLR = 1.5, $\Delta N_{OL} = 20$

The thermal-mechanical fatigue (TMF) test conducted under this task employed sawtooth waveforms for both thermal and mechanical cycling. Temperature and load cycling were applied 180° out-of-phase as shown in Figure 96, and the test specimen was of through-thickness center crack geometry as shown in Figure 11a. The applied cyclic frequency was 0.0167 Hz (1 cpm) which required heating and cooling rates of 556°C (1000°F) per minute for temperature cycling between 427°C (800°F) and 704°C (1300°F).

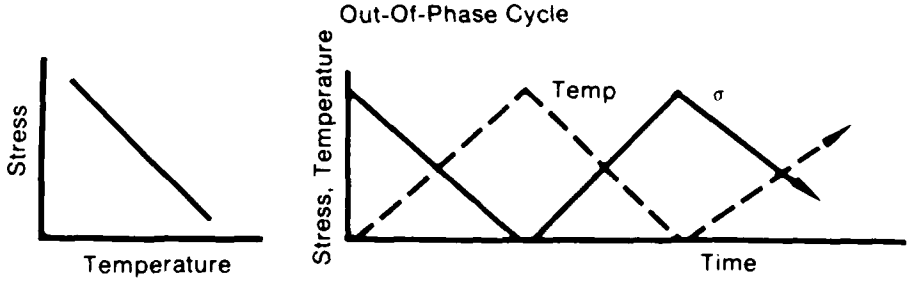

Figure 96. Thermal-Mechanical Fatigue Cycle

Specimen heating was accomplished with electrical induction, and forced air was used to achieve the proper cooling rate. An investigation of the through-thickness thermal gradient in the specimen was conducted by mounting thermocouples on the specimen surface and in a drill hole located at the specimen center. The internal temperature lagged the surface temperature by a maximum of 56°C (100°F) for a 556°C (1000°F) per minute cooling rate.

Figure 97 compares the thermal-mechanical FCP observed under out-of-phase cycling (maximum temperature occurring at minimum load) with crack growth under isothermal conditions at the same frequency and stress ratio (0.0167 Hz (10 cpm), R = 0.10). The four SINH curves represent isothermal crack growth at a series of temperatures which spans the range of thermal cycling (427°C (800°F) to 704°C (1300°F)). The TMF data are observed to correlate well with results of isothermal tests conducted at 427°C. This temperature coincides with the temperature at which peak loading occurs during the TMF cycle, signifying the importance of the peak load vs temperature condition. This result indicates that TMF behavior is more closely related to isothermal FCP than originally thought.

f. Effect of Specimen Thickness

An investigation of the effect of specimen thickness on elevated temperature crack propagation of Waspaloy (PWA 1007) was conducted at 427°C (800°F) and 649°C (1200°F). At each temperature, specimens of three thicknesses (2.54, 7.62, and 12.70 mm) (0.1, 0.3, and 0.5 in.) were tested at similar conditions (0.0167 Hz (10 cpm), R = 0.05). The results of these tests are illustrated in Figure 98 and 99. At each temperature, equivalent rates of crack growth are observed for the 7.62 and 12.70 mm thick specimens, while a much slower rate of crack propagation occurred in the 2.54 mm thick specimen. From these findings it is concluded that the rate of FCP of Waspaloy (PWA 1007) becomes thickness independent at some thickness less than 7.62 mm (0.30 in.).

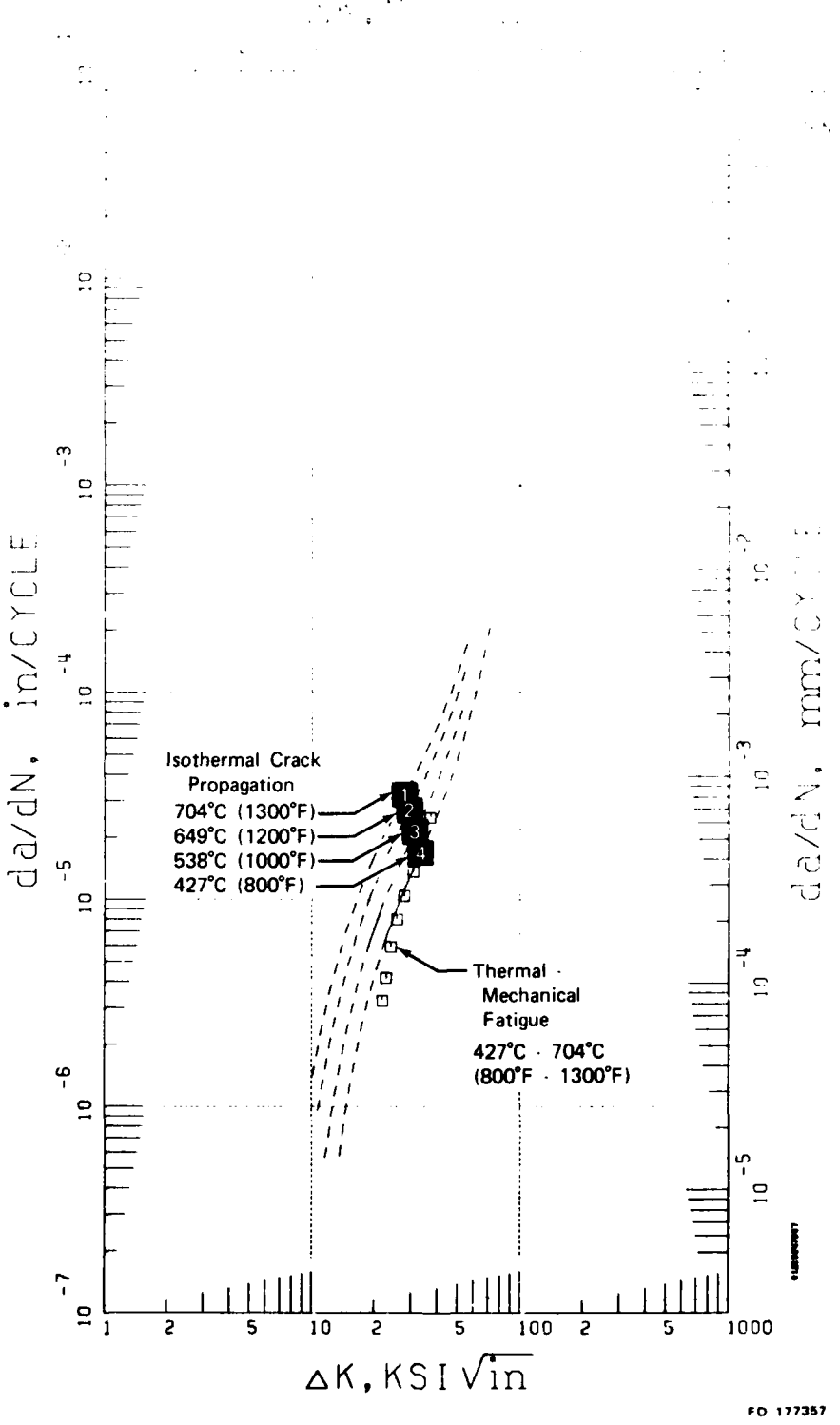

Figure 97. IN100 (PWA 1073) Crack Propagation, Thermal-Mechanical Fatigue, R = 0.10, 0.167 Hz (10 cpm)

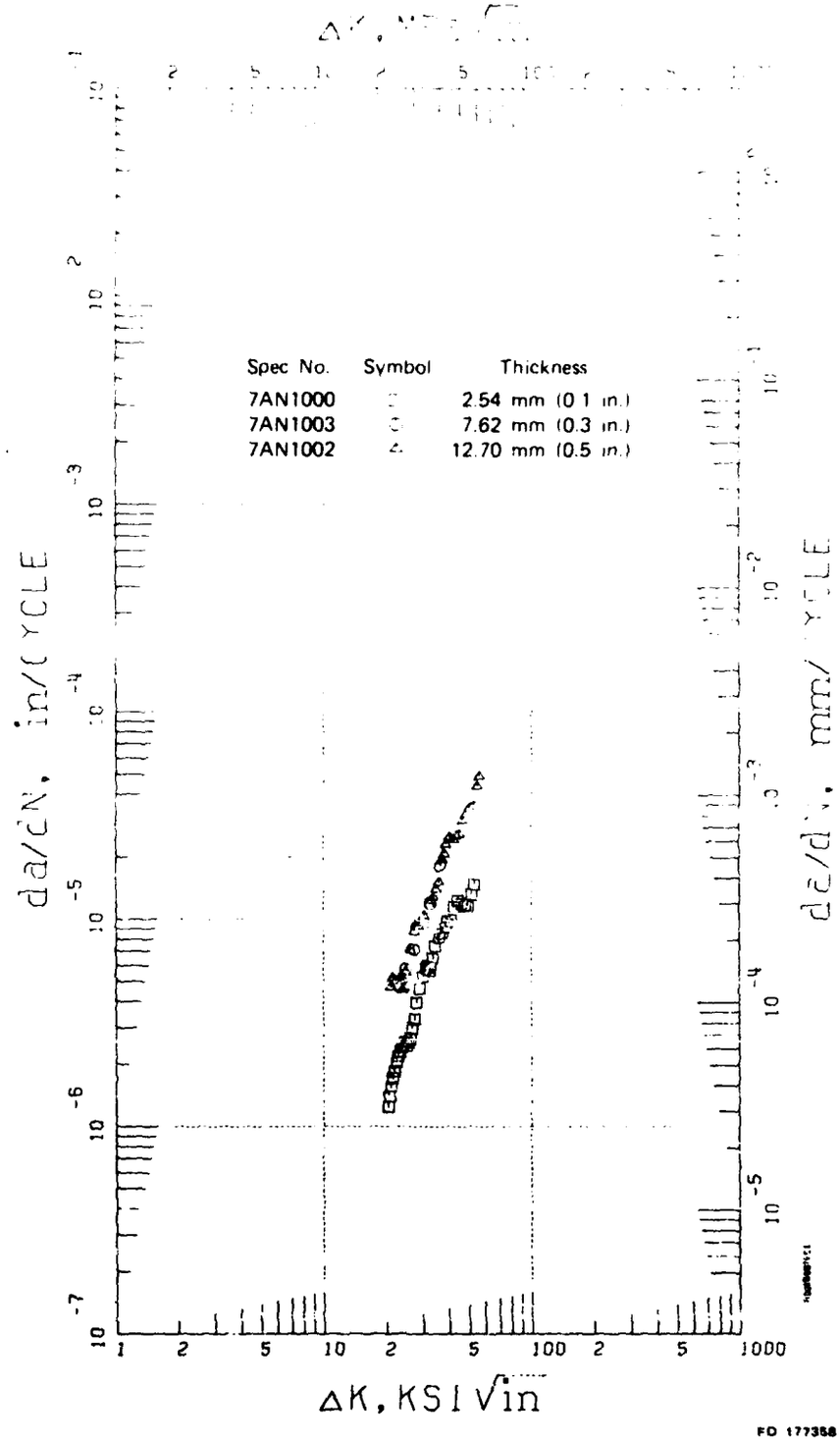

Figure 98. Waspaloy (PWA 1007) Crack Propagation, Effect of Specimen Thickness, R = 0.05, 0.167 Hz (10 cpm), 427°C (800°F)

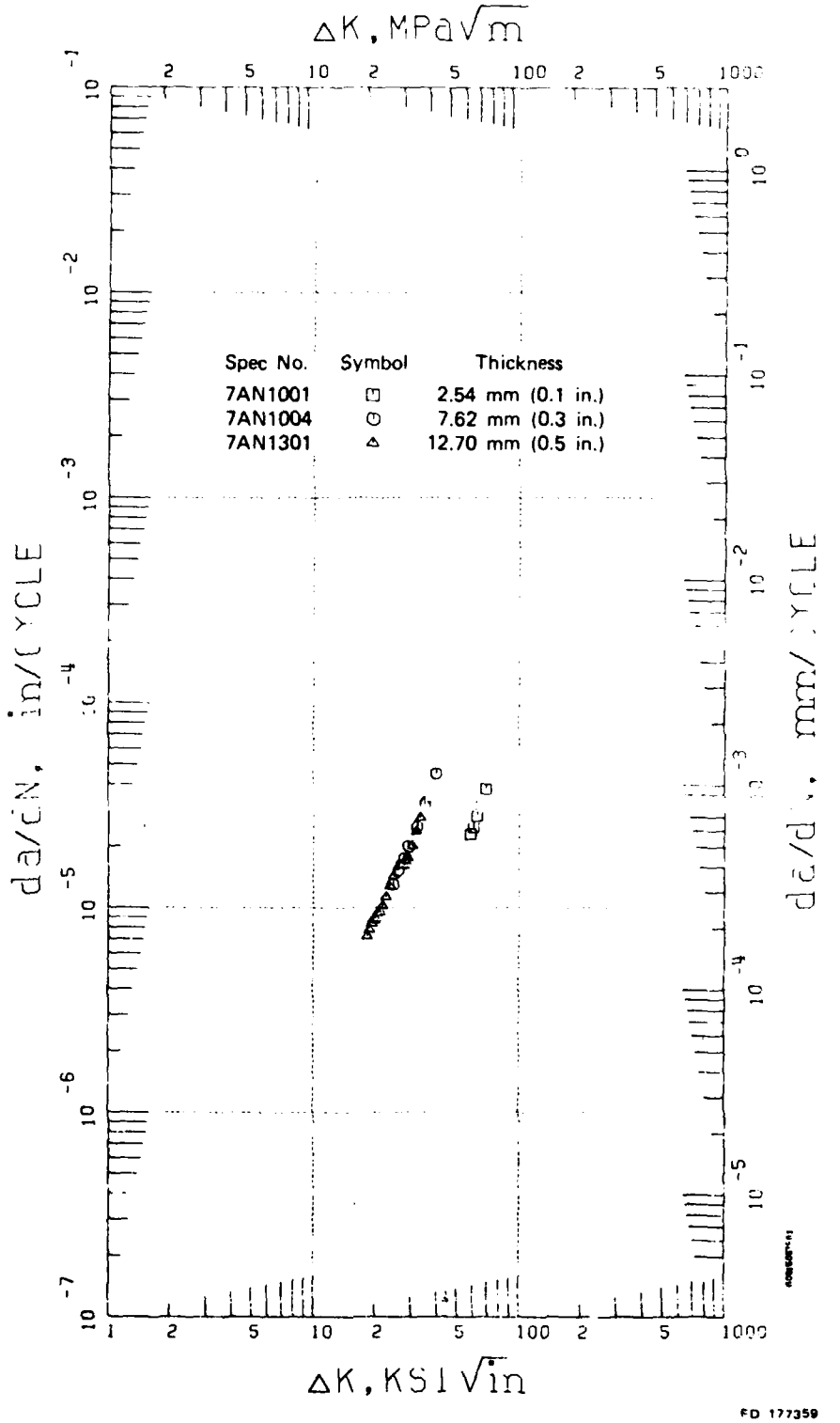

Figure 99. Waspaloy (PWA 1007) Crack Propagation, Effect of Specimen Thickness, R = 0.05, 0.167 Hz (10 cpm), 649°C (1200°F)

D. PHASE IV — MODEL DEMONSTRATION

The goal of this phase of the program was to demonstrate the accuracy of the developed crack propagation model. During the initial step of this effort, the Air Force project engineer provided two mission profiles upon which life history (a vs N) predictions were made. Subsequently, crack propagation tests of Waspaloy (PWA 1007) and IN100 (PWA 1073) were conducted under repetitive application of the provided missions in two specimen geometries — compact and surface flaw.

1. Demonstration Missions

The two demonstration missions supplied by the Air Force are illustrated in Figures 100 and 101. In order to fully exercise the predictive capability of the crack growth model, these missions were chosen to be extreme cases. They were not defined to simulate enigne operation. The first mission, Figure 100, was composed of a series of major load excursions, followed by series of load dwells of increasing magnitude, and ending with a flurry of fatigue cycles at a high load ratio. This was contrasted with the second demonstration mission, shown in Figure 101, which contained much more prominent load sequence effects.

2. Mission Segregation and Life Prediction

Cumulative damage segmentation of the model demonstration missions presented in Figure 100 and 101 was accomplished by use of the segregation algorithm discussed earlier. This computerized procedure characterized the individual loading cycles in terms of basic fatigue parameters such as maximum load (P_{max}), load ration (r), and frequency. Furthermore, the segregation algorithm accounted for load sequence effects which result in crack growth synergism. Major load excursions were identified and load sequence parameters describing overload ratio and occurence frequency were defined by the algorithm.

For example, model demonstration mission number 1 begins with four major load excursions. These were defined in terms of P_{max}, R, and frequency, and the fourth of these cycles were identified as an overload affecting subsequent cycles. All of the remaining cycles in this mission were of reduced maximum load and are therefore influenced by the overload. The number of overload affected cycles (ΔN_{OL}) was defined, and the overload ratios P_{OL}/P_{max}) were calculated for the individual post-overload cycles. Note that the subsequent repetitive mission marks the end of the cycles influenced by the overload, since the overload ratio returns to 1.0

The occurrence of the series of stairstep load dwells within mission 1 posed an unusual situation. As discussed earlier, testing under LCF-Dwell load sequencing revealed that the crack growth resulting from the intermittent load dwells was significantly slower than observed for equivalent repetitive load dwells. This behavior occurred in both Waspaloy and IN100 and agrees with the findings of Macha, Grandt, and Wicks. (Reference 10.) These researchers, performing elevated temperature crack propagation testing of IN100, observed minimal effect of load dwells in a representative mission load sequence. This finding is incorporated in the segregation algorithm by defining as zero the crack growth associated with sustained load mission segments. Crack propagation produced by a load dwell cycle was assumed to result entirely from the initial load excursion in the dwell cycle. In the event that successive, increasing load dwells occurred, the stairstep loading sequence was reduced to a single monotonic load excursion. Therefore, the stairstep sequence of mission 1 was characterized as a single loading cycle which occurred during the indicated time interval.

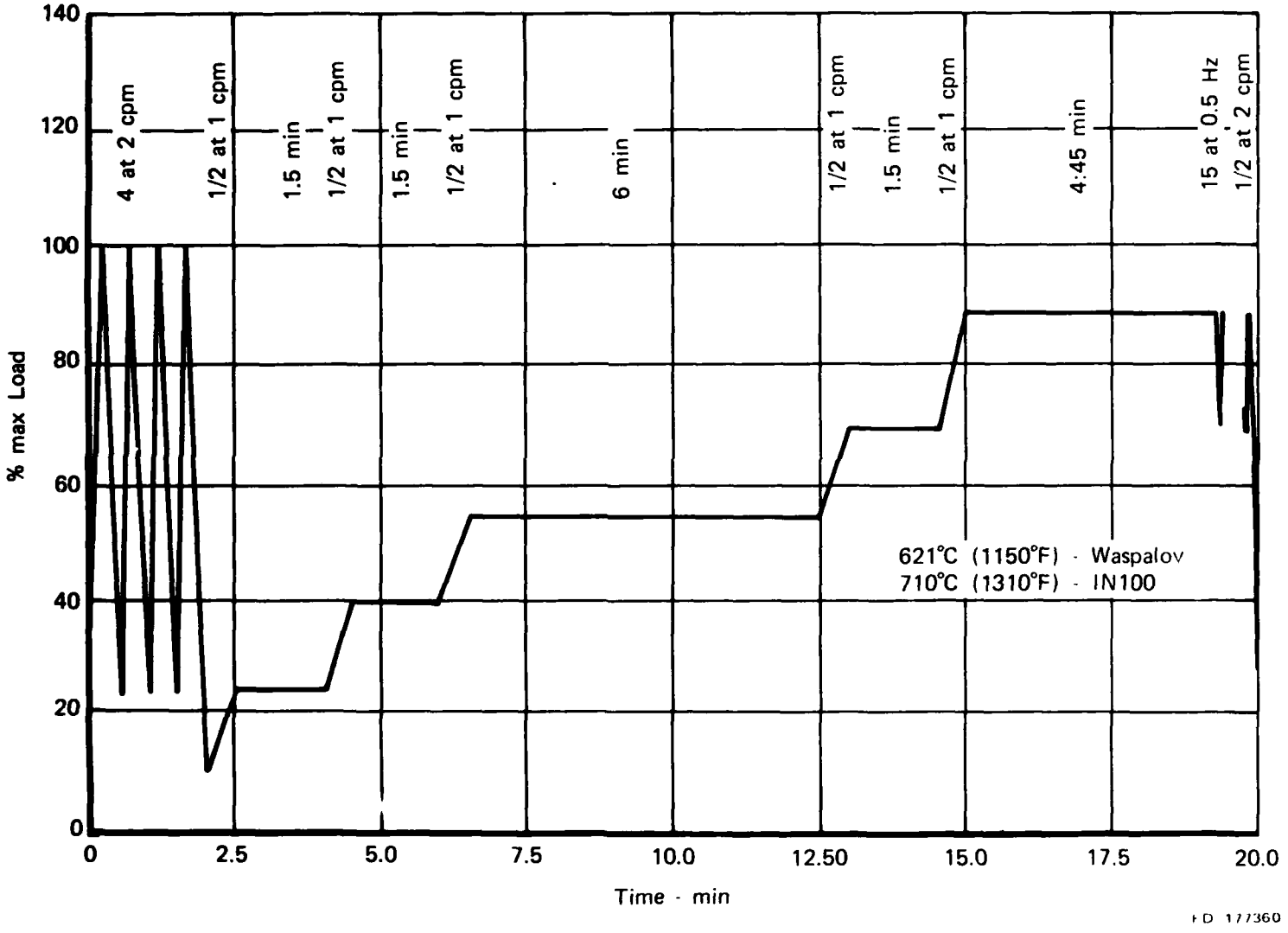

Figure 100. Model Demonstration Mission, No. 1

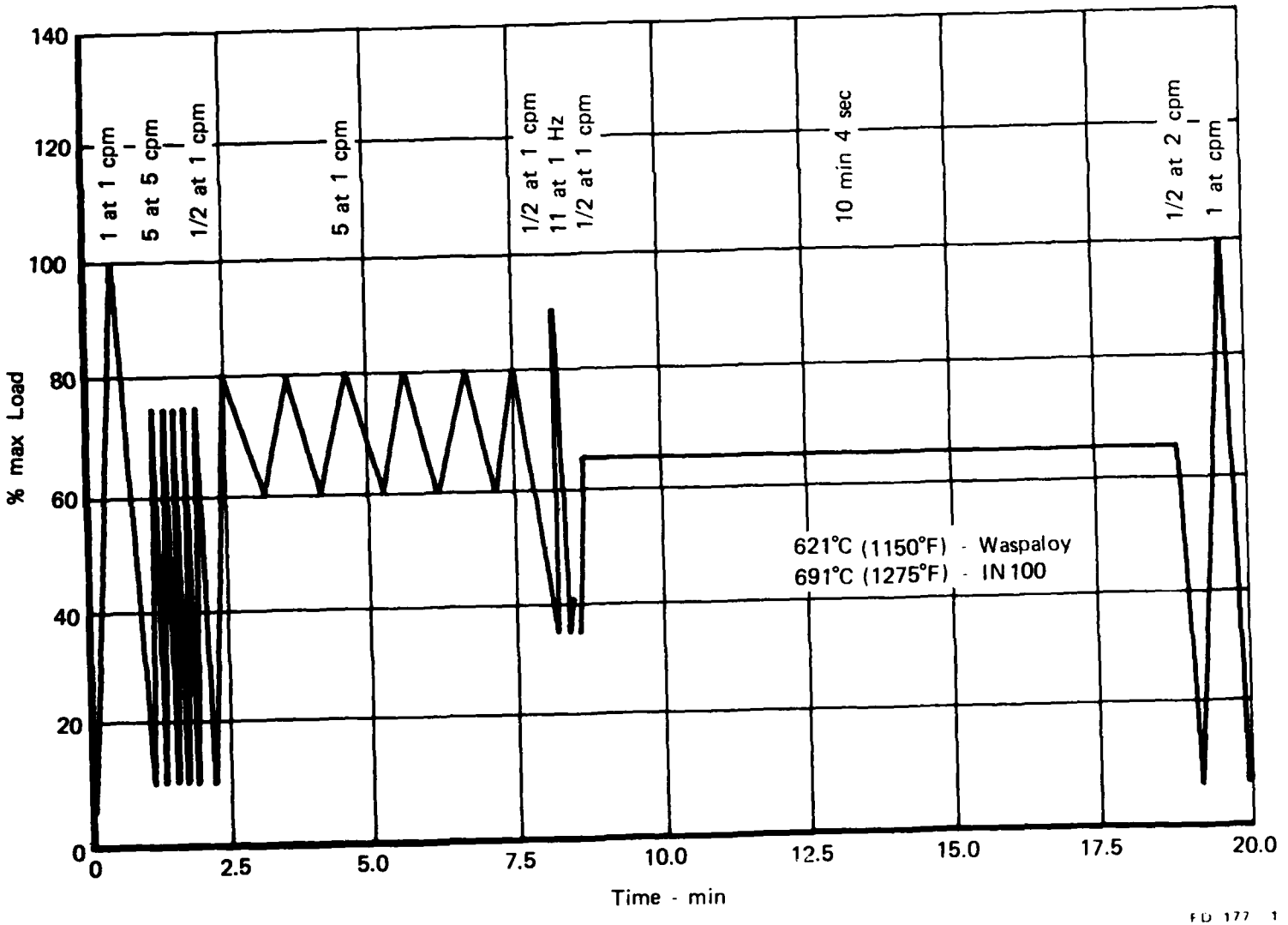

Figure 101. Model Demonstration Mission, No. 2

Segregation of model demonstration mission number 2 (Figure 101) was also performed by the computer algorithm. All cycles were defined in terms of load, load ratio, and frequency, and the first cycle was identified as an overload. The lsat cycle in the mission, being equivalent to the overload cycle, terminated the calculated effect of the initial overload. The number of overload affected crack growth cycles was determined and the individual ratios were calculated.

The mission segregations discussed above were the basis of a synergistic model life prediction accounting for load sequence interactions. A cycle-by-cycle partitioning of the test missions assuming that load sequence does not affect crack growth (i.e. that linear damage summation method) was performed by truncating the load sequence parameters from the output of the synergistic segregation algorithm. This abbreviated mission segregation formed the basis of the SINH Linear Damage Model life prediction.

The segregated missions were subsequently input into the interpolation algorithm which defined a characteristic crack growth curve for each unique loading condition. The output of this routine was that used in a cycle-by-cycle integration of crack growth, known as the Computational Algorithm, to obtain life calculations for a total of eight demonstration specimens. There were four specimens in each material, Waspaloy (PWA 1007) and IN100 (PWA 1073). Two specimen geometries (compact and surface flaw) were tested under each of the two missions (Figures 100 and 101). Since a linear damage and a synergistic model life prediction was calculated for each of the eight specimens, a total of sixteen life calculations were performed. These were recorded with the Air Force project engineer prior to mechanical testing.

3. Demonstration Testing

The two specimen geometries used in demonstration testing were the compact (Figure 11b) and the surface flaw specimen (Figure 102). The compact specimen has a well characterized stress intensity solution (Reference 5) and was used extensively during the test program, while the surface flaw specimen is less familiar and was unused in data generation. The stress intensity solution for this specimen was taken from calculations performed by P&WA/ Commercial Products Division (Reference 11). Figure 103 compares this analytically determined surface flaw K-solution and a solution calculated using handbook values (Reference 12).

Experimental verification of the accuracy of the stress intensity solution was performed by testing a Waspaloy (PWA 1007) surface flaw specimen at fatigue conditions equivalent to baseline data generated, under the test program of this contract. This data is illustrated in Figure 104 with $2b/w \leq 0.45$, and good correlation with the SINH curve generated from baseline data is observed.

All testing was performed on servocontrolled hydraulic machines operated under load control with mission profile described by either an MTS minicomputer or a DATATRAK® controller. The atmosphere was laboratory air, and specimen heating was accomplished using clamshell resistance furnaces.

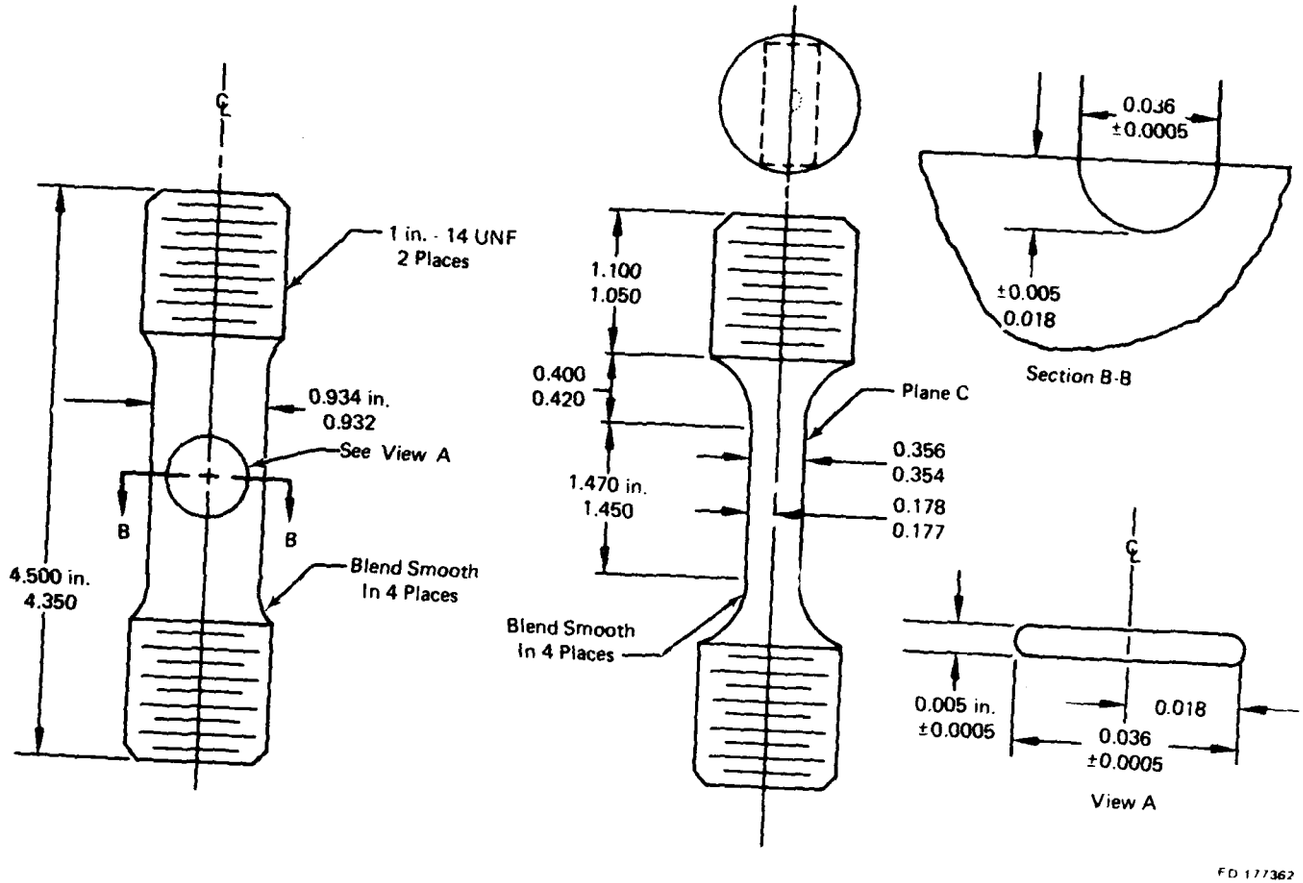

Figure 102. Surface Flaw Specimen

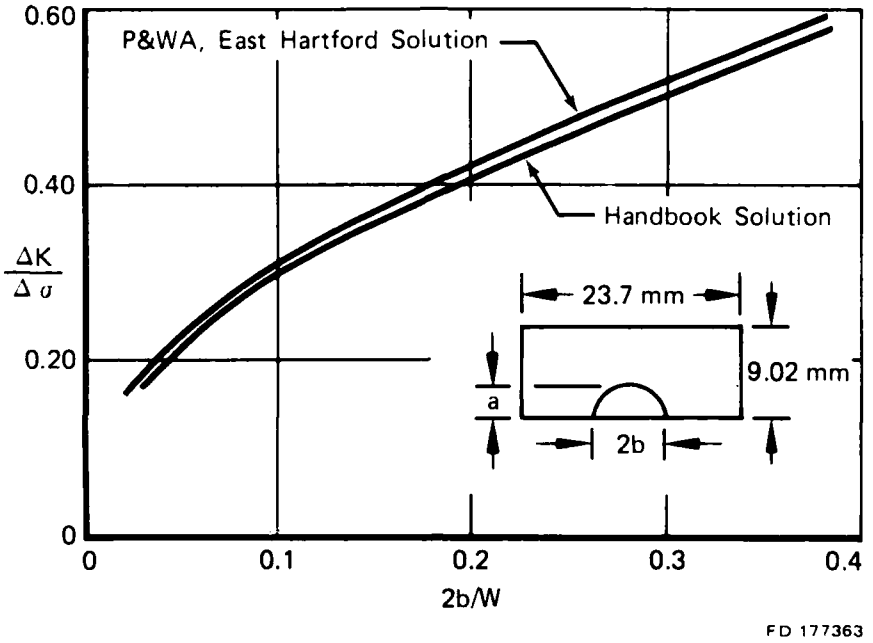

Figure 103. Comparison of K-Calibration Curves for Surface Flaw Specimen

4. Model Verification

Model demonstration tests were conducted to determine the accuracy of the crack propagation models developed under this program. The procedure of modeling crack growth under complex loading conditions was equivalent for both Waspaloy and IN100. The test data from all specimens were treated in a uniform fashion. In order to eliminate transient effects on crack propagation commonly associated with change from room temperature precracking conditions to elevated temperature test conditions, the initial 0.635 mm (0.025 in.) of crack growth was deleted from all data sets.

a. Waspaloy (PWA 1007)

All mission testing to evaluate the effectiveness of the Waspaloy (PWA 1007) crack propagation model was conducted at a single temperature: 621°C (1150°F). The results of tests performed under Mission 1 (Figure 100) using compact and surface flaw specimens are presented in Figures 105 and 106, respectively. For both specimens, the life predictions agree well with the data.

A parameter which may be used to sample the accuracy of the live prediction is the ratio of calculated cycles to failure vs actual cycles to failure (N_c/N_A). For the compact specimen (Figure 105) this parameter demonstrates the superior accuracy of the synergistic model as compared to the life prediction using linear damage summation.

The results of the test of the surface flaw specimen, Figure 106, indicate that the total life prediction is more accurate using SINH linear damage summation. However, the accuracy of the surface flaw stress intensity factor solution diminishes for $2b/w > 0.45$ due to the proximity of the edges and back surface of the specimen. For the surface flaw specimens tested in this program, this corresponds to a half crack length of approximately 5.3 mm (0.210 in.). Therefore, the data of crack length greater than this value are not entirely valid and should not be used for model evaluation. These data are shown as solid triangles.

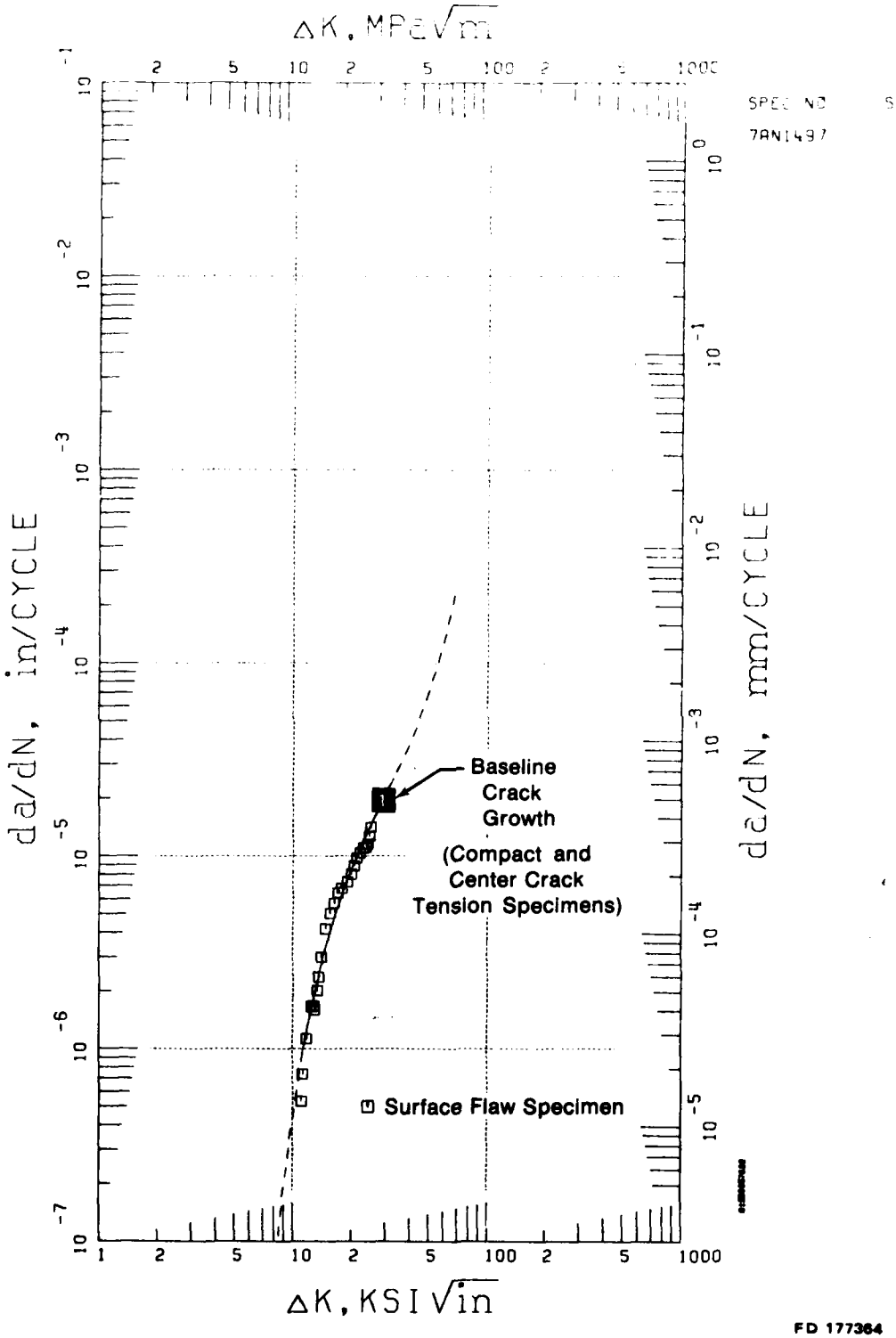

Figure 104. Waspaloy (PWA 1007) Crack Propagation, Comparison of Data Generated in a Surface Flaw Specimen With Baseline Data, R = 0.05, 0.167 Hz (10 cpm), 649°C (1200°F)

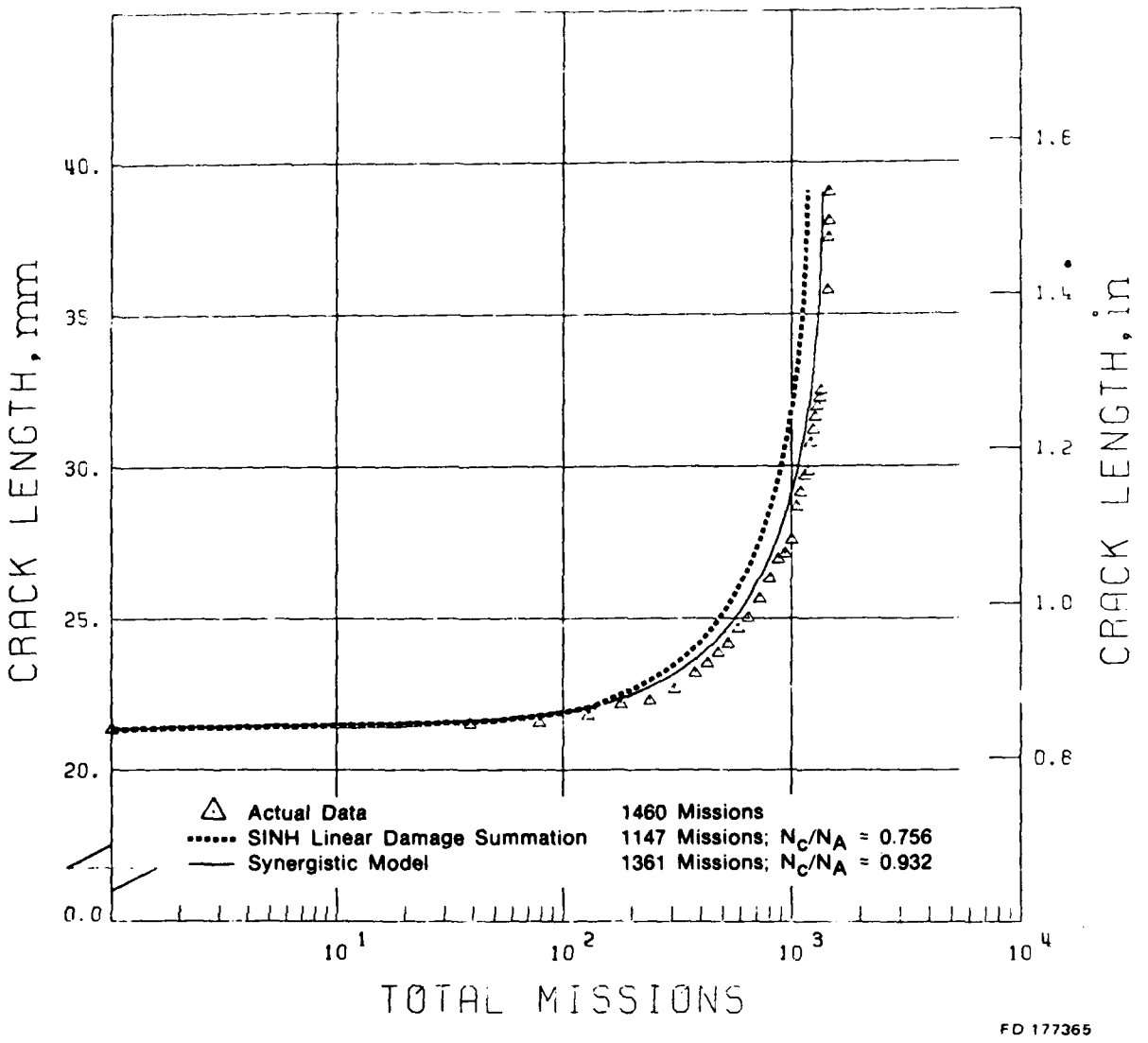

Figure 105. Waspaloy (PWA 1007) Model Description Test, Mission 1, Compact Specimen No. 1565, 621°C (1150°F)

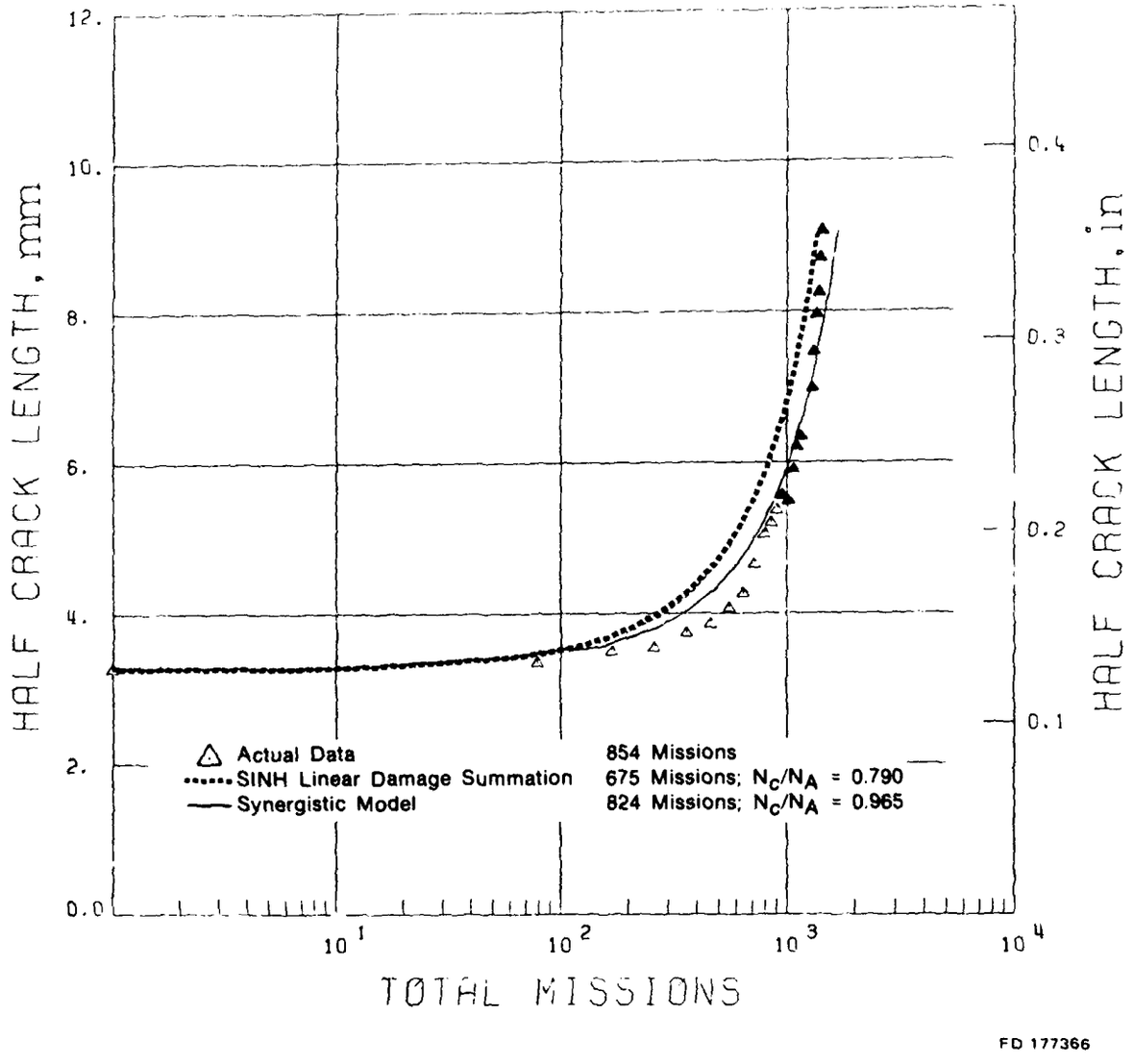

Figure 106. Waspaloy (PWA 1007) Model Demonstration Test, Mission 1, Surface Flaw Specimen No. 1500, 621°C (1150°F)

Model demonstration tests of Waspaloy fatigued according to Mission 2 (Figure 101) were also predicted well by the SINH model. Test results from the compact specimen, Figure 107, revealed good accuracy for both the SINH linear damage and the synergistic SINH models. Early in the life of the specimen the prediction using SINH linear damage methods corresponds closely to the actual fatigue data, while the synergistic prediction is superior when considering the total life of the specimen.

Both synergistic and SINH linear damage calculations of crack growth resulting from Mission 2 loading were less adequate in predicting the life of the surface flaw specimen. These predictions and the actual data, are presented in Figure 108. The three, inconsistently long, crack length measurements which are highlighted, are the work of an inexperienced technician. Discounting these isolated data points and recalling that the stress intensity factor solution for this specimen loses accuracy for half crack length greater than approximately 5.3 mm (0.210 in.), both life calculations are demonstrated as conservative. The approximate values N_{calc}/N_{actual} for the linear damage and synergistic models are 0.58 and 0.73 respectively for the 5.3 mm crack.

b. IN100 (PWA 1073)

The IN100 demonstration specimen life predictions of Mission 1 (Figure 101) calculated using the interpolative SINH models were less accurate than the Waspaloy predictions. Both synergistic and SINH linear damage calculations gave anticonservative life predictions of both specimen geometries, tested at 710°C (1310°F), as shown in Figures 109 and 110. Test results of the compact specimen (Figure 109) show the synergistic and linear damage calculations to overpredict the actual specimen life as demonstrated by the respective values of N_c/N_A of 3.76 and 2.94. The prediction errors for the surface flaw specimens were similar (synergistic model: $N_c/N_A = 1.57$; linear damage summation: $N_c/N_A = 1.25$).

The capability of the IN100 interpolative SINH model demonstrated much more effective in predicting crack growth in the Mission 2 (Figure 101) loading sequence. In test at 691°C (1275°F) of a compact specimen (Figure 111) the synergistic model prediction was extremely accurate ($N_c/N_A = 0.96$), while the life calculation using methods of linear damage summation indicate a much shorter life ($N_c/N_A = 0.64$). In a similar Mission 2 model demonstration test using a surface flaw specimen (Figure 112) the synergistic model prediction exhibited reasonable accuracy ($N_c/N_A = 0.67$), while the linear damage summation calculation was significantly conservative ($N_c/N_A = 0.36$).

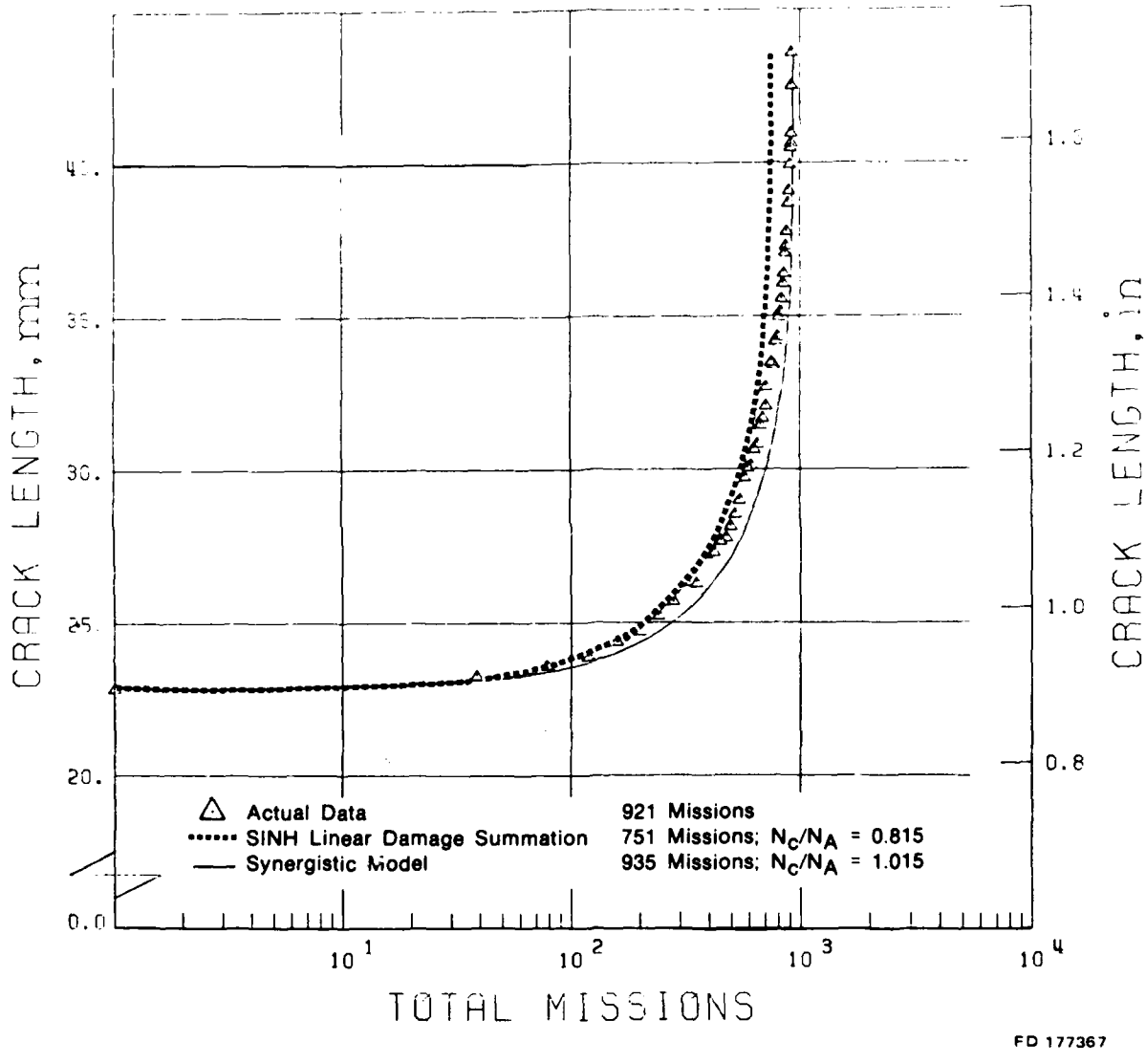

Figure 107. Waspaloy (PWA 1007) Model Demonstration Test, Mission 2, Compact Specimen No. 1563, 621°C (1150°F)

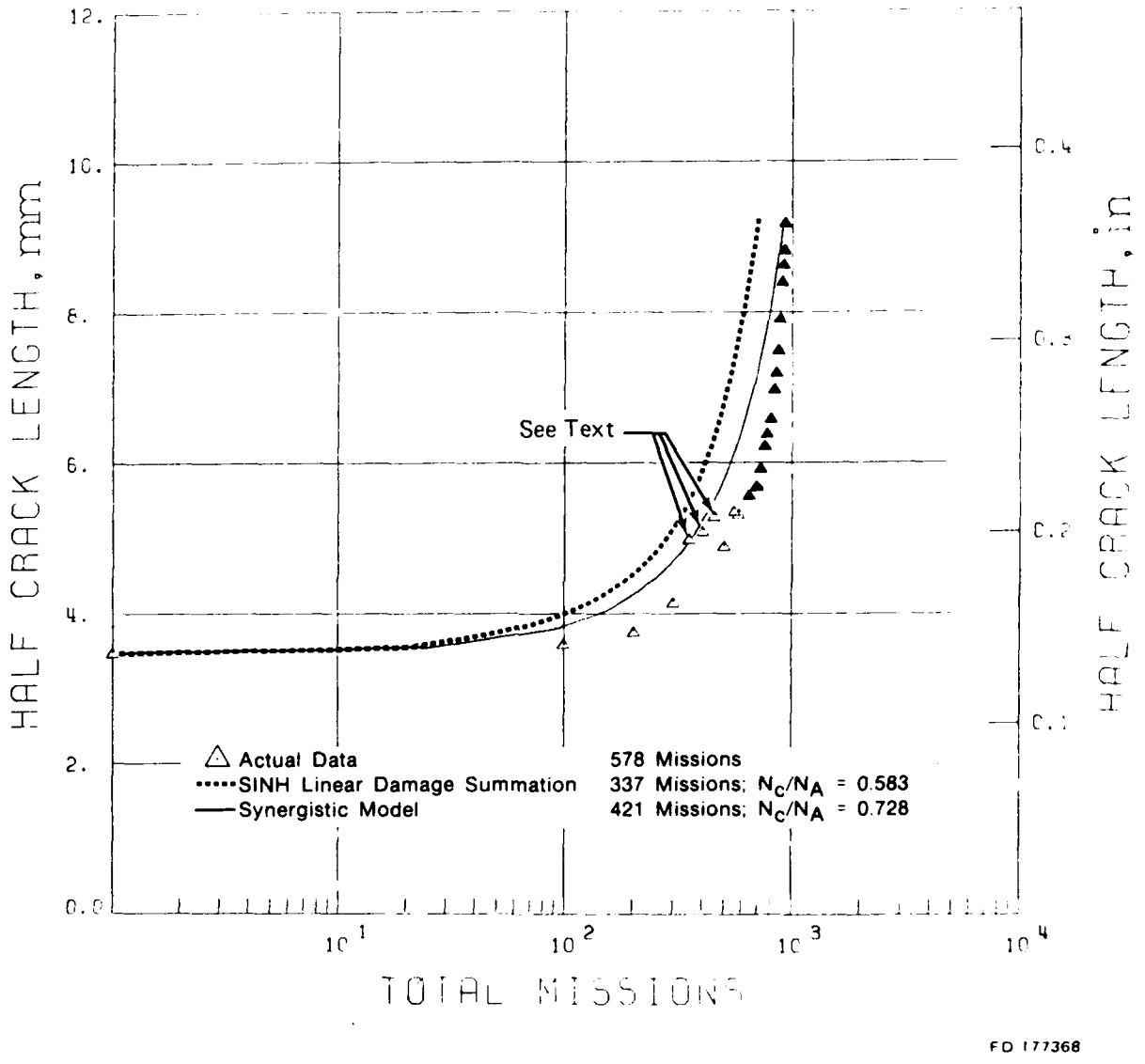

Figure 108. Waspaloy (PWA 1007) Model Demonstration Test, Mission 2, Surface Flaw Specimen No. 1498, 621°C (1150°F)

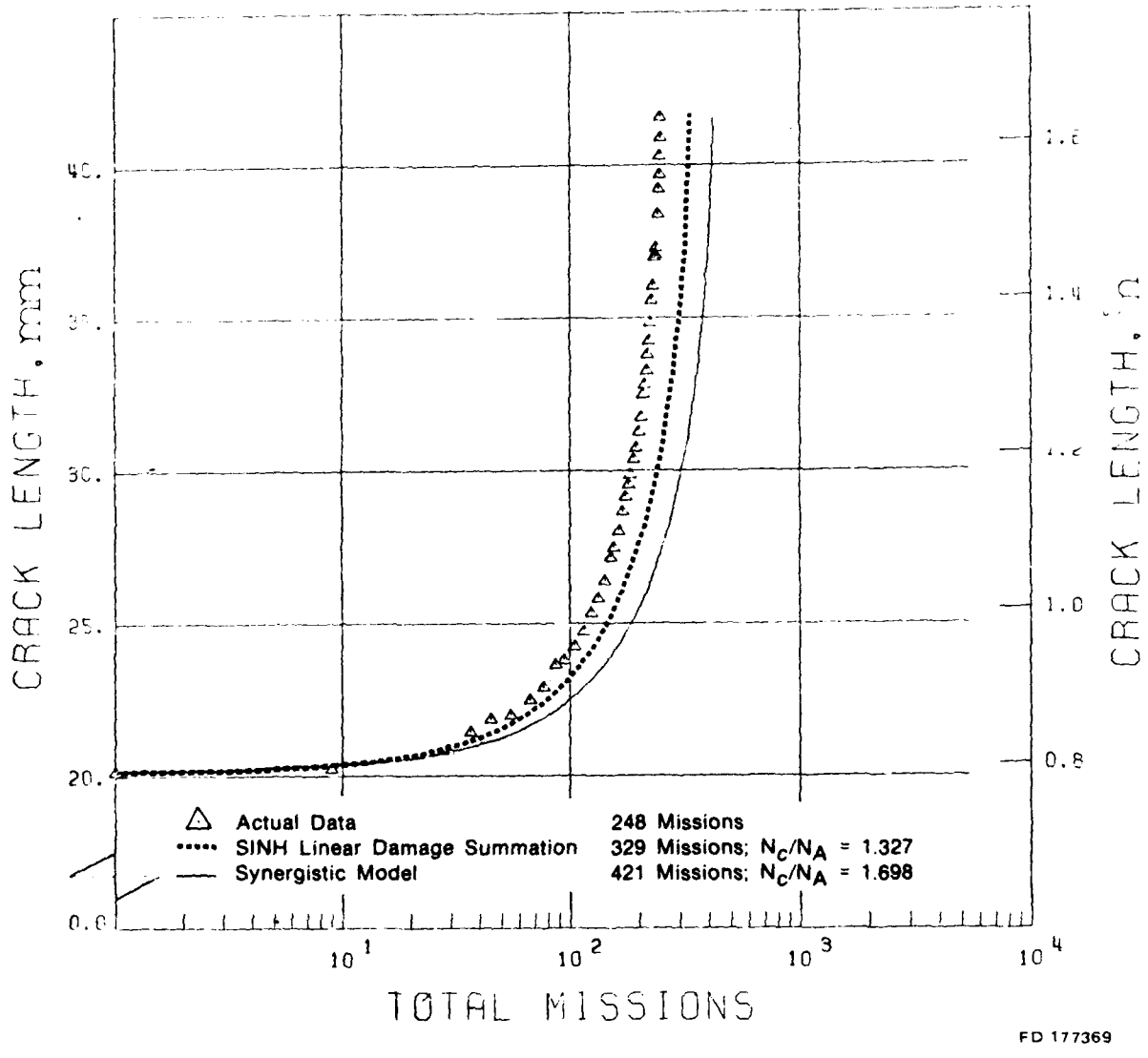

Figure 109. IN100 (PWA 1073) Model Demonstration Test, Mission 1, Compact Specimen No. 1334, 710°C (1310°F)

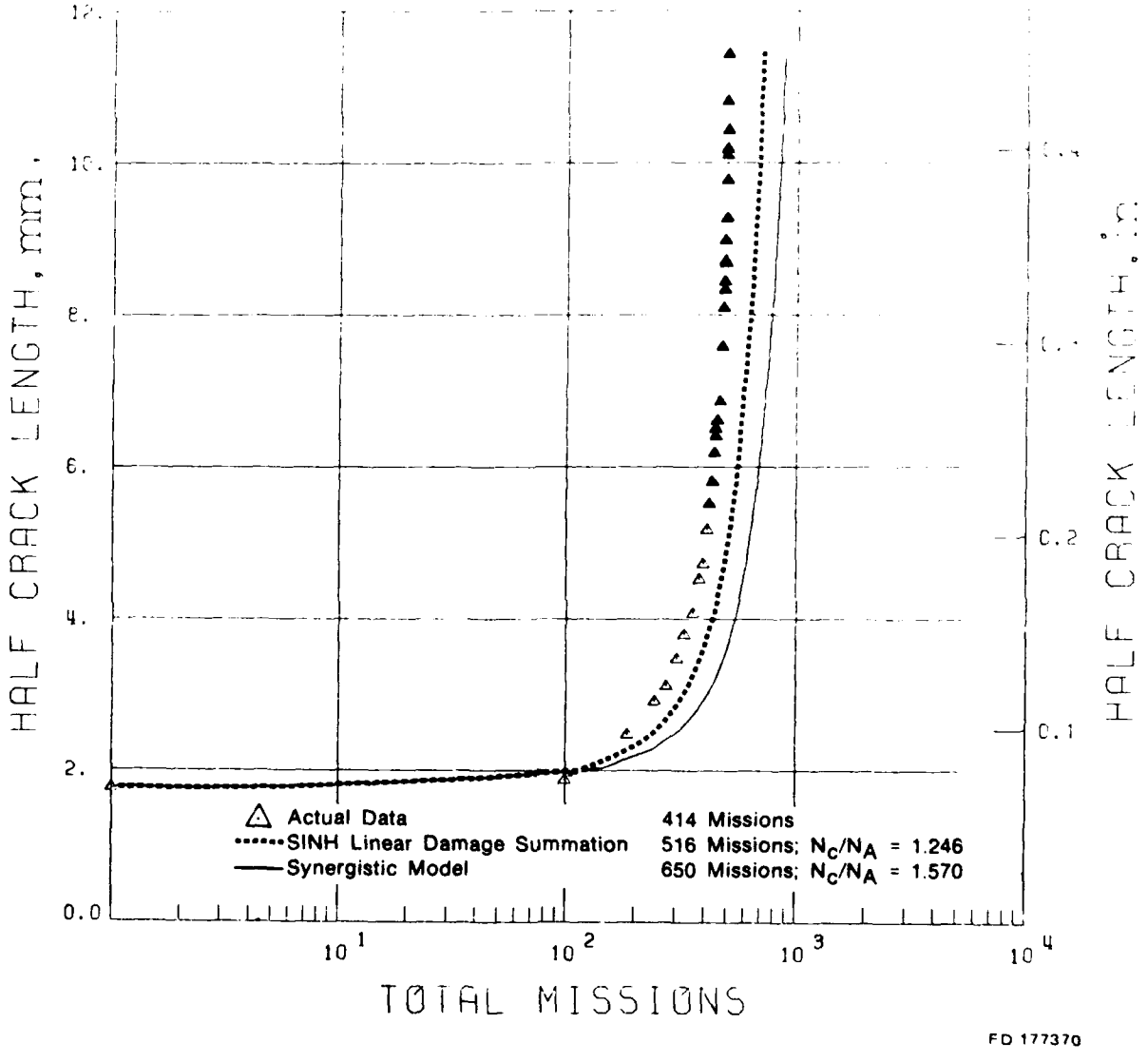

Figure 110. IN100 (PWA 1073) Model Demonstration Test, Mission 1, Surface Flaw Specimen No. 1473, 710°C (1310°F)

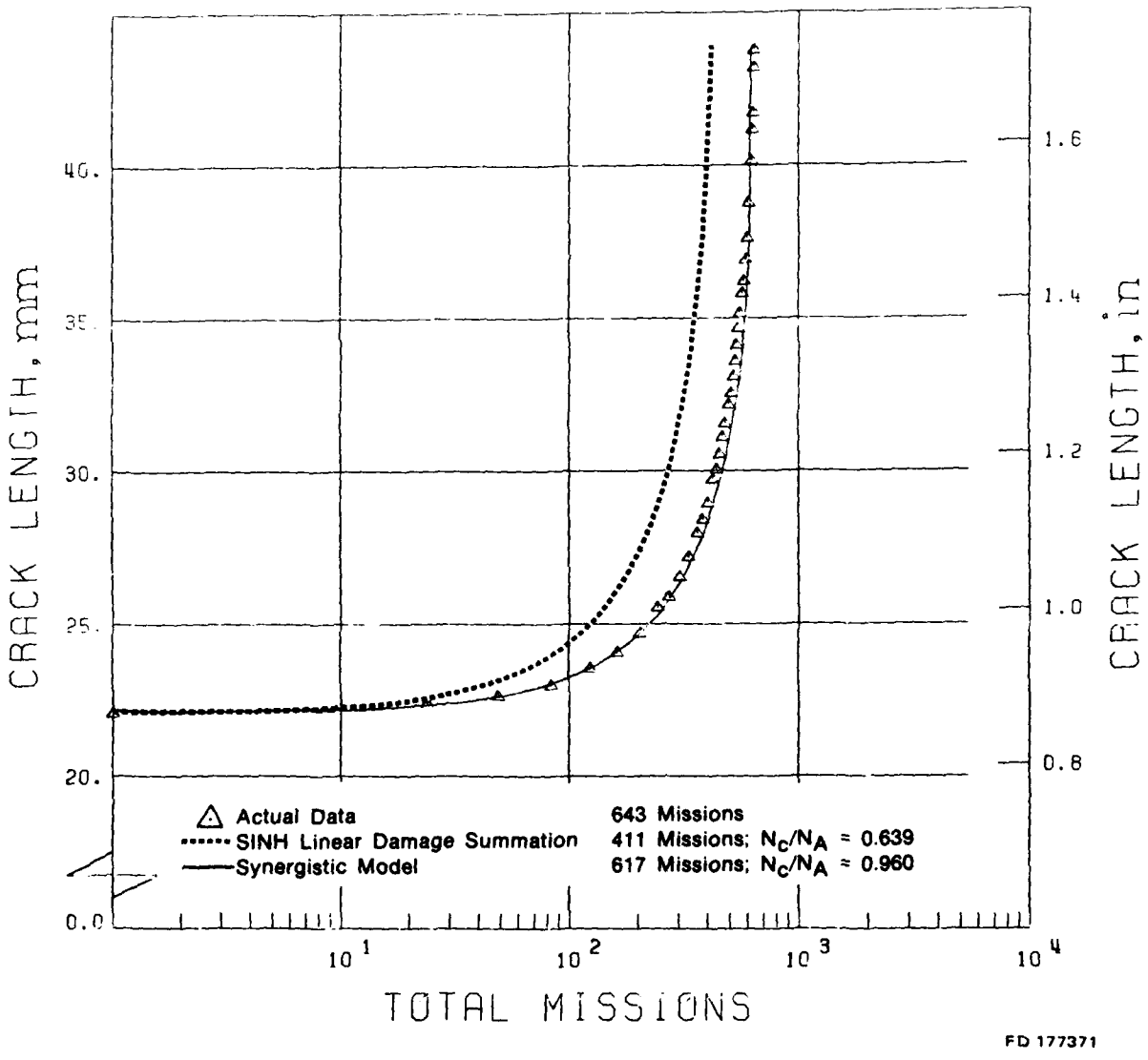

Figure 111. IN100 (PWA 1073) Model Demonstration Test, Mission 2, Compact Specimen No. 1333, 691°C (1275°F)

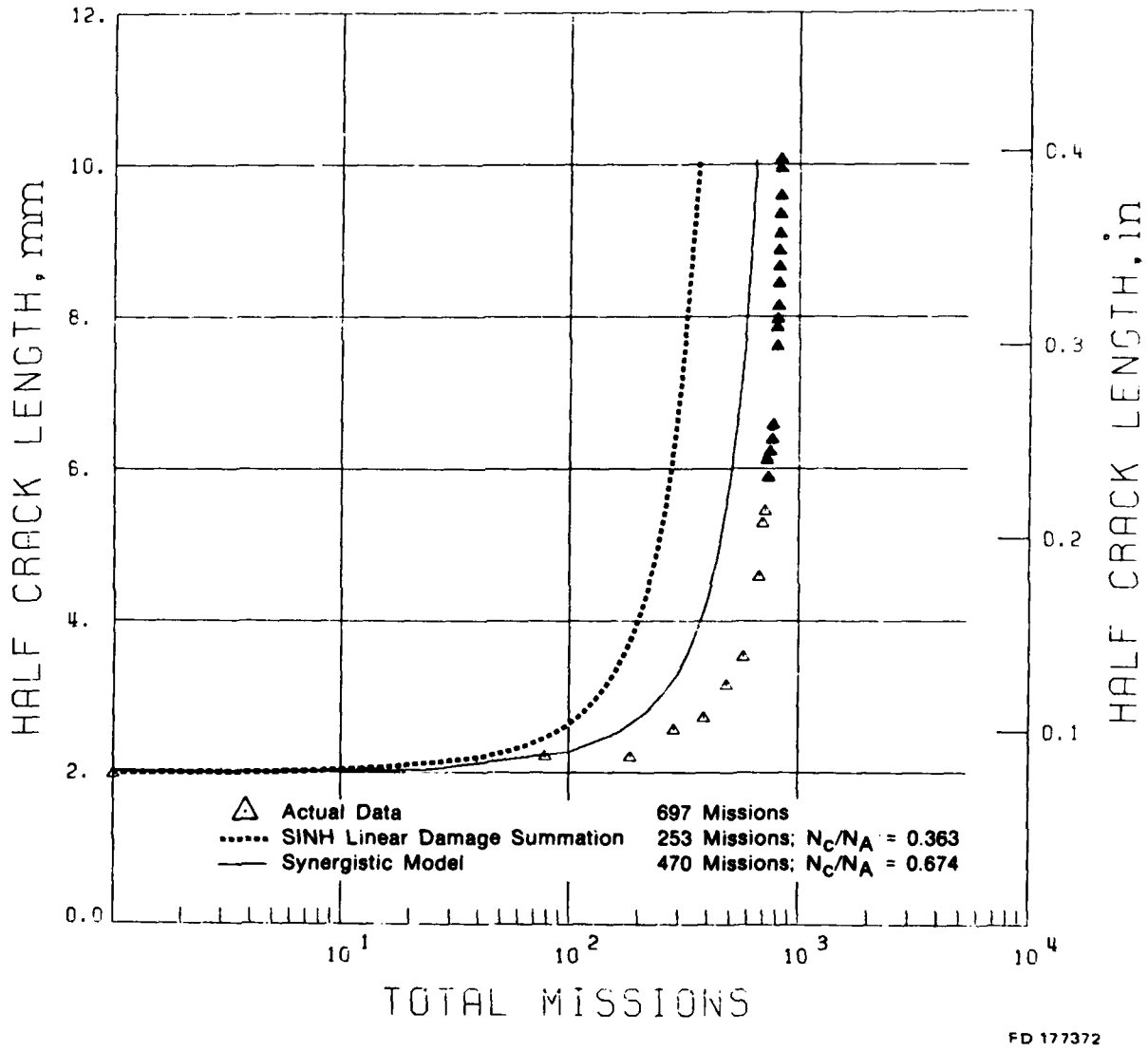

Figure 112. IN100 (PWA 1073) Model Demonstration Test, Mission 2, Surface Specimen No. 1575, 691°C (1275°F)

5. Critique

The basic goal of the model demonstration program was to determine the effectiveness of the crack propagation models to predict elevated temperature fatigue crack growth in Waspaloy (PWA 1007) and IN100 (PWA 1073) under load sequencing representative of turbine disk operation. This evaluation tests the capability of the three-part specimen life prediction procedure composed of the segregation, interpolation, and computation algorithms.

An assessment of the results of the model demonstration program may be accomplished by constructing a log-normal probability plot of values of $N_{Calculated}/N_{Actual}$ for the collection of demonstration specimens. Such a plot is presented in Figure 113. Values of N_c/N_A which are less than 1.0 indicate conservative life predictions while values greater than 1.0 are anticonservative, the statistical analysis of the test results provided by this plot shows the mean of all values of N_c/N_A to be 1.07. That is, the average life prediction given by the synergistic model is 7% greater than the actual specimen life. This highly accurate result demonstrates the excellent capability of this model to describe cumulative damage effects on crack growth in Waspaloy and IN100. This may be contrasted with a similar analysis of results of the SINH Linear Damage Model. The mean value of these predictive errors is 20% less than the actual specimen life. While the error associated with the nonsynergistic model was not excessive for these demonstration tests, a considerably more significant load sequence effect may be expected under more representative missions. In order to permit usage of available testing machines, the model demonstration missions were of limited cycle count. More representative mission load sequences have less frequently occurring overloads, resulting in increased crack growth synergism (greater error in the nonsynergistic life calculation).

While the average model behavior is represented by the statistical mean, the distribution of the sample of values of N_c/N_A about the mean provides an assessment of the variability in predictive assuracy. For example, the plot of the synergistic model results (Figure 113) indicates that for one hundred future life calculations, the maximum prediction error should be anticonservative by a factor of approximately 2.2. One in 1000 future predictions may be anticonservative by a factor of 3.0. Similar results occur for an analysis of the SINH Linear Damage Model predictions.

The above worst case analysis considers the Waspaloy and IN100 data together. However, the prediction errors for Waspaloy were generally less than for IN100. The maximum and minimum errors were observed in IN100. The primary source of this defference is not believed to be the difference in material. Rather, a difference in testing temperature for the two materials appears to be responsible. All Waspaloy demonstration testing was conducted at 621°C (1150°F), while the Mission 1 and Mission 2 IN100 tests were run at 710°C (1310°F) and 691°C (1275°F) respectively. At the lower temperture, Waspaloy displays relatively limited creep crack growth; however crack propagation in IN100 under sustained load becomes more appreciable in the indicated temperture ranges for these tests. Both demonstration missions have significant load dwell components, and at the IN100 operating temperatures cracking tends to violate Linear Elastic Fracture Mechanics. Since variability in creep crack growth data is generally much more severe than observed by cyclic fatigue crack growth, it is not suprising that the IN100 results are more extreme than the Waspaloy findings.

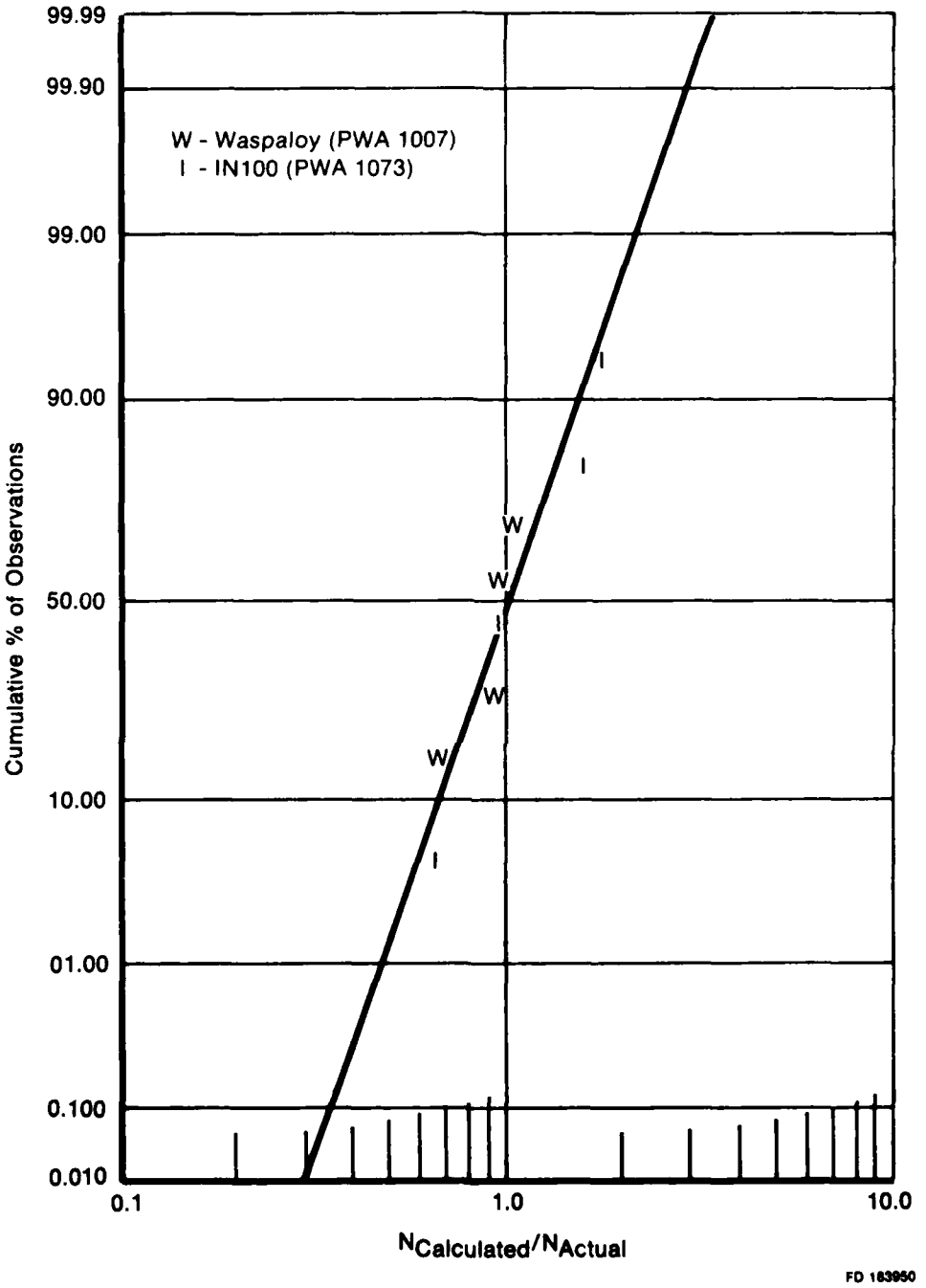

Figure 113. Log-Normal Probability Plot of Synergistic Model Demonstration of Test Results

In order to examine the hypothesis that test-to-test variability in crack growth was responsible for much of the scatter in the IN100 model demonstration results, a number of replicate tests were performed. The most severe creep conditions were selected: Mission 1 and 710°C (1301°F). The results of five such tests are presented in Figure 114. The variability of these data is significantly more severe than observed for the collection of the separate demonstration tests of Figure 113. The extreme data scatter for the replicate tests indicates that much of the variability in values of N^a/N^A for the original eight specimens was the result of test-to-test material scatter rather than an arbitrary error in the cumulative damage model prediction.

Another source of model prediction error was extrapolation of ΔK to values beyond the limits of the data base used in model development. The range in ΔKover which data ws generated in the initial test program wsa necessarily limited by the scope of the contract.

While it is difficult to assess the relative contribution of errors in Cumulative Damage Model and intrinsic material data scatter, the combination of these errors is represnted by model demonstration results of Figure 113. The capability of the synergistic model to predict crack propagation under loading similar to demonstration missions 1 and 2 is described by this plot. As stated earlier, these missions were chosen to be extreme cases which would exercise the model. Typical operating missions for turbine disks are expected to be less severe, therefore, more accurate life predictions are expected for field usage than was observed for the demonstration test program.

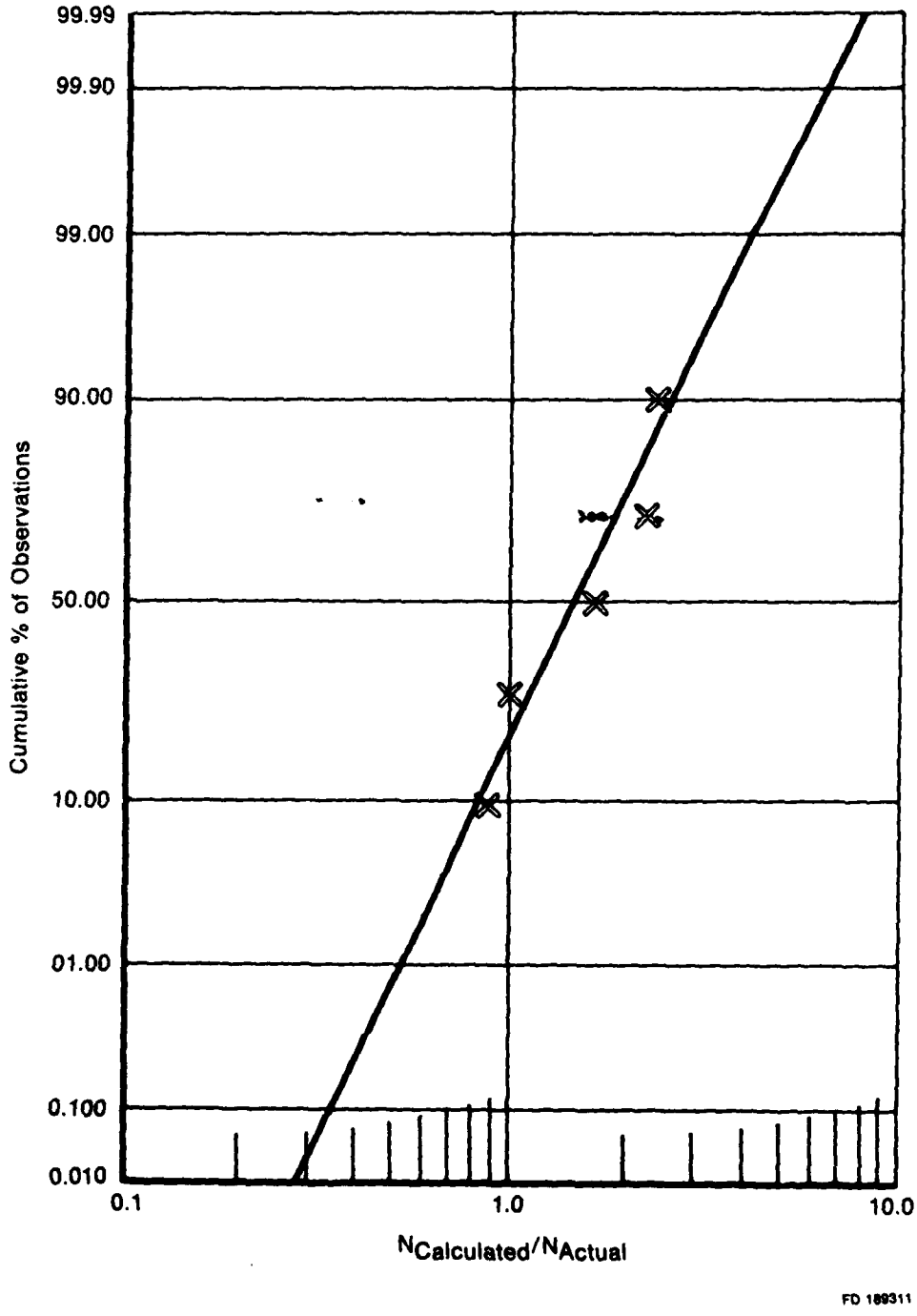

Figure 114. Log-Normal Probability Plot of Results of Replicate Demonstration Tests. IN100, 710°C (1310°F), Mission 1.

SECTION III
CONCLUSIONS

The primary accomplishment of this contract was the development of a computer based mathematical model for prediction of elevated temperature crack propagation of Waspaloy (PWA 1007) and GATORIZED® IN100 (PWA 1073) subject to load sequencing representative of turbine disk operation. The following conclusions are drawn from the results of testing and analysis which supported construction of the model.

1. Loading spectra representative of turbine disk operation contain major and minor load excursions, as well as load dwells, which lead to synergistic effects on crack propagation. In the missions evaluated, the occurrence frequency of major load excursions (overloads) was high (generally every 50 cycles, or less), and the observed overload ratio (P_{OL}/P_{max}) was generally less than 1.5. Compressive stress excursions may occur in some disks at some location (eg. cooling holes).

2. Crack propagation data (da/dN vs ΔK), generated under constant load amplitude cycling (and repetitive load sequencing) of Waspaloy (PWA 1007) and IN100 (PWA 1073), are effectively described by an equation of the form

$$\log \frac{da}{dN} = 0.5 \text{ SINH } (C_2 (\log \Delta K + C_3)) + C_4$$

where C_2, C_3, and C_4 are empirical functions of the parameters of component operation.

3. For the given material, Waspaloy (PWA 1007) or IN100 (PWA 1073), equations of the form given above provide the capability for multiparameter (eg. frequency, stress ratio, temperature, overload ratio) interpolations to define representative crack growth relationships.

4. Of the two superalloys Waspaloy (PWA 1007) and IN100 (PWA 1073), the former is considerably more prone to test-to-test variability of crack propagation properties. The basis of this variability is the large range of acceptable crystalline grain size for Waspaloy (PWA 1007) as compared to IN100 (PWA 1073).

5. Under constant load amplitude cycling with dwell at peak load, the rate of crack propagation of Waspaloy (PWA 1007) increases with increasing period of load dwell. However, for a period of load dwell of 120 sec, crack propagation in this alloy is significantly more rapid at 649°C (1200°F) than at 732°C (1350°F). The higher temperature apparently promotes creep-induced crack tip blunting which reduces the rate of crack growth in this alloy.

6. Negative stress ratio fatigue of Waspaloy (PWA 1007) and IN100 (PWA 1073) in the range of $-1.0 \leq R < 0.0$ appears to produce slightly more rapid crack growth than observed under R = 0 cycling. This effect on crack propagation of the tensile-compressive cycling is not adequately predicted by an extrapolation of the effect of positive stress ratios.

7. Elevated temperature crack propagation data (da dN vs ΔK) of Waspaloy (PWA 1007) fatigued at representative stresses are conservative as compared to similar crack growth in stress fields approaching the material yield strength.

8. The effect of prior plastic deformation 1.0% strain cycling; ($\epsilon_{mean} = 1/2\,\epsilon_{max}$) on subsequent elevated temperature (649°C) crack propagation of Waspaloy (PWA 1007) is to increase crack propagation slightly above characteristic cracking behavior of virgin (unstrained) material. In IN100 (PWA 1073) the effect of similar prestrain is neglible. Test results of both materials are within the material scatterband.

9. Under repetitive overload-underload-LCF cycling of IN100 (PWA 1073) at 649°C (1200°F), the effect of the compressive load cycle following the overload is to reduce the beneficial effect of the tensile overload.

10. A periodic dwell ($10 \leq \Delta N_{Dwell} \leq 40$) at peak load, interrupting otherwise constant load amplitude cycling (R = 0.1), has a negligible effect on crack propagation of Waspaloy (PWA 1007) and IN100 (PWA 1073) at 649°C (1200°F). The effect of similar periodic load dwells on the 732°C (1350°F) crack propagation of Waspaloy is also insignificant; however, the periodic dwell increases crack growth rate of IN100 at this temperature. At low values of ΔK, this increase is generally predictable using linear damage summation methods.

11. Under constant load amplitude fatigue (R = 0.5) interrupted by periodic overloads, the elevated temperature average crack propagation rate of Waspaloy (PWA 1007) and IN100 (PWA 1073) decreases with increasing overload ratio ($1.0 \leq OLR \leq 1.5$) and with increasing cycles between overloads ($5 \leq \Delta N_{OL} \leq 40$). Over this range of representative loading sequences, the effect of the overloading on crack growth is much more pronounced in IN100 than in Waspaloy.

12. The interpolative model of elevated temperature crack propagation in Waspaloy (PWA 1007) and IN100 (PWA 1073) are effective for prediction of cumulative damage effects under mission loading.

APPENDIX A
OBSERVATION OF CRACK RETARDATION RESULTING FROM LOAD SEQUENCING CHARACTERISTIC OF MILITARY GAS TURBINE OPERATION

J. M. Larsen, C. G. Annis, Jr.

Pratt & Whitney Aircraft Group
Government Products Division
Mechanics of Materials and Structures
P.O. Box 2691
West Palm Beach, FL 33402

ABSTRACT

The nature of crack propagation resulting from flight loading representative of military gas turbine operation is investigated. Mission stress profiles for turbine disks fabricated from the superalloys GATORIZED® IN100 and Waspaloy contain load sequences which produce synergistic effects on crack propagation. Major load throttle excursions, overloads, occur routinely during flight, and a retardation in subsequent crack propagation generally results. Such mission load interaction effects have been addressed in crack propagation testing employing repetitive overload-fatigue sequences. The influences of overload ratio ($P_{overload}/P_{max}$) and the number of fatigue cycles between overloads have been investigated for crack propagation at 649°C (1200°F), and an interpolative model of these effects is presented. A determination of the instantaneous crack retardation following a mission major load excursion is accomplished with an unconventional method. The existence of a deceleration in crack growth rate, delayed retardation, following a mission overload is verified. Typically, this period is greater than the total number of baseline fatigue cycles applied between engine mission overloads, and delayed retardation is largely, if not entirely, responsible for the beneficial effects of the overloading.

Key words: crack propagation, fatigue, retarding, superalloys

Presented at ASTM Symposium on "Effect of Load Spectrum Variables on Fatigue Crack Initiation and Propagation" San Francisco, CA, May 1979. Submitted to ASTM for publication 1979.

INTRODUCTION

Operational loading spectra imposed on rotating disks in a military gas turbine engine contain load sequences which differ significantly from the high cycle loading encountered in flight of an airframe. Fatigue of a superalloy engine disk is a low cycle phenomenon resulting from throttle excursions and associated thermal stresses. Major and minor throttle excursions compose a load sequence from which synergistic crack propagation results, and this load interaction is complicated by elevated temperature operation and concomitant time dependent behavior.

Typical loading spectra are derived from service missions which include ferry, training, and terrain following radar (TFR) activity. A mission composite is presented in Figure A-1 (Reference 1). The loading spectra may conain frequent single or multiple major load excursions (overloads) with a small number (usually no more than 50) of less severe throttle excursions between overloads. As a result of this frequent overloading, crack growth immediately following an overload is of increased significance, while the crack retardation commonly observed many cycles after an overload application is of reduced importance since this retarded growth is soon interrupted by another overload excursion.

This paper reports the finding of an investigation into the effects of frequent overloading on elevated temperature fatigue crack propagation (FCP) of the superalloys GATORIZED* IN100 and Waspaloy. An empirical model of these overload effects is described, and the characteristic retardation of crack growth which follows the frequent overloads is determined.

CRACK RETARDATION

The crack propagation resulting under the complex of loading and environment encountered in a military gas turbine engine is not predicted satisfactorily by residual stress (References 2 and 3) or closure (Reference 4) models, and a need for further study of this isolated problem exists. The current work has employed an empirical model (References 5, 6 and 7) of elevated temperature FCP under spectrum loading. The basic philosophy of this approach is that any complex mission spectrum can be segregated into elemental damage events which can be quantitatively described. The crack propagation life expected under such a spectrum can then be computed as a linear addition of the damage associated with properly segregated events. Mission segregation is based on the definition of an "elemental damage event" as the smallest repeating load-time sequence which results in FCP not predictable by linear damage accumulation alone. A simplified mission consisting of a single overload followed by a block of constant load amplitude fatigue cycles is such an elemental damage event.

Figure A-2a presents a schematic of a crack growth curve, crack length (a) vs number of applied fatigue cycles (N), illustrating the common effects of a single overload on previously unretarded crack growth. When the crack growth produced by constant load amplitude fatigue is interrupted by an overload, crack growth accelerates corresponding to the overload (Reference 8). Thereafter, the rate of crack propagation quickly decelerates, and after a small number of subsequent fatigue cycles the rate of crack growth achieves a minimum. This deceleration to a minimum rate of crack propagation is known as delayed retardation, and the period of delayed retardation is defined as the number (N_{DR}) of post-overload fatigue cycles required to achieve the minimum crack growth rate. Following delayed retardation, crack growth continues at a near minimum rate for an extended period, and the exhaustion of the retardation process is marked by an acceleration of crack growth to regain the unretarded rate. The total period of crack retardation, N*, is defined as the number of cycles during which crack growth rate is retarded following an overload application. The nature of the transient crack propagation behavior which results following an overload is further revealed by differentiating the crack growth curve, Figure A-2a, to give crack propagation rate, da/dN, as a function of N, Figure A-2b.

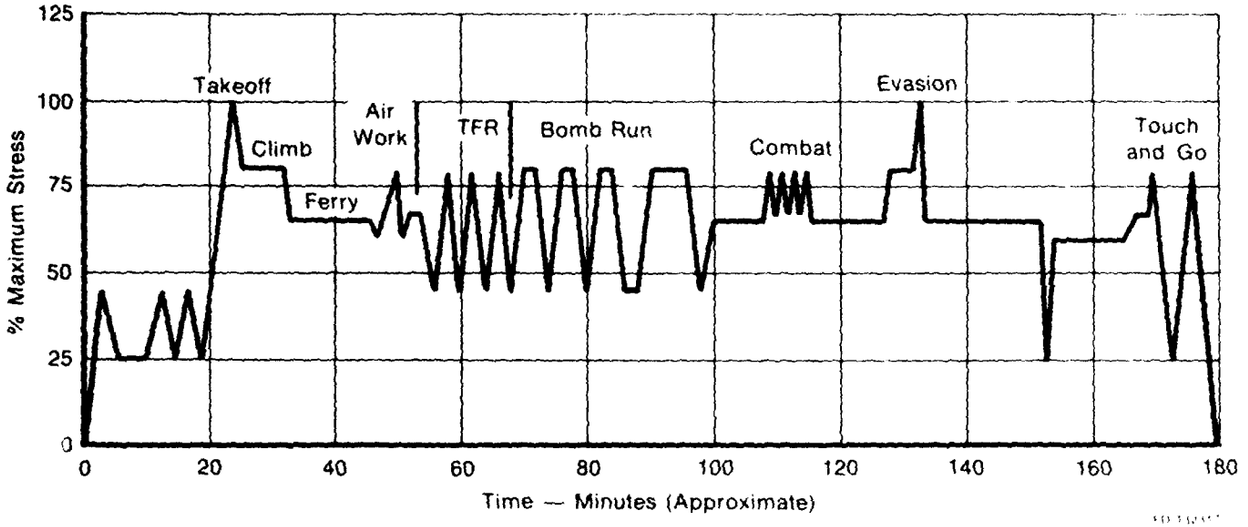

Figure A-1. Composite Mission Stress Profile

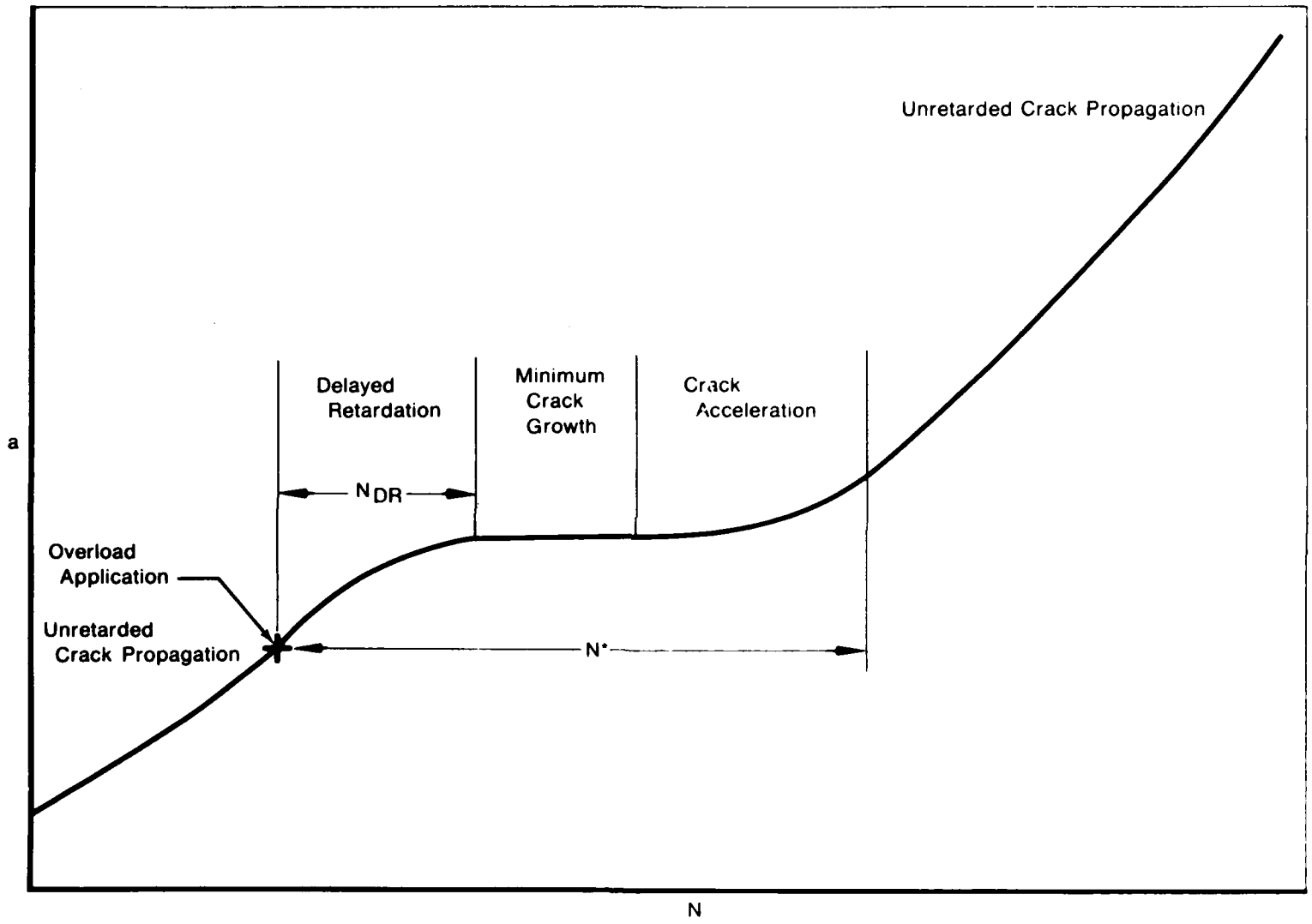

Figure A-2a. Fatigue Crack Retardation Resulting from the Applicatio of a Single Overload

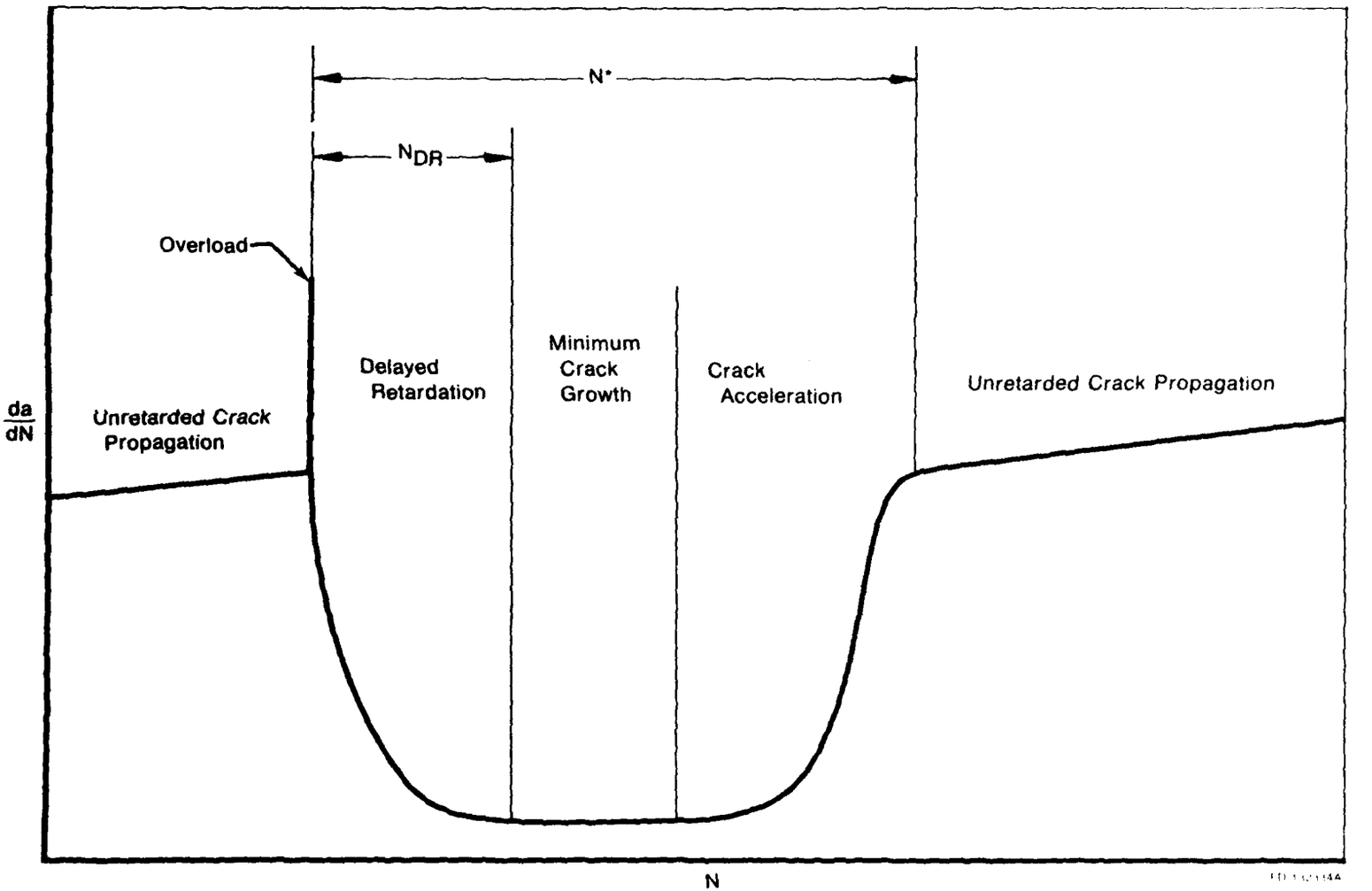

Figure A-2b. Fatigue Crack Retardation Resulting from the Application of a Single Overload

Overloads which occur at cyclic intervals less than N^* interrupt and restart the crack retardation process. The beneficial effect offered by intermittent overloads has been observed to be reduced as the number of cycles between overloads, ΔN_{OL}, is reduced to fewer than N^* cycles (Reference 9 and 10). As ΔN_{OL} becomes small, the relative importance of delayed retardation is increased, and the average crack growth rate associated with the overload-fatigue sequence increases.

PROCEDURE

Fatigue crack propagation tests of the nickel base superalloys GATORIZED IN100 and Waspaloy were conducted on electrohydraulic testing machines operated under load control. All tests were performed in air at 649°C (1200°F) and the loading waveform was that of an isosceles triangle applied at a frequency of 0.167 Hz (10 cpm). Compact specimens (Figure A-3) of C-R (circumferential-radial) orientation (Reference 11) were machined from disk forgings representative of engine disk material. The test specimens were pre-cracked at room temperature using standard procedures (Reference 11).

Testing was designed to evaluate the influence of frequently applied periodic overloads on otherwise constant load amplitude (ΔP) fatigue crack growth. A schematic of the basic loading sequence is presented in Figure A-4. The baseline load ratio (R = minimum load/maximum load = P_{min}/P_{max}) was 0.5 for all tests. The variables of test were the overload ratio (OLR = (P_{OL}/P_{max} 1.25, 1.50) and the number of baseline fatigue cycles between overloads (ΔN_{OL} = 5, 20, and 40).

During propagation testing, crack lengths were measured on both surfaces of the specimen with a traveling microscope. To facilitate this procedure, the test was interrupted, and the mean load was applied while holding the specimen at the temperature of testing. The increment in crack length measurement was 0.50 mm (0.020 in.) and the measurement error was ±0.025 mm (0.001 in.). The resulting "a" vs "N" data were reduced with a seven-point incremental polynomial technique (Reference 12) to produce da/dN vs ΔK data.

RESULTS AND DISCUSSION

The crack retardation associated with a single periodic overload is generally reflected in a local purturbation in the "a" versus "N" crack growth curve. However, as ΔN_{OL} becomes small, the resolution in crack length measurement must be increased in order to perceive the transient variations in crack growth which occur between successive overloads. In the present experiment, ΔN_{OL} is exceedingly small relative to the increment in measurement of surface crack length, and no transient variations in crack growth are observed. Rather, the collection of all "a" versus "N" data represents a trend in crack propagation resulting from very frequent periodic overloads.

Reducing the "a" versus "N" data to the form of da/dN versus ΔK data and performing a least square regression produces analytical functions which represent the average crack growth rate for the specific combination of OLR and ΔN_{OL}. The regression equation was based on the hyperbolic sine function and is given as: (References 5, 6 and 7)

$$\log (da/dN) = C_1 \sinh (C_2 (\log \Delta K + C_3)) + C_4 \qquad \text{(A1)}$$

where C_1 = 0.5, a material constant,
C_2 = horizontal shape coefficient,
C_3 = log (ΔK) at the point of inflection,
C_4 = log (da/dN) at the point of inflection, and
ΔK = baseline stress intensity factor range.

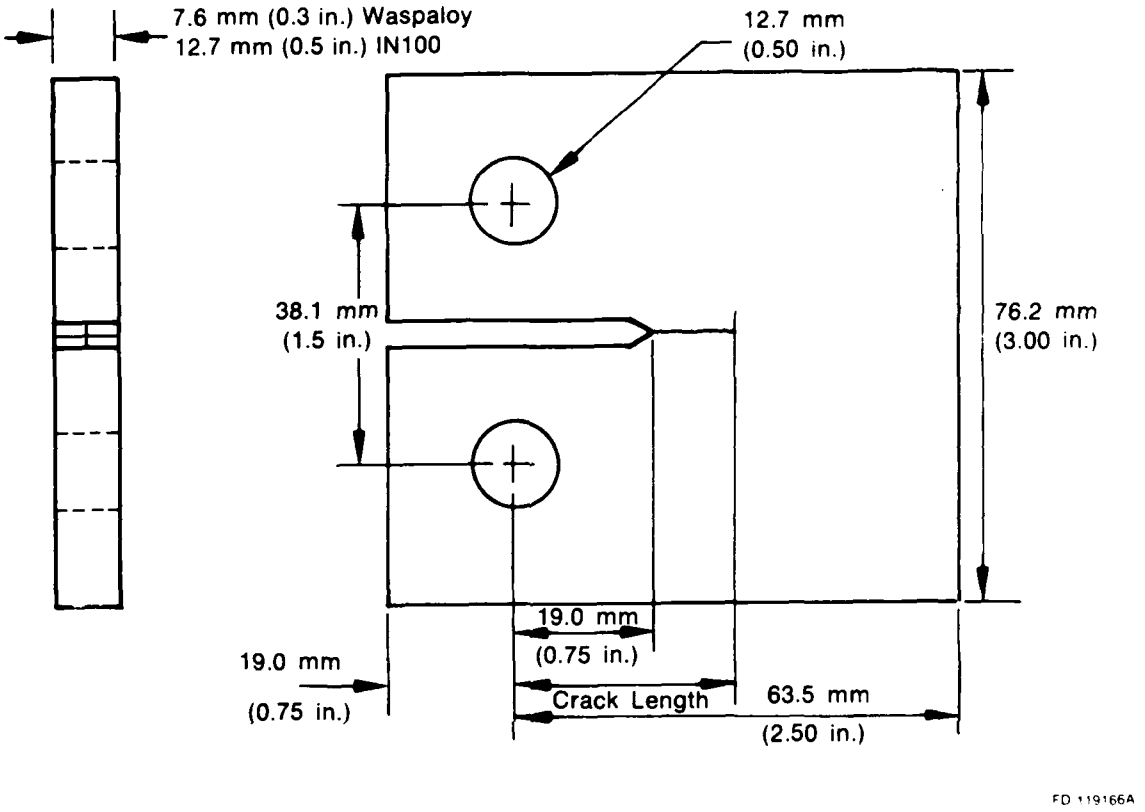

Figure A-3. Compact Specimen

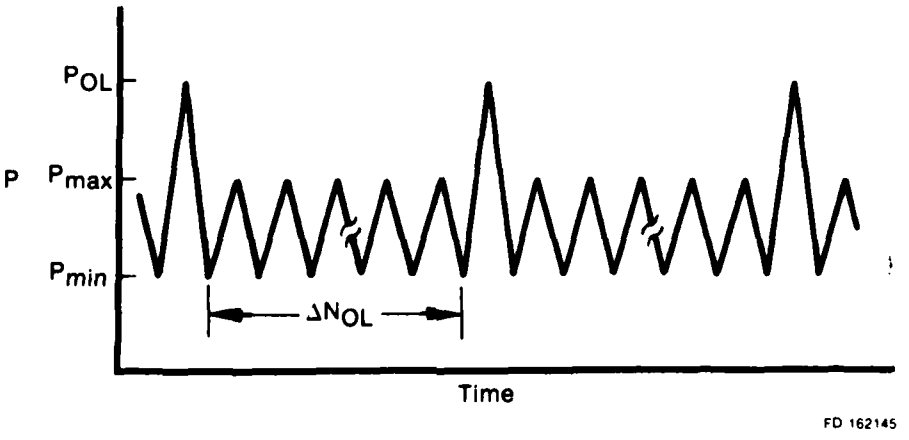

Figure A-4. Periodic Overload Fatigue

The increased magnitude of the overload stress intensity range (ΔK_{OL}) is not reflected in the plotted value of *DK*. Rather, the overload is treated as an isolated variable influencing crack growth, and its impact is revealed in the dependent variable, da dN. Thus, under the load sequencing of Figure 4, *DK* is defined as K_{max}-K_{min} for all cycles (including the overload) and da/dN is the calculated average crack growth per cycle (including the overload).

Defining fatigue with periodic overloading as a succession of repetitive overload-fatigue missions (elemental damage events) as in Figure A-4, one may plot a series of crack growth rate curves for the collection of test missions. Figure A-5 presents such data, illustrating the effect of ΔN_{OL} on elevated temperature fatigue crack propagation in GATORIZED IN100. For purposes of comparison, a single regression curve (without data) representing crack growth under constant amplitude loading has also been plotted. This baseline crack growth is observed to be essentially equivalent to propagation under periodic overloading with ΔN_{OL} = 5 (6 cycles per overload-fatigue mission). The equivalence of crack growth rates results from a balance of overload accelerated crack growth and the subsequent crack retardation. As ΔN_{OL} increases to 20 and 40, the average effect of the overloading becomes more beneficial than damaging, and the resultant propagation rate is reduced significantly below that produced under constant ΔP fatigue.

The dependence of da/dN on ΔN_{OL} may be described by an interpolative model of the associated SINH curves. The coefficients of Equation (A1) are defined as a function of ΔN_{OL}:

$$C_i = a_i + b_i (\Delta N_{OL} + 1) \qquad i = 2, 3, 4 \tag{A2}$$

Thus, over the range $5 \leq \Delta N_{OL} \leq 40$, da/dN is given by a continuous function (Equation A1) for which the three coefficients are uniquely defined (Equation A2). Interpolations on ΔN_{OL} define representative SINH curves giving average crack growth associated with periodic overload fatigue of ΔN_{OL} cycles between overloads. This permits prediction of crack growth where no actual data exist. The relationship of Equation (A2) also provides the capability for limited extrapolation beyond the data base.

The effect of overload ratio on fatigue crack propagation may also be described by an interpolative model of the SINH coefficients. Figure A-6 illustrates this effect for periodic overloading (ΔN_{OL} = 40) with overload ratios of 1.0, 1.25, and 1.5. Data of overload ratio 1.0 is generated under constant ΔP fatigue, and any interpolative model of OLR must converge to this condition regardless of the value of ΔN_{OL}. The expression which defines the SINH coefficients as a function of overload ratio is

$$c_i = d_i + e_i (OLR) \qquad i = 2, 3, 4 \tag{A3}$$

Thus, for periodic overload-fatigue with ΔN_{OL} = 40, the combination of Equations (A1) and (A3) uniquely define crack propagation for $1.0 \leq OLR \leq 1.5$.

Having established that the SINH coefficients are linear functions of overload ratio for the case of ΔN_{OL} = 40, it is assumed that a similar linear relationship describes the dependence of crack propagation for $\Delta N_{OL} \leq 40$. This allows combination of the functions (2) and (3), permitting full interpolation over the region defined by $1.0 \leq OLR \leq 1.5$ and $5 \leq \Delta N_{OL} \leq 40$. The coefficients of Equation (A1) are given by:

$$C_i = \alpha_i + \beta_i (OLR) + \gamma_i (\log (\Delta N_{OL} + 1)) + \delta_i (OLR) (\log (\Delta N_{OL} + 1)) \tag{A4}$$

$i = 2, 3, 4$

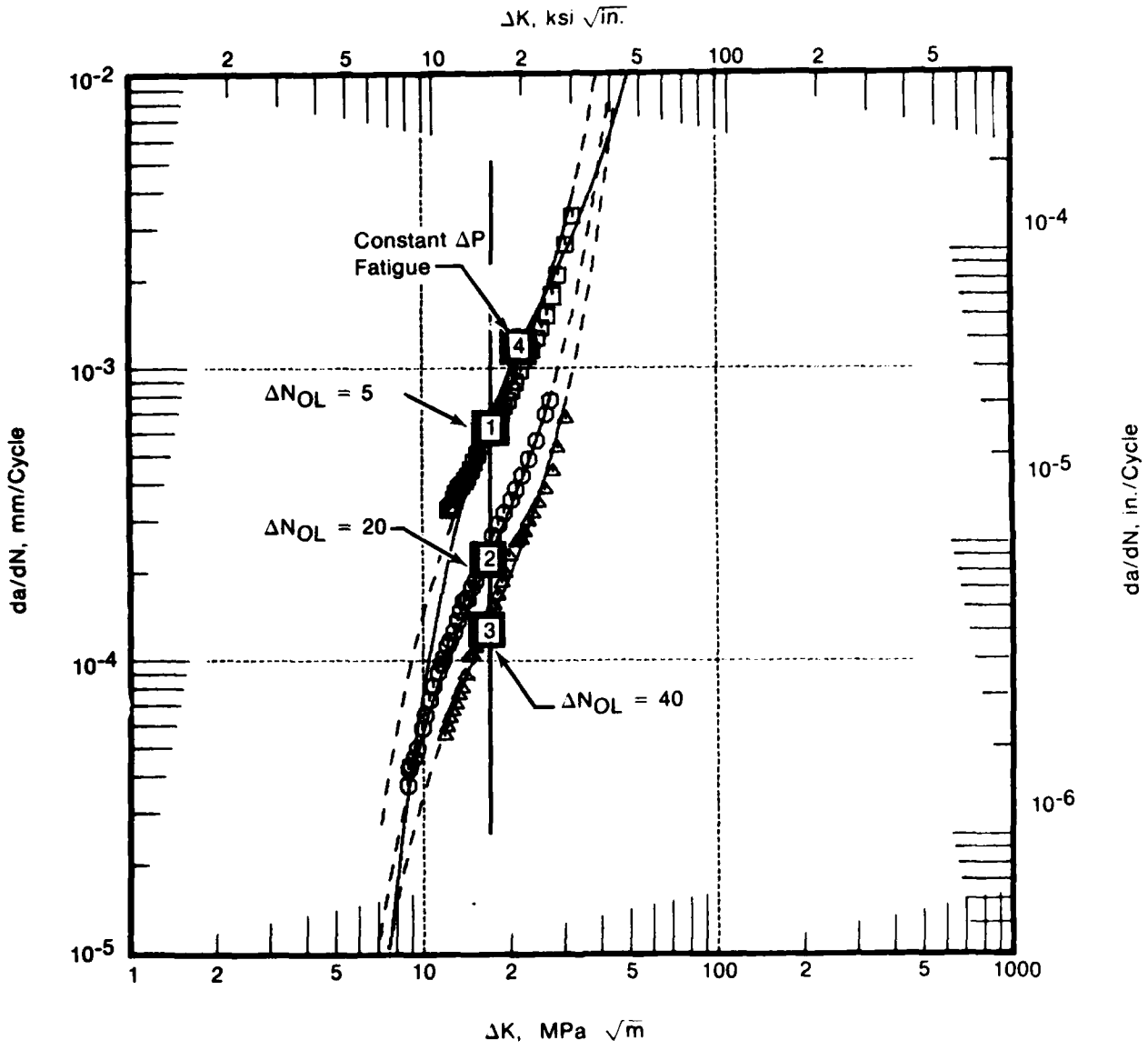

Figure A-5. Effect of Cycles Between Overloads on Fatigue of IN100, OLR = 1.5, 0.167 Hz, 649°C

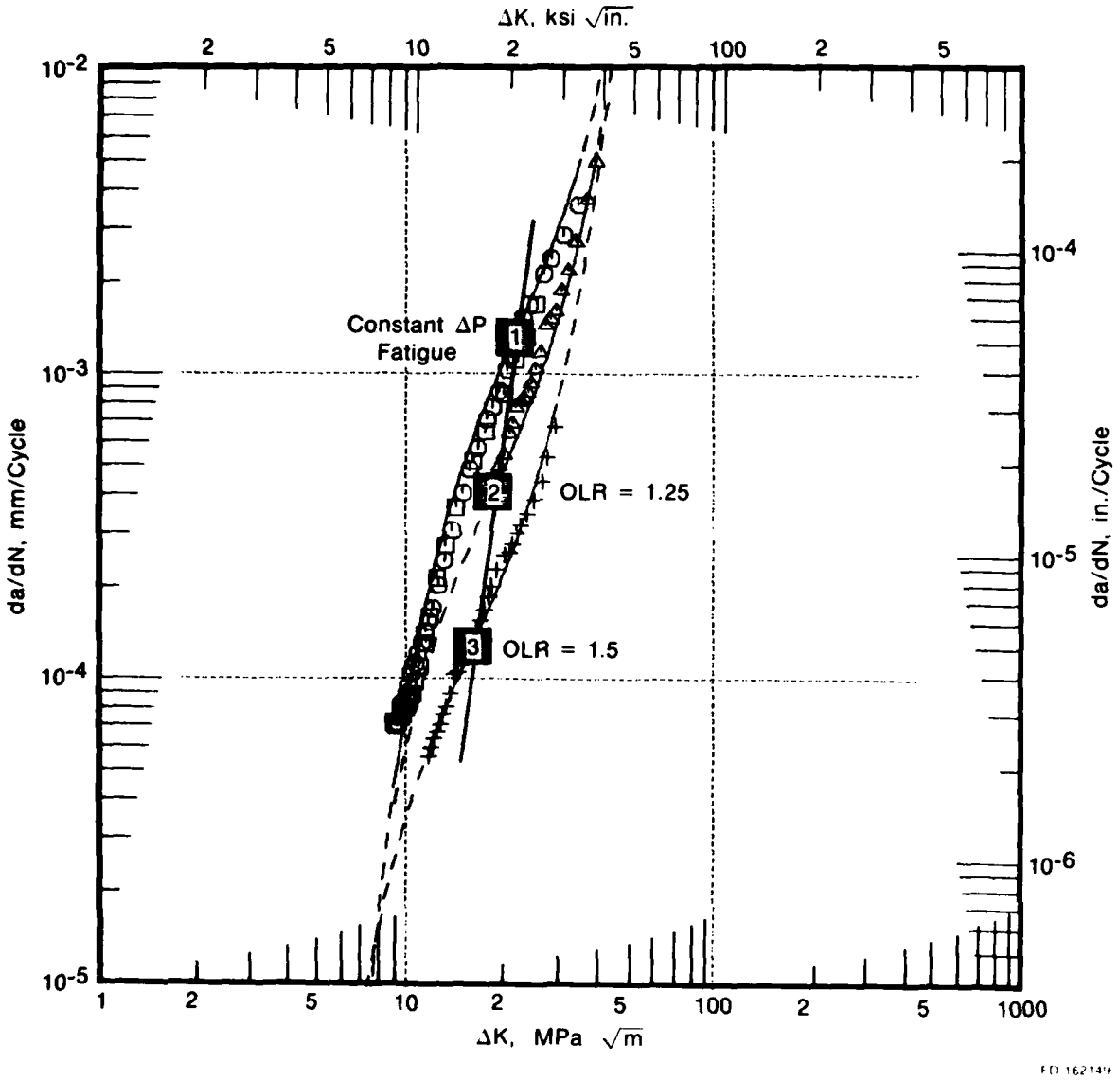

Figure A-6. Effect of Overload Ratio on Fatigue of IN100, ΔN_{OL} = 40, 0.167 Hz, 649°C

This Interpolative SINH Model provides capability for prediction of fatigue crack propagation in IN100 as a function of overload ratio and the number of cycles between overloads. This interpolative model is limited to crack retardation effects under the frequently applied overloads which are characteristic of military gas turbine operation. The applicable range of OLR and ΔN_{OL} may be extended with additional testing.

Development of a similar interpolative model of crack propagation in Waspaloy has also been accomplished. As observed in Figure A-7, the beneficial influence of periodically applied overloads (OLR = 1.5) is much less pronounced in this material than in IN100. Crack growth in Waspaloy with ΔN_{OL} = 5(6 cycles per overload-fatigue mission) is considerably more severe than propagation under constant ΔP fatigue, and the average effect of the overloading becomes beneficial for ΔN_{OL} = 20 and 40. In spite of the significantly different retardation behavior between Waspaloy and IN100, an interpolative function of the form of Equation (A2) is satisfactory representation of the effect of ΔN_{OL} on crack growth in this alloy.

The model of the effect of overload ratio (ΔN_{OL} = 40) on crack propagation in Waspaloy, Figure A-8, also demonstrates a much more limited effect than was observed in IN100. A relationship of the form of Equation (A3) describes SINH coefficients for Waspaloy crack propagation as a function of overload ratio. Combining the models of the effects of cycles between overloads and overload ratio provides interpolative capability for both variables simultaneously (Equation A4).

The coefficients of Equation (A4) are given in Table A-1 for crack propagation of IN100 and Waspaloy at 649°C (1200°F), 0.167 Hz (10 cpm), and R = 0.5. Substitution into Equation (A1) gives crack propagation rate as a function of OLR and ΔN_{OL}.

POST-OVERLOAD CRACK RETARDATION

An Interpolative SINH Model representing crack growth under frequently applied periodic overloads is an effective method for prediction of crack growth resulting during a specific overload-fatigue sequence. However, the instantaneous response of a crack to the overload-fatigue block is not evident. From knowledge of the process of crack retardation resulting from application of a single overload, a hypothesis concerning crack growth in response to frequent periodic overloading may be established.

The crack growth curve is expected to range between two general extremes depending upon the form of post-overload crack retardation. For a given value of ΔN_{OL}, these curves are illustrated in Figure A-9. Assuming delayed retardation does not occur, the minimum crack growth rate should immediately follow the overload. If delayed retardation is present, the minimum crack growth rate should be observed some number of cycles following the overload. If ΔN_{OL} is less than the period of delayed retardation, N_{DR}, a subsequent overload interrupts the delayed retardation process, and the minimum crack growth rate should immediately precede the overload.

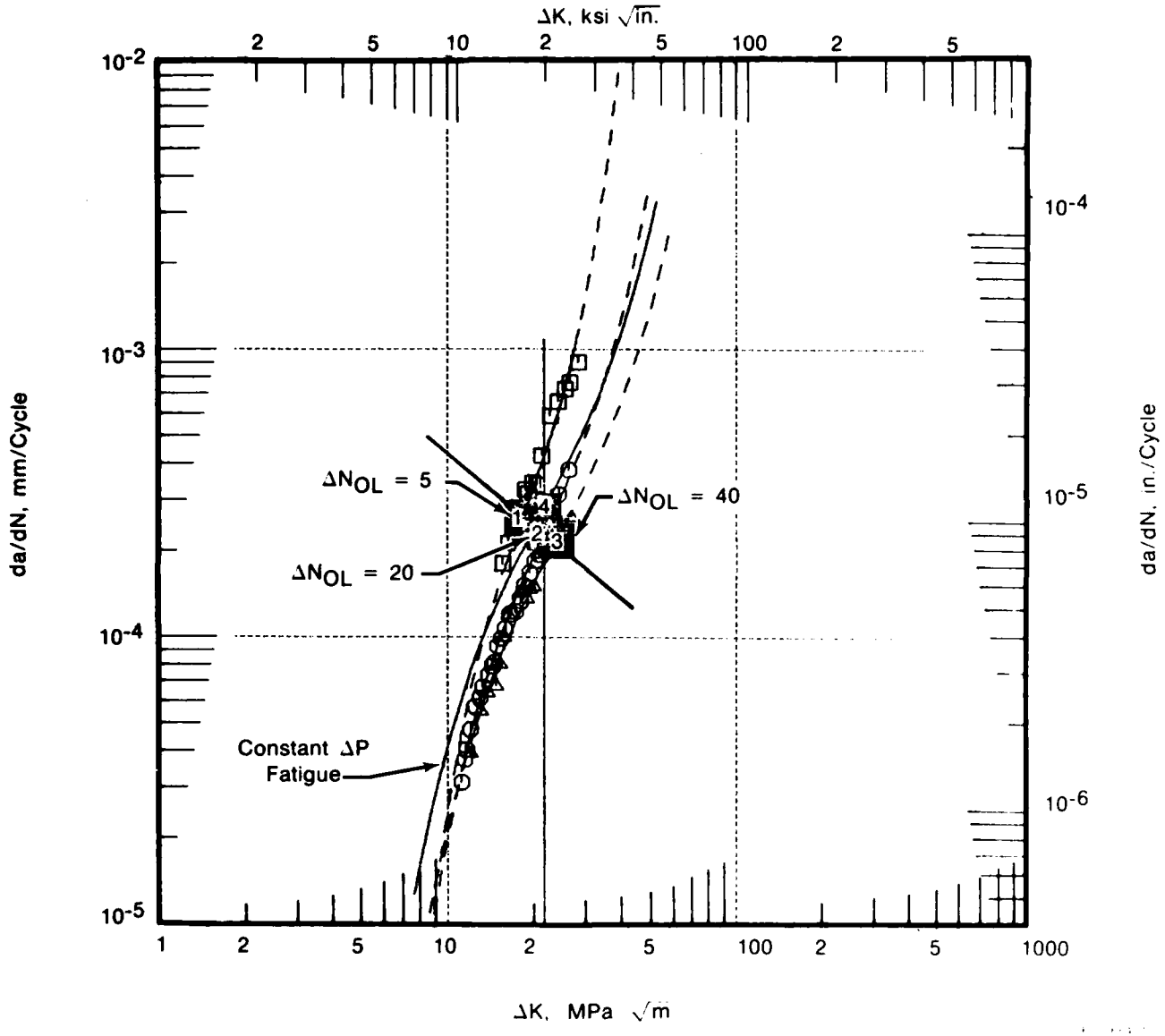

Figure A-7. Effect of Cycles Between Overloads on Fatigue of Waspaloy OLR = 1.5, 0.167 Hz, 649°C

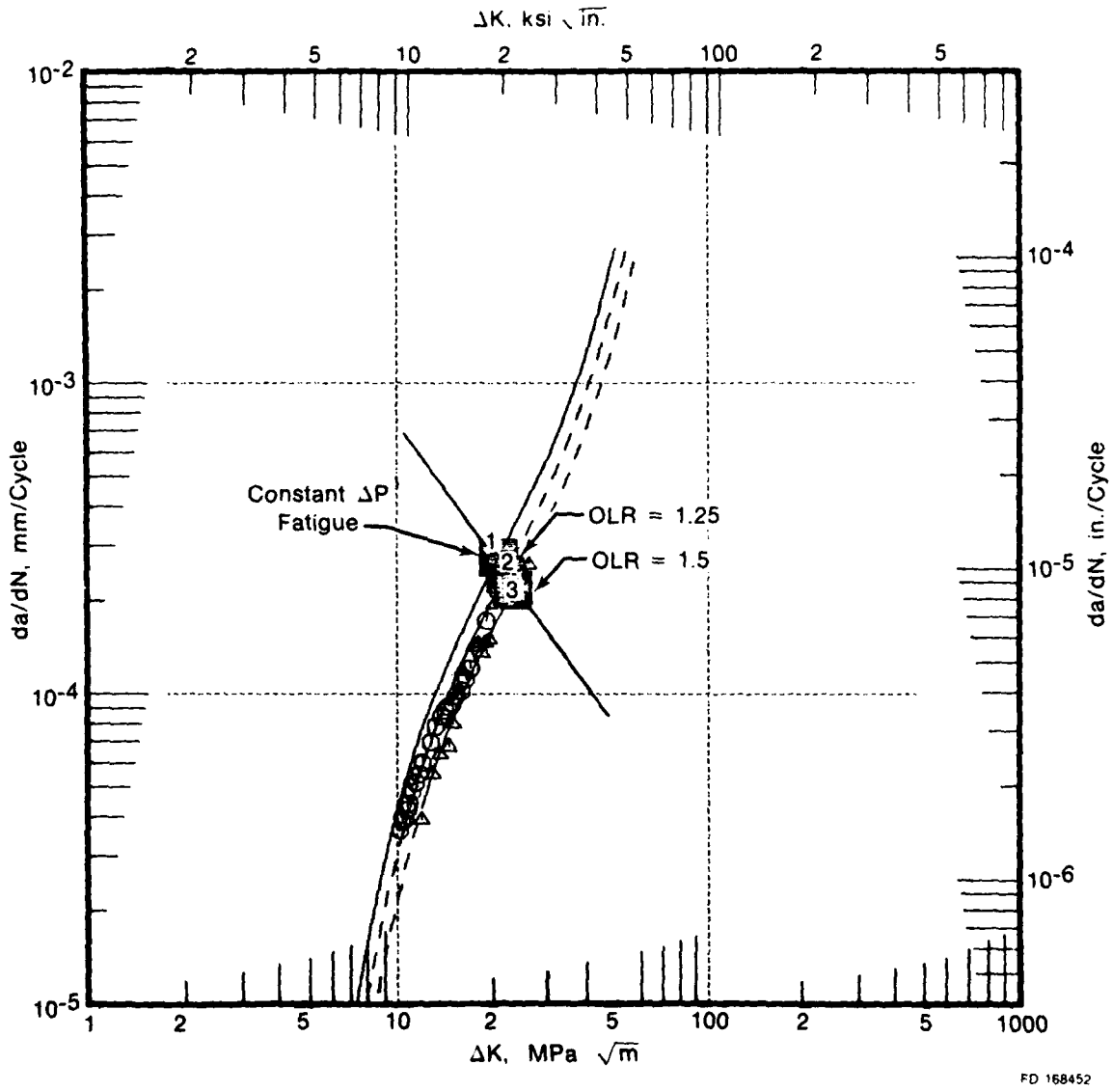

Figure A-8. Effect of Overload Ratio on Fatigue of Waspaloy, ΔN_{OL} = 40, 0.167 Hz, 649°C

TABLE A1. COEFFICIENTS OF EQUATION 4

	IN 100				*Waspaloy*			
	α	β	δ	ζ	α	β	δ	ζ
C_2	4.8410	−0.2140	0	0	−2.9984	6.8424	4.2414	−4.2414
C_3	−1.5448	0.1928	−0.0503	0.0503	−1.6853	0.3563	0.2780	−0.2780
C_4	−3.5196	0.6386	1.6534	−1.6534	−3.6536	0.0916	0.1845	−0.1845

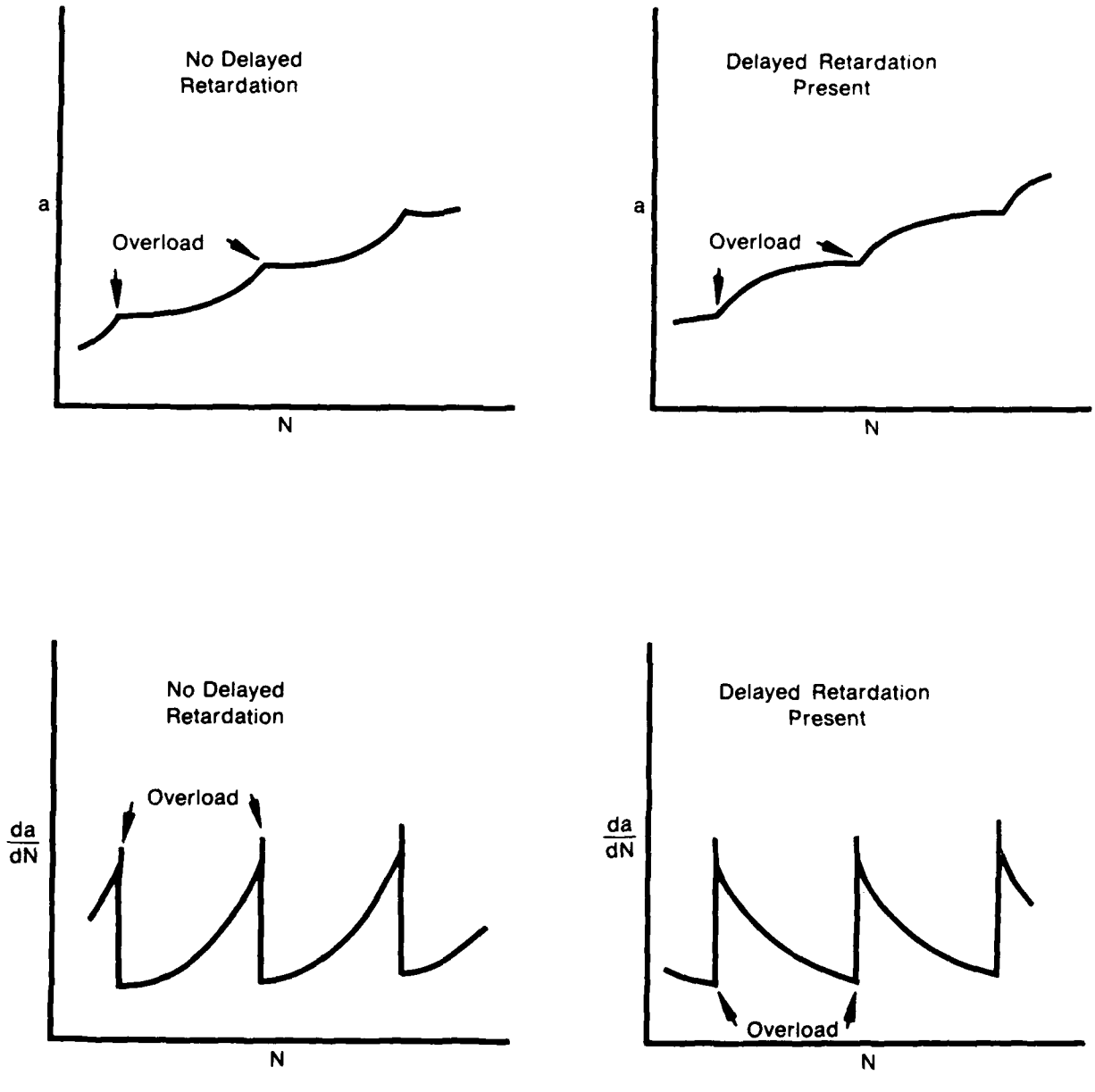

Figure A-9. Fatigue Crack Propagation Under Periodic Overload Fatigue

Experimental determination of the nature of the instantaneous crack growth curve in response to periodic overloading is, however, a formidable task. As previously noted, it is extremely difficult to obtain accurate, meaningful measurement of crack advance between very frequent overloads using standard optical techniques. Additionally, measurement of crack length at the specimen surface is complicated by any discontinuities in crack advance due to microstructural variations. Such discontinuous fatigue crack growth is common in Waspaloy and to a lesser extent in IN100. Even if precise measurement of the surface crack length were accomplished without microstructural interference, a question would remain concerning the shape of the crack front. That is, does the crack front geometry remain constant during periodic overloading, or do periodic changes in crack curvature accompany the overloads? The latter phenomenon is certain to complicate data interpretation. Measurement of incremental crack growth by determination of fatigue striation spacing was prevented by formation of a heavy oxide on the crack face during elevated temperature testing.

It is possible, however, to determine the form of the instantaneous crack propagation curve indirectly. Unlike direct measurement, a SINH curve describing crack propagation under periodic overloading gives average behavior over the period of many overloads. The SINH representation also averages crack growth discontinuities due to variations in microsctructure, crack front geometry, and judgment on the part of the technician. Thus, each curve represents a *statistical mean of the microscopic crack growth rate as ΔK increases with crack length.*

As noted earlier, increasing the number of fatigue cycles between successive overloads produces an increase in crack retardation and a corresponding reduction in average crack growth rate. Alternately, decreasing ΔN_{OL} reduces crack retardation, and, in the limit of zero cycles between overloads, the da/dN versus ΔK curve should approach the crack growth curve corresponding to constant overload fatigue. For the current example of constant ΔP fatigue (R = 0.5) interrupted by periodic overloads (OLR = P_{OL}/P_{max} = 1.5), the parameters defining constant overload fatigue are R = P_{min}/P_{OL} = 0.33 and

$$\Delta K_{OL} = \Delta K_{baseline} [(OLR - R)/(1 - R)] = 2\Delta K_{baseline} \quad (A5)$$

The propagation curve for R = 0.333 fatigue is obtained from an interpolative model of the effect of load ratio (Reference 13). Maintaining the convention of assigning the value of $\Delta K_{baseline}$ to all overload cycles, the R = 0.333 constant ΔP curve is translated by $\Delta K_{baseline} = \Delta K_{OL}/2$ in order to represent the case of constant overload fatigue. For IN100, this curve is presented in Figure A-10 and its relationship to the SINH curves representing periodic overload-fatigue is illustrated. A similar presentation of Waspaloy data appears in Figure A-11.

From the collection of curves for a single material, one may deduce an approximation to the instantaneous form of post-overload crack propagation due to periodic overloading. One assumption is required: the form of the post-overload crack propagation curve is similar for ΔN_{OL} = 5, 20, and 40. Noting that the increase in crack length between successive overloads is very small, the associated increase in ΔK is determined to be correspondingly small and of little significance. Calculating crack growth rate at a specific value of ΔK from each of the overload curves gives the average advance per cycle under the indicated loading condition. The crack growth during each of the individual overload-fatigue missions is then calculated, and the difference in the crack growth for two different missions defines a point on the post-overload da/dN vs N curve. For example, by subtracting the crack advance due to a 21-cycle mission from the crack advance due to a 41-cycle mission, the *Da* corresponding to cycles 21 to 41 after the overload is obtained. The average value of da/dN for the cycle interval of 21 to 41 cycles after the overload may now be obtained by dividing $\Delta a_{21\ to\ 41}$ by the corresponding ΔN. This procedure is given by:

$$da/dN_{21\ to\ 41} = [41\ (da/dN)_{41} - 21\ (da/dN)_{21}]/(41-21) \quad (A6)$$

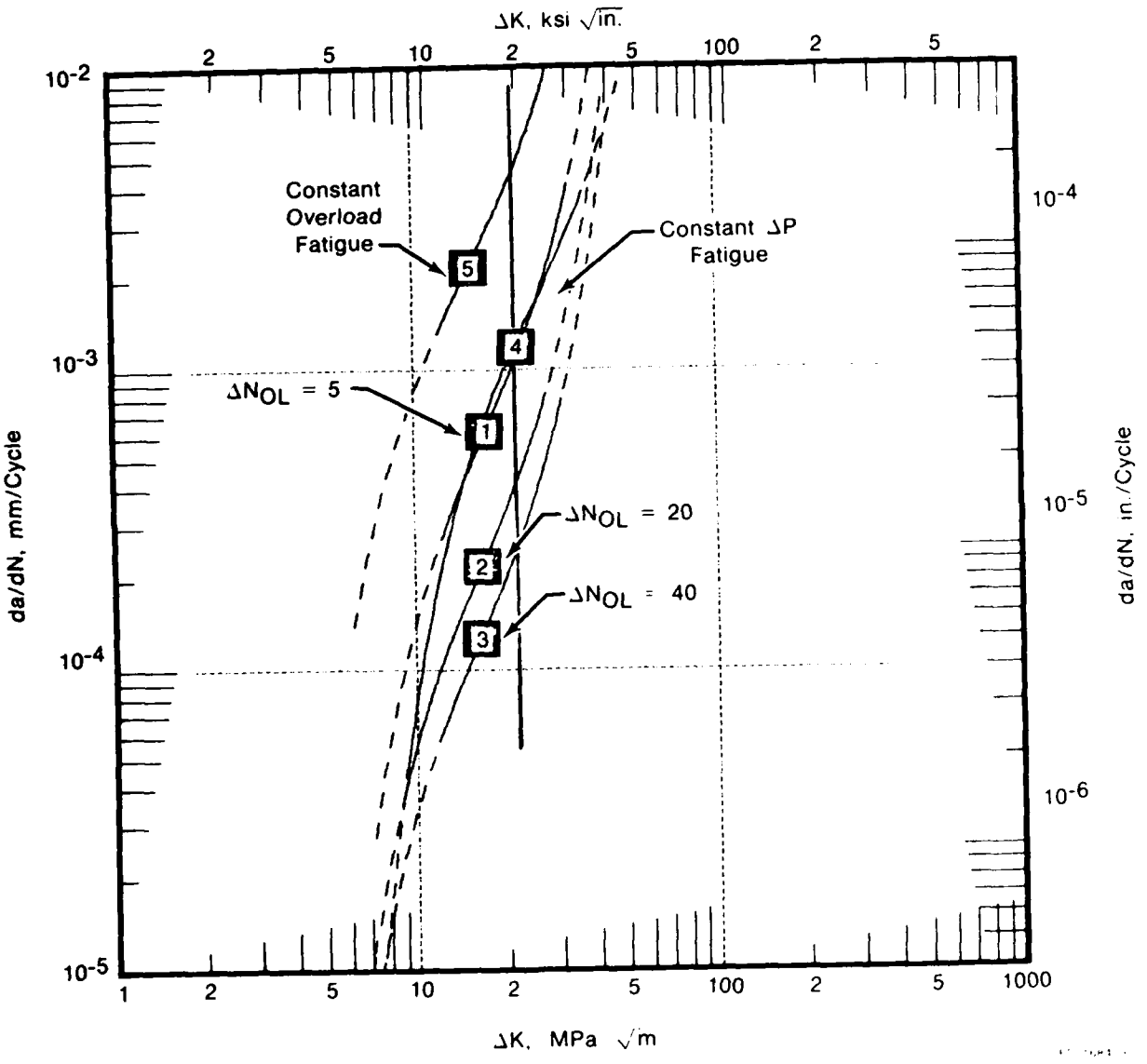

Figure A-10. Effect of Cycles Between Overloads on Fatigue of IN100, OLR = 1.5

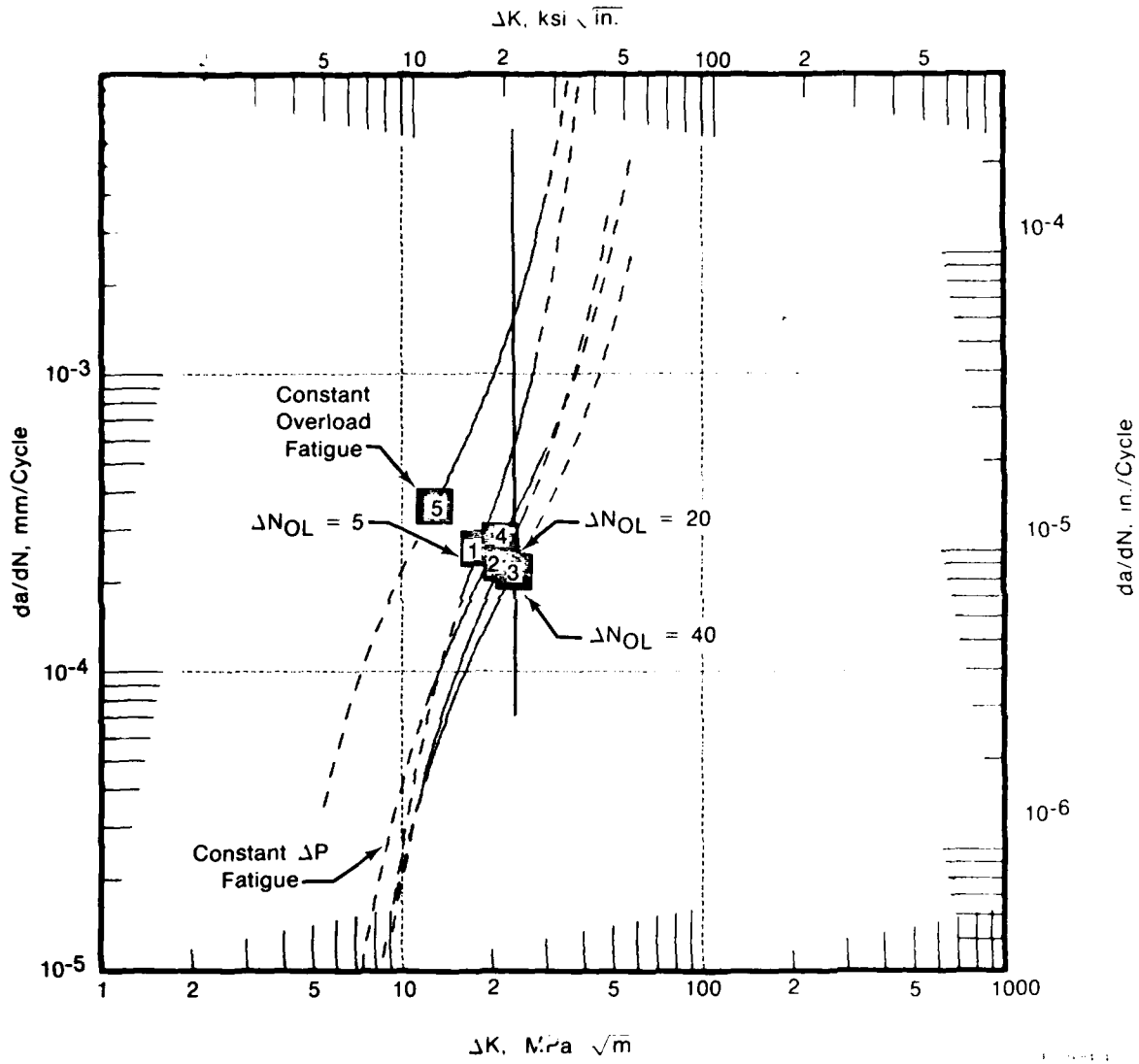

Figure A-11. Effect of Cycles Between Overloads on Fatigue of Waspaloy, OLR = 1.5

The value of $da/dN_{6\ to\ 21}$ may be obtained similarly, and $da/dN_{1\ to\ 6}$ may also be determined by subtracting the standard crack growth for one cycle of fatigue at the overload conditions from the 6-cycle mission data.

Plotting the calculated values of da/dN at the midpoints of the cycle intervals (e.g., N = 31 for the interval of 21 to 41 cycles) gives an approximation of the instantaneous crack propagation rate following an overload. For IN100 and Waspaloy at $\Delta K = 22$ MPa this data is presented in Figure A-12. While the exact path of the immediate post-overload crack propagation rate curve is unclear, as indicated by the broken line, the existence of delayed retardation is confirmed. In each alloy the crack growth rate is maximized at the time of the overload and the average crack growth rate decreases in each of the subsequent cycle intervals, i.e., 1 to 6, 6 to 21, and 21 to 41.

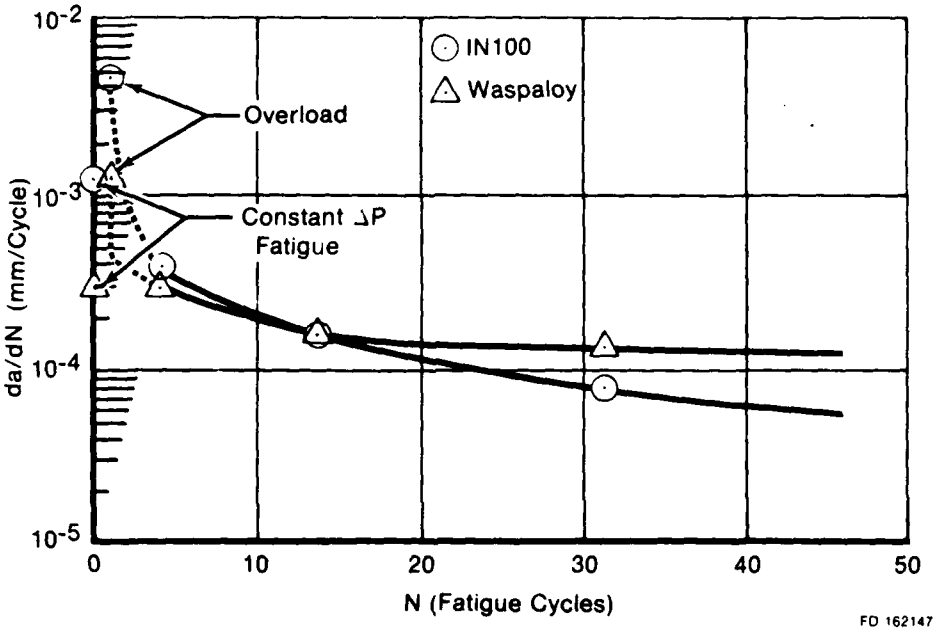

Figure A-12. Post Overload Crack Growth Exhibiting Delayed Retardation, OLR = 1.5, ΔK = 22 MPa $\sqrt{m}$

This finding is verification of the general crack behavior which was hypothesized earlier for mission crack growth subject to delayed retardation. That is, in IN100 and Waspaloy a crack subjected to constant load amplitude fatigue interrupted by periodic overloading will display a general decrease in the average macroscopic crack propagation rate, but, as illustrated in Figure A-13, the instantaneous response of a crack to such overloading is more complex. The full extent of crack retardation does not develop immediately following the application of an overload; rather, post-overload crack growth rate decelerates throughout the period of delayed retardation. Typically, this period is greater than the total number of baseline fatigue cycles applied between mission overload, and delayed retardation is responsible for all beneficial effects of the overloading. Since crack growth rate decelerates during the entire period of delayed retardation, fatigue cycles immediately following an overload are considerably more damaging than later cycles.

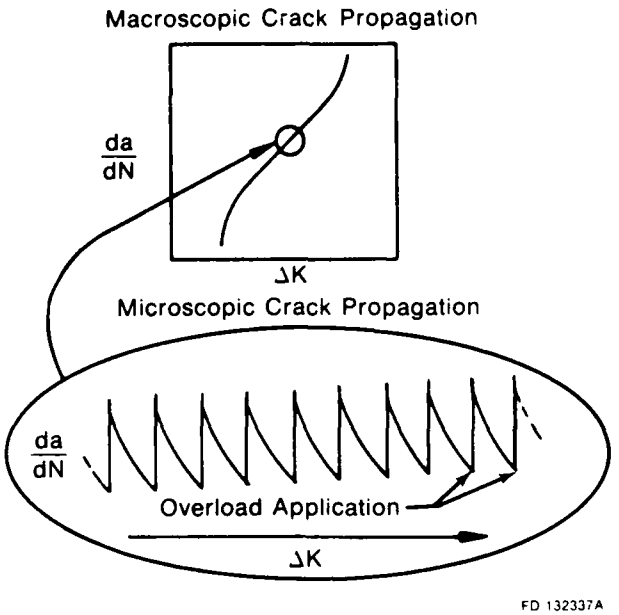

Figure A-13. Fatigue Crack Propagation with Frequent Overloads

This behavior deviates significantly from the general long-term effects of an overload on FCP; therefore, mission crack growth in IN100 and Waspaloy is difficult to predict by any retardation model which is developed solely from experimental measurements of the total period of retardation N*. Modeling of N* addresses fatigue crack retardation as a steady-state process, while retardation under mission loading is dominated by delayed retardation which is a transient response. Only a model which contains this transient capability is expected to effectively predict the synergistic effects of the frequent overloading which is common to engine operation.

CONCLUSIONS

1. The rate of elevated temperature FCP of IN100 and Waspaloy subjected to constant load amplitude interrupted by periodic overloads, decreases with increasing overload ratio and number of cycles between overload.

2. The combined effects of overload ratio ($1.0 \leq OLR \leq 1.5$) and number of cycles between overloads ($5 \leq \Delta N_{OL} \leq 40$) on crack propagation of IN100 and Waspaloy are effectively described by an interpolative model based on the hyperbolic sine function.

3. Post-overload crack retardation resulting from frequently applied overloads (OLR = 1.5, $\Delta N_{OL} \leq 40$) exhibits delayed retardation in IN100 and Waspaloy. The delayed retardation is not exhausted between successive overloads and is entirely responsible for any reduction in crack growth rate in these alloys.

ACKNOWLEDGEMENT

The authors wish to acknowledge the support of the Air Force Materials Laboratory on Contract F33615-75-C-5197, "Application of Fracture Mechanics at Elevated Temperatures," and Contract F33615-77-C-5153, "Cumulative Damage Fracture Mechanics Under Engine Spectra."

LIST OF SYMBOLS

a	crack length
C_1	SINH material coefficient = 0.5
C_2	SINH horizontal scaling coefficient
C_3	SINH horizontal inflection coefficient
C_4	SINH vertical inflection coefficient
da/dN	cyclic rate of crack growth
ΔK	applied stress intensity factor range
ΔN_{OL}	number of fatigue cycles applied between periodic overloads
K	stress intensity factor
K_{max}	maximum stress intensity factor
K_{min}	minimum stress intensity factor
K_{OL}	overload stress intensity factor
N	number of cycles
N*	number of cycles during which crack growth rate is retarded following an overload application
N_{DR}	period of delayed retardation
P	applied load
P_{max}	maximum applied load
P_{min}	minimum applied load
P_{OL}	magnitude of applied overload
P	load ratio (P_{min}/P_{max})

REFERENCES

1. Larsen, J. L., and Annis, C.G., "Cumulative Damage Fracture Mechanics Under Engine Spectra," Annual Report on Air Force Material Laboratory Contract F33615-77-C-5153, Pratt & Whitney Aircraft/Government Products Division, September 1978.

2. Wheeler, O.E., "Spectrum Loading and Crack Growth," *Journal of Basic Engineering*, American Society for Mechanical Engineering, 1972, pp. 181-186.

3. Willenborg, J., Engle, R.M., and Wood, H.A., "A Crack Growth Retardation Model Using an Effective Stress Concept," AFFDL-TM-71-1-FRR, Air Force Flight Dynamics Lab, 1971.

4. Elber, Wolf, "The Significance of Fatigue Crack Closure," *Damage Tolerance in Aircraft Structures, ASTM STP 486*, American Society for Testing and Materials, 1971, pp. 230-242.

5. Annis, C.G., Wallace, R.M., and Sims, D.L., "An Interpolative Model for Elevated Temperature Fatigue Crack Propagation," Technical Report AFML-TR-76-176, Part I, Air Force Materials Laboratory, November 1976.

6. Wallace, R.M., Annis, C.G., and Sims, D.L., "Application of Fracture Mechanics at Elevated Temperature," Technical Report AFML-TR-76-176, Part III, Air Force Materials Laboratory, November 1976.

7. Sims, D.L., Annis, C.G., and Wallace, R.M., "Cumulative Damage Fracture Mechanics at Elevated Temperature," Technical Report AFML-TR-76-176, Part III, Air Force Materials Laboratory, November 1976.

8. Corbly, D.M., and Packman, P.F., "On the Influence of Single and Multiple Peak Overloads on Fatigue Crack Propagation in 7075-T6511 Aluminum," *Engineering Fracture Mechanics*, 1973, pp. 479-497.

9. Rice, R.C., and Stephens, R.I., "Overload Effects of Subcritical Crack Growth in Austenitic Manganese Steel," *Progress in Flaw Growth and Fracture Toughness Testing, ASTM STP 536*, American Society for Testing and Materials, 1973. pp. 95-114.

10. Gardner, F.H., and Stephens, R.I., "Subcritical Crack Growth Under Single and Multiple Periodic Overloads in Cold-Rolled Steel," *Fracture Toughness and Slow-Stable Cracking, ASTM STP 559*, American Society for Testing and Materials, 1974, pp. 225-244.

11. "Plane-Strain Fracture Toughness of Metallic Materials," ASTM E399 72, American Society for Testing and Materials.

12. Hudak, S.J., Jr., Saxena, A., Bucci, R.J., and Malcolm, R.C., "Development of Standard Methods of Testing and Analyzing Fatigue Crack Growth Rate Data," Technical Report AFML-TR-78-40, Air Force Materials Laboratory, May 1978.

13. Larsen, J.M., "Cumulative Damage Fracture Mechanics Under Engine Spectra," Interim Technical Report on Air Force Materials Laboratory Contract F33615-77-C-5153, Pratt & Whitney Aircraft/Government Products Division, March 1979.

APPENDIX B. CUMULATIVE DAMAGE CRACK PROPAGATION TESTS

Specimen Number	*Material*	*Test Temperature*	*Atmosphere*	*Frequency*	*Load Ratio*	*Specimen Geometry*	*Thickness*	*Comment*
1000793	PWA 1073	427C	AIR	.167 HZ	R=-1.	CC[1]	7.62	
1001000	PWA 1007	427C	AIR	.167 HZ	R=.05	C[2]	2.64	
1001001	PWA 1007	649C	AIR	.167 HZ	R=.05	C	2.59	
1001002	PWA 1007	427C	AIR	.167 HZ	R=.05	C	12.67	
1001003	PWA 1007	427C	AIR	.167 HZ	R=.05	CC	7.70	
1001004	PWA 1007	649C	AIR	.167 HZ	R=.05	CC	7.65	
1001005	PWA 1007	427C	AIR	.167 HZ	R=.5	CC	7.62	
1001006	PWA 1007	649C	AIR	.167 HZ	R=.55	CC	7.29	
1001007	PWA 1007	427C	AIR	.167 HZ	R=.8	CC	7.62	
1001008	PWA 1007	649C	AIR	.167 HZ	R=.8	CC	7.62	
1001009	PWA 1007	TMF	AIR	.0167 HZ	R=.05	CC	7.62	TMF800-1300F
1001010	PWA 1007	732C	AIR	.167 HZ	R=.05	CC	7.65	
1001011	PWA 1007	732C	AIR	.167 HZ	R=.05	C	2.72	
1001013	PWA 1007	649C	AIR	.167 HZ	R=.1	C	8.08	
1001014	PWA 1007	427C	AIR	.167 HZ	R=.05	C	7.62	PARTIAL
1001015	PWA 1007	732C	AIR	2 MDWL	R=.1	C	7.62	PARTIAL
1001017	PWA 1007	649C	AIR	20 HZ	R=.8	C	7.62	
1001018	PWA 1007	427C	AIR	.167 HZ	R=.05	C	7.57	
1001019	PWA 1007	649C	AIR	.167 HZ	R=.5	C	7.59	OL1.50+5CY
1001021	PWA 1007	649C	AIR	.167 HZ	R=.5	C	7.67	OL1.50+40CY
1001022	PWA 1007	649C	AIR	.167 HZ	R=.5	C	7.62	OL1.25+5CY
1001024	PWA 1007	649C	AIR	.167 HZ	R=.5	C	7.62	OL1.25+40 PA
1001025	PWA 1007	649C	AIR	.167 HZ	R=.5	C	7.62	OL1.50+20CY
1001026	PWA 1007	649C	AIR	.167 HZ	R=.5	C	7.57	OL1.25+20CY
1001027	PWA 1007	732C	AIR	2 MDWL	R=.1	C	7.59	
1001028	PWA 1007	649C	AIR	.167 HZ	R=.5	C	7.65	OL1.25+40CY
1001029	PWA 1007	649C	AIR	.167 HZ	R=.1	C	7.62	OL1.50+20CY
1001030	PWA 1007	649C	AIR	.167 HZ	R=.1	C	7.59	OL1.25+20CY
1001031	PWA 1007	649C	AIR	DA/DT		C	12.75	
1001033	PWA 1007	649C	AIR	DA/DT		C	12.75	
1001034	PWA 1007	649C	AIR	DA/DT		C	12.73	
1001035	PWA 1007	649C	AIR	DA/DT		C	12.75	
1001036	PWA 1007	732C	AIR	DA/DT		C	12.80	
1001037	PWA 1007	732C	AIR	DA/DT		C	12.80	
1001039	PWA 1007	732C	AIR	DA/DT		C	12.80	
1001041	PWA 1007	732C	AIR	DA/DT		C	12.24	
1001042	PWA 1007	649C	AIR	DA/DT		C	12.29	
1001044	PWA 1073	732C	AIR	.0083 HZ	R=.1	C	7.67	
1001046	PWA 1073	732C	AIR	.167 HZ	R=.1	C	7.62	OL1.25+20CY
1001047	PWA 1073	732C	AIR	.167 HZ	R=.1	C	7.65	OL1.50+20CY
1001048	PWA 1073	649C	AIR	.167 HZ	R=.8	C	7.67	
1001052	PWA 1073	649C	AIR	.0083 HZ	R=.1	C	7.24	
1001053	PWA 1073	649C	AIR	.167 HZ	R=.1	C	7.59	
1001055	PWA 1073	649C	AIR	.167 HZ	R=.5	CC	7.82	OL1.5-.3+20

APPENDIX B. CUMULATIVE DAMAGE CRACK PROPAGATION TESTS

Specimen Number	Material	Test Temperature	Atmosphere	Frequency	Load Ratio	Specimen Geometry	Thickness	Comment
1001058	PWA 1073	649C	AIR	.167 HZ	R=-.5	CC	7.85	
1001196	PWA 1007	649C	AIR	20 HZ	R=.05	C	19.13	
1001301	PWA 1007	649C	AIR	.167 HZ	R=.05	C	12.73	
1001302B	PWA 1007	649C	AIR	.167 HZ	R=.5	C	12.75	OL1.50+20CY
1001303	PWA 1007	649C	AIR	.167 HZ	R=.1	C	12.70	2MDWL+20CY
1001304	PWA 1007	649C	AIR	20 HZ	R=.1	C	12.70	
1001307	PWA 1007	427C	AIR	20 HZ	R=.1	C	7.80	
1001308	PWA 1007	649C	AIR	20 HZ	R=.1	C	7.67	
1001309	PWA 1007	649C	AIR	.167 HZ	R=.1	C	7.72	2MDWL+40CY
1001310	PWA 1007	649C	AIR	.167 HZ	R=.1	C	7.42	2MDWL+20CY
1001312	PWA 1007	649C	AIR	.167 HZ	R=.1	C	7.54	2MDWL+20CY
1001313	PWA 1007	732C	AIR	.167 HZ	R=.1	C	7.67	2MDWL+40CY
1001314	PWA 1007	732C	AIR	.167 HZ	R=.1	C	7.47	2MDWL+20CY
1001315	PWA 1007	732C	AIR	.167 HZ	R=.1	C	7.59	2MDWL+10CY
1001316	PWA 1007	732C	AIR	.167 HZ	R=.5	C	7.47	2MDWL+20CY
1001317	PWA 1007	649C	AIR	.167 HZ	R=.1	C	7.67	2MDWL+10CY
1001318	PWA 1007	732C	AIR	.167 HZ	R=.1	C	7.67	OL1.50+20CY
1001319	PWA 1007	732C	AIR	.167 HZ	R=.5	C	7.57	OL1.50+20CY
1001320	PWA 1007	732C	AIR	.167 HZ	R=.5	CC	7.59	OL1.25+20CY
1001321	PWA 1007	649C	AIR	.167 HZ	R=.1	CC	7.42	PRESTRAIN
1001323	PWA 1007	649C	AIR	.167 HZ	R=.1	CC	7.54	PRESTRAIN
1001324	PWA 1007	427C	AIR	.167 HZ	R=-.5	CC	7.57	
1001326	PWA 1007	649C	AIR	.167 HZ	R=-.5	CC	7.57	
1001327	PWA 1007	649C	AIR	.167 HZ	R=-1.	CC	7.62	
1001328	PWA 1007	649C	AIR	.0083 HZ	R=.1	CC	7.59	
1001329	PWA 1007	732C	AIR	.167 HZ	R=.1	CC	7.62	OL1.25+20CY
1001330	PWA 1007	732C	AIR	15 MDWL	R=.1	CC	7.59	
1001337	PWA 1073	649C	AIR	.167 HZ	R=.1	CC	7.32	PRESTRAIN
1001341	PWA 1073	649C	AIR	.167 HZ	R=.1	CC	7.52	
1001342	PWA 1073	649C	AIR	.167 HZ	R=-1.	CC	7.59	
1001343	PWA 1073	427C	AIR	.167 HZ	R=-.5	CC	5.79	
1001349	PWA 1007	649C	AIR	.167 HZ	R=.05	CC	7.59	HIGH STRESS
1001350	PWA 1007	427C	AIR	.167 HZ	R=-1.	CC	7.54	
1001426	PWA 1007	649C	AIR	.167 HZ	R=.05	CC	7.57	HIGH STRESS
1001456	PWA 1007	649C	AIR	.167 HZ	R=.5	C	12.75	2MDWL+20CY

1 CC = through thickness center crack specimen (figure 11a)
2 C = compact specimen (figure 11b)

APPENDIX C. CRACK PROPAGATION DATA FOR SPECIMENS TESTED

7AN0326A PWA 1073 1350F AIR 2 M7AN
R= 0.10 THICKNESS=11.074 MM
PMAX= 5.280 KN WIDTH=63.373 MM
COMPACT SPECIMEN

NO.	CYCLES	A(MM)	DEL K (MPA√M)	DA/DN (MM/CYCLE)
1	0.	27.08		
2	390.	28.17		
3	503.	28.48		
4	706.	29.20	14.58	3.156E-03
5	841.	29.56	14.84	3.309E-03
6	1074.	30.22	15.39	3.537E-03
7	1254.	31.03	15.82	3.985E-03
8	1374.	31.56	16.13	4.984E-03
9	1569.	32.19	16.87	6.703E-03
10	1749.	33.34	17.90	9.776E-03
11	1894.	35.20	19.42	1.342E-02
12	2014.	36.62	21.47	2.053E-02
13	2089.	38.24		
14	2134.	39.13		
15	2254.	43.61		

1000330 PWA 1073 1350F AIR 10 CPM
R= 0.10 THICKNESS=12.700 MM
PMAX= 6.045 KN WIDTH=63.602 MM
COMPACT SPECIMEN

NO.	CYCLES	A(MM)	DEL K (MPA√M)	DA/DN (MM/CYCLE)
1	0.	26.81		
2	8040.	27.38	13.29	7.092E-05

7AN0334 PWA 1073 1200F AIR 10 CPM
R= 0.50 THICKNESS=12.725 MM
PMAX= 8.976 KN WIDTH=63.409 MM
COMPACT SPECIMEN

NO.	CYCLES	A(MM)	DEL K (MPA√M)	DA/DN (MM/CYCLE)
1	0.	21.24		
2	2000.	21.51		
3	6000.	21.94		
4	14400.	22.33	9.15	7.141E-05
5	21000.	22.80	9.30	6.987E-05
6	28000.	23.30	9.47	7.156E-05
7	34400.	23.77	9.64	7.415E-05
8	41000.	24.25	9.82	7.610E-05
9	48000.	24.79	10.03	8.041E-05
10	55000.	25.35	10.25	8.480E-05
11	62000.	25.93	10.51	8.894E-05
12	69300.	26.68	10.78	9.756E-05
13	76200.	27.32	11.08	1.096E-04
14	84800.	28.14	11.53	1.303E-04
15	92000.	29.22	12.01	1.597E-04
16	99000.	30.38	12.62	2.125E-04
17	105000.	31.53	13.40	2.718E-04
18	111000.	33.13	14.53	3.630E-04
19	117000.	35.61	16.48	5.140E-04
20	120000.	37.10	18.08	6.410E-04
21	123100.	39.12	20.78	8.549E-04
22	124650.	40.64	22.71	1.107E-03
23	125640.	41.71		
24	126500.	43.08		
25	127400.	44.33		

7AN0337 PWA 1073 1200F AIR 2 MDWL
R= 0.10 THICKNESS=11.201 MM
PMAX= 7.895 KN WIDTH=63.416 MM
COMPACT SPECIMEN

NO.	CYCLES	A(MM)	DEL K (MPA√M)	DA/DN (MM/CYCLE)
1	0.	21.08		
2	1011.	23.27		
3	1240.	23.72		
4	1460.	24.23	17.64	2.229E-03
5	1700.	24.68	18.01	2.009E-03
6	2000.	25.56	18.48	2.322E-03
7	2200.	25.85	18.81	2.376E-03
8	2665.	26.92	19.67	2.687E-03
9	3110.	28.25	20.75	2.929E-03
10	3500.	29.46	21.91	2.912E-03
11	3900.	31.06	23.14	3.000E-03
12	4200.	31.72	24.06	3.782E-03
13	4397.	31.82	24.79	4.217E-03
14	4710.	33.43	26.29	5.239E-03
15	5100.	35.97	29.99	7.749E-03
16	5200.	36.85	31.53	8.396E-03
17	5300.	37.34	33.14	1.034E-02
18	5400.	38.55	35.07	1.166E-02
19	5500.	39.66	37.99	1.428E-02
20	5640.	42.01	44.81	1.802E-02
21	5650.	42.18	45.39	2.024E-02
22	5665.	42.49	46.46	2.142E-02
23	5680.	42.78		
24	5700.	43.28		
25	5720.	43.77		

APPENDIX C. CRACK PROPAGATION DATA FOR SPECIMENS TESTED (Continued)

7AN0371 PWA 1073 1350F AIR 10CPM
R= 0.10 THICKNESS=12.751 MM
PMAX= 9.016 KN WIDTH=63.469 MM
COMPACT SPECIMEN

NO.	CYCLES	A(MM)	DEL K (MPA√M)	DA/DN (MM/CYCLE)
1	0.	21.29		
2	500.	21.73		
3	1340.	22.19		
4	2210.	22.61	16.68	5.382E-04
5	3040.	23.04	16.91	5.092E-04
6	4000.	23.62	17.20	5.185E-04
7	5100.	23.96	17.57	5.539E-04
8	6500.	24.86	18.11	6.473E-04
9	7740.	25.68	18.71	7.711E-04
10	8340.	26.15	19.09	8.301E-04
11	9000.	26.76	19.53	8.787E-04
12	9650.	27.34	20.00	9.611E-04
13	10310.	28.00	20.54	1.049E-03
14	11110.	28.78	21.29	1.190E-03
15	11900.	29.80	22.22	1.400E-03
16	12400.	30.53	22.94	1.582E-03
17	12900.	31.33	23.82	1.786E-03
18	13400.	32.25	24.88	2.016E-03
19	13800.	33.12	25.92	2.213E-03
20	14100.	33.80	26.84	2.364E-03
21	14400.	34.54	27.88	2.545E-03
22	14660.	35.20	28.85	2.840E-03
23	14940.	35.96	30.17	3.273E-03
24	15200.	36.77	31.72	3.806E-03
25	15470.	37.95	33.90	4.384E-03
26	15580.	38.51	35.00	4.459E-03
27	15700.	39.04	36.31	4.829E-03
28	15820.	39.66	37.80	4.700E-03
29	15950.	40.17	39.32	5.005E-03
30	16070.	40.99	40.89	6.278E-03
31	16100.	41.18	42.92	8.691E-03
32	16290.	42.14		
33	16350.	43.28		
34	16400.	44.20		

7AN0393 PWA 1073 1200F AIR 10 CPM
R= 0.50 THICKNESS=12.700 MM
PMAX= 9.061 KN WIDTH=63.635 MM
COMPACT SPECIMEN

NO.	CYCLES	A(MM)	DEL K (MPA√M)	DA/DN (MM/CYCLE)
1	26220.	23.56		
2	32050.	24.06		
3	38020.	24.52		
4	44310.	25.15	10.23	9.397E-05
5	50210.	25.80	10.45	1.038E-04
6	56110.	26.18	10.72	1.115E-04
7	61100.	26.86	10.96	1.204E-04
8	66000.	27.60	11.23	1.302E-04
9	70800.	28.10	11.56	1.425E-04
10	75600.	28.86	11.88	1.534E-04
11	80300.	29.58	12.25	1.694E-04
12	85370.	30.39	12.74	2.014E-04
13	90350.	31.47	13.34	2.425E-04
14	95320.	32.64	14.16	3.046E-04
15	100000.	34.17	15.31	4.044E-04
16	102380.	35.17	16.10	4.827E-04
17	104540.	36.18	17.10	5.683E-04
18	106540.	37.52	18.34	7.073E-04
19	107450.	38.10	19.07	7.707E-04
20	108400.	38.80	20.02	8.737E-04
21	109350.	39.83	21.15	1.026E-03
22	109820.	40.12	21.87	1.134E-03
23	110420.	40.91	22.96	1.346E-03
24	110920.	41.57	24.06	1.534E-03
25	111270.	42.11		
26	112043.	43.59		
27	112390.	44.40		

7AN0527 PWA 1073 1200F AIR 20 HZ
R= 0.10 THICKNESS= 6.274 MM
PMAX= 4.448 KN WIDTH=63.703 MM
COMPACT SPECIMEN

NO.	CYCLES	A(MM)	DEL K (MPA√M)	DA/DN (MM/CYCLE)
1	0.	21.75		
2	5000.	22.42		
3	9000.	23.01		
4	13000.	23.57	17.20	1.460E-04
5	17000.	24.12	17.59	1.508E-04
6	21000.	24.75	18.00	1.570E-04
7	25000.	25.41	18.45	1.644E-04
8	29000.	26.06	18.95	1.726E-04
9	33000.	26.78	19.49	1.816E-04
10	36000.	27.31	19.93	1.867E-04
11	39000.	27.89	20.41	1.979E-04
12	42000.	28.51	20.93	2.073E-04
13	45000.	29.13	21.51	2.190E-04
14	48000.	29.81	22.14	2.327E-04
15	50000.	30.27	22.60	2.431E-04
16	52000.	30.77	23.11	2.541E-04
17	54000.	31.30	23.66	2.638E-04
18	56000.	31.84	24.26	2.823E-04
19	56043.	31.84	24.26	2.829E-04
20	58000.	32.38	24.92	3.006E-04
21	60000.	33.04	25.70	3.200E-04
22	61510.	33.55	26.34	3.320E-04
23	63000.	34.04	27.02	3.466E-04
24	64500.	34.55	27.75	3.705E-04
25	66000.	35.09	28.59	3.960E-04
26	67500.	35.71	29.56	4.264E-04
27	68500.	36.21	30.30	4.499E-04
28	69500.	36.62	31.11	4.776E-04
29	70500.	37.10	31.99	5.075E-04
30	71500.	37.62	32.98	5.449E-04
31	72500.	38.18	34.19	5.788E-04
32	73500.	38.80	35.44	6.570E-04
33	74500.	39.48	37.05	7.184E-04
34	75550.	40.07	39.01	8.569E-04
35	76350.	41.07	40.98	9.477E-04
36	77000.	41.45	42.94	9.996E-04
37	77700.	42.46		
38	78300.	42.99		
39	78800.	43.47		

APPENDIX C. CRACK PROPAGATION DATA FOR SPECIMENS TESTED (Continued)

7AN0528 PWA 1073 1000F AIR 10 CPM
R= 0.10 THICKNESS= 6.350 MM
PMAX= 4.484 KN WIDTH=63.563 MM
COMPACT SPECIMEN

NO.	CYCLES	A(MM)	DEL K (MPA*√M)	DA/DN (MM/CYCLE)
1	0.	20.63		
2	1000.	21.04		
3	3800.	21.49		
4	5810.	22.00	16.23	2.441E-04
5	7000.	22.53	16.52	2.537E-04
6	10000.	23.04	16.86	2.661E-04
7	12200.	23.60	17.23	2.818E-04
8	14400.	24.28	17.65	2.967E-04
9	16400.	24.89	18.08	3.152E-04
10	18500.	25.60	18.57	3.337E-04
11	20500.	26.22	19.07	3.504E-04
12	22500.	26.96	19.63	3.702E-04
13	24110.	27.58	20.12	3.877E-04
14	26100.	28.37	20.80	4.182E-04
15	28000.	29.16	21.53	4.429E-04
16	29820.	29.98	22.32	4.731E-04
17	30900.	30.56	22.84	4.940E-04
18	31900.	31.01	23.37	5.092E-04
19	33000.	31.59	24.01	5.163E-04
20	34100.	32.20	24.65	5.249E-04
21	35200.	32.78	25.36	5.442E-04
22	36300.	33.30	26.09	5.743E-04
23	37400.	33.97	26.95	6.025E-04
24	38400.	34.59	27.83	6.412E-04
25	39410.	35.33	28.87	6.835E-04
26	40300.	35.86	29.88	7.179E-04
27	41220.	36.56	31.02	7.708E-04
28	42050.	37.20	32.19	8.330E-04
29	42920.	37.92	33.73	9.104E-04
30	43000.	38.78	35.53	1.017E-03
31	44570.	39.62	37.48	1.149E-03
32	45100.	40.13	39.08	1.267E-03
33	45600.	40.85	40.89	1.409E-03
34	46120.	41.60	43.17	1.610E-03
35	46500.	42.29		
36	46950.	43.01		
37	47350.	43.92		

7AN0534 PWA 1073 1200F AIR 10 CPM
R= 0.10 THICKNESS=12.725 MM
PMAX= 6.676 KN WIDTH=63.640 MM
COMPACT SPECIMEN

NO.	CYCLES	A(MM)	DEL K (MPA*√M)	DA/DN (MM/CYCLE)
1	0.	22.73		
2	50000.	25.17		
3	60000.	26.86		
4	66000.	28.16	15.34	2.319E-04
5	68000.	28.61	15.63	2.717E-04
6	70000.	29.17	15.99	3.133E-04
7	72000.	29.84	16.42	3.485E-04
8	74000.	30.53	16.97	3.993E-04
9	76000.	31.44	17.63	4.488E-04
10	77280.	31.98	18.13	4.978E-04
11	78600.	32.68	18.75	5.819E-04
12	78970.	32.84	18.92	6.389E-04
13	79570.	33.27	19.29	6.822E-04
14	80170.	33.75	19.71	7.494E-04
15	80770.	34.20	20.20	8.057E-04
16	81330.	34.59	20.68	8.607E-04
17	81900.	35.17	21.24	9.103E-04
18	82400.	35.59	21.78	1.003E-03
19	82900.	36.14	22.40	1.147E-03
20	83400.	36.62	23.14	1.296E-03
21	83900.	37.34	24.12	1.462E-03
22	84400.	38.21	25.30	1.612E-03
23	84800.	38.89	26.44	1.775E-03
24	85100.	39.34	27.37	1.979E-03
25	85400.	39.89	28.44	2.232E-03
26	85700.	40.61	29.83	2.440E-03
27	85900.	41.23	30.95	2.695E-03
28	86100.	41.79	32.23	2.965E-03
29	86300.	42.20		
30	86640.	43.45		
31	86800.	44.12		

7AN0535 PWA 1073 1200F AIR 1 MDWL
R= 0.10 THICKNESS=11.811 MM
PMAX= 8.309 KN WIDTH=63.500 MM
COMPACT SPECIMEN

NO.	CYCLES	A(MM)	DEL K (MPA*√M)	DA/DN (MM/CYCLE)
1	0.	25.97		
2	720.	26.71		
3	2100.	28.22		
4	2700.	29.04	21.41	1.489E-03
5	3250.	29.93	22.21	1.651E-03
6	3700.	30.79	22.99	1.842E-03
7	4125.	31.44	23.84	2.088E-03
8	4558.	32.35	24.88	2.481E-03
9	4900.	33.25	25.94	2.992E-03
10	5200.	34.15	27.22	3.977E-03
11	5404.	34.95	28.38	4.808E-03
12	5600.	35.78	29.88	6.040E-03
13	5800.	37.31	32.14	7.909E-03
14	6009.	38.71	35.13	1.107E-02
15	6100.	39.97	38.80	1.376E-02
16	6170.	40.99	41.55	1.813E-02
17	6200.	41.66	43.31	1.817E-02
18	6230.	42.24		
19	6260.	42.90		
20	6330.	44.19		

APPENDIX C. CRACK PROPAGATION DATA FOR SPECIMENS TESTED (Continued)

7AN0536 PWA 1073 1200F AIR 10CPM
R= 0.10 THICKNESS=11.938 MM
PMAX= 5.338 KN WIDTH=63.787 MM
COMPACT SPECIMEN

NO.	CYCLES	A(MM)	DEL K (MPA√M)	DA/DN (MM/CYCLE)
1	0.	26.92		
2	100.	27.06		
3	200.	27.16		
4	300.	27.27	12.52	1.231E-03
5	487.	27.50	12.64	1.345E-03
6	587.	27.66	12.71	1.421E-03
7	687.	27.80	12.79	1.557E-03
8	787.	27.95	12.87	1.671E-03
9	887.	28.11	12.96	1.829E-03
10	987.	28.32	13.07	1.985E-03
11	1087.	28.52	13.18	2.242E-03
12	1187.	28.76	13.31	2.535E-03
13	1287.	28.97	13.46	2.838E-03
14	1387.	29.32	13.62	3.317E-03
15	1487.	29.66	13.82	3.954E-03
16	1587.	30.03	14.08	4.690E-03
17	1687.	30.54	14.37	5.520E-03
18	1887.	31.82	15.20	8.753E-03
19	1987.	32.59		
20	2087.	33.67		
21	2187.	35.42		

7AN0537 PWA 1073 1200F AIR MIX
R= 0.10 THICKNESS=12.027 MM
PMAX= 6.672 KN WIDTH=63.906 MM
COMPACT SPECIMEN

NO.	CYCLES	A(MM)	DEL K (MPA√M)	DA/DN (MM/CYCLE)
1	0.	27.68		
2	100.	28.69		
3	200.	28.51		
4	300.	28.84	16.61	3.379E-03
5	400.	29.27	16.76	3.184E-03
6	500.	29.59	17.07	3.959E-03
7	600.	29.99	17.38	4.127E-03
8	700.	30.43	17.70	4.255E-03
9	800.	30.91	18.05	4.506E-03
10	900.	31.32	18.41	4.923E-03
11	1000.	31.78	18.84	5.239E-03
12	1100.	32.30	19.31	5.824E-03
13	1200.	33.05	19.88	6.682E-03
14	1300.	33.57	20.58	7.636E-03
15	1400.	34.42	21.38	9.181E-03
16	1500.	35.37	22.45	1.120E-02
17	1600.	36.40	24.01	1.409E-02
18	1700.	38.03	26.25	1.871E-02
19	1750.	38.97	27.82	2.319E-02
20	1800.	40.02	30.08	2.922E-02
21	1850.	41.50	33.12	3.938E-02
22	1900.	43.45	38.91	7.237E-02
23	1925.	44.97		
24	1950.	46.95		
25	1975.	51.99		

7AN0540 PWA 1073 1200F AIR 20 HZ
R= 0.10 THICKNESS=11.227 MM
PMAX= 7.735 KN WIDTH=63.348 MM
COMPACT SPECIMEN

NO.	CYCLES	A(MM)	DEL K (MPA√M)	DA/DN (MM/CYCLE)
1	0.	19.99		
2	5000.	20.43		
3	9000.	20.82		
4	13000.	21.17	15.46	9.620E-05
5	17500.	21.64	15.70	9.333E-05
6	22000.	22.05	15.95	1.007E-04
7	26600.	22.58	16.23	1.032E-04
8	31000.	23.00	16.50	1.056E-04
9	35500.	23.47	16.80	1.071E-04
10	40000.	23.97	17.11	1.083E-04
11	44500.	24.49	17.44	1.103E-04
12	49000.	24.94	17.79	1.160E-04
13	53500.	25.51	18.16	1.181E-04
14	58000.	26.05	18.54	1.202E-04
15	62500.	26.62	18.97	1.333E-04
16	67000.	27.14	19.45	1.419E-04
17	71600.	27.83	20.00	1.514E-04
18	75600.	28.54	20.54	1.616E-04
19	79600.	29.19	21.14	1.743E-04
20	83500.	29.84	21.79	1.911E-04
21	87400.	30.59	22.52	2.111E-04
22	90000.	31.16	23.11	2.242E-04
23	92600.	31.83	23.78	2.591E-04
24	95000.	32.53	24.47	2.553E-04
25	97400.	33.37	25.20	2.799E-04
26	99700.	33.61	26.01	3.241E-04
27	101900.	34.24	26.97	3.066E-04
28	103700.	35.03	28.14	4.439E-04
29	104200.	35.39	28.50	4.834E-04
30	105000.	35.76	29.17	5.297E-04
31	105500.	36.26	29.50	5.691E-04
32	106000.	36.53	30.70	5.917E-04
33	107400.	37.17	31.63	6.[illegible]E-04
34	106200.	37.70	32.60	6.9[illegible] 04
35	109000.	38.22	33.78	8.301E-04
36	109500.	38.76	35.17	1.004E-03
37	110600.	39.59	37.07	1.381E-03
38	111100.	40.43	39.07	1.516E-03
39	111400.	40.93		
40	111600.	41.63		
41	112400.	42.72		

7AN0541 PWA 1073 1200F AIR 10 CPM
R= 0.10 THICKNESS=12.687 MM
PMAX= 11.978 KN WIDTH=63.393 MM
COMPACT SPECIMEN

NO.	CYCLES	A(MM)	DEL K (MPA·√M)	DA/DN (MM/CYCLE)
1	0.	20.52		
2	300.	20.84		
3	700.	21.20		
4	1200.	21.58	21.46	8.450E-04
5	1800.	22.05	21.83	8.421E-04
6	2550.	22.70	22.34	8.900E-04
7	3130.	23.24	22.78	9.461E-04
8	4000.	24.06	23.53	1.028E-03
9	4500.	24.62	24.01	1.085E-03
10	5000.	25.17	24.52	1.170E-03
11	5500.	25.73	25.11	1.255E-03
12	6000.	26.37	25.75	1.383E-03
13	6450.	27.05	26.42	1.554E-03
14	6850.	27.62	27.15	1.654E-03
15	7250.	28.36	27.96	1.746E-03
16	7600.	29.10	28.72	1.815E-03
17	7890.	29.50	29.41	1.896E-03
18	8220.	30.15	30.20	2.031E-03
19	8500.	30.70	30.97	2.120E-03
20	8800.	31.36	31.96	2.294E-03
21	9050.	32.07	32.87	2.315E-03
22	9250.	32.42	33.61	2.500E-03
23	9500.	33.11	34.64	2.822E-03
24	9700.	33.48	35.61	3.044E-03
25	9850.	34.15	36.54	3.099E-03
26	10000.	34.74	37.51	3.194E-03
27	10150.	35.12	38.54	3.389E-03
28	10330.	35.63	39.73	3.330E-03
29	10550.	36.38	41.42	3.592E-03
30	10700.	37.02	42.80	4.008E-03
31	10850.	37.58	44.46	4.359E-03
32	11020.	38.28	46.62	4.894E-03
33	11150.	39.06	48.59	5.466E-03
34	11250.	39.52	50.50	5.794E-03
35	11350.	40.18	52.64	6.297E-03
36	11450.	40.86	55.00	6.784E-03
37	11570.	41.59	58.57	7.597E-03
38	11650.	42.28	61.31	8.296E-03
39	11700.	42.72		
40	11750.	43.15		
41	11800.	43.62		

7AN0542 PWA 1073 1200F AIR 40HZ
R= 0.10 THICKNESS=12.700 MM
PMAX= 5.693 KN WIDTH=63.500 MM
COMPACT SPECIMEN

NO.	CYCLES	A(MM)	DEL K (MPA·√M)	DA/DN (MM/CYCLE)
1	0.	27.69		
2	106.	28.46		
3	206.	29.25		
4	306.	30.14	14.27	9.255E-03
5	406.	31.06	14.83	1.053E-02
6	506.	32.07	15.65	1.237E-02
7	606.	33.36	16.68	1.545E-02
8	656.	34.20	17.34	1.840E-02
9	706.	35.07	18.21	2.247E-02
10	756.	36.17	19.31	2.825E-02
11	806.	37.61	21.03	3.722E-02
12	856.	39.49		
13	906.	42.17		
14	931.	44.13		

7AN0544 PWA 1073 1200F AIR .5 CPM
R= 0.10 THICKNESS=11.913 MM
PMAX= 6.699 KN WIDTH=63.396 MM
COMPACT SPECIMEN

NO.	CYCLES	A(MM)	DEL K (MPA·√M)	DA/DN (MM/CYCLE)
1	0.	28.13		
2	500.	28.48		
3	1000.	28.76		
4	1500.	29.07	17.14	5.526E-04
5	2000.	29.32	17.33	5.211E-04
6	2500.	29.57	17.49	5.056E-04
7	3495.	30.01	17.88	5.323E-04
8	3995.	30.30	18.08	5.538E-04
9	6000.	31.56	19.17	7.141E-04
10	7357.	32.58	20.16	8.226E-04
11	8357.	33.54		
12	8857.	33.88		
13	9357.	34.42		

7AN0546 PWA 1073 1200F AIR 10 CPM
R= 0.30 THICKNESS=12.776 MM
PMAX= 20.016 KN WIDTH=63.421 MM
COMPACT SPECIMEN

NO.	CYCLES	A(MM)	DEL K (MPA·√M)	DA/DN (MM/CYCLE)
1	32900.	26.66		
2	35000.	27.32		
3	37000.	28.22		
4	39540.	29.07	10.50	4.452E-04
5	40450.	29.34	10.75	4.691E-04
6	41500.	29.80	10.93	5.109E-04
7	42400.	30.16	11.16	5.517E-04
8	43500.	30.69	11.50	5.805E-04
9	44500.	31.50	11.83	5.932E-04
10	45390.	32.07	12.11	6.039E-04
11	46140.	32.46	12.40	5.944E-04
12	47300.	33.14	12.80	6.220E-04
13	48220.	33.70	13.17	6.071E-04
14	49000.	34.19	13.55	7.102E-04
15	49900.	34.69	13.97	7.603E-04
16	50800.	35.40	14.40	8.291E-04
17	51440.	36.13	15.06	9.411E-04
18	52100.	36.81	15.60	1.044E-03
19	52700.	37.42	16.22	1.183E-03
20	53350.	38.49	17.36	1.446E-03
21	53950.	39.12	18.04	1.609E-03
22	54360.	39.76	18.65	1.620E-03
23	54750.	40.51		
24	55130.	41.28		
25	55400.	42.00		

APPENDIX C. CRACK PROPAGATION DATA FOR SPECIMENS TESTED (Continued)

1000602AF PWA 1073 1200F AIR 2 MDWL
R= 0.10 THICKNESS= 6.350 MM
PMAX= 5.604 KN WIDTH=61.874 MM
COMPACT SPECIMEN

NO.	CYCLES	A(MM)	DEL K (MPA·√M)	DA/DN (MM/CYCLE)
1	0.	20.32		
2	51.	20.39	19.81	1.295E-03
3	200.	20.64	19.92	1.713E-03
4	500.	21.24	20.22	1.998E-03
5	800.	21.92	20.69	2.261E-03
6	1103.	22.56	21.20	2.104E-03
7	1400.	23.19	21.72	2.108E-03
8	1704.	23.57	22.15	1.270E-03
9	2054.	24.28	22.63	2.021E-03
10	2369.	25.02	23.29	2.338E-03
11	2625.	25.60	23.92	2.282E-03
12	2875.	26.25	24.54	2.506E-03
13	3100.	27.09	25.32	3.759E-03
14	3230.	27.53	26.02	3.409E-03
15	3335.	28.12	26.61	4.684E-03
16	3400.	28.55	27.21	3.465E-03
17	3510.	28.76	27.60	6.774E-03
18	3570.	29.05	27.90	4.868E-03
19	3691.	29.44	28.34	3.243E-03
20	3816.	30.05	28.99	4.846E-03
21	3936.	30.84	29.95	6.593E-03
22	4039.	31.22	30.81	4.094E-03
23	4113.	31.58	31.37	4.300E-03
24	4230.	32.34	32.25	6.459E-03
25	4326.	32.63	33.12	3.093E-03
26	4420.	33.25	33.92	6.580E-03
27	4512.	34.01	35.19	8.283E-03
28	4600.	34.94	36.87	1.054E-02
29	4650.	35.61	38.59	1.331E-02
30	4687.	36.12	39.97	1.380E-02
31	4720.	36.60	41.21	1.474E-02
32	4753.	37.10	42.49	1.497E-02
33	4788.	37.65	43.94	1.578E-02
34	4824.	38.30	45.73	1.806E-02
35	4853.	38.89	47.68	1.711E-02
36	4882.	39.72	50.12	2.462E-02
37	4910.	40.04	52.25	1.771E-02
38	4935.	40.74	54.28	2.630E-02
39	4955.	41.33	57.00	2.915E-02
40	4980.	42.57	61.23	3.560E-02

7AN0604AF PWA 1073 1200F AIR .5 CPM
R= 0.10 THICKNESS= 6.350 MM
PMAX= 6.214 KN WIDTH=61.900 MM
COMPACT SPECIMEN

NO.	CYCLES	A(MM)	DEL K (MPA·√M)	DA/DN (MM/CYCLE)
1	0.	27.98		
2	200.	28.43		
3	340.	28.76		
4	660.	29.44	31.64	2.317E-03
5	900.	29.94	32.48	2.414E-03
6	1160.	30.63	33.47	2.573E-03
7	1360.	31.27	34.42	2.783E-03
8	1600.	31.81	35.51	2.995E-03
9	1810.	32.45	36.64	3.357E-03
10	2000.	33.14	37.90	3.677E-03
11	2150.	33.64	39.10	3.903E-03
12	2300.	34.39	40.45	4.067E-03
13	2400.	34.72	41.41	4.204E-03
14	2520.	35.23	42.66	4.388E-03
15	2640.	35.74	43.95	4.486E-03
16	2760.	36.32	45.46	4.955E-03
17	2870.	36.86	47.04	5.459E-03
18	2980.	37.41	48.93	6.139E-03
19	3080.	38.10	51.03	6.736E-03
20	3160.	38.67	53.03	7.336E-03
21	3240.	39.30	55.41	7.889E-03
22	3300.	39.72	57.39	8.022E-03
23	3370.	40.36	59.86	8.383E-03
24	3420.	40.80	61.84	8.443E-03
25	3490.	41.33	64.74	9.017E-03
26	3540.	41.85		
27	3590.	42.21		
28	3640.	42.85		

7AN0605AF PWA 1073 1200F AIR .5 CPM
R= 0.10 THICKNESS= 6.350 MM
PMAX= 5.596 KN WIDTH=61.900 MM
COMPACT SPECIMEN

NO.	CYCLES	A(MM)	DEL K (MPA·√M)	DA/DN (MM/CYCLE)
1	3560.	28.53		
2	3760.	28.83		
3	3970.	29.27		
4	4180.	29.54	28.67	1.693E-03
5	4530.	30.22	29.56	1.867E-03
6	4930.	30.78	30.41	2.193E-03
7	5190.	31.44	31.44	2.553E-03
8	5450.	32.19	32.51	3.122E-03
9	5660.	32.85	33.68	3.561E-03
10	5860.	33.48	35.04	4.041E-03
11	6040.	34.46	36.53	4.467E-03
12	6130.	34.75	37.39	4.903E-03
13	6250.	35.35	38.78	5.132E-03
14	6360.	35.86	40.02	5.650E-03
15	6470.	36.69	41.69	6.773E-03
16	6540.	36.94	42.91	7.746E-03
17	6640.	37.77	45.27	9.794E-03
18	6700.	38.46	47.04	1.113E-02
19	6750.	39.04	49.10	1.176E-02
20	6790.	39.63	50.96	1.238E-02
21	6830.	40.03	52.86	1.265E-02
22	6870.	40.58	54.73	1.368E-02
23	6910.	41.03		
24	6950.	41.63		
25	7000.	42.63		

AD-A084 934 PRATT AND WHITNEY AIRCRAFT GROUP WEST PALM BEACH FL G--ETC F/G 21/5
CUMULATIVE DAMAGE FRACTURE MECHANICS UNDER ENGINE SPECTRA.(U)
JAN 80 J N LARSEN, B J SCHWARTZ, C G ANNIS F33615-77-C-5183
UNCLASSIFIED PWA-FR-11044 AFML -TR-79-4199 NL

3 OF 3
AD A084934

END
DATE FILMED
7-80
DTIC

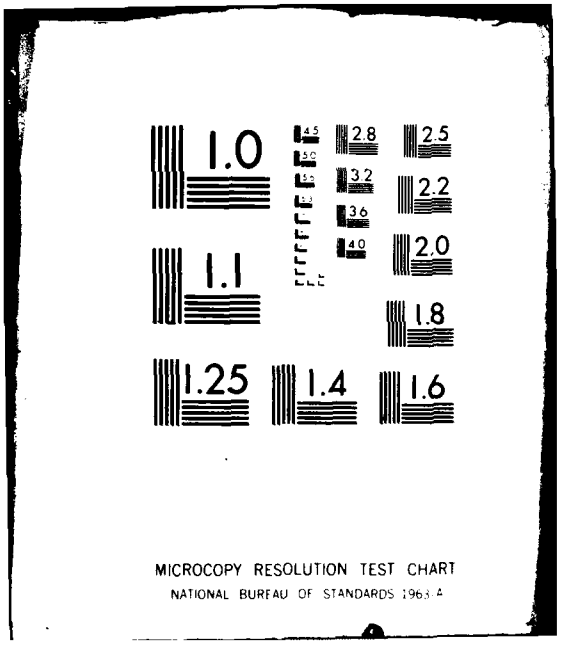
1.0
1.1
1.25
1.4
1.6
1.8
2.0
2.2
2.5
2.8
3.2
3.6
4.0
4.5
MICROCOPY RESOLUTION TEST CHART
NATIONAL BUREAU OF STANDARDS 1963-A

APPENDIX C. CRACK PROPAGATION DATA FOR SPECIMENS TESTED (Continued)

1000607AF PWA 1073 1200F AIR .5 CPM
R= 0.50 THICKNESS= 6.274 MM
PMAX= 6.307 KN WIDTH=63.767 MM
COMPACT SPECIMEN

NO.	CYCLES	A(MM)	DEL K (MPA√M)	DA/DN (MM/CYCLE)
1	0.	28.05		
2	100.	28.12	16.18	7.112E-04
3	600.	28.40	16.30	5.588E-04
4	1110.	28.72	16.50	6.425E-04
5	1700.	29.04	16.73	5.424E-04
6	2300.	29.41	16.98	6.160E-04
7	3100.	29.84	17.27	5.350E-04
8	3980.	30.41	17.65	6.408E-04
9	5000.	31.01	18.12	5.927E-04
10	6000.	31.82	18.71	8.115E-04
11	6970.	32.65	19.44	8.510E-04
12	7630.	33.27	20.12	9.390E-04
13	8290.	33.95	20.78	1.031E-03
14	8890.	34.59	21.49	1.073E-03
15	9440.	35.21	22.22	1.127E-03
16	10000.	36.02	23.09	1.442E-03
17	10380.	36.53	23.95	1.340E-03
18	10760.	37.17	24.76	1.698E-03
19	11000.	37.67	25.61	2.053E-03
20	11250.	38.17	26.39	1.996E-03
21	11480.	38.52	27.10	1.540E-03
22	11750.	39.06	27.88	2.013E-03
23	11910.	39.43	28.71	2.302E-03
24	12070.	39.79	29.41	2.254E-03
25	12340.	40.58	30.57	2.916E-03
26	12500.	41.00	31.87	2.603E-03
27	12670.	41.55	32.98	3.235E-03
28	12840.	42.18	34.42	3.713E-03
29	13000.	42.94	36.25	4.747E-03
30	13140.	43.36	37.91	2.984E-03
31	13300.	44.25	39.91	5.596E-03

1000608AF PWA 1073 1200F AIR .5 CPM
R= 0.50 THICKNESS= 6.325 MM
PMAX= 6.672 KN WIDTH=63.546 MM
COMPACT SPECIMEN

NO.	CYCLES	A(MM)	DEL K (MPA√M)	DA/DN (MM/CYCLE)
1	0.	28.15		
2	50.	28.19	17.13	8.890E-04
3	250.	28.49	17.26	1.499E-03
4	400.	28.57	17.40	5.418E-04
5	650.	28.88	17.54	1.229E-03
6	1000.	29.39	17.85	1.455E-03
7	1350.	29.95	18.27	1.611E-03
8	1700.	30.48	18.72	1.513E-03
9	2000.	31.00	19.16	1.723E-03
10	2300.	31.53	19.62	1.757E-03
11	2600.	32.27	20.21	2.476E-03
12	2800.	32.68	20.78	2.051E-03
13	3010.	33.18	21.24	2.377E-03
14	3220.	33.55	21.70	1.754E-03
15	3460.	34.14	22.24	2.482E-03
16	3600.	34.54	22.82	2.848E-03
17	3880.	35.19	23.46	2.318E-03
18	4100.	35.77	24.25	2.632E-03
19	4310.	36.67	25.28	4.288E-03
20	4600.	37.85	26.86	4.064E-03
21	4620.	37.82	27.82	-1.538E-03
22	4760.	38.49	28.38	4.808E-03
23	4820.	38.81	29.29	5.440E-03
24	5000.	39.89	30.66	5.976E-03
25	5100.	40.80	32.80	9.106E-03
26	5150.	41.16	34.30	7.189E-03
27	5210.	41.48	35.16	5.376E-03
28	5270.	42.07	36.34	9.758E-03
29	5330.	42.62	37.92	9.208E-03
30	5390.	43.40	39.89	1.295E-02
31	5430.	43.83	41.83	1.089E-02
32	5470.	44.16	43.13	8.255E-03

1000613AF PWA 1073 1350F AIR 20MDWL
R= 0.10 THICKNESS= 6.325 MM
PMAX= 6.067 KN WIDTH=62.840 MM
COMPACT SPECIMEN

NO.	CYCLES	A(MM)	DEL K (MPA√M)	DA/DN (MM/CYCLE)
1	0.	29.04		
2	5.	31.67	31.49	5.260E-01
3	7.	33.17	34.73	7.512E-01
4	8.	34.48	37.30	1.304E+00
5	9.	36.18	40.48	1.703E+00
6	10.	37.99	44.89	1.815E+00
7	11.	39.40	49.75	1.402E+00
8	12.	43.85	61.26	4.458E+00

APPENDIX C. CRACK PROPAGATION DATA FOR SPECIMENS TESTED (Continued)

1000614AF PWA 1073 1200F AIR 20MDWL
R= 0.10 THICKNESS= 6.401 MM
PMAX= 7.575 KN WIDTH=62.934 MM
COMPACT SPECIMEN

NO.	CYCLES	A(MM)	DEL K (MPA·√M)	DA/DN (MM/CYCLE)
1	0.	23.97		
2	8.	24.05	29.71	9.525E-03
3	35.	24.22	29.86	6.585E-03
4	90.	24.89	30.36	1.210E-02
5	135.	25.38	31.06	1.101E-02
6	180.	25.84	31.65	1.002E-02
7	226.	26.22	32.19	8.365E-03
8	275.	26.95	32.92	1.488E-02
9	310.	27.60	33.88	1.865E-02
10	340.	28.20	34.78	2.007E-02
11	385.	29.30	36.07	2.433E-02
12	415.	30.08	37.58	2.591E-02
13	442.	30.67	38.77	2.211E-02
14	467.	31.36	39.93	2.753E-02
15	488.	32.18	41.38	3.895E-02
16	500.	32.48	42.52	2.540E-02
17	515.	33.02	43.41	3.565E-02
18	530.	33.70	44.76	4.521E-02
19	545.	34.28	46.25	3.912E-02
20	555.	34.89	47.75	6.032E-02
21	565.	35.26	49.04	3.721E-02
22	580.	35.78	50.29	3.505E-02
23	595.	36.51	52.14	4.860E-02
24	601.	36.86	53.82	5.694E-02
25	611.	37.61	55.64	7.531E-02
26	617.	38.02	57.70	6.816E-02
27	623.	38.60	59.56	9.695E-02
28	629.	39.24	62.00	1.063E-01
29	634.	39.95	64.91	1.430E-01
30	638.	40.42	67.66	1.172E-01
31	642.	40.70	69.50	7.080E-02
32	647.	41.38	71.96	1.351E-01
33	651.	42.14	75.91	1.895E-01
34	654.	42.92	80.55	2.616E-01

7AN0621AF PWA 1073 1350F AIR MIX
R= 0.10 THICKNESS= 6.020 MM
PMAX= 4.804 KN WIDTH=63.678 MM
COMPACT SPECIMEN

NO.	CYCLES	A(MM)	DEL K (MPA·√M)	DA/DN (MM/CYCLE)
1	0.	24.08		
2	20.	24.54		
3	40.	25.16		
4	60.	25.79	21.09	3.055E-02
5	80.	26.38	21.63	3.195E-02
6	100.	27.10	22.20	3.290E-02
7	120.	27.67	22.81	3.437E-02
8	140.	28.40	23.48	3.664E-02
9	155.	28.95	24.02	3.914E-02
10	170.	29.54	24.66	4.286E-02
11	185.	30.19	25.36	4.752E-02
12	200.	30.92	26.23	5.109E-02
13	212.	31.53	27.02	5.422E-02
14	224.	32.35	27.88	5.863E-02
15	236.	32.91	28.86	6.400E-02
16	248.	33.69	29.99	7.129E-02
17	256.	34.34	30.87	7.631E-02
18	262.	34.84	31.67	8.438E-02
19	268.	35.32	32.61	8.389E-02
20	274.	35.78	33.56	8.291E-02
21	280.	36.53	34.49	8.501E-02
22	286.	36.78	35.50	8.850E-02
23	292.	37.29	36.62	9.359E-02
24	298.	37.95	37.81	1.053E-01
25	302.	38.33	38.93	1.162E-01
26	306.	38.81	40.12	1.292E-01
27	310.	39.36	41.49	1.404E-01
28	314.	39.92	43.25	1.479E-01
29	318.	40.65	45.16	1.549E-01
30	322.	41.31	47.23	1.608E-01
31	326.	41.80	49.48	1.690E-01
32	330.	42.50	51.93	1.840E-01
33	333.	43.10		
34	336.	43.71		
35	339.	44.41		

7AN0622AF PWA 1073 1200F AIR 20 HZ
R= 0.80 THICKNESS= 5.220 MM
PMAX= 4.595 KN WIDTH=63.472 MM
COMPACT SPECIMEN

NO.	CYCLES	A(MM)	DEL K (MPA·√M)	DA/DN (MM/CYCLE)
1	0.	23.51		
2	25000.	23.92		
3	50000.	24.19		
4	80000.	24.31	4.92	9.208E-06
5	120000.	24.67	4.93	8.799E-06
6	197250.	25.42	5.13	1.182E-05
7	240000.	26.05	5.27	1.379E-05
8	303700.	26.96	5.45	1.594E-05
9	353500.	27.82	5.65	1.750E-05
10	390000.	28.39	5.81	1.866E-05
11	426000.	29.16	5.98	1.956E-05
12	446000.	29.50	6.08	2.029E-05
13	470000.	30.05	6.22	2.132E-05
14	494000.	30.53	6.36	2.199E-05
15	518000.	31.07	6.52	2.397E-05
16	532000.	31.42	6.62	2.467E-05
17	556000.	31.93	6.82	2.647E-05
18	580000.	32.98	7.12	2.894E-05
19	600500.	33.30	7.25	3.001E-05
20	636000.	34.33	7.67	3.229E-05
21	653000.	34.97	7.90	3.373E-05
22	668000.	35.51	8.12	3.541E-05
23	683150.	35.97	8.38	3.791E-05
24	698300.	36.56	8.65	4.031E-05
25	713300.	37.18	8.97	4.596E-05
26	727000.	37.84	9.34	5.116E-05
27	740000.	38.53	9.76	5.508E-05
28	751000.	39.22	10.17	5.960E-05
29	752000.	39.61	10.46	6.366E-05
30	766000.	40.05	10.83	6.309E-05
31	775000.	40.73	11.30	7.608E-05
32	782000.	41.30	11.76	8.495E-05
33	789000.	41.65	12.31	9.578E-05
34	796000.	42.59		
35	801000.	43.24		
36	807000.	43.89		

APPENDIX C. CRACK PROPAGATION DATA FOR SPECIMENS TESTED (Continued)

7AN0625AF PWA 1073 1200F AIR MIX
R= 0.10 THICKNESS= 6.452 MM
PMAX= 5.338 KN WIDTH=63.729 MM
COMPACT SPECIMEN

NO.	CYCLES	A(MM)	DEL K (MPA√M)	DA/DN (MM/CYCLE)
1	0.	23.75		
2	35.	24.37		
3	70.	24.86		
4	95.	25.24	21.39	1.605E-02
5	120.	25.60	21.71	1.678E-02
6	145.	26.03	22.08	1.795E-02
7	170.	26.53	22.50	1.927E-02
8	195.	27.03	22.96	2.069E-02
9	220.	27.55	23.46	2.259E-02
10	245.	28.11	24.03	2.423E-02
11	265.	28.59	24.54	2.514E-02
12	285.	29.21	25.10	2.625E-02
13	305.	29.71	25.67	2.800E-02
14	325.	30.21	26.31	2.976E-02
15	345.	30.79	27.01	3.185E-02
16	365.	31.53	27.85	3.488E-02
17	385.	32.24	28.83	3.816E-02
18	400.	32.82	29.66	4.021E-02
19	415.	33.42	30.54	4.513E-02
20	425.	33.89	31.24	4.826E-02
21	435.	34.32	32.03	5.180E-02
22	455.	35.52	34.02	5.878E-02
23	463.	35.99	34.94	6.273E-02
24	471.	36.50	35.99	6.504E-02
25	479.	36.96	37.10	6.664E-02
26	487.	37.62	38.31	7.133E-02
27	493.	37.99	39.37	7.043E-02
28	499.	38.40	40.46	7.237E-02
29	505.	38.96	41.54	7.284E-02
30	511.	39.23	42.76	7.621E-02
31	517.	39.76	44.08	7.848E-02
32	523.	40.24	45.45	8.354E-02
33	529.	40.76	47.19	9.191E-02
34	535.	41.25	49.04	1.013E-01
35	541.	41.95	51.36	1.100E-01
36	545.	42.36	53.12	1.178E-01
37	549.	42.93		
38	553.	43.34		
39	557.	43.94		

7AN0626AF PWA 1073 1350F AIR MIX
R= 0.10 THICKNESS= 6.096 MM
PMAX= 4.955 KN WIDTH=61.951 MM
COMPACT SPECIMEN

NO.	CYCLES	A(MM)	DEL K (MPA√M)	DA/DN (MM/CYCLE)
1	0.	22.13		
2	10.	22.26		
3	25.	22.84		
4	40.	23.41	20.33	3.579E-02
5	55.	23.87	20.78	4.051E-02
6	70.	24.42	21.29	4.436E-02
7	85.	25.23	21.89	4.960E-02
8	100.	26.00	22.63	5.529E-02
9	110.	26.56	23.18	5.944E-02
10	120.	27.15	23.76	6.472E-02
11	130.	27.80	24.46	6.861E-02
12	140.	28.53	25.24	7.380E-02
13	150.	29.40	26.12	8.442E-02
14	155.	29.63	26.64	8.410E-02
15	160.	30.11	27.17	8.792E-02
16	165.	30.75	27.73	9.149E-02
17	170.	30.99	28.41	9.716E-02
18	175.	31.57	28.99	1.101E-01
19	180.	32.08	29.78	1.234E-01
20	185.	32.58	30.87	1.420E-01
21	190.	33.67	32.13	1.514E-01
22	195.	34.39	33.61	1.732E-01
23	198.	34.82	34.69	1.748E-01
24	201.	35.23	35.66	1.849E-01
25	203.	35.96	36.48	1.939E-01
26	205.	36.13	37.41	2.031E-01
27	207.	36.55	38.40	2.119E-01
28	209.	37.00	39.31	2.098E-01
29	211.	37.43	40.49	2.378E-01
30	213.	37.92	41.75	2.637E-01
31	215.	38.39	43.26	3.009E-01
32	217.	39.04	45.22	3.334E-01
33	219.	39.80	47.57	3.639E-01
34	220.	40.25	48.95	3.858E-01
35	221.	40.48	50.40	4.079E-01
36	222.	40.91	51.98	4.084E-01
37	223.	41.42	53.70	4.109E-01
38	224.	41.88	55.49	4.573E-01
39	225.	42.21	57.34	5.186E-01
40	226.	42.61		
41	227.	43.36		
42	228.	44.22		

7AN0629AF PWA 1073 1350F AIR MIX
R= 0.10 THICKNESS= 6.375 MM
PMAX= 5.338 KN WIDTH=57.097 MM
COMPACT SPECIMEN

NO.	CYCLES	A(MM)	DEL K (MPA√M)	DA/DN (MM/CYCLE)
1	0.	20.25		
2	10.	20.84		
3	20.	21.50		
4	35.	22.70	22.94	8.610E-02
5	50.	24.06	24.41	9.759E-02
6	55.	24.60	24.97	1.001E-01
7	60.	25.15	25.57	1.037E-01
8	65.	25.59	26.19	1.120E-01
9	70.	26.15	26.69	1.185E-01
10	75.	26.73	27.68	1.300E-01
11	80.	27.53	28.65	1.434E-01
12	85.	28.17	29.74	1.600E-01
13	90.	29.04	31.05	1.868E-01
14	94.	29.70	32.32	2.143E-01
15	98.	30.60	34.01	2.358E-01
16	100.	31.27	34.98	2.554E-01
17	102.	31.73	35.15	2.673E-01
18	104.	32.12	37.39	2.744E-01
19	106.	32.86	38.61	2.928E-01
20	108.	33.38	40.16	3.338E-01
21	110.	33.94	42.14	3.693E-01
22	112.	34.84	44.39	4.472E-01
23	113.	35.35	45.90	5.117E-01
24	114.	35.67	47.80	5.453E-01
25	115.	36.38	49.96	5.591E-01
26	116.	37.09	52.21	6.166E-01
27	117.	37.59	55.14	6.546E-01
28	118.	38.09	57.97	7.040E-01
29	119.	39.08	61.33	8.299E-01
30	120.	39.64		
31	121.	40.75		
32	122.	42.21		

APPENDIX C. CRACK PROPAGATION DATA FOR SPECIMENS TESTED (Continued)

1000630AF PWA 1073 1200F AIR MIX
R= 0.50 THICKNESS= 6.426 MM
PMAX= 5.418 KN WIDTH=57.132 MM
COMPACT SPECIMEN

NO.	CYCLES	A(MM)	DEL K (MPA√M)	DA/DN (MM/CYCLE)
1	271.	21.11		
2	350.	21.67	12.13	7.057E-03
3	430.	21.71	12.29	5.874E-04
4	516.	22.01	12.37	3.411E-03
5	600.	22.67	12.63	7.907E-03
6	696.	22.84	12.86	1.786E-03
7	800.	22.86	12.92	1.710E-04
8	952.	23.80	13.19	6.166E-03
9	1023.	24.44	13.66	9.105E-03
10	1088.	24.98	14.04	8.206E-03
11	1156.	24.99	14.21	1.681E-04
12	1220.	25.01	14.22	2.778E-04
13	1290.	24.99	14.23	-1.633E-04
14	1360.	25.70	14.46	1.001E-02
15	1422.	26.50	14.98	1.297E-02
16	1465.	26.49	15.27	-1.183E-04
17	1510.	27.16	15.52	1.482E-02
18	1550.	27.20	15.79	1.080E-03
19	1601.	27.24	15.82	6.721E-04
20	1700.	28.92	16.52	1.702E-02
21	1745.	29.70	17.62	1.724E-02
22	1784.	30.48	18.39	1.993E-02
23	1810.	30.74	18.94	1.011E-02
24	1840.	30.78	19.10	1.227E-03
25	1880.	31.56	19.57	1.969E-02
26	1915.	32.30	20.48	2.097E-02
27	1941.	33.16	21.53	3.321E-02
28	1960.	33.20	22.17	1.738E-03
29	1987.	33.25	22.23	2.070E-03
30	2020.	33.23	22.26	-4.999E-04
31	2060.	34.56	23.26	3.312E-02
32	2100.	36.42	26.06	4.661E-02
33	2115.	37.30	28.95	5.817E-02
34	2140.	38.92	32.05	6.482E-02
35	2152.	39.95	35.94	8.583E-02
36	2158.	40.60	38.77	1.092E-01
37	2162.	40.89	40.50	7.303E-02
38	2166.	41.40	42.03	1.257E-01
39	2170.	42.06	44.41	1.651E-01
40	2174.	42.80	47.52	1.867E-01

1000631AF PWA 1073 1350F AIR MIX
R= 0.50 THICKNESS= 6.248 MM
PMAX= 5.311 KN WIDTH=63.678 MM
COMPACT SPECIMEN

NO.	CYCLES	A(MM)	DEL K (MPA√M)	DA/DN (MM/CYCLE)
1	35.	23.43		
2	75.	24.55	11.65	2.810E-02
3	96.	25.07	12.02	2.467E-02
4	116.	25.62	12.27	2.718E-02
5	149.	26.45	12.61	2.525E-02
6	175.	27.17	13.01	2.755E-02
7	198.	27.81	13.37	2.794E-02
8	218.	28.49	13.75	3.397E-02
9	233.	29.19	14.15	4.665E-02
10	246.	29.74	14.54	4.250E-02
11	257.	30.19	14.86	4.087E-02
12	271.	30.75	15.19	3.973E-02
13	286.	31.44	15.63	4.640E-02
14	296.	31.97	16.07	5.283E-02
15	306.	32.56	16.50	5.855E-02
16	315.	33.00	16.92	4.995E-02
17	325.	33.40	17.27	3.988E-02
18	336.	34.00	17.71	5.403E-02
19	347.	34.69	18.30	6.269E-02
20	357.	35.36	18.97	6.756E-02
21	366.	35.89	19.60	5.814E-02
22	372.	36.50	20.23	1.031E-01
23	378.	36.87	20.81	6.096E-02
24	385.	37.36	21.34	6.931E-02
25	392.	38.03	22.09	9.561E-02
26	399.	38.67	23.01	9.271E-02
27	404.	39.21	23.90	1.074E-01
28	410.	40.07	25.03	1.439E-01
29	416.	40.53	26.17	7.556E-02
30	426.	42.04	28.05	1.516E-01
31	431.	42.99	30.71	1.890E-01
32	435.	43.64	32.65	1.635E-01

7AN0633AF PWA 1073 1200F AIR 10 CPM
R= 0.10 THICKNESS= 6.350 MM
PMAX= 4.030 KN WIDTH=63.797 MM
COMPACT SPECIMEN

NO.	CYCLES	A(MM)	DEL K (MPA√M)	DA/DN (MM/CYCLE)
1	1490.	25.54		
2	2570.	25.94		
3	3700.	26.40		
4	4930.	26.87	17.48	4.257E-04
5	6150.	27.41	17.85	4.560E-04
6	7350.	27.97	18.27	4.887E-04
7	8550.	28.58	18.74	5.354E-04
8	9840.	29.29	19.31	5.980E-04
9	10900.	29.90	19.85	6.709E-04
10	11900.	30.60	20.47	7.371E-04
11	12900.	31.38	21.20	8.130E-04
12	13600.	32.04	21.79	8.853E-04
13	14230.	32.52	22.39	9.528E-04
14	14800.	33.07	22.98	1.050E-03
15	15420.	33.77	23.74	1.177E-03
16	15900.	34.31	24.47	1.293E-03
17	16460.	35.12	25.47	1.446E-03
18	16820.	35.64	26.22	1.550E-03
19	17180.	36.19	27.08	1.667E-03
20	17510.	36.78	27.93	1.769E-03
21	18130.	37.92	29.93	2.136E-03
22	18450.	38.58	31.26	2.373E-03
23	18750.	39.29	32.77	2.546E-03
24	19000.	40.10	34.26	2.690E-03
25	19180.	40.55	35.47	2.872E-03
26	19360.	40.98	36.87	2.811E-03
27	19540.	41.54	38.17	2.800E-03
28	19720.	42.20	39.55	2.977E-03
29	20010.	42.78		
30	20160.	43.37		
31	20300.	44.01		

APPENDIX C. CRACK PROPAGATION DATA FOR SPECIMENS TESTED (Continued)

1000662AF PWA 1073 1350F AIR 20 HZ
R= 0.80 THICKNESS= 6.375 MM
PMAX= 4.479 KN WIDTH=63.622 MM
COMPACT SPECIMEN

NO.	CYCLES	A(MM)	DEL K (MPA√M)	DA/DN (MM/CYCLE)
1	16540.	24.22		
2	18335.	25.17		
3	19800.	25.96		
4	20125.	26.02	4.16	4.655E-04
5	21100.	26.39	4.23	4.694E-04
6	22155.	26.86	4.31	4.920E-04
7	23100.	27.40	4.40	5.640E-04
8	24100.	28.01	4.51	6.334E-04
9	25000.	28.57	4.63	6.892E-04
10	26130.	29.40	4.79	7.337E-04
11	27000.	30.10	4.93	8.100E-04
12	27803.	30.74	5.08	8.895E-04
13	28502.	31.23	5.22	1.006E-03
14	29203.	32.10	5.40	1.137E-03
15	29550.	32.47	5.50	1.243E-03
16	30205.	33.34	5.75	1.440E-03
17	30500.	33.70	5.87	1.495E-03
18	31200.	34.91	6.22	1.625E-03
19	31500.	35.44	6.40	1.715E-03
20	31833.	36.00	6.61	1.865E-03
21	32100.	36.34	6.78	2.020E-03
22	32400.	37.06	7.03	2.334E-03
23	32650.	37.67	7.29	2.640E-03
24	32850.	38.22	7.55	2.959E-03
25	33000.	38.68	7.77	3.146E-03
26	33200.	39.30	8.10	3.505E-03
27	33400.	40.08	8.52	3.717E-03
28	33550.	40.63	8.86	4.122E-03
29	33711.	41.38	9.28	5.067E-03
30	33800.	41.57		
31	34000.	42.75		
32	34115.	43.96		

1000663AF PWA 1073 1350F AIR MIX
R= 0.80 THICKNESS= 6.350 MM
PMAX= 5.338 KN WIDTH=63.792 MM
COMPACT SPECIMEN

NO.	CYCLES	A(MM)	DEL K (MPA√M)	DA/DN (MM/CYCLE)
1	5285.	27.72		
2	5505.	27.97	5.35	1.126E-03
3	5730.	28.34	5.42	1.637E-03
4	5945.	28.61	5.50	1.246E-03
5	6150.	28.98	5.57	1.834E-03
6	6600.	29.32	5.66	7.507E-04
7	6860.	29.54	5.72	8.450E-04
8	7150.	29.91	5.80	1.288E-03
9	7412.	30.09	5.87	6.689E-04
10	7683.	30.45	5.94	1.345E-03
11	7960.	30.95	6.05	1.788E-03
12	8245.	31.25	6.16	1.065E-03
13	8550.	31.66	6.26	1.345E-03
14	8860.	32.05	6.38	1.262E-03
15	9150.	32.55	6.52	1.708E-03
16	9437.	33.11	6.68	1.965E-03
17	9720.	33.80	6.89	2.437E-03
18	9920.	33.95	7.04	7.619E-04
19	10144.	34.97	7.25	4.519E-03
20	10364.	35.71	7.60	3.383E-03
21	10564.	36.21	7.86	2.476E-03

1000664AF PWA 1073 1350F AIR MIX
R= 0.80 THICKNESS= 6.325 MM
PMAX= 4.399 KN WIDTH=63.896 MM
COMPACT SPECIMEN

NO.	CYCLES	A(MM)	DEL K (MPA√M)	DA/DN (MM/CYCLE)
1	0.	21.09		
2	50.	21.84	3.47	1.494E-02
3	90.	23.09	3.59	3.150E-02
4	110.	24.18	3.75	5.410E-02
5	117.	24.33	3.84	2.195E-02
6	137.	25.04	3.90	3.537E-02
7	150.	25.42	3.98	2.940E-02
8	166.	26.10	4.07	4.239E-02
9	185.	27.04	4.20	4.940E-02
10	200.	28.21	4.38	7.798E-02
11	206.	28.65	4.53	7.366E-02
12	212.	29.31	4.64	1.105E-01
13	218.	29.46	4.72	2.413E-02
14	225.	29.95	4.78	6.985E-02
15	232.	30.26	4.87	4.463E-02
16	242.	31.09	4.99	8.293E-02
17	253.	32.00	5.19	8.336E-02
18	263.	33.15	5.45	1.151E-01
19	273.	34.27	5.76	1.113E-01
20	280.	35.67	6.15	1.999E-01
21	285.	36.45	6.52	1.565E-01
22	288.	37.03	6.78	1.943E-01
23	291.	37.74	7.04	2.371E-01
24	293.	38.34	7.32	2.978E-01
25	295.	38.82	7.57	2.426E-01
26	298.	39.31	7.81	1.626E-01
27	299.	40.35	8.22	1.043E+00
28	301.	40.76	8.63	2.032E-01
29	302.	41.18	8.88	4.217E-01
30	303.	41.68	9.18	5.016E-01
31	304.	42.03	9.46	3.454E-01
32	305.	42.74	9.84	7.112E-01
33	306.	43.08	10.24	3.404E-01
34	307.	43.68	10.61	5.944E-01

APPENDIX C. CRACK PROPAGATION DATA FOR SPECIMENS TESTED (Continued)

1000665AF PWA 1073 1350F AIR MIX
R= 0.10 THICKNESS= 6.248 MM
PMAX= 4.359 KN WIDTH=63.726 MM
COMPACT SPECIMEN

NO.	CYCLES	A(MM)	DEL K (MPA·√M)	DA/DN (MM/CYCLE)
1	0.	22.35		
2	30.	22.39	16.20	1.439E-03
3	70.	22.42	16.22	6.985E-04
4	157.	22.58	16.27	1.825E-03
5	240.	22.68	16.35	1.255E-03
6	400.	22.79	16.41	6.350E-04
7	800.	23.51	16.66	1.800E-03
8	1000.	23.71	16.95	1.041E-03
9	1250.	24.24	17.19	2.098E-03
10	1500.	24.68	17.50	1.748E-03
11	1750.	25.36	17.88	2.718E-03
12	1920.	25.63	18.22	1.591E-03
13	2110.	25.94	18.43	1.638E-03
14	2300.	26.40	18.71	2.453E-03
15	2460.	27.18	19.18	4.842E-03
16	2615.	27.32	19.54	9.177E-04
17	2864.	27.67	19.74	1.408E-03
18	3112.	27.91	19.98	9.525E-04
19	3607.	29.56	20.79	3.346E-03
20	3809.	29.88	21.69	1.578E-03
21	4050.	30.68	22.23	3.325E-03
22	4253.	30.95	22.77	1.314E-03
23	4472.	31.92	23.42	4.431E-03
24	4585.	32.39	24.22	4.192E-03

Continued Next Column

1000665AF PWA 1073 1350F AIR MIX
R= 0.10 THICKNESS= 6.248 MM
PMAX= 4.359 KN WIDTH=63.726 MM
COMPACT SPECIMEN

NO.	CYCLES	A(MM)	DEL K (MPA·√M)	DA/DN (MM/CYCLE)
25	4700.	32.72	24.69	2.849E-03
26	4830.	33.32	25.25	4.591E-03
27	4930.	34.03	26.08	7.125E-03
28	5010.	34.45	26.84	5.191E-03
29	5090.	34.88	27.44	5.366E-03
30	5170.	35.51	28.22	7.874E-03
31	5250.	36.09	29.17	7.255E-03
32	5330.	36.81	30.26	9.033E-03
33	5412.	37.08	31.15	3.314E-03
34	5523.	38.01	32.29	8.421E-03
35	5624.	38.54	33.77	5.218E-03
36	5670.	39.28	35.16	1.612E-02
37	5700.	39.68	36.49	1.308E-02
38	5732.	40.10	37.49	1.318E-02
39	5760.	40.63	38.73	1.891E-02
40	5788.	40.96	39.90	1.175E-02
41	5818.	41.80	41.61	2.824E-02
42	5835.	42.32	43.74	3.063E-02
43	5850.	42.61	45.08	1.913E-02
44	5865.	42.98	46.22	2.489E-02
45	5880.	43.32	47.50	2.261E-02
46	5895.	43.92	49.26	3.979E-02
47	5910.	44.39	51.40	3.150E-02

1000669AF PWA 1073 1200F AIR MIX
R= 0.10 THICKNESS= 5.994 MM
PMAX= 4.208 KN WIDTH=64.049 MM
COMPACT SPECIMEN

NO.	CYCLES	A(MM)	DEL K (MPA·√M)	DA/DN (MM/CYCLE)
1	100.	21.34		
2	200.	21.63	15.69	2.896E-03
3	300.	21.90	15.84	2.743E-03
4	450.	22.41	16.06	3.429E-03
5	600.	23.13	16.42	4.801E-03
6	750.	23.90	16.87	5.080E-03
7	850.	24.56	17.32	6.629E-03
8	950.	24.99	17.69	4.318E-03
9	1050.	25.48	18.00	4.877E-03
10	1150.	26.02	18.37	5.372E-03
11	1250.	26.80	18.85	7.849E-03
12	1350.	27.53	19.43	7.315E-03
13	1490.	28.57	20.15	7.411E-03
14	1550.	29.00	20.77	7.218E-03
15	1610.	29.46	21.17	7.535E-03
16	1670.	29.85	21.55	6.540E-03
17	1730.	30.33	21.96	8.065E-03
18	1790.	30.91	22.48	9.588E-03
19	1850.	31.67	23.17	1.270E-02
20	1910.	32.46	24.01	1.319E-02
21	1960.	32.85	24.69	7.849E-03
22	2010.	33.36	25.23	1.013E-02
23	2060.	33.81	25.82	8.992E-03
24	2110.	34.31	26.44	9.957E-03
25	2160.	34.89	27.19	1.173E-02
26	2210.	35.75	28.24	1.717E-02
27	2260.	36.41	29.43	1.316E-02
28	2300.	37.08	30.56	1.680E-02
29	2340.	37.92	31.94	2.105E-02
30	2370.	38.33	33.16	1.346E-02
31	2400.	38.96	34.24	2.095E-02
32	2430.	39.59	35.64	2.100E-02
33	2460.	40.38	37.35	2.654E-02
34	2475.	40.85	38.98	3.090E-02
35	2490.	41.21	40.11	2.396E-02
36	2505.	41.82	41.51	4.089E-02
37	2520.	42.29	43.18	3.166E-02
38	2535.	42.99	45.09	4.640E-02
39	2545.	43.50	47.19	5.118E-02
40	2555.	43.95	48.97	4.470E-02
41	2565.	44.40	50.72	4.508E-02

APPENDIX C. CRACK PROPAGATION DATA FOR SPECIMENS TESTED (Continued)

1000670AF PWA 1073 1200F AIR MIX
R= 0.50 THICKNESS= 6.375 MM
PMAX= 4.408 KN WIDTH=63.718 MM
COMPACT SPECIMEN

NO.	CYCLES	A(MM)	DEL K (MPA·√M)	DA/DN (MM/CYCLE)
1	300.	22.31		
2	650.	22.44	8.91	3.701E-04
3	1100.	22.64	8.96	4.431E-04
4	1150.	22.68	9.00	8.382E-04
5	1902.	23.05	9.07	4.914E-04
6	2800.	23.48	9.21	4.837E-04
7	3720.	24.00	9.37	5.618E-04
8	4579.	24.59	9.57	6.831E-04
9	5585.	25.41	9.83	8.218E-04
10	6300.	26.19	10.14	1.083E-03
11	6801.	26.72	10.41	1.065E-03
12	7300.	27.40	10.67	1.364E-03
13	7700.	28.01	10.96	1.534E-03
14	8100.	28.74	11.27	1.823E-03
15	8400.	29.33	11.59	1.964E-03
16	8657.	29.79	11.85	1.774E-03
17	8950.	30.48	12.15	2.371E-03
18	9173.	31.07	12.50	2.614E-03
19	9404.	31.61	12.83	2.342E-03
20	9650.	32.49	13.26	3.598E-03
21	9820.	32.83	13.65	1.965E-03
22	10010.	33.57	14.01	3.890E-03
23	10200.	34.15	14.48	3.088E-03
24	10391.	34.98	15.02	4.335E-03
25	10535.	35.60	15.61	4.330E-03
26	10687.	36.46	16.26	5.615E-03
27	10790.	36.97	16.91	4.932E-03
28	10890.	37.65	17.51	6.845E-03
29	10960.	38.42	18.30	1.096E-02
30	11034.	38.86	19.01	6.007E-03
31	11100.	39.38	19.61	7.832E-03
32	11160.	39.99	20.35	1.020E-02
33	11250.	41.01	21.52	1.137E-02
34	11295.	41.76	22.91	1.659E-02
35	11338.	42.44	24.14	1.586E-02
36	11390.	43.03	25.32	1.131E-02
37	11400.	43.56	26.43	5.334E-02
38	11430.	44.19	27.66	2.087E-02

7AN0671AF PWA 1073 1200F AIR MIX
R= 0.50 THICKNESS= 6.426 MM
PMAX= 4.390 KN WIDTH=64.206 MM
COMPACT SPECIMEN

NO.	CYCLES	A(MM)	DEL K (MPA·√M)	DA/DN (MM/CYCLE)
1	455.	21.57		
2	605.	21.77		
3	805.	21.95		
4	1005.	22.31	8.66	9.494E-04
5	1205.	22.33	8.71	8.691E-04
6	1460.	22.50	8.77	8.168E-04
7	1760.	22.77	8.85	7.850E-04
8	2100.	23.12	8.94	8.925E-04
9	2450.	23.37	9.05	9.246E-04
10	3150.	24.08	9.27	9.731E-04
11	3850.	24.73	9.52	1.044E-03
12	4400.	25.38	9.73	1.129E-03
13	4900.	25.87	9.95	1.217E-03
14	5400.	26.53	10.19	1.345E-03
15	5900.	27.21	10.47	1.512E-03
16	6400.	27.97	10.82	1.711E-03
17	6900.	28.87	11.23	1.912E-03
18	7250.	29.64	11.57	2.044E-03
19	7490.	30.10	11.82	2.146E-03
20	7730.	30.61	12.09	2.346E-03
21	7970.	31.15	12.40	2.461E-03
22	8210.	31.75	12.75	2.627E-03
23	8450.	32.56	13.14	2.875E-03
24	8610.	32.88	13.44	3.084E-03
25	8770.	33.35	13.77	3.331E-03
26	8930.	33.97	14.14	3.410E-03
27	9090.	34.55	14.58	3.648E-03
28	9250.	35.22	15.03	3.852E-03
29	9410.	35.68	15.52	4.055E-03
30	9570.	36.35	16.08	4.436E-03
31	9720.	37.09	16.70	4.970E-03
32	9840.	37.68	17.33	5.635E-03
33	9960.	38.36	18.08	6.105E-03
34	10080.	39.13	18.96	6.721E-03
35	10200.	40.07	20.04	7.428E-03
36	10280.	40.54	20.87	8.086E-03
37	10360.	41.25	21.83	8.983E-03
38	10440.	41.95	22.94	1.027E-02
39	10520.	42.79		
40	10590.	43.67		
41	10625.	44.25		

7AN0673AF PWA 1073 1200F AIR MIX
R= 0.50 THICKNESS= 6.274 MM
PMAX= 7.219 KN WIDTH=63.637 MM
COMPACT SPECIMEN

NO.	CYCLES	A(MM)	DEL K (MPA·√M)	DA/DN (MM/CYCLE)
1	770.	25.91		
2	820.	26.70		
3	855.	27.21		
4	890.	27.59	18.25	1.620E-02
5	930.	28.32	18.75	1.702E-02
6	970.	29.01	19.33	1.865E-02
7	1010.	29.92	20.01	2.038E-02
8	1050.	30.60	20.76	2.209E-02
9	1090.	31.56	21.64	2.608E-02
10	1110.	32.04	22.15	2.813E-02
11	1130.	32.61	22.78	3.183E-02
12	1150.	33.41	23.54	3.328E-02
13	1165.	33.76	24.18	3.406E-02
14	1180.	34.50	24.84	3.577E-02
15	1195.	34.86	25.49	3.822E-02
16	1210.	35.39	26.33	4.246E-02
17	1225.	36.09	27.23	4.804E-02
18	1240.	36.90	28.49	5.914E-02
19	1250.	37.42	29.58	6.196E-02
20	1260.	38.10	30.79	6.585E-02
21	1270.	39.01	32.05	7.678E-02
22	1280.	39.47	33.74	8.964E-02
23	1290.	40.27	35.84	1.112E-01
24	1300.	41.71	38.91	1.419E-01
25	1305.	42.32		
26	1310.	43.28		
27	1315.	44.06		

APPENDIX C. CRACK PROPAGATION DATA FOR SPECIMENS TESTED (Continued)

7AN0675AF PWA 1073 1200F AIR MIX
R= 0.50 THICKNESS= 6.375 MM
PMAX= 5.489 KN WIDTH=63.645 MM
COMPACT SPECIMEN

NO.	CYCLES	A(MM)	DEL K (MPA√M)	DA/DN (MM/CYCLE)
1	1790.	22.67		
2	2000.	23.04		
3	2250.	23.49		
4	2500.	24.09	11.84	2.271E-03
5	2732.	24.60	12.09	2.435E-03
6	2940.	25.15	12.34	2.611E-03
7	3150.	25.71	12.62	2.749E-03
8	3340.	26.21	12.89	2.907E-03
9	3540.	26.85	13.19	3.128E-03
10	3732.	27.43	13.53	3.310E-03
11	3930.	28.09	13.92	3.640E-03
12	4115.	28.66	14.33	3.685E-03
13	4250.	29.28	14.66	4.210E-03
14	4385.	29.97	15.03	4.589E-03
15	4600.	30.86	15.74	4.951E-03
16	4700.	31.49	16.12	5.306E-03
17	4800.	32.12	16.53	5.632E-03
18	4900.	32.44	17.01	5.951E-03
19	5001.	33.27	17.50	6.343E-03
20	5080.	33.69	17.94	6.035E-03
21	5160.	34.22	18.49	7.584E-03
22	5230.	34.80	18.97	8.183E-03
23	5305.	35.43	19.65	9.289E-03
24	5410.	36.38	20.85	1.040E-02
25	5470.	37.21	21.65	1.052E-02
26	5500.	37.51	22.08	1.130E-02
27	5550.	37.98	22.85	1.226E-02
28	5600.	38.52	23.69	1.305E-02
29	5650.	39.31	24.83	1.418E-02
30	5700.	40.12	26.13	1.580E-02
31	5750.	40.97	27.68	1.814E-02
32	5782.	41.27	28.78	2.178E-02
33	5820.	42.18	30.60	2.756E-02
34	5850.	42.82		
35	5882.	43.65		
36	5876.	44.09		

1000676AF PWA 1073 1200F AIR MIX
R= 0.50 THICKNESS= 5.817 MM
PMAX= 5.373 KN WIDTH=64.112 MM
COMPACT SPECIMEN

NO.	CYCLES	A(MM)	DEL K (MPA√M)	DA/DN (MM/CYCLE)
1	0.	22.38		
2	150.	22.59	11.87	1.448E-03
3	553.	23.09	12.02	1.232E-03
4	973.	23.59	12.24	1.197E-03
5	1350.	24.04	12.46	1.189E-03
6	1732.	24.57	12.69	1.393E-03
7	2132.	25.18	12.97	1.508E-03
8	2500.	25.69	13.25	1.394E-03
9	2863.	26.29	13.54	1.641E-03
10	3208.	26.83	13.85	1.587E-03
11	3540.	27.53	14.20	2.089E-03
12	3840.	28.12	14.58	1.994E-03
13	4156.	28.78	14.96	2.082E-03
14	4445.	29.47	15.39	2.373E-03
15	4710.	30.06	15.81	2.252E-03
16	4975.	30.77	16.27	2.679E-03
17	5100.	31.24	16.70	3.729E-03
18	5230.	31.55	16.99	2.364E-03
19	5500.	32.43	17.46	3.260E-03
20	5650.	32.90	18.03	3.166E-03
21	5800.	33.53	18.51	4.182E-03
22	5930.	33.97	19.00	3.351E-03
23	6065.	34.51	19.48	4.064E-03
24	6200.	35.19	20.10	5.014E-03
25	6316.	35.67	20.73	4.160E-03
26	6450.	36.34	21.39	4.985E-03
27	6608.	37.22	22.34	5.586E-03
28	6700.	37.82	23.33	6.502E-03
29	6790.	38.54	24.27	7.930E-03
30	6893.	39.17	25.31	6.177E-03
31	6990.	39.91	26.45	7.568E-03
32	7060.	40.50	27.64	8.527E-03
33	7140.	41.27	28.96	9.541E-03
34	7200.	41.80	30.30	8.826E-03
35	7260.	42.62	31.83	1.378E-02
36	7300.	43.20	33.53	1.441E-02
37	7342.	43.75	35.00	1.315E-02
38	7380.	44.43	36.71	1.775E-02

7AN0677AF PWA 1073 1200F AIR 10MDWL
R= 0.10 THICKNESS= 6.401 MM
PMAX= 7.117 KN WIDTH=63.609 MM
COMPACT SPECIMEN

NO.	CYCLES	A(MM)	DEL K (MPA√M)	DA/DN (MM/CYCLE)
1	0.	21.31		
2	60.	22.06		
3	112.	22.73		
4	150.	23.28	26.77	1.479E-02
5	200.	24.05	27.55	1.601E-02
6	240.	24.81	28.26	1.657E-02
7	270.	25.15	28.83	1.694E-02
8	300.	25.80	29.42	1.706E-02
9	330.	26.26	29.99	1.799E-02
10	360.	26.81	30.66	1.997E-02
11	390.	27.29	31.39	2.185E-02
12	420.	28.08	32.31	2.479E-02
13	450.	28.88	33.39	2.892E-02
14	470.	29.44	34.32	2.908E-02
15	490.	30.04	35.24	2.942E-02
16	510.	30.86	36.20	3.039E-02
17	530.	31.20	37.18	3.206E-02
18	550.	31.85	38.25	3.453E-02
19	570.	32.56	39.49	3.811E-02
20	590.	33.42	41.16	4.503E-02
21	605.	34.11	42.65	4.915E-02
22	620.	34.80	44.41	5.363E-02
23	630.	35.49	45.74	5.633E-02
24	640.	35.99	47.22	6.156E-02
25	650.	36.61	49.02	6.288E-02
26	660.	37.23	50.84	6.541E-02
27	670.	38.09	53.00	7.127E-02
28	676.	38.24	54.45	7.277E-02
29	682.	38.80	55.96	8.072E-02
30	688.	39.35	57.65	8.628E-02
31	694.	39.73	59.91	1.006E-01
32	700.	40.51	62.43	1.119E-01
33	706.	41.10	65.56	1.324E-01
34	711.	41.83	69.05	1.549E-01
35	714.	42.26	71.35	1.776E-01
36	717.	42.85		
37	720.	43.45		
38	723.	44.20		

1000679AF PWA 1073 1350F AIR 10 CPM
R= 0.50 THICKNESS= 6.350 MM
PMAX= 4.395 KN WIDTH=63.605 MM
COMPACT SPECIMEN

NO.	CYCLES	A(MM)	DEL K (MPA√M)	DA/DN (MM/CYCLE)
1	425.	26.46		
2	475.	26.82	10.52	7.315E-03
3	565.	27.74	10.80	1.023E-02
4	645.	28.67	11.22	1.159E-02
5	685.	29.46	11.63	1.969E-02
6	725.	30.83	12.19	3.435E-02
7	745.	31.17	12.67	1.664E-02
8	765.	31.59	12.89	2.102E-02
9	785.	32.78	13.38	5.975E-02
10	800.	33.59	14.05	5.385E-02
11	815.	34.91	14.82	8.839E-02
12	830.	36.75	16.13	1.221E-01
13	835.	37.26	17.25	1.019E-01
14	840.	38.15	17.99	1.786E-01
15	845.	38.94	18.96	1.580E-01
16	850.	39.93	20.09	1.989E-01
17	855.	41.32	21.79	2.776E-01
18	862.	42.65	24.02	1.894E-01
19	864.	43.27	25.85	3.124E-01
20	866.	43.91	27.15	3.181E-01

7AN0680AF PWA 1073 1200F AIR MIX
R= 0.50 THICKNESS= 6.375 MM
PMAX= 5.827 KN WIDTH=63.754 MM
COMPACT SPECIMEN

NO.	CYCLES	A(MM)	DEL K (MPA√M)	DA/DN (MM/CYCLE)
1	150.	22.49		
2	225.	22.60		
3	425.	23.04		
4	625.	23.41	12.23	1.960E-03
5	825.	23.81	12.41	1.991E-03
6	1025.	24.12	12.60	2.025E-03
7	1250.	24.70	12.82	2.144E-03
8	1475.	25.11	13.07	2.234E-03
9	1700.	25.65	13.34	2.324E-03
10	1925.	26.23	13.62	2.373E-03
11	2150.	26.72	13.92	2.474E-03
12	2375.	27.28	14.24	2.559E-03
13	2600.	27.88	14.58	2.691E-03
14	2825.	28.47	14.96	2.858E-03
15	3050.	29.15	15.39	3.031E-03
16	3275.	29.87	15.86	3.252E-03
17	3475.	30.49	16.32	3.555E-03
18	3675.	31.20	16.87	3.766E-03
19	3850.	31.90	17.41	3.961E-03
20	4025.	32.72	18.02	4.136E-03
21	4150.	33.13	18.49	4.276E-03
22	4275.	33.68	18.99	4.440E-03
23	4400.	34.24	19.51	4.627E-03
24	4525.	34.84	20.14	5.024E-03
25	4650.	35.48	20.84	5.385E-03
26	4775.	36.16	21.66	5.865E-03
27	4900.	36.93	22.62	6.387E-03
28	5000.	37.57	23.52	6.895E-03
29	5100.	38.31	24.57	7.578E-03
30	5175.	38.85	25.47	8.262E-03
31	5250.	39.48	26.55	9.079E-03
32	5325.	40.19	27.80	1.042E-02
33	5385.	40.83	29.04	1.251E-02
34	5445.	41.50	30.68	1.586E-02
35	5495.	42.29	32.56	1.972E-02
36	5530.	43.10		
37	5550.	43.70		
38	5570.	44.08		

1000681AF PWA 1073 1350F AIR 10 CPM
R= 0.50 THICKNESS= 6.401 MM
PMAX= 4.381 KN WIDTH=63.896 MM
COMPACT SPECIMEN

NO.	CYCLES	A(MM)	DEL K (MPA√M)	DA/DN (MM/CYCLE)
1	0.	22.19		
2	15.	22.24	8.74	3.302E-03
3	100.	22.61	8.81	4.436E-03
4	185.	22.97	8.92	4.228E-03
5	270.	23.55	9.08	6.858E-03
6	355.	23.80	9.22	2.943E-03
7	450.	24.36	9.36	5.842E-03
8	545.	25.13	9.60	8.128E-03
9	620.	25.83	9.88	9.279E-03
10	695.	26.09	10.06	3.471E-03
11	770.	26.34	10.16	3.302E-03
12	845.	26.91	10.33	7.654E-03
13	920.	27.46	10.57	7.366E-03
14	1055.	28.72	10.97	9.351E-03
15	1130.	29.68	11.50	1.280E-02
16	1190.	30.03	11.82	5.673E-03
17	1265.	30.59	12.06	7.506E-03
18	1330.	31.27	12.40	1.036E-02
19	1395.	31.76	12.73	7.561E-03
20	1456.	32.56	13.12	1.318E-02
21	1521.	34.02	13.85	2.243E-02
22	1556.	34.41	14.51	1.118E-02
23	1590.	34.98	14.88	1.685E-02
24	1625.	35.69	15.39	2.010E-02
25	1655.	36.34	15.98	2.189E-02
26	1685.	37.03	16.59	2.295E-02
27	1715.	37.66	17.25	2.095E-02
28	1745.	38.50	18.03	2.798E-02
29	1775.	39.11	18.87	2.040E-02
30	1805.	39.94	19.76	2.747E-02
31	1835.	40.68	20.83	2.476E-02
32	1855.	41.37	21.89	3.429E-02
33	1870.	41.95	22.91	3.912E-02
34	1885.	42.63	23.99	4.487E-02
35	1895.	43.12	25.06	4.915E-02
36	1905.	43.59	26.01	4.763E-02

APPENDIX C. CRACK PROPAGATION DATA FOR SPECIMENS TESTED (Continued)

1000682AF PWA 1073 1300F AIR 10 CPM
R= 0.10 THICKNESS= 6.426 MM
PMAX= 5.951 KN WIDTH=63.645 MM
COMPACT SPECIMEN

NO.	CYCLES	A(MM)	DEL K (MPA√M)	DA/DN (MM/CYCLE)
1	300.	22.61		
2	700.	23.03	21.89	1.032E-03
3	1200.	23.52	22.26	9.881E-04
4	1720.	24.01	22.67	9.378E-04
5	2200.	24.55	23.12	1.130E-03
6	2660.	25.05	23.58	1.077E-03
7	3130.	25.66	24.10	1.316E-03
8	3620.	26.30	24.70	1.301E-03
9	4060.	26.85	25.29	1.244E-03
10	4500.	27.55	25.94	1.588E-03
11	4870.	28.17	26.66	1.696E-03
12	5230.	28.76	27.34	1.630E-03
13	5580.	29.48	28.11	2.043E-03
14	5900.	30.40	29.13	2.889E-03
15	6150.	30.77	29.97	1.458E-03
16	6500.	31.52	30.74	2.159E-03
17	6750.	32.13	31.73	2.428E-03
18	7030.	32.92	32.80	2.812E-03
19	7200.	33.49	33.91	3.399E-03
20	7350.	34.00	34.84	3.361E-03
21	7500.	34.45	35.70	3.023E-03
22	7650.	34.94	36.59	3.260E-03
23	7800.	35.54	37.68	4.030E-03
24	7950.	36.16	38.97	4.115E-03
25	8090.	36.79	40.37	4.508E-03
26	8230.	37.45	41.92	4.690E-03
27	8330.	37.81	43.23	3.645E-03
28	8450.	38.63	44.83	6.784E-03
29	8550.	39.05	46.63	4.255E-03
30	8700.	39.88	48.59	5.537E-03
31	8800.	40.53	51.07	6.452E-03
32	8880.	41.16	53.40	7.906E-03
33	8930.	41.60	55.47	8.712E-03
34	9040.	42.30	57.83	6.385E-03
35	9140.	43.15	61.30	8.509E-03
36	9190.	43.42	64.01	5.385E-03

7AN0685AF PWA 1073 1200F AIR 10 CPM
R= 0.10 THICKNESS=22.098 MM
PMAX= 15.657 KN WIDTH=63.688 MM
COMPACT SPECIMEN

NO.	CYCLES	A(MM)	DEL K (MPA√M)	DA/DN (MM/CYCLE)
1	1400.	20.99		
2	2600.	21.34		
3	3800.	21.75		
4	5000.	22.10	16.29	3.056E-04
5	6500.	22.52	16.56	3.115E-04
6	8000.	22.98	16.84	3.220E-04
7	9760.	23.58	17.20	3.473E-04
8	11850.	24.31	17.70	3.819E-04
9	13000.	25.10	18.24	4.221E-04
10	15100.	25.66	18.63	4.656E-04
11	16400.	26.24	19.09	5.115E-04
12	17760.	26.95	19.65	5.678E-04
13	19100.	27.80	20.30	6.476E-04
14	19990.	28.36	20.81	7.218E-04
15	20830.	28.94	21.36	8.031E-04
16	21700.	29.68	22.01	9.059E-04
17	22300.	30.28	22.57	9.849E-04
18	23500.	31.49	23.93	1.139E-03
19	24130.	32.34	24.78	1.224E-03
20	24500.	32.74	25.33	1.297E-03
21	24940.	33.29	26.06	1.386E-03
22	25300.	33.81	26.70	1.449E-03
23	25700.	34.44	27.55	1.593E-03
24	26170.	35.19	28.72	1.762E-03
25	26450.	35.67	29.52	1.860E-03
26	26730.	36.25	30.42	1.940E-03
27	27000.	36.79	31.38	2.059E-03
28	27270.	37.35	32.43	2.205E-03
29	27540.	37.90	33.59	2.400E-03
30	27870.	38.72	35.39	2.689E-03
31	28120.	39.44	37.04	2.971E-03
32	28300.	40.06	38.45	3.222E-03
33	28490.	40.58	40.17	3.439E-03
34	28680.	41.29	42.10	3.782E-03
35	28880.	41.79	43.52	3.915E-03
36	28920.	42.22	45.14	4.245E-03
37	29050.	42.85		
38	29160.	43.25		
39	29200.	43.94		

1000687AF PWA 1073 1200F AIR 10NOWL
R= 0.10 THICKNESS=21.742 MM
PMAX= 17.792 KN WIDTH=63.754 MM
COMPACT SPECIMEN

NO.	CYCLES	A(MM)	DEL K (MPA√M)	DA/DN (MM/CYCLE)
1	1300.	24.59		
2	1400.	25.09		
3	1500.	25.62		
4	1600.	26.10	21.92	5.185E-03
5	1700.	26.65	22.36	5.445E-03
6	1800.	27.29	22.87	5.477E-03
7	1900.	27.61	23.40	5.517E-03
8	2000.	28.45	23.92	5.938E-03
9	2070.	28.68	24.34	6.064E-03
10	2160.	29.19	24.93	6.799E-03
11	2250.	29.98	25.57	7.264E-03
12	2335.	30.45	26.33	8.448E-03
13	2430.	31.56	27.59	9.844E-03
14	2570.	32.76	29.26	1.159E-02
15	2632.	33.60	30.39	1.200E-02
16	2675.	34.10	31.25	1.393E-02
17	2700.	34.40	31.80	1.505E-02
18	2750.	35.25	33.07	1.779E-02
19	2786.	35.81	34.20	2.177E-02
20	2820.	36.58	35.65	2.790E-02
21	2845.	37.28	37.33	3.403E-02
22	2865.	38.00	39.03	4.181E-02
23	2880.	38.75	40.65	4.673E-02
24	2890.	39.21	41.95	5.265E-02
25	2901.	39.80	43.65	5.840E-02
26	2911.	40.29	45.33	6.562E-02
27	2921.	41.11	47.61	7.772E-02
28	2929.	41.66	49.26	9.043E-02
29	2935.	42.22	50.81	1.017E-01
30	2941.	42.90		
31	2945.	43.37		
32	2950.	44.01		

7AN0703 PWA 1073 1200F AIR 20 HZ
R= 0.05 THICKNESS= 6.325 MM
PMAX= 3.594 KN WIDTH=63.538 MM
COMPACT SPECIMEN

NO.	CYCLES	A(MM)	DEL K (MPA√M)	DA/DN (MM/CYCLE)
1	0.	21.73		
2	29000.	24.68		
3	33000.	25.21		
4	37000.	25.60	15.80	1.099E-04
5	41000.	26.01	16.13	1.096E-04
6	50500.	27.09	16.77	9.210E-05
7	55100.	27.63	16.96	1.246E-04
8	59500.	27.65	17.35	1.439E-04
9	64000.	28.15	17.83	1.462E-04
10	71000.	30.12	18.79	1.595E-04
11	74100.	30.62	19.35	1.594E-04
12	78000.	30.91	20.00	1.473E-04
13	83000.	31.57	20.34	1.359E-04
14	87000.	32.06	20.87	1.500E-04
15	91000.	32.69	21.56	1.679E-04
16	94000.	33.32	22.10	1.780E-04
17	97000.	33.78	22.73	1.949E-04
18	100000.	34.39	23.44	2.100E-04
19	103000.	35.01	24.23	2.297E-04
20	106000.	35.77	25.22	2.585E-04
21	109000.	36.53	26.40	2.899E-04
22	111000.	37.16	27.33	3.287E-04
23	113000.	37.80	28.43	3.739E-04
24	115000.	38.50	29.84	4.261E-04
25	117000.	39.49	31.63	5.000E-04
26	119000.	40.53	34.03	6.229E-04
27	120000.	41.08	35.60	6.811E-04
28	121000.	41.81	37.42	7.736E-04
29	122000.	42.76	39.76	8.332E-04
30	122500.	43.03	41.16	9.035E-04
31	123000.	43.60		
32	123400.	43.82		
33	123800.	44.42		

7AN0730 PWA 1007 1200F AIR 20 CPM
R= 0.05 THICKNESS=11.354 MM
PMAX= 14.935 KN WIDTH=63.586 MM
COMPACT SPECIMEN

NO.	CYCLES	A(MM)	DEL K (MPA√M)	DA/DN (MM/CYCLE)
1	0.	21.52		
2	1160.	21.86		
3	2400.	22.55		
4	3600.	23.13	33.31	5.003E-04
5	4800.	23.68	34.13	5.293E-04
6	6500.	24.68	35.33	5.546E-04
7	7310.	25.15	35.96	5.699E-04
8	8390.	25.70	36.88	5.852E-04
9	9420.	26.35	37.73	6.263E-04
10	10230.	26.85	38.51	6.812E-04
11	11000.	27.30	39.38	7.239E-04
12	11850.	28.03	40.43	7.689E-04
13	12520.	28.61	41.39	7.644E-04
14	13100.	29.01	42.20	7.868E-04
15	13860.	29.66	43.22	7.954E-04
16	14500.	30.00	44.15	8.250E-04
17	15500.	30.89	45.88	9.333E-04
18	16200.	31.64	47.30	1.022E-03
19	17040.	32.50	49.45	1.109E-03
20	17600.	33.17	51.02	1.163E-03
21	18000.	33.66	52.21	1.245E-03
22	18400.	34.09	53.58	1.312E-03
23	18800.	34.63	55.12	1.335E-03
24	19200.	35.28	56.67	1.480E-03
25	19600.	35.84	58.64	1.610E-03
26	20000.	36.31	60.83	1.777E-03
27	20400.	37.31	63.51	1.865E-03
28	20600.	37.57	65.08	1.916E-03
29	20900.	38.27	67.59	2.002E-03
30	21200.	38.73	69.76	2.427E-03
31	21540.	39.46	74.07	3.335E-03
32	21740.	40.10	77.54	4.816E-03
33	21880.	41.03	81.58	6.559E-03
34	21930.	41.26		
35	22000.	41.88		
36	22060.	42.42		

1000731 PWA 1007 1200F AIR 15NDNL
R= 0.05 THICKNESS=10.592 MM
PMAX= 15.386 KN WIDTH=63.673 MM
COMPACT SPECIMEN

NO.	CYCLES	A(MM)	DEL K (MPA√M)	DA/DN (MM/CYCLE)
1	0.	19.74		
2	3.	19.77	32.54	7.197E-03
3	30.	19.84	32.59	2.369E-03
4	130.	19.93	32.70	1.321E-03
5	330.	20.47	33.03	2.491E-03
6	530.	20.69	33.41	1.111E-03
7	800.	21.43	33.98	2.916E-03
8	1050.	22.15	34.85	2.713E-03
9	1300.	22.96	35.78	3.231E-03
10	1500.	23.47	36.65	2.521E-03
11	1790.	24.01	37.37	2.711E-03
12	1900.	24.93	38.43	4.622E-03
13	2100.	25.55	39.59	3.111E-03
14	2300.	26.22	40.61	3.303E-03
15	2475.	27.10	41.83	5.086E-03
16	2595.	27.77	43.23	5.567E-03
17	2715.	28.67	44.65	7.451E-03
18	2815.	29.23	46.02	5.335E-03
19	2915.	30.07	47.44	8.699E-03
20	2990.	31.00	49.44	1.339E-02
21	3025.	31.52	51.09	1.266E-02
22	3060.	31.68	51.80	4.663E-03
23	3100.	32.17	52.59	1.232E-02
24	3140.	32.65	53.62	1.197E-02
25	3180.	33.18	55.15	1.333E-02
26	3220.	33.75	56.69	1.406E-02
27	3260.	34.60	58.75	2.101E-02
28	3290.	34.93	60.67	1.253E-02
29	3320.	35.92	62.25	3.133E-02
30	3340.	36.17	64.97	1.257E-02
31	3365.	36.93	66.87	3.032E-02
32	3385.	38.00	70.75	5.721E-02
33	3395.	39.02	75.47	9.411E-02
34	3400.	39.69	79.53	1.351E-01
35	3405.	40.23	82.81	1.067E-01
36	3410.	40.60	85.43	7.518E-02
37	3415.	41.56	89.53	1.913E-01
38	3417.	41.93	93.92	1.841E-01
39	3419.	42.73	98.28	4.000E-01

APPENDIX C. CRACK PROPAGATION DATA FOR SPECIMENS TESTED (Continued)

7AN0732 PWA 1007 1200F AIR 15MDWL
R= 0.05 THICKNESS=10.719 MM
PMAX= 11.102 KN WIDTH=63.741 MM
COMPACT SPECIMEN

NO.	CYCLES	A(MM)	DEL K (MPA√M)	DA/DN (MM/CYCLE)
1	100.	23.19		
2	250.	23.24		
3	500.	23.32		
4	750.	23.50	26.36	4.282E-04
5	1054.	23.57	26.54	5.242E-04
6	1514.	23.74	26.84	6.047E-04
7	2060.	24.36	27.19	6.271E-04
8	2600.	24.59	27.52	6.578E-04
9	3600.	25.20	28.25	6.821E-04
10	4400.	25.73	28.77	6.814E-04
11	6482.	27.33		
12	7099.	27.72		
13	7553.	28.43		

7AN0732A PWA 1007 1200F AIR 15MDWL
R= 0.05 THICKNESS=10.719 MM
PMAX= 14.336 KN WIDTH=63.741 MM
COMPACT SPECIMEN

NO.	CYCLES	A(MM)	DEL K (MPA√M)	DA/DN (MM/CYCLE)
1	0.	28.43		
2	75.	28.95		
3	253.	30.47		
4	315.	30.82	46.21	7.634E-03
5	390.	31.46	47.27	8.028E-03
6	457.	31.92	48.45	9.573E-03
7	517.	32.36	49.73	1.063E-02
8	567.	33.01	51.16	1.215E-02
9	618.	33.95	52.99	1.330E-02
10	660.	34.26	54.55	1.508E-02
11	711.	35.15	56.79	1.694E-02
12	751.	35.63	58.67	1.932E-02
13	822.	37.24	64.37	2.755E-02
14	847.	37.91	67.03	3.429E-02
15	864.	38.58	69.67	4.150E-02
16	882.	39.28	72.91	5.106E-02
17	900.	40.11	77.82	6.652E-02
18	912.	41.09	82.46	8.438E-02
19	918.	41.63	85.62	1.144E-01
20	924.	42.19		
21	930.	42.87		
22	934.	44.15		

7AN0736 PWA 1007 1200F AIR 20 HZ
R= 0.05 THICKNESS=10.973 MM
PMAX= 7.210 KN WIDTH=63.551 MM
COMPACT SPECIMEN

NO.	CYCLES	A(MM)	DEL K (MPA√M)	DA/DN (MM/CYCLE)
1	0.	27.19		
2	3500.	27.71		
3	12700.	28.61		
4	18600.	29.12	21.18	1.060E-04
5	25000.	29.89	21.80	1.074E-04
6	28630.	30.25	22.17	1.126E-04
7	32800.	30.75	22.65	1.196E-04
8	39300.	31.44	23.46	1.276E-04
9	49300.	32.85	25.06	1.531E-04
10	52300.	33.40	25.65	1.606E-04
11	55300.	33.80	26.30	1.720E-04
12	58300.	34.36	26.96	1.816E-04
13	64700.	35.53	28.83	2.180E-04
14	68200.	36.33	30.17	2.436E-04
15	71200.	37.22	31.53	2.652E-04
16	73200.	37.63	32.62	2.745E-04
17	75200.	38.26	33.77	2.946E-04
18	77000.	38.77	34.83	3.125E-04
19	78800.	39.29	36.27	3.398E-04
20	80600.	39.99	37.75	3.764E-04
21	82600.	40.75	39.89	4.262E-04
22	84000.	41.29	41.67	4.732E-04
23	86400.	42.58	45.60	5.787E-04
24	86890.	42.81		
25	88000.	43.54		
26	89010.	44.25		

APPENDIX C. CRACK PROPAGATION DATA FOR SPECIMENS TESTED (Continued)

7AN0737 PWA 1007 1200F AIR 2 MDWL
R= 0.05 THICKNESS= 8.026 MM
PMAX= 8.660 KN WIDTH=63.716 MM
COMPACT SPECIMEN

NO.	CYCLES	A(MM)	DEL K (MPA√M)	DA/DN (MM/CYCLE)
1	0.	21.31		
2	505.	21.57		
3	1511.	21.95		
4	2600.	22.22	27.12	4.862E-04
5	3222.	22.88	27.40	5.651E-04
6	3873.	23.13	27.82	5.618E-04
7	4528.	23.41	28.27	5.878E-04
8	5200.	24.10	28.61	5.702E-04
9	5823.	24.16	29.03	6.050E-04
10	6600.	24.66	29.56	6.339E-04
11	7350.	25.27	30.04	6.917E-04
12	8050.	25.67	30.69	8.357E-04
13	8750.	26.19	31.42	9.411E-04
14	9463.	27.00	32.32	1.042E-03
15	9960.	27.63	33.10	1.062E-03
16	10450.	28.15	33.89	1.092E-03
17	11016.	28.77	34.76	1.068E-03
18	11532.	29.21	35.51	1.099E-03
19	12012.	29.80	36.28	1.228E-03
20	12512.	30.31	37.23	1.414E-03
21	13214.	31.31	39.13	1.815E-03
22	13562.	32.17	40.32	2.068E-03
23	13962.	32.76	41.61	2.389E-03
24	14187.	33.48	43.35	2.555E-03
25	14412.	34.10	44.59	2.807E-03
26	14637.	34.93	46.15	3.091E-03
27	14812.	35.20	47.66	2.987E-03
28	15018.	36.07	49.29	3.260E-03
29	15162.	36.58	50.47	3.736E-03
30	15312.	36.70	52.25	4.361E-03
31	15462.	37.64	54.19	5.282E-03
32	15562.	38.30	55.99	6.431E-03
33	15666.	38.83	58.79	8.252E-03
34	15812.	39.97	63.85	1.109E-02
35	15882.	40.89	67.34	1.224E-02
36	15915.	41.66	69.49	1.435E-02
37	15941.	41.75	71.45	1.635E-02
38	15982.	42.08		
39	16032.	43.40		
40	16052.	44.04		

7AN0739 PWA 1007 1200F AIR 5 MDWL
R= 0.05 THICKNESS= 9.576 MM
PMAX= 13.602 KN WIDTH=63.602 MM
COMPACT SPECIMEN

NO.	CYCLES	A(MM)	DEL K (MPA√M)	DA/DN (MM/CYCLE)
1	223.	30.57		
2	232.	30.61		
3	260.	30.75		
4	310.	30.98	49.49	5.699E-03
5	345.	31.27	50.02	6.040E-03
6	382.	31.36	50.54	6.574E-03
7	442.	31.98	51.55	7.398E-03
8	475.	32.02	52.17	7.412E-03
9	515.	32.45	52.89	9.165E-03
10	557.	32.80	53.67	1.170E-02
11	592.	33.00	55.13	1.313E-02
12	633.	33.82	56.83	1.441E-02
13	673.	34.80	58.61	1.657E-02
14	730.	35.32	61.73	1.949E-02
15	780.	36.19	65.10	2.158E-02
16	832.	37.59	69.62	2.632E-02
17	870.	38.79	74.62	3.241E-02
18	905.	39.56	80.99	4.692E-02
19	931.	40.68		
20	951.	41.89		
21	961.	43.78		

7AN0793 PWA 1073 800F AIR 10 CPM
R= 0.0 THICKNESS= 7.569 MM
PMAX= 23.379 KN WIDTH=25.400 MM
CENTER CRACK SPECIMEN

NO.	CYCLES	A(MM)	DEL K (MPA√M)	DA/DN (MM/CYCLE)
1	32000.	3.74		
2	42000.	3.94		
3	52000.	4.12		
4	62000.	4.44	15.51	3.247E-05
5	72000.	4.81	16.33	3.961E-05
6	80000.	5.10	17.15	4.650E-05
7	90000.	5.60	18.33	5.766E-05
8	98000.	6.08	19.67	7.155E-05
9	102000.	6.37	20.50	8.055E-05
10	106000.	6.73	21.49	9.439E-05
11	110000.	7.10	22.77	1.204E-04
12	111041.	7.22	23.13	1.393E-04
13	113041.	7.50	24.09	1.648E-04
14	115041.	7.85	25.33	2.061E-04
15	117000.	8.45	28.27	3.296E-04
16	118600.	8.69		
17	119400.	9.03		
18	120200.	9.56		

APPENDIX C. CRACK PROPAGATION DATA FOR SPECIMENS TESTED (Continued)

7AN1000 PWA 1007 800F AIR 10 CPM
R= 0.05 THICKNESS= 2.642 MM
PMAX= 2.473 KN WIDTH=63.602 MM
COMPACT SPECIMEN

NO.	CYCLES	A(MM)	DEL K (MPA·√M)	DA/DN (MM/CYCLE)
1	0.	21.16		
2	6000.	21.25		
3	12100.	21.43		
4	24000.	21.68	22.51	3.156E-05
5	36000.	22.23	22.86	3.557E-05
6	48000.	22.71	23.22	3.915E-05
7	60000.	23.11	23.65	4.319E-05
8	72020.	23.59	24.09	4.679E-05
9	84000.	24.25	24.63	5.170E-05
10	93000.	24.73	25.11	5.554E-05
11	103000.	25.31	25.70	5.817E-05
12	113020.	25.91	26.29	6.111E-05
13	123000.	26.54	26.95	6.458E-05
14	131080.	26.99	27.57	6.197E-05
15	140000.	27.69	28.19	6.446E-05
16	148000.	28.25	28.79	6.710E-05
17	156090.	28.47	29.42	7.583E-05
18	164030.	29.27	30.16	8.377E-05
19	171060.	29.80	30.94	1.010E-04
20	178410.	30.72	32.13	1.178E-04
21	184000.	31.20	33.11	1.338E-04
22	189420.	32.18	34.32	1.464E-04
23	192150.	32.45	34.98	1.496E-04
24	194700.	32.94	35.73	1.431E-04
25	197200.	33.28	36.25	1.488E-04
26	199750.	33.65	36.90	1.645E-04
27	203350.	34.01	38.03	1.897E-04
28	206900.	34.95	39.62	2.073E-04
29	209900.	35.74	41.11	2.174E-04
30	212400.	36.35	42.55	2.300E-04
31	214400.	36.48	43.52	2.478E-04
32	217000.	37.20	45.19	2.534E-04
33	219090.	37.80	46.58	2.922E-04
34	221000.	38.60	48.62	3.142E-04
35	223100.	38.88	50.88	3.023E-04
36	225140.	40.00	52.98	2.939E-04
37	226590.	40.15	54.30	2.931E-04
38	228500.	40.61	56.44	3.331E-04
39	230460.	41.26	58.39	3.743E-04
40	233000.	42.10		
41	234500.	43.22		
42	236020.	44.24		

7AN1001 PWA 1007 1200F AIR 10 CPM
R= 0.05 THICKNESS= 2.578 MM
PMAX= 3.096 KN WIDTH=63.627 MM
COMPACT SPECIMEN

NO.	CYCLES	A(MM)	DEL K (MPA·√M)	DA/DN (MM/CYCLE)
1	3100.	36.41		
2	5750.	37.44		
3	7300.	38.21		
4	8300.	38.94	63.89	5.814E-04
5	9100.	39.47	66.00	6.240E-04
6	10100.	39.79	68.61	7.068E-04
7	11140.	40.70	72.06	8.074E-04
8	12110.	41.42	76.47	9.610E-04
9	13360.	42.88		
10	14000.	43.61		
11	14600.	44.40		

7AN1002 PWA 1007 800F AIR 10 CPM
R= 0.05 THICKNESS=12.675 MM
PMAX= 11.449 KN WIDTH=63.622 MM
COMPACT SPECIMEN

NO.	CYCLES	A(MM)	DEL K (MPA·√M)	DA/DN (MM/CYCLE)
1	7040.	22.09		
2	11040.	22.34		
3	16100.	22.93		
4	20110.	23.87	23.24	1.199E-04
5	24210.	24.09	23.65	1.316E-04
6	28090.	24.69	24.23	1.280E-04
7	32020.	25.13	24.78	1.266E-04
8	36060.	26.32	25.54	1.307E-04
9	40200.	26.81	26.37	1.150E-04
10	44900.	27.08	26.56	1.290E-04
11	50450.	27.44	26.93	1.183E-04
12	55020.	27.84	27.50	1.407E-04
13	61050.	28.94	28.71	1.810E-04
14	66000.	29.82	29.91	2.210E-04
15	69540.	30.63	30.72	2.337E-04
16	70200.	30.69	31.29	2.359E-04
17	72040.	31.43	32.03	2.427E-04
18	74500.	32.03	32.81	2.419E-04
19	76700.	32.37	33.70	2.639E-04
20	81300.	33.56	35.72	3.037E-04
21	82500.	34.03	36.37	3.144E-04
22	83800.	34.52	37.21	3.265E-04
23	85350.	34.93	38.29	3.559E-04
24	87010.	35.52	39.43	3.839E-04
25	88250.	36.19	41.12	4.907E-04
26	89600.	36.67	42.00	5.227E-04
27	90300.	36.99	42.93	5.800E-04
28	91300.	37.71	44.66	6.310E-04
29	92350.	38.26	46.64	6.157E-04
30	93000.	38.89	47.69	6.407E-04
31	93900.	39.35	49.58	6.521E-04
32	94600.	39.76	51.44	7.591E-04
33	95400.	40.49	53.69	8.151E-04
34	96220.	40.95	55.74	8.679E-04
35	96960.	41.64	58.29	8.994E-04
36	97400.	42.06	60.34	1.115E-03
37	97700.	42.33	61.76	1.033E-03
38	98150.	42.82		
39	98400.	43.07		
40	98750.	44.01		

7AN1003 PWA 1007 800F AIR 10 CPM
R= 0.05 THICKNESS= 7.696 MM
PMAX= 59.230 KN WIDTH=25.316 MM
CENTER CRACK SPECIMEN

NO.	CYCLES	A(MM)	DEL K (MPA·√M)	DA/DN (MM/CYCLE)
1	0.	1.61		
2	2000.	1.79		
3	5000.	2.11		
4	8000.	2.37	25.41	1.213E-04
5	11000.	2.73	27.60	1.460E-04
6	14000.	3.17	30.09	1.816E-04
7	17000.	3.83	33.27	2.404E-04
8	19000.	4.23	35.90	3.022E-04
9	21500.	4.97	40.39	4.600E-04
10	23500.	5.84		
11	24500.	6.51		
12	25500.	7.74		

7AN1004 PWA 1007 1200F AIR 10 CPM
R= 0.05 THICKNESS= 7.645 MM
PMAX= 51.210 KN WIDTH=25.359 MM
CENTER CRACK SPECIMEN

NO.	CYCLES	A(MM)	DEL K (MPA·√M)	DA/DN (MM/CYCLE)
1	0.	1.79		
2	4000.	2.64		
3	6000.	3.05		
4	7000.	3.32	27.11	3.302E-04
5	8000.	3.72	28.55	3.826E-04
6	9000.	4.18	30.53	4.402E-04
7	9800.	4.45	32.17	5.053E-04
8	11000.	5.11	35.22	6.301E-04
9	12000.	5.68	38.52	8.197E-04
10	13000.	6.57	43.93	1.151E-03
11	13500.	7.15		
12	14000.	7.87		
13	14200.	8.45		

1001005 PWA 1007 800F AIR 10 CPM
R= 0.50 THICKNESS= 7.620 MM
PMAX= 68.473 KN WIDTH=25.293 MM
CENTER CRACK SPECIMEN

NO.	CYCLES	A(MM)	DEL K (MPA·√M)	DA/DN (MM/CYCLE)
1	0.	2.59		
2	2000.	2.77	16.75	9.239E-05
3	3500.	2.88	17.25	7.112E-05
4	6000.	3.17	17.94	1.179E-04
5	8500.	3.50	18.99	1.321E-04
6	11000.	3.69	19.86	7.544E-05
7	13500.	4.10	20.84	1.610E-04
8	15500.	4.42	22.07	1.648E-04
9	17500.	4.68	23.06	1.267E-04
10	19500.	5.10	24.24	2.121E-04
11	21500.	5.52	25.75	2.086E-04
12	23500.	5.97	27.38	2.276E-04
13	25500.	6.69	29.75	3.597E-04
14	26500.	7.03	32.09	3.391E-04
15	27500.	7.49	34.01	4.534E-04

1001006 PWA 1007 1200F AIR 10 CPM
R= 0.55 THICKNESS= 7.290 MM
PMAX= 64.838 KN WIDTH=25.314 MM
CENTER CRACK SPECIMEN

NO.	CYCLES	A(MM)	DEL K (MPA·√M)	DA/DN (MM/CYCLE)
1	0.	1.62		
2	1000.	1.69	11.57	6.223E-05
3	5000.	2.19	12.57	1.264E-04
4	10500.	3.12	14.90	1.697E-04
5	13000.	3.65	17.12	2.103E-04
6	15500.	4.20	18.72	2.184E-04
7	18000.	5.01	20.77	3.244E-04
8	19500.	5.55	22.90	3.594E-04
9	21000.	6.17	24.87	4.191E-04
10	22300.	6.92	27.40	5.739E-04
11	23300.	7.70	30.62	7.817E-04

1001007 PWA 1007 800F AIR 10 CPM
R= 0.80 THICKNESS= 7.620 MM
PMAX= 83.075 KN WIDTH=25.372 MM
CENTER CRACK SPECIMEN

NO.	CYCLES	A(MM)	DEL K (MPA·√M)	DA/DN (MM/CYCLE)
1	1000.	1.69		
2	3000.	1.74	6.37	2.349E-05
3	10000.	1.87	6.55	1.930E-05
4	15000.	1.89	6.68	8.890E-07
5	20000.	1.97	6.77	1.854E-05
6	30000.	1.99	6.83	2.159E-06
7	40000.	2.16	7.06	1.740E-05
8	50000.	2.25	7.29	8.699E-06
9	60000.	2.46	7.55	2.064E-05
10	70000.	2.65	7.89	1.962E-05
11	80000.	2.85	8.22	1.981E-05
12	90000.	3.11	8.60	2.570E-05
13	100000.	3.30	8.96	1.867E-05
14	110000.	3.64	9.40	3.467E-05
15	120000.	3.87	9.86	2.242E-05
16	138900.	4.51	10.56	3.408E-05
17	148900.	4.96	11.46	4.515E-05
18	158000.	5.36	12.18	4.039E-05
19	168000.	5.81	12.94	4.413E-05
20	178000.	6.40	13.91	5.950E-05

APPENDIX C. CRACK PROPAGATION DATA FOR SPECIMENS TESTED (Continued)

7AN1008 PWA 1007 1200F AIR 10 CPM
R= 0.80 THICKNESS= 7.620 MM
PMAX= 80.344 KN WIDTH=25.298 MM
CENTER CRACK SPECIMEN

NO.	CYCLES	A(MM)	DEL K (MPA√M)	DA/DN (MM/CYCLE)
1	0.	1.62		
2	3000.	1.65		
3	5500.	1.72		
4	9000.	1.78	6.34	2.750E-05
5	19000.	2.17	7.02	4.238E-05
6	30000.	2.71	7.92	5.417E-05
7	35000.	3.05	8.38	6.094E-05
8	40000.	3.28	8.87	6.957E-05
9	45000.	3.64	9.42	7.667E-05
10	50000.	4.06	10.04	8.636E-05
11	54000.	4.47	10.64	9.527E-05
12	58000.	4.80	11.27	1.053E-04
13	63000.	5.37	12.15	1.251E-04
14	67000.	5.82		
15	71000.	6.44		
16	73500.	6.99		

1001009 PWA 1007 TMF AIR 1 CPM
R= 0.05 THICKNESS= 7.620 MM
PMAX= 57.598 KN WIDTH=25.311 MM
CENTER CRACK SPECIMEN

NO.	CYCLES	A(MM)	DEL K (MPA√M)	DA/DN (MM/CYCLE)
1	1600.	1.78		
2	2600.	1.93	21.94	1.448E-04
3	3600.	2.01	22.65	8.382E-05
4	4600.	2.14	23.28	1.251E-04
5	5600.	2.18	23.78	4.635E-05
6	6100.	2.23	24.04	8.255E-05
7	8000.	2.41	24.69	9.492E-05
8	10000.	2.59	25.72	9.144E-05
9	12000.	3.01	27.41	2.121E-04
10	14000.	3.36	29.51	1.753E-04
11	16000.	3.98	32.10	3.092E-04
12	17500.	4.54	35.26	3.746E-04
13	19000.	5.14	38.43	3.971E-04
14	20000.	5.77	41.96	6.344E-04
15	20800.	6.55	46.33	9.660E-04
16	21400.	7.24	51.45	1.161E-03

1001010 PWA 1007 1350F AIR 10 CPM
R= 0.05 THICKNESS= 7.645 MM
PMAX= 50.605 KN WIDTH=25.301 MM
CENTER CRACK SPECIMEN

NO.	CYCLES	A(MM)	DEL K (MPA√M)	DA/DN (MM/CYCLE)
1	0.	1.76		
2	3000.	2.55	20.81	2.616E-04
3	5500.	3.46	24.99	3.642E-04
4	7500.	4.48	29.52	5.109E-04
5	8000.	4.97	33.10	9.741E-04
6	8500.	5.44	35.43	9.487E-04
7	9000.	5.91	37.93	9.390E-04
8	9500.	6.49	40.83	1.154E-03
9	9900.	7.11	44.48	1.556E-03

1001011 PWA 1007 1350F AIR 10 CPM
R= 0.05 THICKNESS= 2.705 MM
PMAX= 2.277 KN WIDTH=63.337 MM
COMPACT SPECIMEN

NO.	CYCLES	A(MM)	DEL K (MPA√M)	DA/DN (MM/CYCLE)
1	500.	27.72		
2	1000.	27.84	25.74	2.286E-04
3	2330.	28.27	26.03	3.247E-04
4	4030.	28.96	26.66	4.086E-04
5	5030.	29.46	27.35	4.915E-04
6	5850.	29.87	27.90	5.095E-04
7	6600.	30.34	28.45	6.181E-04
8	7300.	30.70	28.98	5.189E-04
9	8060.	31.14	29.51	5.765E-04
10	8800.	31.48	30.05	4.634E-04
11	9650.	32.00	30.66	6.081E-04
12	10400.	32.16	31.16	2.184E-04
13	11200.	32.52	31.56	4.493E-04
14	12000.	33.25	32.41	9.160E-04
15	12500.	33.56	33.26	6.070E-04
16	13200.	34.04	33.93	6.912E-04
17	13900.	34.44	34.72	5.715E-04
18	14720.	34.99	35.60	6.691E-04
19	15610.	35.47	36.61	5.408E-04
20	16400.	35.77	37.41	3.794E-04
21	17200.	36.39	38.40	7.779E-04
22	18100.	36.72	39.47	3.627E-04
23	18910.	37.12	40.33	4.907E-04
24	19550.	37.64	41.46	8.136E-04
25	20100.	38.07	42.69	7.805E-04
26	20670.	38.35	43.66	4.991E-04
27	21750.	38.94	44.89	5.421E-04
28	22750.	39.76	47.02	8.217E-04
29	23590.	40.23	49.14	5.624E-04
30	24410.	41.06	51.43	1.013E-03
31	25020.	41.79	54.41	9.000E-04
32	26000.	42.46	57.30	8.515E-04
33	26700.	43.15	60.35	9.906E-04
34	27400.	44.12	64.44	1.389E-03
35	27800.	44.37	67.69	6.319E-04

7AN1013 PWA 1007 1200F AIR 10 CPM
R= 0.10 THICKNESS= 8.064 MM
PMAX= 5.609 KN WIDTH=63.094 MM
COMPACT SPECIMEN

NO.	CYCLES	A(MM)	DEL K (MPA√M)	DA/DN (MM/CYCLE)
1	0.	24.61		
2	2000.	24.93		
3	4540.	25.65		
4	6800.	25.96	18.78	1.631E-04
5	10800.	26.61	19.27	1.873E-04
6	13820.	27.07	19.71	1.920E-04
7	16960.	27.72	20.23	2.224E-04
8	20000.	28.62	20.83	2.572E-04
9	23000.	29.11	21.64	2.714E-04
10	26000.	30.21	22.47	2.861E-04
11	27690.	30.84	22.97	2.908E-04
12	31080.	31.57	24.13	3.115E-04
13	34130.	32.62	25.16	3.357E-04
14	36500.	33.35	26.19	3.981E-04
15	38410.	34.09	27.30	4.488E-04
16	39500.	34.65	27.99	4.938E-04
17	40640.	35.33	28.93	5.119E-04
18	41600.	35.74	29.82	5.285E-04
19	42630.	36.39	30.74	5.461E-04
20	43600.	36.80	31.69	5.618E-04
21	44680.	37.41	32.95	5.876E-04
22	45700.	38.13	34.08	6.818E-04
23	46710.	38.76	35.72	7.906E-04
24	47700.	39.31	37.78	8.644E-04
25	48700.	40.69	40.28	9.575E-04
26	50000.	41.99	44.52	1.080E-03
27	50500.	42.23		
28	51500.	43.53		
29	52000.	44.19		

1001014 PWA 1007 800F AIR 10 CPM
R= 0.05 THICKNESS= 7.620 MM
PMAX= 4.853 KN WIDTH=63.165 MM
COMPACT SPECIMEN

NO.	CYCLES	A(MM)	DEL K (MPA√M)	DA/DN (MM/CYCLE)
1	0.	26.84		
2	1500.	26.88	18.79	2.794E-05
3	8540.	27.19	18.93	4.402E-05
4	16070.	27.37	19.12	2.429E-05
5	26000.	28.00	19.45	6.382E-05
6	35000.	28.61	19.96	6.689E-05
7	43500.	28.98	20.38	4.348E-05
8	53330.	29.24	20.66	2.606E-05
9	63280.	30.00	21.13	7.983E-05
10	71750.	30.50	21.73	5.878E-05
11	80200.	31.03	22.25	6.328E-05

1001015 PWA 1007 1350F AIR 2 MDWL
R= 0.10 THICKNESS= 7.620 MM
PMAX= 8.883 KN WIDTH=63.602 MM
COMPACT SPECIMEN

NO.	CYCLES	A(MM)	DEL K (MPA√M)	DA/DN (MM/CYCLE)
1	604.	28.59		
2	1200.	28.82	34.83	3.793E-04
3	2016.	29.19	35.27	4.576E-04
4	3000.	29.75	35.98	5.627E-04
5	3900.	30.04	36.66	3.316E-04

7AN1017 PWA 1007 1200F AIR 20 HZ
R= 0.80 THICKNESS= 7.620 MM
PMAX= 9.528 KN WIDTH=63.576 MM
COMPACT SPECIMEN

NO.	CYCLES	A(MM)	DEL K (MPA√M)	DA/DN (MM/CYCLE)
1	0.	24.39		
2	57920.	25.17		
3	100000.	26.23		
4	125000.	26.59	7.61	1.995E-05
5	155000.	27.09	7.81	2.114E-05
6	189000.	27.87	8.03	2.231E-05
7	210000.	28.44	8.21	2.140E-05
8	230000.	28.87	8.37	2.179E-05
9	250000.	29.33	8.51	2.140E-05
10	293570.	30.16	8.83	2.352E-05
11	318000.	30.59	9.06	2.517E-05
12	338000.	31.29	9.28	2.701E-05
13	356000.	31.76	9.52	2.769E-05
14	373000.	32.20	9.74	2.794E-05
15	392000.	32.80	9.97	2.767E-05
16	411000.	33.20	10.23	2.886E-05
17	432000.	33.64	10.55	3.099E-05
18	450000.	34.44	10.87	3.239E-05
19	466000.	34.96	11.19	3.408E-05
20	480000.	35.50	11.50	3.425E-05
21	495000.	35.97	11.80	3.768E-05
22	510300.	36.55	12.19	4.204E-05
23	525000.	36.99	12.66	4.443E-05
24	540000.	38.00	13.23	4.689E-05
25	559000.	38.51	13.62	5.619E-05
26	560000.	38.78	14.14	6.403E-05
27	570250.	39.33	14.72	6.957E-05
28	580000.	40.48	15.46	8.312E-05
29	585000.	40.83		
30	596300.	41.67		
31	606000.	42.93		

APPENDIX C. CRACK PROPAGATION DATA FOR SPECIMENS TESTED (Continued)

7AN1018 PWA 1007 800F AIR 10 CPM
R= 0.05 THICKNESS= 7.556 MM
PMAX= 6.303 KN WIDTH=63.635 MM
COMPACT SPECIMEN

NO.	CYCLES	A(MM)	DEL K (MPA$\sqrt{M}$)	DA/DN (MM/CYCLE)
1	0.	25.74		
2	1355.	25.87		
3	3353.	26.22		
4	5400.	26.30	23.87	1.351E-04
5	10088.	26.99	24.62	1.484E-04
6	14140.	27.97	25.27	1.346E-04
7	17116.	28.25	25.71	1.314E-04
8	20000.	28.47	26.07	1.327E-04
9	23207.	28.77	26.41	1.284E-04
10	26220.	29.25	26.90	1.463E-04
11	29210.	29.82	27.52	1.594E-04
12	32420.	30.31	28.19	1.709E-04
13	35745.	30.92	28.95	1.706E-04
14	43347.	32.17	30.71	1.602E-04
15	47000.	32.87	31.55	1.950E-04
16	49500.	33.12	32.30	2.123E-04
17	52036.	33.51	33.08	2.409E-04
18	55000.	34.69	34.38	2.747E-04
19	56540.	34.91	35.29	2.804E-04
20	58070.	35.45	36.24	2.625E-04
21	59532.	35.76	36.89	2.461E-04
22	61000.	36.22	37.64	2.668E-04
23	62517.	36.41	38.39	2.857E-04
24	64000.	36.87	39.42	3.199E-04
25	65500.	37.46	40.60	3.582E-04
26	69700.	39.31	45.62	4.724E-04
27	71250.	39.98	48.04	4.795E-04
28	72500.	40.73	50.19	6.185E-04
29	73500.	41.18	52.03	7.119E-04
30	74800.	41.77	55.81	9.057E-04
31	75800.	43.37		
32	76114.	43.53		
33	76710.	44.15		

7AN1019 PWA 1007 1200F AIR 10 CPM
R= 0.50 THICKNESS= 7.595 MM
PMAX= 6.316 KN WIDTH=63.660 MM
COMPACT SPECIMEN

NO.	CYCLES	A(MM)	DEL K (MPA$\sqrt{M}$)	DA/DN (MM/CYCLE)
1	2200.	25.82		
2	6200.	29.00		
3	7700.	30.50		
4	8700.	31.30	15.51	1.079E-03
5	9700.	32.42	16.28	1.272E-03
6	10800.	33.48	17.44	1.687E-03
7	11500.	35.01	18.58	1.955E-03
8	11700.	35.64	18.96	1.891E-03
9	12000.	36.22	19.70	2.061E-03
10	12300.	36.56	20.30	2.023E-03
11	12700.	37.31	21.15	2.551E-03
12	13100.	38.42	22.63	3.521E-03
13	13350.	39.11	24.05	3.962E-03
14	13550.	40.51	25.47	4.356E-03
15	13650.	40.75	26.35	4.595E-03
16	13350.	41.50	28.19	5.417E-03
17	14050.	42.63		
18	14150.	43.18		
19	14250.	44.37		

7AN1021 PWA 1007 1200F AIR 10 CPM
R= 0.50 THICKNESS= 7.658 MM
PMAX= 5.911 KN WIDTH=63.612 MM
COMPACT SPECIMEN

NO.	CYCLES	A(MM)	DEL K (MPA$\sqrt{M}$)	DA/DN (MM/CYCLE)
1	2600.	25.29		
2	3400.	25.95		
3	4000.	26.39		
4	4600.	26.82	11.99	1.613E-03
5	5600.	28.91	12.99	2.257E-03
6	6100.	30.80	13.74	2.624E-03
7	6600.	31.74	14.68	2.774E-03
8	6850.	32.11	15.18	3.293E-03
9	7100.	33.35	15.70	4.101E-03
10	7275.	33.73	16.25	4.878E-03
11	7575.	35.38	17.76	5.608E-03
12	7675.	36.29	18.33	5.971E-03
13	7750.	36.80	18.88	5.554E-03
14	7825.	36.90	19.34	6.001E-03
15	7925.	37.58	19.90	6.124E-03
16	8025.	38.00	20.64	7.966E-03
17	8125.	39.03	21.92	9.117E-03
18	8200.	39.73	23.03	8.724E-03
19	8260.	40.71	24.02	9.055E-03
20	8320.	40.86	24.92	8.895E-03
21	8380.	41.17	25.73	9.611E-03
22	8440.	41.98	26.69	1.064E-02
23	8490.	42.42		
24	8540.	43.27		
25	8590.	43.87		

1001022 PWA 1007 1200F AIR 10 CPM
R= 0.50 THICKNESS= 7.607 MM
PMAX= 5.507 KN WIDTH=63.500 MM
COMPACT SPECIMEN

NO.	CYCLES	A(MM)	DEL K (MPA√M)	DA/DN (MM/CYCLE)
1	2706.	27.24		
2	5000.	27.52		
3	7000.	28.00		
4	8599.	28.69	12.04	4.229E-04
5	9812.	29.31	12.34	4.884E-04
6	10830.	29.94	12.64	5.239E-04
7	11889.	30.26	12.96	5.606E-04
8	13134.	31.18	13.39	5.902E-04
9	13960.	31.56	13.68	6.558E-04
10	14786.	32.19	14.08	6.878E-04
11	15611.	32.64	14.46	7.098E-04
12	16436.	33.49	14.90	7.825E-04
13	17133.	33.81	15.31	8.299E-04
14	18213.	34.75	16.10	8.863E-04
15	18828.	35.46	16.57	9.008E-04
16	19414.	36.02	17.08	1.011E-03
17	20000.	36.44	17.62	1.098E-03
18	20600.	37.03	18.25	1.233E-03
19	21684.	38.53	20.08	1.603E-03
20	22100.	39.42	21.05	1.749E-03
21	22500.	40.22	22.13	1.923E-03
22	22795.	40.44	23.02	2.056E-03
23	23115.	41.29	24.07	2.149E-03
24	23715.	42.69		
25	24015.	43.51		
26	24315.	44.35		

1001024 PWA 1007 1200F AIR 10 CPM
R= 0.50 THICKNESS= 7.620 MM
PMAX= 4.595 KN WIDTH=63.627 MM
COMPACT SPECIMEN

NO.	CYCLES	A(MM)	DEL K (MPA√M)	DA/DN (MM/CYCLE)
1	100.	28.78		
2	300.	29.05	10.08	1.391E-03
3	433.	29.32	10.19	1.986E-03

7AN1025 PWA 1007 1200F AIR 10 CPM
R= 0.50 THICKNESS= 7.607 MM
PMAX= 5.702 KN WIDTH=63.597 MM
COMPACT SPECIMEN

NO.	CYCLES	A(MM)	DEL K (MPA√M)	DA/DN (MM/CYCLE)
1	0.	25.14		
2	300.	25.28		
3	800.	25.47		
4	1800.	26.16	11.16	6.566E-04
5	2700.	26.55	11.46	7.875E-04
6	3045.	27.12	11.59	8.514E-04
7	3945.	27.86	11.93	1.003E-03
8	4845.	28.74	12.49	1.208E-03
9	5445.	29.53	12.89	1.288E-03
10	5845.	30.10	13.20	1.407E-03
11	6545.	31.20	13.84	1.545E-03
12	6945.	31.64	14.25	1.655E-03
13	7175.	32.22	14.51	1.716E-03
14	7475.	32.64	14.85	1.950E-03
15	7775.	33.25	15.34	2.072E-03
16	8075.	33.80	15.81	2.236E-03
17	8375.	34.84	16.41	2.507E-03
18	8675.	35.19	17.14	2.570E-03
19	8975.	36.25	17.91	2.794E-03
20	9175.	36.89	18.43	3.171E-03
21	9375.	37.17	19.22	3.506E-03
22	9575.	38.06	19.99	3.853E-03
23	9775.	39.04	21.05	4.038E-03
24	9859.	39.25	21.61	4.295E-03
25	9916.	39.47	21.87	4.558E-03
26	10056.	39.97	22.71	4.921E-03
27	10206.	40.85	24.09	6.587E-03
28	10356.	42.02	26.12	7.989E-03
29	10431.	42.60		
30	10506.	43.35		
31	10581.	43.95		

7AN1026 PWA 1007 1200F AIR 10 CPM
R= 0.50 THICKNESS= 7.556 MM
PMAX= 4.568 KN WIDTH=63.586 MM
COMPACT SPECIMEN

NO.	CYCLES	A(MM)	DEL K (MPA√M)	DA/DN (MM/CYCLE)
1	466.	28.93		
2	974.	29.70		
3	1314.	29.96		
4	1694.	30.34	10.81	1.027E-03
5	2093.	30.87	10.98	1.040E-03
6	2450.	31.07	11.18	1.145E-03
7	2850.	31.49	11.42	1.167E-03
8	3064.	31.93	11.54	1.361E-03
9	3264.	32.16	11.71	1.501E-03
10	3464.	32.29	11.90	1.511E-03
11	3722.	32.92	12.10	1.543E-03
12	3969.	33.32	12.36	1.669E-03
13	4219.	33.53	12.64	1.699E-03
14	4520.	34.26	12.95	1.634E-03
15	4726.	34.53	13.17	1.728E-03
16	5030.	35.00	13.54	1.961E-03
17	5330.	35.53	13.95	2.146E-03
18	5630.	36.25	14.52	2.268E-03
19	5941.	37.18	15.17	2.048E-03
20	6011.	37.31	15.32	2.363E-03
21	6170.	37.40	15.65	2.468E-03
22	6329.	37.71	15.96	2.430E-03
23	6491.	38.49	16.41	2.853E-03
24	6630.	38.82	16.93	3.132E-03
25	6784.	39.20	17.49	3.204E-03
26	6973.	39.93	18.12	3.156E-03
27	7164.	40.44	18.83	3.700E-03
28	7355.	41.08	19.87	4.165E-03
29	7550.	41.92		
30	7900.	44.10		
31	8000.	44.35		

APPENDIX C. CRACK PROPAGATION DATA FOR SPECIMENS TESTED (Continued)

7AN1027 PWA 1007 1350F AIR 2 MDWL
R= 0.10 THICKNESS= 7.595 MM
PMAX= 9.950 KN WIDTH=63.800 MM
COMPACT SPECIMEN

NO.	CYCLES	A(MM)	DEL K (MPA√M)	DA/DN (MM/CYCLE)
1	150.	26.04		
2	460.	26.27		
3	1070.	26.66		
4	1690.	27.02	36.26	5.776E-04
5	2308.	27.33	36.76	5.683E-04
6	2827.	27.58	37.16	6.077E-04
7	3400.	27.97	37.73	6.382E-04
8	3880.	28.25	38.26	6.802E-04
9	4803.	29.03	39.35	7.182E-04
10	5600.	29.53	40.30	7.470E-04
11	6400.	30.12	41.37	7.870E-04
12	6990.	30.55	42.15	8.124E-04
13	8400.	31.79	44.61	1.024E-03
14	9100.	32.47	46.21	1.236E-03
15	9400.	32.88	47.03	1.259E-03
16	9700.	33.34	47.89	1.503E-03
17	10000.	33.80	48.96	1.700E-03
18	10300.	34.06	50.30	1.835E-03
19	10750.	35.27	52.84	2.089E-03
20	10950.	35.75	54.14	2.263E-03
21	11170.	36.16	55.82	2.462E-03
22	11400.	36.55	57.44	2.504E-03
23	11645.	37.38	59.59	2.937E-03
24	11775.	37.81	61.06	3.144E-03
25	11931.	38.11	63.09	3.452E-03
26	12108.	38.91		
27	12275.	39.48		
28	12421.	40.12		

1001028 PWA 1007 1200F AIR 10 CPM
R= 0.50 THICKNESS= 7.645 MM
PMAX= 5.275 KN WIDTH=63.721 MM
COMPACT SPECIMEN

NO.	CYCLES	A(MM)	DEL K (MPA√M)	DA/DN (MM/CYCLE)
1	0.	25.15		
2	135.	25.26	9.90	7.902E-04
3	300.	25.57	9.98	1.909E-03
4	559.	25.88	10.10	1.172E-03
5	859.	26.39	10.27	1.710E-03
6	1159.	26.89	10.48	1.676E-03
7	1459.	27.37	10.69	1.609E-03
8	1604.	27.65	10.86	1.874E-03
9	1906.	28.12	11.02	1.573E-03
10	2213.	28.78	11.29	2.159E-03
11	2500.	29.57	11.64	2.744E-03
12	2750.	30.09	11.98	2.068E-03
13	3283.	31.28	12.44	2.230E-03
14	3550.	32.12	13.03	3.144E-03
15	3817.	33.16	13.62	3.924E-03
16	3956.	33.54	14.10	2.677E-03
17	4110.	34.16	14.46	4.016E-03
18	4260.	34.63	14.87	3.166E-03
19	4411.	35.33	15.34	4.634E-03
20	4563.	35.91	15.68	3.802E-03
21	4711.	36.52	16.41	4.136E-03
22	4859.	37.22	17.05	4.754E-03
23	5200.	38.82	18.27	4.689E-03
24	5390.	40.41	20.24	8.819E-03
25	5460.	41.21	21.96	9.938E-03
26	5510.	41.56	22.87	7.010E-03
27	5561.	42.10	23.63	1.076E-02
28	5609.	42.55	24.51	9.207E-03
29	5659.	42.92	25.28	7.442E-03
30	5709.	43.32	26.04	8.128E-03
31	5760.	44.25	27.44	1.823E-02

1001029 PWA 1007 1200F AIR 10 CPM
R= 0.10 THICKNESS= 7.620 MM
PMAX= 5.564 KN WIDTH=63.739 MM
COMPACT SPECIMEN

NO.	CYCLES	A(MM)	DEL K (MPA√M)	DA/DN (MM/CYCLE)
1	0.	23.73		
2	250.	23.96	17.90	9.144E-04
3	504.	24.14	18.04	7.200E-04
4	1000.	25.45	18.56	2.637E-03
5	1300.	26.21	19.32	2.515E-03
6	1500.	26.63	19.78	2.127E-03
7	1750.	27.44	20.28	3.236E-03
8	1960.	28.36	21.01	4.372E-03
9	2152.	28.87	21.65	2.692E-03
10	2348.	29.79	22.32	4.652E-03
11	2500.	30.12	22.93	2.164E-03
12	2700.	30.68	23.38	2.813E-03
13	2900.	31.80	24.28	5.607E-03
14	3050.	32.16	25.13	2.388E-03
15	3207.	32.94	25.82	4.991E-03
16	3330.	33.65	26.78	5.792E-03
17	3550.	34.62	27.94	4.405E-03
18	3696.	35.42	29.26	5.463E-03
19	3840.	36.50	30.80	7.488E-03
20	3915.	36.98	32.20	6.384E-03
21	4000.	37.68	33.34	8.262E-03
22	4089.	38.38	34.79	7.820E-03
23	4194.	39.30	36.60	8.757E-03
24	4273.	40.51	39.26	1.532E-02
25	4310.	41.03	41.67	1.407E-02
26	4353.	41.62	43.34	1.373E-02
27	4412.	42.38	45.53	1.292E-02
28	4462.	43.87	49.58	2.987E-02

APPENDIX C. CRACK PROPAGATION DATA FOR SPECIMENS TESTED (Continued)

1001030 PWA 1007 1200F AIR 10 CPM
R= 0.10 THICKNESS= 7.582 MM
PMAX= 5.467 KN WIDTH=63.754 MM
COMPACT SPECIMEN

NO.	CYCLES	A(MM)	DEL K (MPA√M)	DA/DN (MM/CYCLE)
1	0.	24.04		
2	300.	24.24	17.86	6.646E-04
3	803.	24.65	18.07	8.029E-04
4	1533.	26.15	18.75	2.060E-03
5	2017.	27.06	19.66	1.876E-03
6	2422.	27.88	20.37	2.023E-03
7	2759.	28.83	21.13	2.815E-03
8	3062.	29.55	21.89	2.397E-03
9	3262.	30.20	22.55	3.245E-03
10	3463.	30.61	23.08	2.022E-03
11	3665.	31.11	23.55	2.458E-03
12	3329.	32.16	24.41	6.551E-03
13	3994.	32.59	25.28	2.471E-03
14	4144.	33.49	26.09	5.986E-03
15	4249.	33.67	26.80	1.754E-03
16	4417.	33.97	27.12	1.792E-03
17	4567.	35.13	28.16	7.705E-03
18	4730.	36.09	29.80	5.906E-03
19	4843.	36.79	31.23	6.193E-03
20	4954.	37.36	32.40	5.160E-03
21	5057.	37.93	33.52	5.499E-03
22	5164.	38.52	34.74	5.531E-03
23	5240.	38.99	35.93	6.233E-03
24	5344.	40.02	37.73	9.904E-03
25	5403.	40.84	40.16	1.276E-02
26	5462.	41.59	42.43	1.383E-02
27	5512.	42.00	44.25	8.306E-03
28	5562.	42.77	46.22	1.527E-02

1001044 PWA 1073 1350F AIR .5 CPM
R= 0.10 THICKNESS= 7.671 MM
PMAX= 10.337 KN WIDTH=63.782 MM
COMPACT SPECIMEN

NO.	CYCLES	A(MM)	DEL K (MPA√M)	DA/DN (MM/CYCLE)
1	0.	20.87		
2	100.	21.89	30.19	1.017E-02
3	160.	22.20	30.90	5.249E-03
4	289.	23.15	31.61	7.334E-03
5	370.	23.73	32.50	7.165E-03
6	451.	24.47	33.32	9.141E-03
7	502.	24.83	34.02	7.122E-03
8	555.	25.34	34.60	9.489E-03
9	600.	25.70	35.19	8.184E-03
10	660.	26.28	35.85	9.504E-03
11	720.	26.84	36.67	9.377E-03
12	780.	27.53	37.61	1.160E-02
13	830.	28.07	38.57	1.079E-02
14	870.	28.57	39.42	1.251E-02
15	920.	29.15	40.33	1.161E-02
16	970.	29.81	41.41	1.318E-02
17	1024.	30.67	42.80	1.590E-02
18	1064.	31.55	44.50	2.203E-02
19	1094.	31.95	45.83	1.308E-02
20	1124.	32.28	46.61	1.109E-02
21	1164.	33.40	48.27	2.816E-02
22	1184.	33.88	50.21	2.394E-02
23	1204.	34.35	51.43	2.324E-02
24	1224.	34.86	52.75	2.578E-02
25	1244.	35.43	54.29	2.832E-02
26	1264.	35.90	55.83	2.330E-02
27	1284.	36.56	57.62	3.315E-02
28	1304.	37.30	59.98	3.689E-02
29	1324.	37.81	62.25	2.553E-02
30	1344.	39.00	65.60	5.963E-02
31	1354.	39.58	69.44	5.817E-02
32	1369.	39.96	71.68	2.532E-02
33	1384.	40.62	74.26	4.420E-02
34	1399.	43.34	83.75	1.813E-01

1001046 PWA 1073 1350F AIR 10 CPM
R= 0.10 THICKNESS= 7.620 MM
PMAX= 6.120 KN WIDTH=63.810 MM
COMPACT SPECIMEN

NO.	CYCLES	A(MM)	DEL K (MPA√M)	DA/DN (MM/CYCLE)
1	0.	21.08		
2	300.	24.43	18.87	1.119E-02
3	451.	26.91	21.07	1.641E-02
4	503.	27.95	22.61	1.993E-02
5	540.	28.71	23.47	2.066E-02
6	575.	29.61	24.31	2.555E-02
7	600.	30.19	25.10	2.352E-02
8	630.	31.52	26.18	4.403E-02
9	645.	31.89	27.21	2.472E-02
10	660.	32.63	27.93	4.961E-02
11	677.	33.41	28.98	4.609E-02

APPENDIX C. CRACK PROPAGATION DATA FOR SPECIMENS TESTED (Continued)

1001047 PWA 1073 1350F AIR 10 CPM
R= 0.10 THICKNESS= 7.645 MM
PMAX= 6.036 KN WIDTH=63.690 MM
COMPACT SPECIMEN

NO.	CYCLES	A(MM)	DEL K (MPA√M)	DA/DN (MM/CYCLE)
1	0.	21.50		
2	50.	21.85	17.89	6.960E-03
3	100.	21.98	18.04	2.591E-03
4	175.	22.09	18.12	1.507E-03
5	250.	22.48	18.28	5.148E-03
6	301.	23.14	18.63	1.305E-02
7	467.	24.12	19.21	5.914E-03
8	547.	24.57	19.73	5.572E-03
9	615.	25.12	20.11	8.106E-03
10	690.	25.69	20.56	7.603E-03
11	767.	26.35	21.06	8.527E-03
12	844.	27.14	21.68	1.029E-02
13	910.	27.98	22.41	1.272E-02
14	980.	28.42	23.02	6.314E-03
15	1030.	29.32	23.68	1.791E-02
16	1071.	29.95	24.47	1.540E-02
17	1180.	30.99	25.38	9.531E-03
18	1380.	33.69	27.67	1.354E-02
19	1405.	34.65	30.30	3.846E-02
20	1431.	36.08	32.28	5.476E-02
21	1456.	36.42	33.90	1.367E-02
22	1482.	37.36	35.18	3.610E-02
23	1513.	38.62	37.58	4.064E-02
24	1533.	39.38	40.06	3.791E-02
25	1556.	40.97	43.33	6.935E-02
26	1574.	41.46	46.62	2.716E-02

1001048 PWA 1073 1200F AIR 10 CPM
R= 0.80 THICKNESS= 7.671 MM
PMAX= 8.180 KN WIDTH=63.589 MM
COMPACT SPECIMEN

NO.	CYCLES	A(MM)	DEL K (MPA√M)	DA/DN (MM/CYCLE)
1	30330.	24.12		
2	42221.	24.96	5.99	7.081E-05
3	49100.	25.46	6.14	7.237E-05
4	54000.	25.76	6.24	6.220E-05
5	60060.	26.23	6.34	7.775E-05
6	66000.	26.61	6.45	6.371E-05
7	73000.	27.14	6.56	7.529E-05
8	80000.	27.75	6.72	8.745E-05
9	86000.	28.27	6.88	8.594E-05
10	92000.	28.77	7.03	8.361E-05
11	97400.	29.29	7.18	9.596E-05
12	102400.	29.92	7.36	1.270E-04
13	107000.	30.17	7.51	5.439E-05
14	111820.	30.59	7.62	8.774E-05
15	115000.	31.02	7.77	1.342E-04
16	118000.	31.41	7.91	1.312E-04
17	121060.	31.70	8.04	9.380E-05
18	125000.	32.09	8.17	9.799E-05
19	129000.	32.49	8.32	1.006E-04
20	133000.	33.05	8.51	1.394E-04
21	137000.	33.43	8.71	9.430E-05
22	141560.	34.13	8.95	1.554E-04
23	145170.	34.90	9.30	2.125E-04
24	149200.	35.38	9.62	1.194E-04
25	151450.	36.06	9.93	2.992E-04
26	153430.	36.73	10.31	3.393E-04
27	155400.	37.22	10.66	2.482E-04
28	157400.	37.71	10.98	2.476E-04
29	159400.	38.18	11.31	2.337E-04
30	161350.	38.88	11.74	3.615E-04
31	163000.	39.50	12.25	3.725E-04
32	164600.	40.13	12.77	3.961E-04
33	167400.	41.53	13.70	4.989E-04
34	168400.	42.02	14.67	4.915E-04
35	169420.	42.88	15.42	8.429E-04
36	170100.	43.85	16.56	1.429E-03

7AN1052 PWA 1073 1200F AIR .5 CPM
R= 0.10 THICKNESS= 7.239 MM
PMAX= 10.751 KN WIDTH=63.358 MM
COMPACT SPECIMEN

NO.	CYCLES	A(MM)	DEL K (MPA√M)	DA/DN (MM/CYCLE)
1	0.	20.57		
2	150.	21.11		
3	300.	21.80		
4	450.	22.08	34.39	3.448E-03
5	650.	22.61	35.21	3.798E-03
6	828.	23.44	36.09	4.356E-03
7	960.	24.09	36.97	4.769E-03
8	1060.	24.59	37.72	5.127E-03
9	1150.	24.97	38.38	5.400E-03
10	1250.	25.53	39.22	5.676E-03
11	1360.	26.23	40.25	6.113E-03
12	1463.	26.90	41.35	6.552E-03
13	1555.	27.46	42.41	6.939E-03
14	1630.	28.00	43.34	7.244E-03
15	1700.	28.53	44.28	7.664E-03
16	1770.	29.09	45.33	8.373E-03
17	1840.	29.64	46.52	9.066E-03
18	1900.	30.19	47.72	9.320E-03
19	1980.	31.06	49.43	9.613E-03
20	2020.	31.49	50.35	1.012E-02
21	2060.	31.73	51.29	1.043E-02
22	2120.	32.37	52.76	1.080E-02
23	2183.	33.16	54.67	1.216E-02
24	2225.	33.67	56.20	1.322E-02
25	2265.	34.19	57.80	1.336E-02
26	2305.	34.75	59.57	1.410E-02
27	2330.	35.19	60.72	1.475E-02
28	2375.	35.83	62.99	1.583E-02
29	2415.	36.36	65.29	1.711E-02
30	2460.	37.22	68.39	1.966E-02
31	2502.	38.07	72.14	2.291E-02
32	2530.	38.70	75.34	2.378E-02
33	2555.	39.41	78.45	2.481E-02
34	2570.	39.82	80.57	2.535E-02
35	2586.	40.08	82.83	2.709E-02
36	2601.	40.54	85.03	2.812E-02
37	2615.	40.93	87.48	3.059E-02
38	2635.	41.62	91.83	3.517E-02
39	2650.	42.13	95.68	3.750E-02
40	2665.	42.73		
41	2680.	43.33		
42	2690.	43.78		

APPENDIX C. CRACK PROPAGATION DATA FOR SPECIMENS TESTED (Continued)

7AN1053 PWA 1073 1200F AIR 10 CPM
R= 0.10 THICKNESS= 7.595 MM
PMAX= 6.583 KN WIDTH=63.330 MM
COMPACT SPECIMEN

NO.	CYCLES	A(MM)	DEL K (MPA$\sqrt{M}$)	DA/DN (MM/CYCLE)
1	0.	21.63		
2	1000.	22.41		
3	2000.	23.01		
4	2300.	23.69	21.27	7.580E-04
5	3300.	23.95	21.57	7.855E-04
6	3800.	24.42	21.91	8.197E-04
7	4300.	24.85	22.25	8.441E-04
8	4800.	25.26	22.65	9.062E-04
9	5300.	25.71	23.06	9.195E-04
10	5800.	26.18	23.49	9.701E-04
11	6200.	26.63	23.87	1.041E-03
12	6600.	26.95	24.27	1.119E-03
13	7000.	27.44	24.75	1.164E-03
14	7400.	27.96	25.26	1.184E-03
15	7800.	28.51	25.79	1.269E-03
16	8200.	28.93	26.33	1.337E-03
17	8600.	29.37	26.94	1.420E-03
18	9000.	30.07	27.62	1.602E-03
19	9400.	30.74	28.49	1.690E-03
20	9600.	31.04	28.97	1.681E-03
21	9800.	31.50	29.42	1.721E-03
22	10000.	31.71	29.90	1.766E-03
23	10200.	32.08	30.41	1.793E-03
24	10400.	32.49	30.92	1.834E-03
25	10600.	32.87	31.55	1.885E-03
26	10800.	33.21	32.12	1.928E-03

Continued Next Column

7AN1053 PWA 1073 1200F AIR 10 CPM
R= 0.10 THICKNESS= 7.595 MM
PMAX= 6.583 KN WIDTH=63.330 MM
COMPACT SPECIMEN

NO.	CYCLES	A(MM)	DEL K (MPA$\sqrt{M}$)	DA/DN (MM/CYCLE)
27	11000.	33.66	32.73	2.018E-03
28	11200.	33.94	33.43	2.038E-03
29	11400.	34.45	34.17	2.282E-03
30	11600.	34.96	35.02	2.502E-03
31	11800.	35.34	36.08	2.677E-03
32	12000.	36.01	37.19	2.926E-03
33	12100.	36.33	37.83	3.004E-03
34	12200.	36.53	38.59	2.993E-03
35	12300.	36.92	39.23	2.930E-03
36	12450.	37.38	40.25	2.949E-03
37	12700.	37.97	42.17	3.189E-03
38	12800.	38.40	42.97	3.521E-03
39	12900.	38.72	43.96	3.642E-03
40	13000.	39.10	45.17	3.832E-03
41	13100.	39.57	46.32	3.809E-03
42	13200.	39.88	47.55	4.160E-03
43	13300.	40.28	48.93	4.307E-03
44	13400.	40.73	50.45	4.718E-03
45	13500.	41.28	52.34	5.159E-03
46	13600.	41.78	54.46	5.605E-03
47	13675.	42.22	56.19	6.250E-03
48	13750.	42.64	58.21	6.882E-03
49	13825.	43.16		
50	13900.	43.86		
51	13950.	44.27		

1031055 PWA 1073 1200F AIR 10 CPM
R= 0.50 THICKNESS= 7.823 MM
PMAX= 39.805 KN WIDTH=25.397 MM
CENTER CRACK SPECIMEN

NO.	CYCLES	A(MM)	DEL K (MPA$\sqrt{M}$)	DA/DN (MM/CYCLE)
1	100.	1.83		
2	249.	2.03	7.93	1.286E-03
3	404.	2.17	8.28	8.931E-04
4	550.	2.45	8.72	1.903E-03
5	703.	2.77	9.35	2.054E-03
6	847.	3.15	10.01	2.649E-03
7	960.	3.60	10.60	3.395E-03
8	1057.	3.99	11.51	3.608E-03
9	1120.	4.35	12.21	7.063E-03
10	1247.	4.93	13.19	4.570E-03
11	1390.	6.16	15.02	8.691E-03
12	1440.	6.79	17.12	1.260E-02
13	1500.	7.98	19.54	1.988E-02

APPENDIX C. CRACK PROPAGATION DATA FOR SPECIMENS TESTED (Continued)

7AN1058 PWA 1073 1200F AIR 10 CPM
R= 0.0 THICKNESS= 7.849 MM
PMAX= 29.437 KN WIDTH=26.378 MM
CENTER CRACK SPECIMEN

NO.	CYCLES	A(MM)	DEL K (MPA$\sqrt{M}$)	DA/DN (MM/CYCLE)
1	0.	2.54		
2	2000.	2.88		
3	3500.	3.34		
4	4500.	3.68	16.02	3.866E-04
5	5200.	3.92	16.78	4.718E-04
6	6000.	4.31	17.80	6.080E-04
7	6300.	4.49	18.25	6.786E-04
8	6600.	4.80	18.86	6.647E-04
9	6900.	4.97	19.47	7.291E-04
10	7200.	5.21	20.05	7.405E-04
11	7800.	5.56	21.22	8.633E-04
12	8100.	5.86	21.99	1.083E-03
13	8300.	6.07	22.64	1.204E-03
14	8500.	6.32	23.47	1.276E-03
15	8700.	6.66	24.35	1.362E-03
16	8900.	6.91	25.31	1.442E-03
17	9050.	7.07	26.04	1.658E-03
18	9200.	7.34	26.90	1.838E-03
19	9350.	7.59	28.03	2.130E-03
20	9450.	7.93	29.00	2.306E-03
21	9550.	8.08	30.04	2.490E-03
22	9650.	8.36	31.25	2.696E-03
23	9750.	8.62	32.50	3.021E-03
24	9850.	8.93	34.29	3.718E-03
25	9900.	9.10	35.34	4.261E-03
26	9950.	9.33		
27	10000.	9.61		
28	10050.	9.88		

7AN1196 PWA 1007 1200F AIR 20 HZ
R= 0.05 THICKNESS=19.126 MM
PMAX= 13.344 KN WIDTH=63.627 MM
COMPACT SPECIMEN

NO.	CYCLES	A(MM)	DEL K (MPA$\sqrt{M}$)	DA/DN (MM/CYCLE)
1	498000.	35.79		
2	501000.	36.08		
3	504000.	37.18		
4	507000.	37.87	35.01	3.030E-04
5	509000.	38.64	36.54	3.365E-04
6	511000.	39.24	38.08	3.497E-04
7	513000.	39.89	40.02	3.853E-04
8	515000.	40.85	42.18	4.369E-04
9	516500.	41.33	44.24	5.208E-04
10	518000.	42.12	46.95	6.203E-04
11	519000.	42.79		
12	520000.	43.65		
13	521000.	44.41		

7AN1301 PWA 1007 1200F AIR 10 CPM
R= 0.05 THICKNESS=12.725 MM
PMAX= 7.869 KN WIDTH=63.993 MM
COMPACT SPECIMEN

NO.	CYCLES	A(MM)	DEL K (MPA$\sqrt{M}$)	DA/DN (MM/CYCLE)
1	0.	28.12		
2	500.	28.19		
3	4845.	28.71		
4	10016.	29.77	20.12	1.843E-04
5	13000.	30.26	20.63	1.980E-04
6	16415.	30.95	21.30	2.132E-04
7	19000.	31.56	21.83	2.206E-04
8	21000.	31.98	22.31	2.246E-04
9	23000.	32.49	22.77	2.391E-04
10	25000.	32.91	23.32	2.413E-04
11	27500.	33.47	24.00	2.584E-04
12	30358.	34.40	24.91	2.866E-04
13	33045.	34.94	25.98	3.238E-04
14	35812.	36.02	27.34	3.640E-04
15	37800.	36.77	28.48	4.058E-04
16	39300.	37.39	29.60	4.042E-04
17	40300.	37.79	30.33	4.080E-04
18	41300.	38.28	31.08	4.290E-04
19	42300.	38.59	31.87	4.467E-04
20	43955.	39.32	33.47	5.093E-04
21	45241.	40.07	34.97	5.967E-04
22	46240.	40.69	36.51	6.979E-04
23	47241.	41.30	38.39	8.366E-04
24	48240.	42.20		
25	48740.	42.77		
26	49240.	43.42		

APPENDIX C. CRACK PROPAGATION DATA FOR SPECIMENS TESTED (Continued)

1001302B PWA 1007 1200F AIR 10 CPM
R= 0.50 THICKNESS=12.738 MM
PMAX= 10.057 KN WIDTH=64.018 MM
COMPACT SPECIMEN

NO.	CYCLES	A(MM)	DEL K (MPA√M)	DA/DN (MM/CYCLE)
1	0.	38.64		
2	50.	38.70		
3	100.	39.00		
4	150.	39.16	22.13	4.881E-03
5	250.	39.81	23.00	6.821E-03
6	350.	40.37	24.25	8.184E-03
7	450.	41.58	25.84	8.640E-03
8	500.	42.02	26.74	8.310E-03
9	550.	42.35	27.68	8.064E-03
10	600.	42.57		
11	670.	43.26		
12	720.	43.52		

7AN1303 PWA 1007 1200F AIR 10 CPM
R= 0.10 THICKNESS=12.700 MM
PMAX= 10.386 KN WIDTH=63.840 MM
COMPACT SPECIMEN

NO.	CYCLES	A(MM)	DEL K (MPA√M)	DA/DN (MM/CYCLE)
1	100.	21.20		
2	200.	21.43		
3	294.	21.80		
4	400.	22.09	18.77	3.229E-03
5	520.	22.51	19.03	3.385E-03
6	640.	22.94	19.30	3.572E-03
7	760.	23.29	19.62	3.772E-03
8	880.	23.79	19.98	3.730E-03
9	1000.	24.37	20.32	3.889E-03
10	1120.	24.79	20.68	4.144E-03
11	1240.	25.10	21.06	4.333E-03
12	1400.	25.91	21.65	4.833E-03
13	1500.	26.49	22.10	5.057E-03
14	1600.	27.00	22.61	5.096E-03
15	1700.	27.54	23.10	4.884E-03
16	1800.	28.03	23.54	4.729E-03
17	1900.	28.43	23.97	4.880E-03
18	2000.	28.83	24.42	5.451E-03
19	2100.	29.33	25.01	5.952E-03
20	2200.	30.05	25.74	5.817E-03
21	2250.	30.59	26.08	6.289E-03
22	2300.	30.67	26.42	6.317E-03
23	2450.	31.48	27.48	6.827E-03
24	2600.	32.70	28.95	8.739E-03
25	2675.	33.34	29.98	9.424E-03
26	2750.	34.14	31.16	9.269E-03
27	2825.	35.02	32.33	1.014E-02
28	2875.	35.38	33.27	1.083E-02
29	2925.	35.63	34.28	1.033E-02
30	2975.	36.59	35.27	1.051E-02
31	3005.	36.94	36.03	1.059E-02
32	3064.	37.28	37.48	9.770E-03
33	3084.	37.62	37.70	1.254E-02
34	3104.	37.77	38.26	1.382E-02
35	3124.	38.13	39.10	1.571E-02
36	3160.	38.77	40.51	1.708E-02
37	3190.	39.34	41.94	1.893E-02
38	3220.	39.72	43.54	2.062E-02
39	3250.	40.49	45.34	2.417E-02
40	3280.	41.19	47.95	2.679E-02
41	3310.	42.04		
42	3340.	43.25		
43	3370.	43.98		

7AN1304 PWA 1007 1200F AIR 20 HZ
R= 0.10 THICKNESS=12.700 MM
PMAX= 10.066 KN WIDTH=63.726 MM
COMPACT SPECIMEN

NO.	CYCLES	A(MM)	DEL K (MPA√M)	DA/DN (MM/CYCLE)
1	0.	21.44		
2	60220.	27.51		
3	63060.	27.93		
4	66830.	28.31	23.21	1.223E-04
5	70000.	28.68	23.51	1.363E-04
6	73500.	29.04	23.97	1.599E-04
7	78500.	29.86	24.92	2.012E-04
8	81000.	30.68	25.51	2.051E-04
9	82500.	30.96	25.91	1.956E-04
10	84000.	31.10	26.32	1.931E-04
11	85500.	31.40	26.56	1.744E-04
12	87500.	31.79	27.01	1.890E-04
13	89000.	32.03	27.39	2.087E-04
14	92000.	32.72	28.24	2.430E-04
15	94670.	33.34	29.21	2.651E-04
16	96000.	33.77	29.75	2.732E-04
17	97000.	34.14	30.19	2.704E-04
18	98000.	34.25	30.62	2.846E-04
19	99500.	34.75	31.30	2.768E-04
20	101000.	35.11	32.01	2.786E-04
21	102500.	35.67	32.75	3.010E-04
22	104000.	35.99	33.54	3.145E-04
23	105500.	36.44	34.42	3.548E-04
24	107700.	37.28	36.14	3.984E-04
25	109000.	37.83	37.43	4.081E-04
26	110000.	38.47	38.44	4.250E-04
27	111500.	38.92	40.06	4.468E-04
28	112600.	39.34	41.29	4.752E-04
29	113600.	39.89	42.56	4.983E-04
30	114600.	40.44	44.15	5.703E-04
31	115600.	41.03		
32	116650.	41.60		
33	117500.	42.35		

APPENDIX C. CRACK PROPAGATION DATA FOR SPECIMENS TESTED (Continued)

1001307 PWA 1007 800F AIR 20 HZ
R= 0.10 THICKNESS= 7.798 MM
PMAX= 6.539 KN WIDTH=63.772 MM
COMPACT SPECIMEN

NO.	CYCLES	A(MM)	DEL K (MPA√M)	DA/DN (MM/CYCLE)
1	0.	25.01		
2	17000.	26.28	22.00	7.433E-05
3	25000.	26.80	22.80	6.588E-05
4	32000.	27.39	23.32	8.328E-05
5	37000.	27.68	23.74	5.791E-05
6	44000.	28.37	24.22	9.888E-05
7	50000.	28.89	24.85	8.699E-05
8	56000.	29.50	25.45	1.010E-04
9	61000.	29.91	26.01	8.280E-05
10	66000.	30.45	26.56	1.082E-04
11	71000.	31.18	27.32	1.450E-04
12	76000.	31.66	28.08	9.601E-05
13	81000.	32.32	28.84	1.336E-04
14	86000.	32.94	29.74	1.237E-04
15	90000.	33.49	30.59	1.375E-04
16	94000.	34.08	31.47	1.467E-04
17	97000.	34.77	32.52	2.290E-04
18	102000.	35.64	33.89	1.748E-04
19	105000.	36.16	35.20	1.719E-04
20	108000.	36.81	36.38	2.167E-04
21	110000.	37.37	37.69	2.832E-04
22	113000.	37.86	38.89	1.613E-04
23	116000.	38.86	40.71	3.340E-04
24	118000.	39.70	43.18	4.197E-04
25	119000.	39.93	44.74	2.337E-04
26	120500.	40.45	45.90	3.480E-04
27	122000.	41.06	47.73	4.030E-04
28	123500.	41.70	49.83	4.259E-04
29	125000.	42.55	52.67	5.690E-04
30	126500.	43.91	57.27	9.068E-04

7AN1308 PWA 1007 1200F AIR 20 HZ
R= 0.10 THICKNESS= 7.658 MM
PMAX= 6.187 KN WIDTH=63.957 MM
COMPACT SPECIMEN

NO.	CYCLES	A(MM)	DEL K (MPA√M)	DA/DN (MM/CYCLE)
1	0.	21.00		
2	11000.	21.52		
3	25000.	22.39		
4	35000.	22.93	19.08	6.011E-05
5	45000.	23.64	19.52	6.357E-05
6	55000.	24.22	19.97	6.738E-05
7	65000.	24.82	20.50	7.287E-05
8	75000.	25.63	21.09	7.907E-05
9	85000.	26.49	21.80	8.734E-05
10	90000.	26.91	22.21	8.711E-05
11	97000.	27.54	22.76	9.521E-05
12	104000.	28.26	23.38	1.065E-04
13	109000.	28.55	23.91	1.186E-04
14	115000.	29.50	24.67	1.337E-04
15	119000.	30.05	25.26	1.479E-04
16	123000.	30.65	26.01	1.615E-04
17	126500.	31.15	26.66	1.657E-04
18	130000.	31.86	27.41	1.753E-04
19	133000.	32.40	28.10	1.871E-04
20	136000.	32.87	28.89	1.970E-04
21	139000.	33.50	29.73	2.056E-04
22	141500.	34.09	30.53	2.165E-04
23	144000.	34.60	31.44	2.279E-04
24	146500.	35.18	32.38	2.418E-04
25	149000.	35.79	33.46	2.557E-04
26	151500.	36.40	34.74	2.697E-04
27	154000.	37.21	36.20	2.720E-04
28	156000.	37.76	37.37	2.962E-04
29	158000.	38.29	38.67	3.375E-04
30	160000.	38.76	40.24	3.854E-04
31	162000.	39.72		
32	164000.	40.79		
33	166000.	41.91		

7AN1309 PWA 1007 1200F AIR 10 CPM
R= 0.10 THICKNESS= 7.709 MM
PMAX= 6.432 KN WIDTH=64.021 MM
COMPACT SPECIMEN

NO.	CYCLES	A(MM)	DEL K (MPA√M)	DA/DN (MM/CYCLE)
1	400.	24.40		
2	506.	24.62		
3	608.	25.15		
4	713.	26.22	22.06	7.230E-03
5	774.	26.44	22.51	8.004E-03
6	850.	27.12	23.10	8.450E-03
7	920.	27.67	23.62	8.700E-03
8	990.	28.44	24.26	1.016E-02
9	1060.	29.01	25.00	1.100E-02
10	1135.	29.82	25.96	1.180E-02
11	1195.	30.85	26.80	1.158E-02
12	1225.	31.05	27.26	1.251E-02
13	1275.	31.65	28.03	1.452E-02
14	1312.	31.94	28.59	1.639E-02
15	1350.	32.75	29.54	1.790E-02
16	1375.	33.48	30.26	1.820E-02
17	1392.	33.63	30.79	1.915E-02
18	1417.	33.99	31.46	1.789E-02
19	1442.	34.49	32.03	1.667E-02
20	1517.	35.76	34.66	2.249E-02
21	1530.	36.23	35.22	2.304E-02
22	1543.	36.52	35.80	2.263E-02
23	1557.	36.86	36.61	2.344E-02
24	1572.	37.18	37.15	2.471E-02
25	1587.	37.45	37.97	2.805E-02
26	1602.	37.79	38.93	3.509E-02
27	1617.	38.60	40.36	3.793E-02
28	1627.	38.86	41.55	3.501E-02
29	1637.	39.52	42.66	3.135E-02
30	1647.	39.62	43.33	2.672E-02
31	1657.	39.78	43.97	2.653E-02
32	1667.	39.96	44.48	2.934E-02
33	1677.	40.27	45.51	3.663E-02
34	1687.	40.72	46.49	3.919E-02
35	1697.	41.40	48.49	4.129E-02
36	1707.	41.70	49.85	4.450E-02
37	1717.	41.90	51.33	4.520E-02
38	1727.	42.40	52.93	4.885E-02
39	1737.	43.14		
40	1747.	43.55		
41	1757.	44.26		

APPENDIX C. CRACK PROPAGATION DATA FOR SPECIMENS TESTED (Continued)

7AN1310 PHA 1007 1200F AIR 10 CPM
R= 0.10 THICKNESS= 7.417 MM
PMAX= 6.281 KN WIDTH=63.922 MM
COMPACT SPECIMEN

NO.	CYCLES	A(MM)	DEL K (MPA√M)	DA/DN (MM/CYCLE)
1	100.	20.69		
2	204.	20.85		
3	725.	21.57		
4	925.	22.49	19.57	3.176E-03
5	1025.	22.79	19.80	3.191E-03
6	1102.	22.95	20.05	3.347E-03
7	1250.	23.45	20.36	3.056E-03
8	1400.	23.96	20.73	3.149E-03
9	1553.	24.33	21.10	3.333E-03
10	1700.	24.93	21.49	3.462E-03
11	1850.	25.35	21.94	3.605E-03
12	2012.	26.06	22.45	4.153E-03
13	2125.	26.48	22.89	4.254E-03
14	2290.	27.09	23.60	4.681E-03
15	2460.	28.24	24.37	5.150E-03
16	2630.	28.86	25.36	5.525E-03
17	2812.	29.94	26.54	5.903E-03
18	2953.	31.04	27.47	6.840E-03
19	3082.	31.60	28.67	8.161E-03
20	3184.	32.36	29.84	8.482E-03
21	3284.	33.59	31.11	9.429E-03
22	3357.	34.46	32.42	1.039E-02
23	3500.	35.52	35.22	1.062E-02
24	3550.	36.39	36.17	1.206E-02
25	3585.	36.82	37.01	1.319E-02
26	3620.	37.14	38.10	1.471E-02
27	3668.	37.87	39.71	1.530E-02
28	3710.	38.59	41.56	1.596E-02
29	3758.	39.56	43.68	1.779E-02
30	3804.	40.29	45.97	2.076E-02
31	3843.	40.70		
32	3890.	42.08		
33	3930.	43.53		

1001312 PHA 1007 1200F AIR 10 CPM
R= 0.10 THICKNESS= 7.544 MM
PMAX= 6.521 KN WIDTH=63.485 MM
COMPACT SPECIMEN

NO.	CYCLES	A(MM)	DEL K (MPA√M)	DA/DN (MM/CYCLE)
1	0.	20.73		
2	81.	21.01	19.13	3.465E-03
3	181.	21.06	19.24	5.080E-04
4	381.	21.79	19.50	3.664E-03
5	581.	22.22	19.90	2.159E-03
6	731.	22.77	20.26	2.737E-03
7	931.	23.28	20.65	3.412E-03
8	1081.	23.71	21.02	2.862E-03
9	1206.	24.24	21.40	4.186E-03
10	1340.	24.75	21.83	3.848E-03
11	1460.	25.03	22.17	2.307E-03
12	1580.	25.45	22.47	3.514E-03
13	1720.	26.07	22.94	4.409E-03
14	1820.	26.22	23.29	1.499E-03
15	1982.	26.79	23.63	3.543E-03
16	2150.	27.64	24.32	5.019E-03
17	2270.	28.15	25.01	4.276E-03
18	2390.	28.67	25.56	4.360E-03
19	2510.	29.39	26.25	6.022E-03
20	2610.	29.99	27.01	5.969E-03
21	2710.	30.62	27.76	6.312E-03
22	2813.	31.07	28.44	4.389E-03
23	2913.	32.11	29.43	1.031E-02
24	2979.	32.34	30.32	3.483E-03
25	3060.	33.01	30.99	8.310E-03
26	3130.	33.35	31.77	4.862E-03
27	3200.	34.04	32.61	9.924E-03
28	3250.	34.17	33.30	2.464E-03
29	3330.	34.79	33.95	7.731E-03
30	3411.	35.81	35.49	1.270E-02
31	3451.	36.30	37.02	1.213E-02
32	3500.	36.99	38.29	1.407E-02
33	3540.	37.53	39.72	1.353E-02
34	3580.	38.08	41.06	1.368E-02
35	3620.	38.69	42.58	1.537E-02
36	3660.	39.65	44.81	2.397E-02
37	3700.	39.94	46.72	7.303E-03
38	3757.	40.64	48.33	1.217E-02
39	3802.	42.62	53.19	4.420E-02
40	3836.	43.83	60.05	3.552E-02

7AN1313 PHA 1007 1350F AIR 10 CPM
R= 0.10 THICKNESS= 7.671 MM
PMAX= 6.272 KN WIDTH=63.541 MM
COMPACT SPECIMEN

NO.	CYCLES	A(MM)	DEL K (MPA√M)	DA/DN (MM/CYCLE)
1	0.	21.14		
2	100.	21.57		
3	200.	22.32		
4	300.	23.09	19.50	7.382E-03
5	380.	23.40	19.93	7.622E-03
6	480.	24.32	20.39	7.976E-03
7	512.	24.66	20.74	8.120E-03
8	592.	25.25	21.30	8.533E-03
9	672.	26.01	21.81	9.289E-03
10	717.	26.30	22.19	1.001E-02
11	787.	27.02	22.83	1.044E-02
12	850.	27.90	23.52	1.127E-02
13	890.	28.35	23.99	1.220E-02
14	930.	28.56	24.48	1.272E-02
15	1010.	29.75	25.60	1.334E-02
16	1050.	30.47	26.28	1.474E-02
17	1090.	30.99	27.08	1.476E-02
18	1144.	31.78	28.04	1.601E-02
19	1180.	32.43	28.81	1.582E-02
20	1215.	32.72	29.65	1.561E-02
21	1260.	33.92	30.62	1.807E-02
22	1285.	33.99	31.21	2.017E-02
23	1333.	34.69	32.97	2.705E-02
24	1383.	36.41	35.58	3.603E-02
25	1405.	37.42	37.52	4.005E-02
26	1421.	38.17	39.19	3.607E-02
27	1433.	38.40	40.47	3.239E-02
28	1445.	38.87	41.27	3.156E-02
29	1458.	39.21	42.15	3.066E-02
30	1475.	39.52	43.78	3.545E-02
31	1492.	40.37	45.70	3.901E-02
32	1505.	40.93	47.62	3.023E-02
33	1517.	41.41	49.26	4.369E-02
34	1529.	41.92	50.83	4.589E-02
35	1545.	42.31		
36	1560.	43.51		
37	1572.	44.39		

7AN1314 PWA 1007 1350F AIR 10 CPM
R= 0.10 THICKNESS= 7.468 MM
PMAX= 6.432 KN WIDTH=63.421 MM
COMPACT SPECIMEN

NO.	CYCLES	A(MM)	DEL K (MPA√M)	DA/DN (MM/CYCLE)
1	901.	20.66		
2	1050.	21.13		
3	1100.	21.45		
4	1150.	21.48	19.53	3.775E-03
5	1250.	21.88	19.79	4.055E-03
6	1350.	22.40	20.09	4.270E-03
7	1450.	22.74	20.42	4.928E-03
8	1550.	23.31	20.84	4.872E-03
9	1650.	23.74	21.26	4.541E-03
10	1750.	24.53	21.59	4.600E-03
11	1900.	24.92	22.13	4.300E-03
12	1975.	24.97	22.38	4.243E-03
13	2150.	26.05	22.95	5.262E-03
14	2300.	26.58	23.78	6.882E-03
15	2375.	27.05	24.37	5.963E-03
16	2450.	28.08	24.86	5.917E-03
17	2500.	28.28	25.27	6.804E-03
18	2700.	29.12	26.46	5.569E-03
19	2775.	29.53	26.83	5.289E-03
20	2850.	30.03	27.31	6.065E-03
21	2925.	30.59	27.88	6.774E-03
22	3000.	30.75	28.52	7.589E-03
23	3100.	31.79	29.60	8.896E-03
24	3175.	32.48	30.57	1.083E-02
25	3250.	33.32	32.01	1.218E-02
26	3325.	34.14	33.59	1.282E-02
27	3375.	35.22	34.89	1.191E-02
28	3425.	35.65	35.94	1.349E-02
29	3475.	36.27	37.00	1.527E-02
30	3525.	36.51	38.41	1.707E-02
31	3625.	38.70	43.98	2.531E-02
32	3675.	40.80	48.24	2.547E-02
33	3700.	41.25	50.81	2.163E-02
34	3725.	41.46	53.29	2.333E-02
35	3750.	42.01		
36	3775.	42.35		
37	3800.	43.54		

7AN1315 PWA 1007 1350F AIR 10 CPM
R= 0.10 THICKNESS= 7.595 MM
PMAX= 6.338 KN WIDTH=62.161 MM
COMPACT SPECIMEN

NO.	CYCLES	A(MM)	DEL K (MPA√M)	DA/DN (MM/CYCLE)
1	1009.	22.12		
2	1201.	22.49		
3	1401.	23.49		
4	1502.	23.77	20.91	2.453E-03
5	1756.	23.88	21.37	2.182E-03
6	1900.	24.14	21.50	1.975E-03
7	2150.	24.93	21.98	2.587E-03
8	2296.	25.19	22.43	2.906E-03
9	2601.	26.20	23.32	3.110E-03
10	2756.	26.88	23.79	3.413E-03
11	2900.	27.09	24.32	3.340E-03
12	2999.	27.50	24.66	3.242E-03
13	3120.	28.11	25.05	3.418E-03
14	3220.	28.24	25.47	3.632E-03
15	3323.	28.55	25.84	3.665E-03
16	3423.	29.10	26.30	3.730E-03
17	3723.	30.12	27.87	4.407E-03
18	3811.	30.90	29.41	4.368E-03
19	3920.	31.36	29.42	4.398E-03
20	4080.	31.97	30.08	4.822E-03
21	4180.	32.29	30.75	4.793E-03
22	4280.	32.77	31.65	4.804E-03
23	4381.	33.54	32.44	4.244E-03
24	4460.	33.77	32.94	5.030E-03
25	4546.	33.93	33.66	5.205E-03
26	4641.	34.29	34.58	5.166E-03
27	4740.	35.42	35.73	6.005E-03
28	4800.	35.59	36.61	6.524E-03
29	4900.	35.98	38.03	6.751E-03
30	5000.	36.83	39.42	6.752E-03
31	5100.	37.53	41.37	7.644E-03
32	5200.	38.28	43.69	8.531E-03
33	5277.	39.02	45.54	1.067E-02
34	5347.	39.59	48.05	1.099E-02
35	5400.	40.25	50.54	1.403E-02
36	5449.	41.38	53.39	1.503E-02
37	5475.	41.69	55.53	1.449E-02
38	5513.	42.05		
39	5553.	42.79		
40	5609.	43.41		

1001316 PWA 1007 1350F AIR 10 CPM
R= 0.50 THICKNESS= 7.468 MM
PMAX= 6.249 KN WIDTH=62.202 MM
COMPACT SPECIMEN

NO.	CYCLES	A(MM)	DEL K (MPA√M)	DA/DN (MM/CYCLE)
1	754.	23.82		
2	954.	24.23	11.87	2.032E-03
3	1200.	24.70	12.08	1.900E-03
4	1446.	25.34	12.35	2.617E-03
5	1939.	25.66	12.59	6.402E-04
6	2300.	26.18	12.81	1.463E-03
7	2650.	27.24	13.24	3.012E-03
8	2823.	27.74	13.68	2.914E-03
9	2995.	28.21	13.97	2.732E-03
10	3154.	28.79	14.29	3.626E-03
11	3313.	29.32	14.65	3.307E-03
12	3463.	29.66	14.94	2.328E-03
13	3613.	30.53	15.36	5.800E-03
14	3735.	31.05	15.87	4.216E-03
15	3863.	31.41	16.20	2.848E-03
16	3993.	32.10	16.62	5.275E-03
17	4108.	32.74	17.18	4.741E-03
18	4250.	33.29	17.71	4.487E-03
19	4370.	33.85	18.23	4.657E-03
20	4493.	34.53	18.89	6.138E-03
21	4581.	34.79	19.33	2.261E-03
22	4753.	35.98	20.17	6.948E-03
23	4841.	36.62	21.31	7.259E-03
24	5021.	37.63	22.42	5.581E-03
25	5075.	38.18	23.53	1.030E-02
26	5126.	38.66	24.40	9.308E-03
27	5189.	39.15	25.22	7.721E-03
28	5257.	39.65	26.11	7.396E-03
29	5325.	40.25	27.16	8.815E-03
30	5395.	40.91	28.44	9.471E-03
31	5450.	41.73	30.09	1.489E-02
32	5503.	42.54	32.05	1.524E-02
33	5540.	43.01	33.74	1.287E-02
34	5577.	43.96	35.76	2.557E-02
35	5604.	44.27	37.70	1.167E-02

APPENDIX C. CRACK PROPAGATION DATA FOR SPECIMENS TESTED (Continued)

7AN1317 PWA 1007 1200F AIR 10 CPM
R= 0.10 THICKNESS= 7.671 MM
PMAX= 5.822 KN WIDTH=62.212 MM
COMPACT SPECIMEN

NO.	CYCLES	A(MM)	DEL K (MPA*√M)	DA/DN (MM/CYCLE)
1	0.	21.78		
2	200.	22.20		
3	400.	22.54		
4	600.	22.79	18.52	1.678E-03
5	900.	23.31	18.86	1.608E-03
6	1200.	23.89	19.21	1.634E-03
7	1500.	24.23	19.59	1.676E-03
8	1900.	24.93	20.12	1.690E-03
9	2300.	25.70	20.68	1.777E-03
10	2600.	26.18	21.16	1.841E-03
11	2900.	26.73	21.66	1.842E-03
12	3200.	27.35	22.16	1.926E-03
13	3500.	27.90	22.73	2.065E-03
14	3800.	28.41	23.35	2.245E-03
15	4000.	29.00	23.82	2.346E-03
16	4200.	29.46	24.34	2.590E-03
17	4400.	29.99	24.97	2.700E-03
18	4600.	30.47	25.57	2.892E-03
19	4800.	31.22	26.31	3.115E-03
20	4950.	31.49	26.94	3.261E-03
21	5250.	32.70	28.38	3.574E-03
22	5450.	33.38	29.45	3.705E-03
23	5600.	33.91	30.42	3.968E-03
24	5750.	34.55	31.37	4.250E-03
25	5900.	35.19	32.55	4.702E-03
26	6020.	35.71	33.65	5.315E-03
27	6140.	36.40	34.98	5.894E-03
28	6260.	37.09	36.67	6.278E-03
29	6360.	37.90	38.29	6.702E-03
30	6440.	38.41	39.64	7.770E-03
31	6520.	38.83	41.36	8.493E-03
32	6600.	39.54	43.29	9.947E-03
33	6670.	40.55	45.70	1.144E-02
34	6720.	40.83	47.91	1.257E-02
35	6770.	41.67	50.28	1.439E-02
36	6820.	42.31		
37	6870.	43.09		
38	6910.	44.07		

1001318 PWA 1007 1350F AIR 10 CPM
R= 0.10 THICKNESS= 7.671 MM
PMAX= 6.374 KN WIDTH=62.065 MM
COMPACT SPECIMEN

NO.	CYCLES	A(MM)	DEL K (MPA*√M)	DA/DN (MM/CYCLE)
1	0.	19.98		
2	300.	20.60	18.54	2.079E-03
3	500.	20.77	18.80	8.699E-04
4	900.	21.90	19.24	2.813E-03
5	1332.	23.07	20.07	2.699E-03
6	1483.	23.47	20.68	2.656E-03
7	1635.	23.76	20.96	1.913E-03
8	1835.	24.60	21.43	3.370E-03
9	2085.	25.38	22.14	3.880E-03
10	2254.	25.83	22.70	2.660E-03
11	2400.	26.72	23.34	6.106E-03
12	2600.	28.08	24.47	3.389E-03
13	3000.	29.06	25.74	4.908E-03
14	3200.	29.70	26.70	3.226E-03
15	3350.	30.55	27.63	5.664E-03
16	3500.	31.47	28.81	6.147E-03
17	3650.	32.22	30.01	5.004E-03
18	3757.	33.47	31.57	1.164E-02
19	3857.	34.48	33.52	1.007E-02
20	3910.	35.02	34.99	1.023E-02
21	3960.	35.91	36.47	1.786E-02
22	4010.	36.44	38.05	1.052E-02
23	4077.	37.24	39.64	1.138E-02
24	4127.	37.71	41.28	9.576E-03
25	4180.	38.64	43.24	1.742E-02
26	4220.	39.27	45.60	1.587E-02
27	4260.	39.58	47.14	7.747E-03
28	4305.	40.55	49.38	2.162E-02
29	4352.	41.63	53.31	2.286E-02
30	4392.	42.94	58.51	3.267E-02
31	4412.	43.49	63.12	2.781E-02
32	4432.	44.11	66.29	3.086E-02

1001319 PWA 1007 1350F AIR 10 CPM
R= 0.50 THICKNESS= 7.569 MM
PMAX= 6.023 KN WIDTH=63.332 MM
COMPACT SPECIMEN

NO.	CYCLES	A(MM)	DEL K (MPA*√M)	DA/DN (MM/CYCLE)
1	100.	21.06		
2	300.	21.21	9.91	7.176E-04
3	701.	21.63	10.00	1.055E-03
4	1100.	22.00	10.14	9.135E-04
5	1503.	22.50	10.30	1.264E-03
6	1904.	22.96	10.48	1.134E-03
7	2300.	23.60	10.70	1.610E-03
8	2722.	24.26	10.96	1.562E-03
9	3020.	24.51	11.16	8.609E-04
10	3411.	25.58	11.45	2.739E-03
11	3611.	26.16	11.83	2.877E-03
12	3911.	26.33	12.01	8.381E-04
13	4013.	26.69	12.13	1.792E-03
14	4225.	27.07	12.32	1.791E-03
15	4435.	27.20	12.45	6.531E-04
16	4736.	28.33	12.78	3.755E-03
17	4900.	28.57	13.16	1.448E-03
18	5100.	29.41	13.46	4.210E-03
19	5252.	29.63	13.77	1.387E-03
20	5452.	30.07	13.97	2.203E-03
21	5660.	30.65	14.29	2.790E-03
22	5860.	31.84	14.88	5.950E-03
23	6072.	32.61	15.59	3.648E-03
24	6447.	34.26	16.55	4.409E-03
25	6550.	34.59	17.42	3.144E-03
26	6670.	34.71	17.63	1.016E-03
27	6800.	35.22	17.93	3.947E-03
28	6930.	35.66	18.40	3.361E-03
29	7151.	37.08	19.40	6.436E-03
30	7268.	37.97	20.79	7.620E-03
31	7368.	38.67	21.85	6.972E-03
32	7418.	39.79	23.18	2.235E-02
33	7443.	40.19	24.41	1.621E-02
34	7473.	40.48	25.00	9.609E-03
35	7548.	41.08	25.80	8.043E-03
36	7623.	42.27	27.54	1.578E-02
37	7649.	42.90	29.49	2.437E-02
38	7670.	43.47	30.91	2.728E-02
39	7692.	43.62	31.80	6.638E-03

APPENDIX C. CRACK PROPAGATION DATA FOR SPECIMENS TESTED (Continued)

1001320 PWA 1007 1350F AIR 10 CPM
R= 0.50 THICKNESS= 7.595 MM
PMAX= 39.107 KN WIDTH=25.336 MM
CENTER CRACK SPECIMEN

NO.	CYCLES	A(MM)	DEL K (MPA√M)	DA/DN (MM/CYCLE)
1	125.	2.74		
2	325.	2.82	9.78	4.128E-04
3	1325.	3.67	10.68	8.522E-04
4	2300.	4.77	12.55	1.130E-03
5	2550.	5.41	14.27	2.550E-03
6	2650.	6.46	16.08	1.053E-02

7AN1321 PWA 1007 1200F AIR 10 CPM
R= 0.10 THICKNESS= 7.417 MM
PMAX= 29.424 KN WIDTH=24.714 MM
CENTER CRACK SPECIMEN

NO.	CYCLES	A(MM)	DEL K (MPA√M)	DA/DN (MM/CYCLE)
1	0.	2.08		
2	2500.	2.18		
3	7000.	2.40		
4	11170.	2.79	13.65	7.080E-05
5	16200.	2.95	14.70	9.903E-05
6	20200.	3.48	15.84	1.275E-04
7	22260.	3.67	16.49	1.473E-04
8	25530.	4.32	18.05	1.824E-04
9	27200.	4.55	18.90	2.116E-04
10	28630.	4.85	19.83	2.467E-04
11	30060.	5.22	20.83	2.702E-04
12	31020.	5.52	21.70	3.007E-04
13	32010.	5.89	22.72	3.201E-04
14	33000.	6.09	23.79	3.496E-04
15	34000.	6.54	25.02	4.210E-04
16	34750.	6.76	26.18	5.220E-04
17	35400.	7.11	27.66	6.167E-04
18	35800.	7.45	28.66	7.246E-04
19	36220.	7.75		
20	36520.	7.95		
21	37730.	9.30		

7AN1323 PWA 1007 1200F AIR 10 CPM
R= 0.10 THICKNESS= 7.544 MM
PMAX= 60.471 KN WIDTH=25.349 MM
CENTER CRACK SPECIMEN

NO.	CYCLES	A(MM)	DEL K (MPA√M)	DA/DN (MM/CYCLE)
1	0.	2.33		
2	300.	2.58		
3	960.	2.83		
4	2000.	3.39	30.67	5.409E-04
5	2500.	3.63	32.06	5.775E-04
6	3000.	3.96	33.64	6.577E-04
7	3610.	4.30	35.68	8.863E-04
8	4010.	4.63	37.61	1.131E-03
9	4400.	5.04	40.17	1.375E-03
10	4670.	5.63	42.53	1.534E-03
11	4900.	5.96	44.89	1.763E-03
12	5120.	6.26	47.53	2.020E-03
13	5320.	6.64	50.14	2.152E-03
14	5520.	7.20	53.63	2.586E-03
15	5620.	7.52		
16	5750.	7.68		
17	5800.	8.01		

7AN1324 PWA 1007 800F AIR 10 CPM
R= 0.0 THICKNESS= 7.569 MM
PMAX= 32.204 KN WIDTH=25.298 MM
CENTER CRACK SPECIMEN

NO.	CYCLES	A(MM)	DEL K (MPA√M)	DA/DN (MM/CYCLE)
1	31580.	3.11		
2	34350.	3.25		
3	37600.	3.37		
4	40300.	3.47	18.29	4.274E-05
5	47000.	3.72	19.29	6.225E-05
6	49800.	3.90	19.81	8.356E-05
7	52710.	4.22	20.64	1.065E-04
8	55200.	4.40	21.48	1.346E-04
9	57851.	4.85	22.75	1.650E-04
10	60710.	5.30	24.49	1.967E-04
11	62951.	5.90	26.28	1.987E-04
12	64440.	6.18	27.41	2.290E-04
13	66000.	6.52	28.87	2.555E-04
14	67500.	6.70	30.27	3.014E-04
15	69000.	7.41	32.47	3.750E-04
16	70000.	7.69		
17	70870.	8.15		
18	71200.	8.25		

7AN1326 PWA 1007 1200F AIR 10 CPM
R= 0.0 THICKNESS= 7.556 MM
PMAX= 39.338 KN WIDTH=25.349 MM
CENTER CRACK SPECIMEN

NO.	CYCLES	A(MM)	DEL K (MPA√M)	DA/DN (MM/CYCLE)
1	0.	2.22		
2	1000.	2.32		
3	3850.	2.56		
4	5300.	2.96	20.29	2.073E-04
5	6300.	3.16	21.16	2.425E-04
6	7100.	3.41	22.07	2.390E-04
7	7800.	3.45	22.67	2.399E-04
8	8825.	3.86	23.67	2.384E-04
9	9400.	3.87	24.17	2.392E-04
10	10000.	4.08	24.76	2.571E-04
11	11275.	4.34	25.88	2.673E-04
12	11900.	4.53	26.64	2.700E-04
13	12500.	4.74	27.29	2.544E-04
14	13100.	4.90	27.68	3.314E-04
15	13735.	5.03	28.60	3.650E-04
16	14500.	5.18		
17	15608.	6.17		
18	17445.	7.51		

7AN1327 PWA 1007 1200F AIR 10 CPM
R= 0.0 THICKNESS= 7.620 MM
PMAX= 32.639 KN WIDTH=25.336 MM
CENTER CRACK SPECIMEN

NO.	CYCLES	A(MM)	DEL K (MPA√M)	DA/DN (MM/CYCLE)
1	0.	1.67		
2	1000.	1.74		
3	3100.	1.78		
4	6340.	2.12	14.21	9.868E-05
5	10100.	2.64	15.43	1.231E-04
6	14000.	3.00	17.23	1.530E-04
7	15800.	3.33	18.11	1.789E-04
8	17630.	3.68	19.09	1.974E-04
9	19200.	4.00	20.17	2.316E-04
10	20900.	4.45	21.48	2.560E-04
11	22000.	4.62	22.41	2.776E-04
12	24000.	5.34	24.40	3.370E-04
13	25025.	5.59	25.62	3.805E-04
14	26006.	5.98	27.12	4.201E-04
15	26600.	6.31	27.99	4.796E-04
16	27200.	6.56	29.24	5.443E-04
17	27800.	6.86	30.70	5.870E-04
18	28500.	7.36	32.74	5.964E-04
19	29000.	7.72		
20	29400.	7.93		
21	29930.	8.17		

7AN1328 PWA 1007 1200F AIR .5 CPM
R= 0.10 THICKNESS= 7.595 MM
PMAX= 55.600 KN WIDTH=25.349 MM
CENTER CRACK SPECIMEN

NO.	CYCLES	A(MM)	DEL K (MPA√M)	DA/DN (MM/CYCLE)
1	1800.	1.91		
2	3000.	2.27		
3	3900.	2.49		
4	5000.	2.85	25.61	4.543E-04
5	5970.	3.38	27.84	5.704E-04
6	6400.	3.55	29.03	6.467E-04
7	7000.	4.09	31.10	6.833E-04
8	7300.	4.20	32.14	7.381E-04
9	7650.	4.55	33.52	7.915E-04
10	7900.	4.62	34.33	8.305E-04
11	8300.	5.05	36.26	9.153E-04
12	8500.	5.23	37.09	1.035E-03
13	8750.	5.52	38.63	1.161E-03
14	9010.	5.71	40.15	1.343E-03
15	9400.	6.39	43.63	1.801E-03
16	9560.	6.60	45.52	2.040E-03
17	9720.	7.03	48.12	2.443E-03
18	9840.	7.37		
19	9920.	7.61		
20	10000.	7.75		

1001329 PWA 1007 1350F AIR 10 CPM
R= 0.10 THICKNESS= 7.559 MM
PMAX= 38.733 KN WIDTH=25.339 MM
CENTER CRACK SPECIMEN

NO.	CYCLES	A(MM)	DEL K (MPA√M)	DA/DN (MM/CYCLE)
1	0.	2.01		
2	525.	2.89	16.33	1.681E-03
3	1005.	3.37	18.73	9.902E-04
4	1250.	4.31	21.15	3.839E-03
5	1350.	4.67	23.39	3.067E-03
6	1450.	5.38	25.31	7.973E-03
7	1503.	6.72	29.27	2.524E-02
8	1541.	7.60	34.30	2.314E-02

1001330 PWA 1007 1350F AIR 10 CPM
R= 0.10 THICKNESS= 7.567 MM
PMAX= 43.077 KN WIDTH=25.343 MM
CENTER CRACK SPECIMEN

NO.	CYCLES	A(MM)	DEL K (MPA√M)	DA/DN (MM/CYCLE)
1	73.	1.58		
2	93.	1.92	31.18	2.005E-03
3	133.	1.99	31.67	1.775E-03
4	253.	2.10	32.77	1.592E-03
5	323.	2.27	33.64	1.705E-03
6	403.	2.60	35.97	4.107E-03
7	503.	2.95	38.63	3.511E-03

7AN1337 PWA 1073 1200F AIR 10 CPM
R= 0.10 THICKNESS= 7.315 MM
PMAX= 21.115 KN WIDTH=10.351 MM
CENTER CRACK SPECIMEN

NO.	CYCLES	A(MM)	DEL K (MPA√M)	DA/DN (MM/CYCLE)
1	0.	2.40		
2	200.	2.45		
3	500.	2.47		
4	1000.	2.53	13.13	7.200E-05
5	1700.	2.54	13.22	5.033E-05
6	2750.	2.59	13.46	7.099E-05
7	4170.	2.70	13.84	8.935E-05
8	6013.	2.96	14.43	1.177E-04
9	7410.	3.03	14.93	1.555E-04
10	8000.	3.27	15.63	2.070E-04
11	10315.	3.55	16.58	3.137E-04
12	11745.	4.04	18.34	4.099E-04
13	12300.	4.34	19.31	6.266E-04
14	13071.	4.85		
15	13461.	5.18		
16	13661.	5.48		

APPENDIX C. CRACK PROPAGATION DATA FOR SPECIMENS TESTED (Continued)

7AN1341 PWA 1073 1200F AIR 10 CPM
R= 0.10 THICKNESS= 7.518 MM
PMAX= 31.883 KN WIDTH=25.044 MM
CENTER CRACK SPECIMEN

NO.	CYCLES	A(MM)	DEL K (MPA√M)	DA/DN (MM/CYCLE)
1	0.	2.24		
2	1000.	2.37		
3	3000.	2.62		
4	5140.	2.93	15.12	2.088E-04
5	6640.	3.20	16.10	2.536E-04
6	8000.	3.68	17.15	2.834E-04
7	9520.	4.17	18.55	3.321E-04
8	10000.	4.29	19.06	3.819E-04
9	10700.	4.43	19.73	4.684E-04
10	11400.	4.83	20.65	6.382E-04
11	11900.	5.18	21.72	7.783E-04
12	12200.	5.45	22.55	8.599E-04
13	12500.	5.72	23.41	9.778E-04
14	12800.	5.98	24.42	1.095E-03
15	13100.	6.32	25.62	1.273E-03
16	13400.	6.75	27.15	1.483E-03
17	13560.	6.97	28.17	1.757E-03
18	13700.	7.23	29.23	2.016E-03
19	13820.	7.42	30.31	2.188E-03
20	13940.	7.79	31.70	2.346E-03
21	14030.	8.01	32.89	2.352E-03
22	14120.	8.20	34.03	2.575E-03
23	14210.	8.42		
24	14300.	8.60		
25	14390.	8.98		

7AN1342 PWA 1073 1200F AIR 10 CPM
R= 0.0 THICKNESS= 7.595 MM
PMAX= 38.595 KN WIDTH=25.285 MM
CENTER CRACK SPECIMEN

NO.	CYCLES	A(MM)	DEL K (MPA√M)	DA/DN (MM/CYCLE)
1	0.	2.84		
2	500.	3.01		
3	1000.	3.45		
4	1300.	3.77	23.00	1.106E-03
5	1400.	3.82	23.47	1.137E-03
6	1600.	4.14	24.36	1.225E-03
7	1800.	4.34	25.34	1.320E-03
8	2000.	4.62	26.41	1.424E-03
9	2200.	4.92	27.49	1.526E-03
10	2400.	5.23	28.76	1.772E-03
11	2575.	5.52	30.06	2.010E-03
12	2750.	5.87	31.64	2.261E-03
13	2925.	6.34	33.57	2.464E-03
14	3000.	6.54	34.53	2.618E-03
15	3075.	6.70	35.54	2.668E-03
16	3150.	6.88	36.61	2.906E-03
17	3225.	7.16	37.84	3.114E-03
18	3300.	7.45	39.23	3.502E-03
19	3375.	7.62	40.83	3.961E-03
20	3450.	7.92	42.75	4.65[illegible]E-03
21	3525.	8.32	45.35	5.[illegible]E-03
22	3555.	8.55		
23	3605.	8.83		
24	3645.	9.10		

7AN1343 PWA 1073 800F AIR 10 CPM
R= 0.0 THICKNESS= 5.791 MM
PMAX= 20.799 KN WIDTH=25.108 MM
CENTER CRACK SPECIMEN

NO.	CYCLES	A(MM)	DEL K (MPA√M)	DA/DN (MM/CYCLE)
1	0.	2.57		
2	1800.	2.59		
3	5700.	2.62		
4	9093.	2.67	13.47	2.562E-05
5	13200.	2.84	13.89	4.426E-05
6	17600.	2.99	14.48	5.408E-05
7	20045.	3.25	15.00	6.033E-05
8	23900.	3.50	15.54	6.932E-05
9	26420.	3.55	16.05	7.535E-05
10	29945.	3.76	16.54	7.661E-05
11	31400.	4.03	17.01	8.992E-05
12	33700.	4.21	17.66	1.042E-04
13	36000.	4.39	16.30	1.190E-04
14	38316.	4.79	19.11	1.357E-04
15	[illegible]	4.99	19.91	1.482E-04
16	[illegible]	5.41	21.03	1.661E-04
17	[illegible]	5.55	[illegible]	1.745E-0[illegible]
18	[illegible]	5.90	22.71	2.116E-04
19	[illegible]	6.15	23.31	2.401E-04
[illegible]	[illegible]	[illegible]	[illegible]	2.764E-04
[illegible]	[illegible]	[illegible]	[illegible]	2.914E-04
[illegible]	[illegible]	[illegible]	[illegible]	[illegible].610E-04
[illegible]	[illegible]	[illegible]	[illegible]	3.5[illegible]E-04
[illegible]	[illegible]	[illegible]	[illegible]	4.[illegible]E-04
[illegible]	[illegible]	[illegible]	[illegible]	[illegible]E-04
[illegible]	[illegible]	[illegible]	[illegible]	[illegible]07E-04
[illegible]	[illegible]	[illegible]	[illegible]	1.[illegible]E-03

APPENDIX C. CRACK PROPAGATION DATA FOR SPECIMENS TESTED (Continued)

1001349 PWA 1007 1200F AIR 10 CPM
R= 0.05 THICKNESS= 7.582 MM
PMAX=103.175 KN WIDTH=25.336 MM
CENTER CRACK SPECIMEN

NO.	CYCLES	A(MM)	DEL K (MPA√M)	DA/DN (MM/CYCLE)
1	900.	3.39		
2	1000.	3.45	53.00	3.140E-04
3	1180.	3.61	59.10	1.638E-03
4	1300.	3.75	60.63	1.175E-03
5	1450.	4.05	62.83	1.973E-03

7AN1350 PWA 1007 800F AIR 10 CPM
R= 0.0 THICKNESS= 7.531 MM
PMAX= 32.737 KN WIDTH=25.336 MM
CENTER CRACK SPECIMEN

NO.	CYCLES	A(MM)	DEL K (MPA√M)	DA/DN (MM/CYCLE)
1	15000.	2.51		
2	18000.	2.56		
3	22000.	2.87		
4	25000.	2.93	17.12	5.198E-05
5	29000.	3.15	17.82	5.820E-05
6	33333.	3.42	18.57	6.775E-05
7	37600.	3.71	19.53	8.599E-05
8	41000.	3.99	20.53	1.034E-04
9	44032.	4.36	21.60	1.208E-04
10	47047.	4.74	22.89	1.438E-04
11	49000.	5.02	23.90	1.489E-04
12	51000.	5.34	24.96	1.682E-04
13	53219.	5.78	26.34	2.072E-04
14	54354.	5.84	27.22	2.520E-04
15	55550.	6.24	28.32	2.620E-04
16	56700.	6.60	29.62	2.820E-04
17	57800.	6.89	31.19	3.110E-04
18	58800.	7.24	32.59	3.256E-04
19	59500.	7.39	33.67	3.649E-04
20	60200.	7.71	35.03	4.264E-04
21	60700.	7.87	35.14	4.952E-04
22	61209.	8.16	37.77	5.683E-04
23	61726.	8.46	39.48	7.208E-04
24	62200.	8.83		
25	62707.	9.17		
26	63320.	10.09		

1001426 PWA 1007 1200F AIR 10 CPM
R= 0.05 THICKNESS= 7.569 MM
PMAX=120.096 KN WIDTH=25.349 MM
CENTER CRACK SPECIMEN

NO.	CYCLES	A(MM)	DEL K (MPA√M)	DA/DN (MM/CYCLE)
1	0.	1.82		
2	100.	1.89	46.02	7.366E-04
3	300.	2.00	47.20	5.461E-04
4	450.	2.12	48.64	7.916E-04
5	600.	2.41	51.16	1.926E-03
6	760.	2.66	54.37	1.543E-03
7	900.	3.01	57.84	2.495E-03

1001456 PWA 1007 1200F AIR 10 CPM
R= 0.50 THICKNESS=12.751 MM
PMAX= 8.273 KN WIDTH=63.309 MM
COMPACT SPECIMEN

NO.	CYCLES	A(MM)	DEL K (MPA√M)	DA/DN (MM/CYCLE)
1	350.	30.36		
2	425.	30.42	11.68	7.622E-04
3	575.	30.73	11.78	2.057E-03
4	725.	31.04	11.95	2.100E-03
5	875.	31.40	12.13	2.371E-03
6	1050.	32.01	12.41	3.513E-03
7	1200.	32.18	12.64	1.075E-03
8	1400.	32.82	12.89	3.232E-03
9	1575.	33.30	13.26	2.736E-03
10	1750.	33.82	13.59	2.961E-03
11	1925.	34.39	13.98	3.259E-03
12	2075.	34.98	14.42	3.971E-03
13	2200.	35.50	14.86	4.145E-03
14	2325.	36.00	15.29	4.003E-03
15	2450.	37.07	15.99	8.544E-03
16	2525.	37.23	16.58	2.083E-03
17	2600.	37.81	16.96	7.721E-03
18	2675.	38.17	17.46	4.826E-03
19	2750.	38.93	18.10	1.009E-02
20	2825.	39.60	18.97	9.026E-03
21	2875.	40.24	19.83	1.267E-02
22	2910.	40.77	20.65	1.517E-02
23	2945.	41.40	21.53	1.818E-02
24	2970.	41.84	22.40	1.747E-02
25	2995.	42.49	23.32	2.586E-02
26	3015.	43.05	24.43	2.826E-02
27	3035.	43.74	25.66	3.454E-02
28	3050.	44.34	27.01	3.954E-02

APPENDIX C. CRACK PROPAGATION DATA FOR SPECIMENS TESTED (Continued)

1000784 PWA 1073 1310F AIR MISSION
R= 0.10 THICKNESS=10.282 MM
PMAX= 17.792 KN WIDTH=63.424 MM
COMPACT SPECIMEN

NO.	CYCLES	A(MM)
1	1.	20.60
2	10.	21.09
3	20.	21.47
4	30.	21.75
5	40.	22.19
6	50.	22.54
7	60.	22.93
8	70.	23.33
9	80.	23.83
10	90.	24.25
11	100.	24.58
12	110.	24.93
13	120.	25.52
14	130.	26.26
15	138.	26.69
16	146.	27.05
17	154.	27.35
18	163.	27.96
19	172.	28.59
20	180.	29.31
21	186.	29.68
22	192.	30.17
23	198.	30.69
24	203.	31.25
25	208.	31.70
26	213.	32.30

Continued Next Column

1000784 PWA 1073 1310F AIR MISSION
R= 0.10 THICKNESS=10.282 MM
PMAX= 17.792 KN WIDTH=63.424 MM
COMPACT SPECIMEN

NO.	CYCLES	A(MM)
27	217.	32.74
28	221.	33.08
29	225.	33.68
30	229.	34.08
31	233.	34.86
32	237.	35.40
33	241.	36.08
34	244.	36.69
35	246.	37.11
36	248.	37.60
37	250.	37.99
38	252.	38.44
39	254.	39.07
40	256.	39.65
41	258.	40.32
42	260.	41.04
43	261.	41.38
44	262.	41.91

1001333 PWA 1073 1275F AIR MISSION
R= 0.10 THICKNESS=12.692 MM
PMAX= 16.235 KN WIDTH=63.594 MM
COMPACT SPECIMEN

NO.	CYCLES	A(MM)
1	1.	21.97
2	25.	22.29
3	50.	22.53
4	85.	22.90
5	125.	23.44
6	165.	23.96
7	205.	24.59
8	245.	25.44
9	275.	25.79
10	305.	26.44
11	335.	27.09
12	365.	27.87
13	385.	28.31
14	405.	28.85
15	425.	29.61
16	440.	29.93
17	455.	30.44
18	470.	30.99
19	485.	31.44
20	500.	32.07
21	510.	32.46
22	520.	33.00
23	530.	33.51
24	540.	34.02
25	550.	34.57
26	560.	35.08
27	570.	35.73
28	580.	36.13
29	590.	36.83
30	600.	37.53
31	610.	38.67
32	625.	40.06
33	630.	41.09
34	635.	41.63
35	640.	43.11
36	643.	43.68

APPENDIX C. CRACK PROPAGATION DATA FOR SPECIMENS TESTED (Continued)

1001335 PWA1073 1310F MISSION
R= 0.10 THICKNESS=12.824 MM
PMAX= 22.240 KN WIDTH=63.269 MM
COMPACT SPECIMEN

NO.	CYCLES	A(MM)
1	1.	20.03
2	10.	20.13
3	22.	20.45
4	30.	20.74
5	38.	21.35
6	46.	21.76
7	56.	21.88
8	68.	22.40
9	78.	22.83
10	88.	23.53
11	96.	23.69
12	106.	24.13
13	116.	24.63
14	125.	25.23
15	134.	25.71
16	143.	26.29
17	152.	27.07
18	157.	27.39
19	164.	27.94
20	171.	28.56
21	176.	29.03
22	181.	29.43

Continued Next Column

1001335 PWA1073 1310F MISSION
R= 0.10 THICKNESS=12.824 MM
PMAX= 22.240 KN WIDTH=63.269 MM
COMPACT SPECIMEN

NO.	CYCLES	A(MM)
23	185.	29.78
24	190.	30.28
25	195.	30.66
26	200.	31.17
27	205.	31.64
28	209.	32.39
29	212.	32.72
30	215.	33.17
31	218.	33.70
32	221.	34.14
33	224.	34.75
34	227.	35.47
35	230.	35.95
36	233.	36.91
37	235.	36.98
38	238.	37.20
39	242.	38.29
40	245.	39.13
41	246.	39.61
42	247.	40.19
43	248.	40.80
44	249.	41.48

1001473 PWA1074 1310 AIR MISSION
R= 0.10 THICKNESS= 9.017 MM
PMAX= 80.064 KN WIDTH=23.660 MM
SURFACE FLAW SPECIMEN

NO.	CYCLES	A(MM)
1	1.	1.77
2	100.	1.88
3	187.	2.48
4	245.	2.92
5	275.	3.12
6	305.	3.48
7	330.	3.80
8	345.	4.08
9	780.	4.54
10	395.	4.74
11	410.	5.18
12	420.	5.53
13	431.	5.82
14	436.	6.21
15	441.	6.42
16	446.	6.52
17	456.	6.63
18	466.	6.89
19	476.	7.61
20	480.	8.12
21	482.	8.36
22	484.	8.46
23	486.	8.74
24	488.	9.01
25	490.	8.71
26	493.	9.30
27	494.	9.81
28	495.	10.13
29	496.	10.22
30	497.	10.46
31	498.	10.65
32	499.	11.47

APPENDIX C. CRACK PROPAGATION DATA FOR SPECIMENS TESTED (Continued)

1001498 PWA 1007 1150F MISSION
R= 0.05 THICKNESS= 8.979 MM
PMAX= 88.960 KN WIDTH=23.673 MM
SURFACE FLAW SPECIMEN

NO.	CYCLES	A(MM)
1	1.	3.47
2	100.	3.59
3	204.	3.75
4	304.	4.15
5	354.	4.99
6	406.	5.09
7	464.	5.29
8	502.	4.89
9	555.	5.36
10	629.	5.32
11	649.	5.57
12	699.	5.69
13	729.	5.93
14	761.	6.23
15	808.	6.59
16	839.	6.98
17	854.	7.20
18	869.	7.51
19	887.	7.93
20	905.	8.42
21	918.	8.64
22	926.	8.83
23	937.	9.21

1001500 PWA 1007 1150F AIR MISSION
R= 0.10 THICKNESS= 8.979 MM
PMAX= 88.960 KN WIDTH=23.711 MM
SURFACE FLAW SPECIMEN

NO.	CYCLES	A(MM)
1	1.	3.27
2	80.	3.35
3	170.	3.51
4	260.	3.55
5	360.	3.75
6	460.	3.87
7	560.	4.07
8	680.	4.27
9	760.	4.66
10	840.	5.06
11	855.	5.21
12	905.	5.38
13	955.	5.58
14	1005.	5.49
15	1055.	5.92
16	1105.	6.22
17	1155.	6.36
18	1285.	7.01
19	1320.	7.49
20	1385.	7.98
21	1390.	8.26
22	1418.	8.73
23	1431.	9.09

1001501 PWA 1074 1310F AIR MISSION
R= 0.10 THICKNESS=12.675 MM
PMAX= 22.240 KN WIDTH=63.388 MM
COMPACT SPECIMEN

NO.	CYCLES	A(MM)
1	1.	20.52
2	8.	20.75
3	20.	21.20
4	32.	21.54
5	44.	21.89
6	56.	22.48
7	66.	22.55
8	78.	22.83
9	90.	23.23
10	102.	23.65
11	114.	23.79
12	126.	24.16
13	139.	24.82
14	149.	25.11
15	159.	25.49
16	169.	26.08
17	179.	26.56
18	189.	26.83
19	199.	27.06
20	209.	27.55
21	218.	28.09
22	227.	28.44
23	237.	28.74

Table Data Continued on Next Page

1001501 PWA 1074 1310F AIR MISSION
R= 0.10 THICKNESS=12.675 MM
PMAX= 22.240 KN WIDTH=63.388 MM
COMPACT SPECIMEN

NO.	CYCLES	A(MM)
24	247.	29.37
25	257.	29.84
26	266.	30.37
27	274.	30.90
28	282.	31.50
29	290.	31.97
30	298.	32.73
31	305.	33.28
32	311.	33.78
33	317.	34.25
34	323.	34.95
35	328.	35.53
36	333.	36.16
37	338.	36.86
38	343.	37.45
39	347.	38.29
40	350.	38.88
41	353.	39.71
42	355.	40.17
43	357.	40.83
44	358.	41.02
45	360.	41.93
46	361.	43.01

1001503 PWA 1073 1310F MISSION
R= 0.10 THICKNESS=12.700 MM
PMAX= 22.240 KN WIDTH=64.018 MM
COMPACT SPECIMEN

NO.	CYCLES	A(MM)
1	1.	21.40
2	6.	21.84
3	13.	22.26
4	20.	22.87
5	26.	23.16
6	32.	23.37
7	38.	24.10
8	44.	24.53
9	50.	25.10
10	55.	25.63
11	60.	25.89
12	66.	26.38
13	72.	27.15
14	77.	27.27
15	82.	28.14
16	88.	28.79
17	93.	29.50
18	97.	29.97
19	101.	30.46
20	105.	31.01
21	109.	31.68
22	112.	32.13
23	115.	32.72
24	118.	33.29
25	121.	33.77
26	124.	34.52
27	127.	35.27
28	130.	35.66
29	133.	36.46
30	136.	37.55
31	138.	38.51
32	139.	39.35
33	141.	39.85
34	142.	40.42
35	143.	41.61

1001504 PWA 1073 1310F AIR MISSION
R= 0.10 THICKNESS=12.700 MM
PMAX= 22.240 KN WIDTH=63.431 MM
COMPACT SPECIMEN

NO.	CYCLES	A(MM)
1	1.	20.50
2	15.	21.36
3	27.	22.13
4	35.	22.65
5	45.	23.36
6	52.	23.88
7	59.	24.55
8	66.	25.13
9	71.	25.44
10	77.	26.10
11	82.	26.65
12	87.	27.43
13	91.	27.95
14	95.	28.11
15	101.	28.51
16	107.	29.19
17	113.	29.98
18	118.	30.70
19	122.	31.21
20	126.	32.00
21	129.	32.54
22	132.	33.18
23	135.	33.85
24	139.	34.68
25	142.	35.52
26	144.	35.91
27	146.	36.42
28	148.	37.09
29	151.	37.97
30	153.	38.36
31	155.	39.47
32	157.	40.24
33	158.	40.93

APPENDIX C. CRACK PROPAGATION DATA FOR SPECIMENS TESTED (Continued)

1001563 PWA 1007 1150F AIR MISSION
R= 0.10 THICKNESS= 12.848 MM
PMAX= 22.240 KN WIDTH=63.500 MM
COMPACT SPECIMEN

NO.	CYCLES	A(MM)
1	1.	22.73
2	40.	23.17
3	80.	23.50
4	120.	23.80
5	160.	24.26
6	200.	24.62
7	240.	25.12
8	280.	25.59
9	320.	26.21
10	355.	26.19
11	390.	27.15
12	420.	27.20
13	450.	27.56
14	475.	27.66
15	500.	28.05
16	525.	28.45
17	550.	28.89
18	575.	29.63
19	595.	29.94
20	615.	30.02
21	635.	30.54
22	655.	30.71
23	675.	31.34

Continued Next Column

1001563 PWA 1007 1150F AIR MISSION
R= 0.10 THICKNESS= 12.848 MM
PMAX= 22.240 KN WIDTH=63.500 MM
COMPACT SPECIMEN

NO.	CYCLES	A(MM)
24	695.	31.57
25	705.	31.98
26	715.	32.60
27	755.	33.41
28	770.	33.32
29	785.	34.11
30	800.	34.26
31	815.	34.87
32	825.	35.05
33	835.	35.48
34	845.	35.99
35	855.	36.30
36	865.	36.97
37	873.	37.20
38	891.	37.67
39	895.	38.61
40	901.	39.01
41	907.	39.85
42	910.	40.54
43	913.	40.41
44	914.	40.88
45	917.	42.44
46	921.	43.51

1001565 PWA1007 1150F AIR MISSION
R= 0.10 THICKNESS=12.695 MM
PMAX= 26.688 KN WIDTH=63.515 MM
COMPACT SPECIMEN

NO.	CYCLES	A(MM)
1	1.	21.23
2	40.	21.43
3	80.	21.46
4	130.	21.68
5	180.	22.05
6	240.	22.18
7	310.	22.57
8	380.	23.10
9	430.	23.41
10	480.	23.75
11	530.	24.06
12	590.	24.56
13	650.	24.92
14	730.	25.53
15	810.	26.21
16	880.	26.86
17	940.	27.02
18	1000.	27.46
19	1040.	28.58
20	1100.	29.04
21	1140.	29.59
22	1180.	29.74
23	1210.	30.68
24	1240.	31.11
25	1265.	31.53
26	1290.	31.88
27	1305.	32.14
28	1340.	32.40
29	1345.	35.69
30	1350.	37.43
31	1355.	37.99
32	1460.	38.94

1001575 PWA 1073 1275F AIR MISSION
R= 0.05 THICKNESS= 9.017 MM
PMAX= 80.064 KN WIDTH=23.647 MM
SURFACE FLAW SPECIMEN

NO.	CYCLES	A(MM)	DEL K (MPA*√M)	DA/DN (MM/CYCLE)
1	1.	1.97		
2	80.	2.22	22.19	3.135E-03
3	227.	2.20	22.79	-1.123E-04
4	287.	2.57	23.67	6.075E-03
5	387.	2.73	24.94	1.638E-03
6	487.	3.16	26.30	4.280E-03
7	577.	3.53	28.02	4.078E-03
8	677.	4.59	30.87	1.067E-02
9	697.	5.29	34.07	3.499E-02
10	723.	5.46	35.52	6.252E-03
11	728.	6.13	36.88	1.349E-01
12	738.	5.90	37.58	-2.311E-02
13	753.	6.24	37.75	2.269E-02
14	763.	6.40	38.52	1.626E-02
15	773.	6.59	39.04	1.842E-02
16	799.	7.63	40.84	4.000E-02
17	805.	7.87	42.65	4.106E-02
18	809.	7.99	43.15	2.921E-02
19	813.	8.16	43.53	4.191E-02
20	817.	8.46	44.16	7.525E-02
21	820.	8.68	44.85	7.408E-02
22	823.	8.88	45.40	6.773E-02
23	826.	9.11	45.95	7.408E-02
24	829.	9.37	46.56	8.721E-02
25	832.	9.61	47.19	8.043E-02
26	833.	9.98	47.94	3.658E-01

LIST OF SYMBOLS

Symbol	Definition	Units: Metric (SI)	Units: English
a	crack length	mm	in.
B	specimen thickness	mm	in.
C_1	SINH material coefficient = 0.5	dimensionless	dimensionless
C_2	SINH horizontal scaling coefficient	dimensionless	dimensionless
C_3	SINH horizontal inflection coefficient	log (ΔK)	log (ΔK)
C_4	SINH vertical inflection coefficient	log (da/dN)	log (da/dN)
CC	center crack specimen		
CS	compact specimen		
d	differential	–	
da/dN	cyclic rate of crack growth	mm/cycle	in./cycle
da/dt	sustained load rate of crack growth	mm/hr	in./hr
Δ	algebraic difference		
$\Delta a/\Delta N$	growth rate determined from direct secant	mm/cycle	in./cycle
ΔK	applied stress intensity = $K_{max} - K_{min}$	MPa$\sqrt{m}$	ksi$\sqrt{in.}$
ΔN_{OL}	number of fatigue cycles applied between periodic overloads	cycles	cycles
ΔN_{Dwell}	number of fatigue cycles applied between period load dwells		–
f(subscript)	final value of parameter subscripted	–	
f,g	functions		
i(subscript)	initial value of parameter subscripted	–	–
K	stress intensity factor	MPa$\sqrt{m}$	ksi$\sqrt{in.}$
LCF	low cycle fatigue	–	
LEFM	linear elastic fracture mechanics	–	–
N	number of cycles	cycle	cycle
N_A	number of cycles to specimen failure (actual)	–	–
N_c	number of cycles to specimen failure (calculated)	–	
N*	period of crack retardation	cycle	cycle
N_{DR}	period of delayed retardation	cycle	cycle
ν	test frequency	Hz	Hz, cpm (cycles/minute)
P	load	N	Kips
P_{max}	maximum load	N	Kips
P_{min}	minimum load	N	Kips
P_{ol}	magnitude of overload	N	Kips
R	load ratio = P_{min}/P_{max}	–	–

LIST OF SYMBOLS (Continued)

Symbol	*Definition*	*Units*	
		Metric (SI)	*English*
σ	stress	MPa	ksi
t	time	seconds	seconds
T	temperature	^{o}C	^{o}F
W	specimen width	mm	in.

REFERENCES

1. Annis, C. G., R. M. Wallace, and D. L. Sims, "An Interpolative Model for Elevated Temperature Fatigue Crack Propagation," AFML TR-76-176, Part I, November 1976.

2. Wallace, R. M., C. G. Annis, and D. L. Sims, "Application of Fracture Mechanics at Elevated Temperature," AFML TR-76-176, Part II, November 1976.

3. Sims, D. L., C. G. Annis, and R. M. Wallace, "Cumulative Damage Fracture Mechanics at Elevated Temperature," AFML-TR-76-176, Part III, November 1976.

4. Cruse, T. A. and Meyer T. G., "Structural Life Prediction and Analysis Technology," AFAPL-TR-78-106, December 1978.

5. Tada, H., Paris, P. C., Irwin, G. R., "The Stress Analysis of Cracks Handbook," Del Research Corporation, Hellertown, Pennsylvania, 1973.

6. Larsen, J.M. and C.G. Annis, "Observation of Crack Retardation Resulting From Load Sequencing Characteristic of Military Gas Turbine Operation", Submitted for Publication - American Society for Testing and Materials, 1979.

7. Cowles, B. A., D. L. Sims, and J. R. Warren, "Evaluation of the Cyclic Behavior of Aircraft Turbine Disc Alloys," NASA CR-159409, August 1978, Contract NAS3-20367.

8. Hudak, S. J., Jr., A. Saxena, R. J. Bucci, and R. C. Malcolm, "Development of Standard Methods of Testing and Analyzing Fatigue Crack Growth Rate Data," Technical Report AFML-TR-78-40, May 1978.

9. Elber, W., "The Significance of Fatigue Crack Closure," Damage Tolerance in Aircraft Structures, ASTM STP 486, American Society for Testing and Materials, 1971, pages 230–242.

10. Macha, D.E., A.F. Grandt, Jr., and B.J. Wicks, "Effects of Gas Turbine Engine Load Spectrum Variables on Crack Propagation", Submitted for Publication - American Society for Testing and Materials, 1979.

11. Meyers, G. J., "Design & K-Calibration of Surface Flaw Test Specimen," Pratt & Whitney Aircraft, Commercial Products Division Memo, June 22, 1976.

12. Shah, R. C. and A. S. Kobayashi, "On The Surface Flaw Problem," *The Surface Crack: Physical Problems and Computational Solutions,* New York: The American Society of Mechanical Engineers, 1972.

*U.S.Government Printing Office: 1980 — 657-084/617

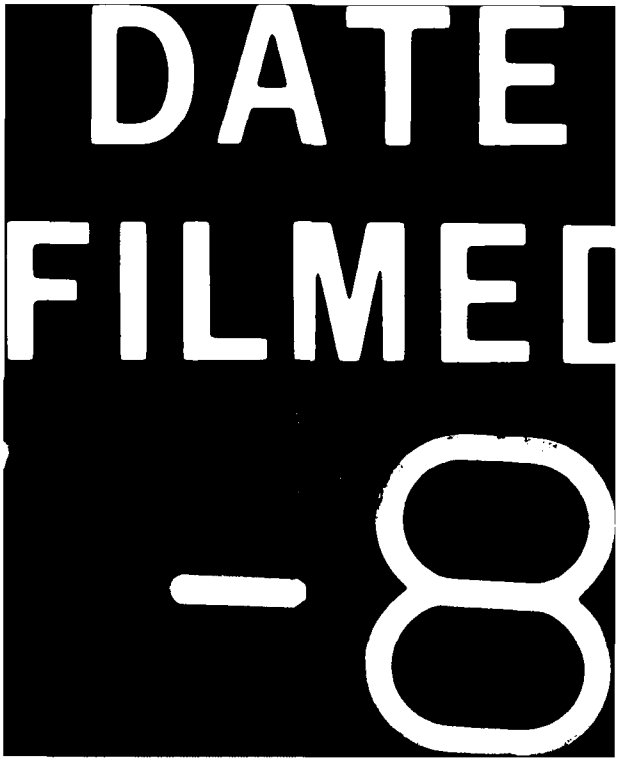
DATE
FILMED
-8